Combinatorial Reid's Recipe for Consistent Dimer Models

Tapia Amador, Jesus

Award date:
2015

Awarding institution:
University of Bath

Combinatorial Reid's Recipe for Consistent Dimer Models

submitted by

Jesus Tapia Amador

for the degree of Doctor of Philosophy

of the

University of Bath

Department of Mathematical Sciences

November 2014

ABSTRACT

The aim of this thesis is to generalise Reid's recipe as first defined by Reid [Rei97] for G-Hilb $\left(\mathbb{C}^3\right)$ (G a finite abelian subgroup of $\mathrm{SL}(3,\mathbb{C})$) to the setting of consistent dimer models. We study the θ-stable representations of a quiver Q with relations $\mathcal{R}$ dual to a consistent dimer model Γ in order to introduce a well-defined recipe that marks interior lattice points and interior line segments of a cross-section of the toric fan Σ of the moduli space $\mathcal{M}_A(\theta)$ with vertices of Q, where $A = \mathbb{C}Q/\langle\mathcal{R}\rangle$. After analysing the behaviour of 'meandering walks' on a consistent dimer model Γ and assuming two technical conjectures, we introduce an algorithm - the arrow contraction algorithm - that allows us to produce new consistent dimer models from old. This algorithm could be used in the future to show that in doing combinatorial Reid's recipe, every vertex of Q appears 'once' and that combinatorial Reid's recipe encodes the relations of the tautological line bundles of $\mathcal{M}_A(\theta)$ in $\mathrm{Pic}(\mathcal{M}_A(\theta))$.

CONTENTS

LIST OF FIGURES

LIST OF TABLES

ACKNOWLEDGEMENTS

Writing this thesis would had been impossible without the help and support of many people.

Firstly, I would like to express my gratitude to my supervisor, Alastair Craw. I could not have hoped for a better supervisor. He has been an inspiring and patient teacher. Thank you for your time and commitment. Your enthusiasm and passion for Mathematics have been a reliable source of encouragement, even in the toughest of days. It has been a wonderful journey.

I would also like to thank my family for their constant support in every respect. Thank you mom and dad for always being there. Your example has taught me so much, and I count myself blessed for having you both as my parents. To my three wonderful sisters, thank you for teaching me to always face challenges with courage, determination and a smile on my face.

I am grateful to Raf Bocklandt for providing me with a large number of examples of dimer models to play with. Thanks to Alastair King and Timothy Logvinenko for their constructive criticisms which significantly improved this thesis. I would like to thank the members of the Departments of Mathematics both at the University of Glasgow and the University of Bath. I am especially thankful to Nathan Prabhu-Naik for the countless mathematical and procrastination sessions. To those I shared offices with and made this experience a more pleasant one, to many other inspiring teachers who encouraged me to pursue the study of Mathematics, to my friends in Mexico, Glasgow and Bath, especially Chik-Wai Ho.

I am also grateful to CONACYT for their financial support through the generous scholarship which funded this project.

Last, words cannot express my gratitude to God, from whom all good comes and to whom all glory belongs. “For where I found Truth, there found I my God, the Truth itself.” *Ad maiorem Dei gloriam.*

INTRODUCTION

In the late nineties, Reid [Rei97] described a recipe to mark the interior line segments and interior lattice points of a cross section of the toric fan of the G-Hilbert scheme, a crepant resolution of the quotient $\mathbb{C}^3/G$, by irreducible representations of G, for G a finite abelian subgroup of $\mathrm{SL}(3,\mathbb{C})$. One of the main features of this recipe is that it encodes the relations between the tautological line bundles of $G\text{-Hilb}(\mathbb{C}^3)$ in $\mathrm{Pic}(G\text{-Hilb}(\mathbb{C}^3))$. Some years later, Craw [Cra05] proved that the recipe can be done for any finite abelian subgroup G of $\mathrm{SL}(3,\mathbb{C})$.

The quotient $\mathbb{C}^3/G$ and crepant resolution $G\text{-Hilb}(\mathbb{C}^3)$ are examples of affine Gorenstein toric threefolds and crepant resolutions arising from the study of dimer models and moduli spaces of quiver representations. Therefore, it is natural to consider a generalisation of Reid's recipe for dimer models. Dimer models are combinatorial objects which encode quivers with relations. To any dimer model Γ, we associate a quiver Q with relations $\mathcal{R}$ and a complex algebra A. When Γ satisfies some 'consistency' conditions, the centre of the algebra A is the coordinate ring of an affine Gorenstein toric threefold X. For some stability parameter θ, the fine moduli space $\mathcal{M}_A(\theta)$ of θ-stable representations of A with dimension vector $(1,1,\ldots,1)$ satisfying the relations $\mathcal{R}$ is a crepant resolution of X. In the case when the dimer model is hexagonal, there is a special choice of parameter θ for which $\mathcal{M}_A(\theta)$ is $G\text{-Hilb}(\mathbb{C}^3)$ for some $G \subset \mathrm{SL}(3,\mathbb{C})$.

Reid's recipe for consistent dimer models marks each interior lattice point and interior line segment in a cross-section of the fan Σ of $\mathcal{M}_A(\theta)$ by a vertex or vertices of the quiver Q. Some progress has been done towards generalising Reid's recipe to consistent dimer models. The work of Cautis–Logvinenko [CL09] and Logvinenko [Log10] for the G-Hilbert scheme inspired Bocklandt–Craw–Quintero-Vélez [BCQV15, Theorem 1.4] to introduce *Geometric Reid's Recipe* for consistent dimer models. In their paper, Bocklandt–Craw–Quintero-Vélez study the images of vertex simples S_v under one of the functors

$$\Psi : D^b(\mathrm{mod}-A) \longrightarrow D^b(\mathrm{coh}(\mathcal{M}_A(\theta)))$$

which gives the equivalence between the bounded derived category of finitely-generated A-modules and the bounded derived category of coherent sheaves on $\mathcal{M}_A(\theta)$. The insight of geometric Reid's recipe, due to Cautis–Logvinenko [CL09], and expanded upon by Logvinenko [Log10] and Craw–Cautis–Logvinenko [CCL12], is that the support of the object $\Psi(S_v)$ is closely related to classical Reid's recipe for the G-Hilbert scheme. The results of Bocklandt–Craw–Quintero-Vélez [BCQV15, Theorem 1.4] suggest how interior lattice points and certain interior line segments of a cross-section of Σ might

be marked by vertices v of Q. This thesis presents a more combinatorial approach to the problem.

In order to define combinatorial Reid's recipe for consistent dimer models, we study the θ-stable representations of A with dimension vector $(1, 1, \ldots, 1)$ satisfying the relations $\mathcal{R}$, for a special choice of stability parameter θ. This enables us to introduce a well-defined recipe which marks every interior lattice point and interior line segment of the fan Σ by a vertex of Q. Combinatorial Reid's recipe is compatible with both classical Reid's recipe from Reid [Rei97] and Craw [Cra05], and with geometric Reid's recipe. With the aim to show that every vertex appears 'once' and that the marking encodes the relations of the line bundles of $\mathcal{M}_A(\theta)$ in $\mathrm{Pic}(\mathcal{M}_A(\theta))$, we introduce a 'localisation' algorithm, called the arrow contraction algorithm.

As a word of warning to the reader, at times throughout this thesis we will need to simultaneously refer to dimer models, quivers and toric fans of crepant resolutions, which we identify with their cross-sections at height one. All three of these have zero-dimensional and one-dimensional components. In order to avoid confusion we give to each of them different names. Table 1 summarises this information and introduces the symbol we normally use to denote each of them.

	Zero-dimensional	One-dimensional	Two-dimensional
Dimer model (Γ)	Nodes ($\mathfrak{n}$)	Edges ($\mathfrak{e}$)	Tiles ($\mathfrak{t}$)
Quiver (Q)	Vertices (v)	Arrows (a)	
Fan (Σ)	Lattice points (ρ)	Line segments (τ)	Triangles (σ)

Table 1: *Convention of names and symbols used for dimer models, quivers and toric fans*

Structure of the thesis

This thesis comes in four parts. The first two chapters present some background material and define some important notions, such as fundamental hexagons and meandering walks. Chapter 3 uses some of the results from Chapter 2 to introduce a well-defined generalisation of Reid's recipe to the setting of consistent dimer models. The third part of this thesis (Chapters 4, 5 and 6) defines an algorithm, called the arrow contraction algorithm, which enables us to produce new consistent dimer models from old. In this part of the thesis, we assume two conjectures which we make based on numerous computational evidence. Finally, Chapter 7 aims to bring the latter two parts of the thesis together, suggesting future work and a link between combinatorial Reid's recipe for consistent dimer models and the arrow contraction algorithm.

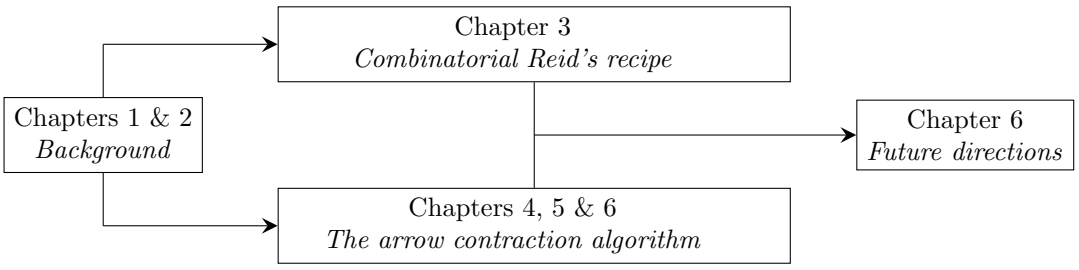

Chapter 1 provides a basic introduction to dimer models and moduli spaces of quiver representations. We start by defining dimer models, their quivers with relations, perfect matchings and zigzag and characteristic polygons. Throughout this thesis we will only be interested in dimer models in the two-torus $\mathbb{T}$ which satisfy a 'nondegeneracy' condition. This is weaker than the consistency condition assumed in Chapters 3−7. Section 1.3 gives some background material on toric varieties. We recall King's construction of moduli spaces of quiver representations and introduce two equivalent notions of consistency for dimer models. The following theorem due to Ishii–Ueda [IU08], Craw–Quintero-Vélez [CQV12] and Broomhead [Bro12], brings most of the background material together:

Theorem 1.48. *Let Γ be a consistent dimer model with θ generic. The moduli space $\mathcal{M}_A(\theta)$ is a toric variety that gives a crepant resolution $f : \mathcal{M}_A(\theta) \to X$ of the Gorenstein affine toric threefold $X := \operatorname{Spec}(Z(A))$.*

At the end of Chapter 1 we remind the reader of classical Reid's recipe, as first described by Reid [Rei97] and proved by Craw [Cra05], for G a finite abelian subgroup of $\mathrm{SL}(3,\mathbb{C})$.

In Chapter 2, we introduce the notion of a fundamental hexagon. Fundamental hexagons were first studied by Ishii–Ueda [IU08] to define toric coordinates on each of the charts U_σ of $\mathcal{M}_A(\theta)$, for any three-dimensional cone σ of the fan Σ of $\mathcal{M}_A(\theta)$, Γ a nondegenerate dimer model and θ generic. They are fundamental domains of the universal cover of Γ associated to each torus-invariant θ-stable representation of $\mathcal{M}_A(\theta)$. Section 2.2 is expository and summarises results from Ishii–Ueda [IU08]. Section 2.3 introduces the notion of meandering walks on a nondegenerate dimer model Γ. Meandering walks are subsets of edges of Γ which lie on the boundary of fundamental hexagons. They generalise the notion of zigzag paths and are defined in terms of symmetric differences of perfect matchings. Meandering walks will play an important role throughout the thesis, especially when defining the arrow contraction algorithm.

As an example, consider the dimer model Γ in Figure 1 depicted next to its associated quiver Q. The fan of $\mathcal{M}_A(\theta)$ for $\theta = (-7, 1, 1, \ldots, 1)$ is presented in Figure 2. It has eight lattice points $\rho_1, \rho_2, \ldots, \rho_8$, marked by $1, 2, \ldots, 8$ in the picture.

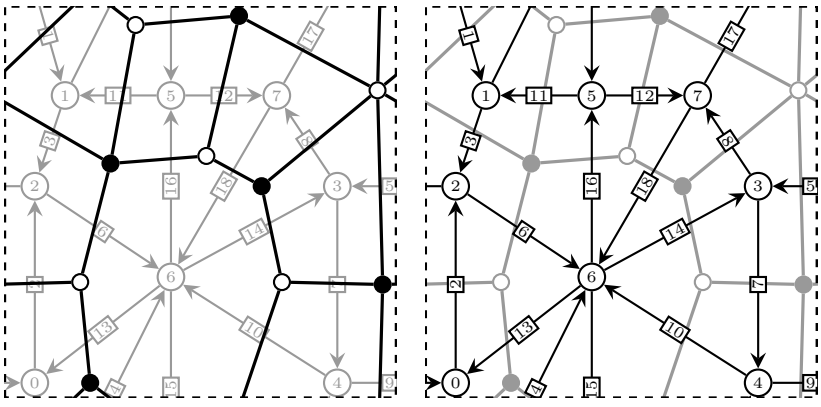

(a) The dimer model Γ (b) The dual quiver Q

Figure 1: *A dimer model Γ with its dual quiver Q*

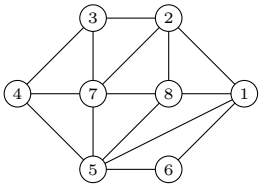

Figure 2: *Fan Σ of $\mathcal{M}_A(\theta)$*

Fundamental hexagons are defined uniquely up to translations by $\mathbb{Z}^2$. Figure 3 shows a tiling of $\mathbb{R}^2$ by a fundamental hexagon. Any choice of vertex 0 in the universal cover of Γ determines a connected subset of $\mathbb{R}^2$ and thus a fundamental hexagon. Note that each of the eight tiles of Γ appears once in the fundamental hexagon. Moreover, the fundamental hexagon has six trivalent nodes along its boundary, three white and three black. The quiver depicted in the fundamental hexagon supports a θ-stable representation 'associated' to the cone σ with lattice points ρ_2, ρ_7 and ρ_8.

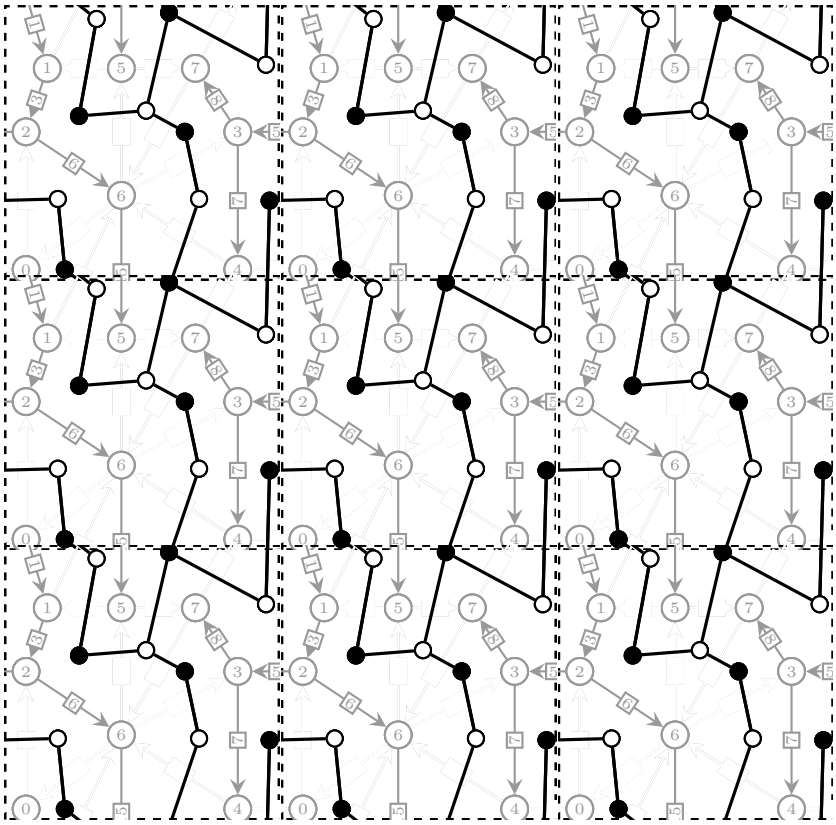

Figure 3: *A tiling of $\mathbb{R}^2$ by a fundamental hexagon*

We conclude Chapter 2 by generalising Nakamura's G-igsaw transformations to the setting of dimer models. Nakamura [Nak01] introduced an algorithm to produce the crepant resolution G-Hilb$(\mathbb{C}^3)$ of $\mathbb{C}^3/G$ for a finite abelian subgroup $G \subset \mathrm{SL}(3,\mathbb{C})$. This algorithm is generalised to the setting of consistent dimer models by using our understanding of fundamental hexagons and the meandering walks on their boundaries. For two adjacent cones σ_+ and σ_- with common line segment τ, we can consider their θ-stable representations M_+ and M_-. We cut the corresponding fundamental hexagon

of M_+, denoted $\mathrm{Hex}(\sigma_+)$, using a subset of edges c_- in Γ which lie along the boundary of $\mathrm{Hex}(\sigma_-)$. We call the set of edges c_- the cut of $\mathrm{Hex}(\sigma_+)$ by $\mathrm{Hex}(\sigma_-)$. This cut splits $\mathrm{Hex}(\sigma_+)$ into connected components called jigsaw pieces.

Theorem 2.21 (Generalised jigsaw transformation)**.** *Given the θ-stable A-module M_+, we may cut the corresponding fundamental hexagon* $\mathrm{Hex}(\sigma_+)$ *along the edges of c_- and rearrange the resulting jigsaw pieces (i.e., translate each piece by a carefully chosen element of $\mathbb{Z}^2$) in order to obtain* $\mathrm{Hex}(\sigma_-)$ *and hence produce the corresponding θ-stable A-module M_-.*

Figure 4 shows a tiling of $\mathbb{R}^2$ by translates of the fundamental hexagon associated to the cone with ray generators ρ_2, ρ_3 and ρ_7. This cone is adjacent to the cone which defines the fundamental hexagon from Figure 3.

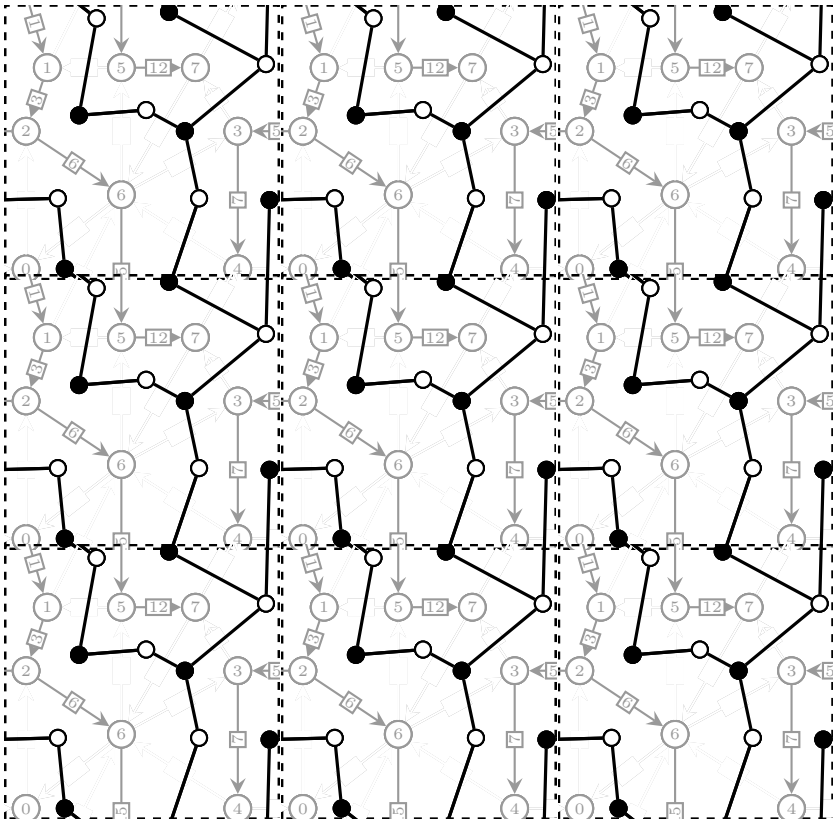

Figure 4: *A tiling of $\mathbb{R}^2$ by the fundamental hexagon of an adjacent cone*

Note that we obtain the fundamental hexagon from Figure 4 by splitting the fundamental hexagon from Figure 3 into two connected components, one containing the tile dual to the vertex 7 and the complement of this tile. By rearranging these tiles, i.e. choosing a different lift of the tile dual to the vertex 7 in the universal cover, we can obtain the fundamental hexagon from Figure 4.

In Chapter 3, we continue our study of jigsaw pieces. From this chapter onwards we assume Γ is a consistent dimer model and θ is a '0-generated' stability parameter. Every 0-generated stability parameter is generic. Among all jigsaw pieces of $\mathrm{Hex}(\sigma_-)$ and $\mathrm{Hex}(\sigma_-)$ we distinguish the zero jigsaw piece $\mathrm{Jig}_\tau(0)$ and the one jigsaw piece

$\mathrm{Jig}_\tau(1)$. Much of Section 3.2 is dedicated to showing that the one jigsaw piece $\mathrm{Jig}^+_\tau(1)$ of $\mathrm{Hex}(\sigma_+)$ coincides with the one jigsaw piece $\mathrm{Jig}^-_\tau(1)$ of $\mathrm{Hex}(\sigma_-)$ up to translation in the universal cover of Γ. More importantly, this implies that the 'sources' of the two subquivers $Q_+(\tau)$ and $Q_-(\tau)$ of the support of M_+ and M_-, as introduced in Definition 3.19, coincide. We use this last result to define Reid's recipe for interior line segments of Σ (see Definition 3.21). Reid's recipe for interior lattice points of Σ is defined using 'socles' in a way reminiscent of Craw–Ishii [CI04, Proposition 9.1] (see Definition 3.23). We show compatibility of combinatorial Reid's recipe with classical Reid's recipe:

Theorem 3.27 (**Reid's recipe for the G-Hilbert scheme**). *Let G be a finite abelian subgroup of $\mathrm{SL}(3,\mathbb{C})$ and let Σ be the fan of the G-Hilbert scheme. Reid's recipe for Σ as in Definitions 3.21 and 3.23 agrees with the classical recipe from Reid [Rei97] and Craw [Cra05].*

We also show that the marking of interior lattice points by vertices of Q according to Definition 3.23 is compatible with the geometric Reid's recipe for consistent dimer models as stated by Bocklandt–Craw–Quintero-Vélez [BCQV15, Theorem 1.4]:

Theorem 3.32 (**Geometric Reid's recipe for lattice points**). *Let $v \in Q_0$ be a nonzero vertex and let $\rho \in \Sigma(1)$ be an interior lattice point of the triangulation Σ. Then v marks ρ according to Reid's recipe if and only if the divisor D_ρ is contained in the support of the sheaf $\Psi(S_v)$.*

New phenomena can be observed in combinatorial Reid's recipe for consistent dimer models which did not appear in classical Reid's recipe: two vertices of Q can mark a single line segment; a vertex can mark more than one lattice point; and the recipe for lattice points is not determined purely by the shape of the incoming line segments and their markings. Section 3.6 computes geometric and combinatorial Reid's recipe for three examples depicting some of these interesting features.

In the example above, the one jigsaw piece consists of a single tile, the tile dual to the vertex 7, while the zero jigsaw piece contains every other tile of Γ. This is one of the simplest examples of a jigsaw transformation. The two subquivers $Q_+(\tau)$ and $Q_-(\tau)$ coincide in this case, they are the quiver with a single vertex, 7, and no arrows. Reid's recipe marks the common line segment to both cones by the 'sources' of the quiver $Q_+(\tau)$, in this case 7.

The aim of Chapters 4, 5 and 6 is to introduce an algorithm - the arrow contraction algorithm - which takes a consistent dimer model Γ to a new consistent dimer model Γ' such that for any 0-generated stability parameters θ and θ', the moduli space of θ'-stable A'-modules $\mathcal{M}_{A'}(\theta')$, for A' the Jacobian algebra of Q', is an open subvariety of $\mathcal{M}_A(\theta)$.

Chapter 4 motivates the arrow contraction algorithm. Section 4.1 introduces an example which illustrates many of the results presented in the remaining of the thesis. We then recall the tautological $\mathbb{C}$-algebra isomorphism $\phi\colon A \to \mathrm{End}_{\mathcal{O}_{\mathcal{M}_A(\theta)}}(T)$ between the Jacobian algebra A and the endomorphism algebra of the tautological bundle T of $\mathcal{M}_A(\theta)$. This isomorphism associates to each path p in Q a torus-invariant section $\phi(p) = x^{\mathrm{div}(p)}$ of the line bundle $L_{\mathsf{h}(p)} \otimes L^{-1}_{\mathsf{t}(p)}$, where the label on p is the torus-invariant

divisor $\mathrm{div}(p) = \sum_{a \in \mathrm{supp}(p)} \mathrm{div}(a) \in \mathbb{N}^{\Sigma(1)}$ on $\mathcal{M}_A(\theta)$. We prove that for any arrow α in Q with tail at vertex 0, there exists consecutive boundary divisors $D_1, D_2, \ldots, D_r$ such that $\mathrm{div}(\alpha) = D_1 + D_2 + \ldots + D_r$. We then associate to α a convex polygon Δ' and a fan $\Sigma' := \{\sigma \in \Sigma \mid \rho_i \nsubseteq \sigma \text{ for all } 1 \leq i \leq r\}$, where Σ denotes the toric fan of $\mathcal{M}_A(\theta)$. Finally, we show that for a consistent dimer model Γ dual to Q and θ 0-generated, the toric variety defined by Σ' is an open subvariety of $\mathcal{M}_A(\theta)$:

Theorem 4.8. *Suppose Δ' is a nondegenerate polygon. Let Y' denote the toric variety defined by the fan Σ' and let $\sigma' := \left\{\sum_{\lambda_\rho \geq 0} \lambda_\rho u_\rho \in N_{\mathbb{R}} \mid u_\rho \in \Delta'\right\}$ denote the cone over Δ'. Then:*

1. *Y' is the open subvariety of $\mathcal{M}_A(\theta)$ satisfying $Y' = \mathcal{M}_A(\theta) \setminus \mathrm{supp}(\mathrm{div}(\alpha))$;*
2. *Y' is a crepant resolution of the affine Gorenstein toric variety $U_{\sigma'}$.*

In the arrow contraction algorithm, Δ' will be the characteristic polygon of Γ', while Y' will be the moduli space $\mathcal{M}_{A'}(\theta')$, for θ' a 0-generated stability parameter. Lemma 4.9 gives the first link between combinatorial Reid's recipe and the toric fan of Y'.

In order to define Γ' we need to determine a subset of edges $\mathcal{S}_\alpha$ of Γ that will be removed. Chapter 5 defines the set $\mathcal{S}_\alpha$ in terms of the meandering walks of line segments in a strip of triangles $\mathrm{strip}(\alpha)$. Most of the results in this chapter assume a technical conjecture (Conjecture 5.7) about some of the edges in the meandering walks associated to the line segments between the triangles in the strip. Section 5.2 studies the behaviour of the meandering walks of Γ associated to all the line segments in $\mathrm{strip}(\alpha)$. It partitions two of them into subsets of edges linking trivalent nodes of the fundamental hexagons of the triangles in $\mathrm{strip}(\alpha)$. Each segment corresponds to a jump between two adjacent triangles in $\mathrm{strip}(\alpha)$, and the behaviour of the walks depends on whether the two triangles in $\mathrm{strip}(\alpha)$ are 'lower' or 'upper'. This understanding allows us to give two alternative characterisations of the edges in $\mathcal{S}_\alpha$ (see Proposition 5.15 and Theorem 5.16).

For any $\alpha \in Q_1$ with tail at vertex 0, Theorem 5.16 associates to some of the line segments in $\mathrm{strip}(\alpha)$ one or three of the edges in $\mathcal{S}_\alpha$. This result is key in proving that the dimer model obtained from Γ by removing the edges in $\mathcal{S}_\alpha$ is consistent. At the end of the chapter, we summarise all the information we have about the meandering walks of line segments in $\mathrm{strip}(\alpha)$ in a single diagram, called the circuit diagram of α. The circuit diagram also contains all the edges in $\mathcal{S}_\alpha$.

Chapter 6 makes use of the results from Chapters 4 and 5 to finally introduce the arrow contraction algorithm. We define a bicoloured graph Γ' associated to a consistent dimer model Γ and an arrow α in its dual quiver with tail at vertex 0. The bicoloured graph Γ' is obtained from Γ by removing the set of edges $\mathcal{S}_\alpha$. We need to assume another technical conjecture (Conjecture 6.4) about the cycles made by the arrows dual to the edges in $\mathcal{S}_\alpha$, in order to prove that Γ' is indeed a dimer model. Once this fact is established, we recall the definition of the zigzag polygon of a dimer model Γ, defined as the convex hull of points obtained using the homology classes of the zigzag paths of Γ. We make further use of the results from Chapter 5 to show that the zigzag polygon of Γ' is the convex polygon Δ' associated to the arrow α. Using a result by Gulotta [Gul08, Theorem 3.1], we prove the following:

Theorem 6.15. *Assume Conjectures 5.7 and 6.4. The dimer model Γ' is consistent.*

In a manner similar to that of Ishii–Ueda [IU09], we show that for 0-generated stability parameters θ and θ' there is an open immersion $j : \mathcal{M}_{A'}(\theta') \hookrightarrow \mathcal{M}_A(\theta)$ whose image is the complement of the support of $\mathrm{div}(\alpha)$. This leads to a geometric characterisations of the arrows dual to the edges in $\mathcal{S}_\alpha$ (see Corollary 6.19).
We are then ready to state the arrow contraction algorithm:

Algorithm 6.20 (The Arrow Contraction Algorithm)**.** *Let Γ be a consistent dimer model with dual quiver Q and Jacobian algebra A. We assume Γ has no bivalent nodes and Conjectures 5.7 and 6.4 hold for Γ.*

1. *Pick an arrow $\alpha \in Q_0$ with tail at vertex 0. By Proposition 4.6, we can associate to α a convex polygon Δ'. Assume α is such that Δ' is nondegenerate.*

2. *Find the set of edges $\mathcal{S}_\alpha$ using Definition 5.4 or either characterisations of the sets $\mathcal{S}_\alpha$ (see Proposition 5.15 and Theorem 5.16) or S_α (see Corollary 6.19).*

3. *Remove the edges in $\mathcal{S}_\alpha$ and all nodes of Γ connected only to edges in $\mathcal{S}_\alpha$ from Γ to obtain a new dimer model Γ' with characteristic polygon $\Delta(\Gamma') = \Delta'$.*

4. *The dimer model Γ' is consistent and for 0-generated stability parameters θ and θ', there exists an open immersion $\mathcal{M}_{A'}(\theta') \hookrightarrow \mathcal{M}_A(\theta)$, so that the toric fan of $\mathcal{M}_{A'}(\theta')$ is $\Sigma' := \{\sigma \in \Sigma \mid \rho_i \nsubseteq \sigma \text{ for all } 1 \leq i \leq r\}$, where Σ is the fan of $\mathcal{M}_A(\theta)$.*

5. *Since Γ' is consistent, and therefore nondegenerate, we may remove all bivalent nodes of Γ' without altering the number and direction of its zigzag paths or the Jacobian algebra of its dual quiver (see Remark 1.38).*

One can now repeat using Γ' and θ'.

The arrow contraction algorithm coincides with Ishii–Ueda's algorithm [IU09] in the special case when the 'label' of the arrow α is a torus-invariant prime divisor. We briefly discuss the connection between these two algorithms. In the last section of Chapter 5, we study the restrictions of the tautological bundle T of $\mathcal{M}_A(\theta)$ to weak toric Fano surfaces. Craw, King and (independently) Logvinenko observed that for some compact surfaces $Z \subset Y = G\text{-Hilb}(\mathbb{C}^3)$, the restriction of the tautological bundle, after removing all redundant summands, is tilting on Z. The arrow contraction algorithm gives a partial explanation for this phenomenon.

Theorem 6.22. *Let Γ be a consistent dimer model with Jacobian algebra A. If we can obtain a dimer model Γ' with Jacobian algebra A' from Γ by performing the arrow contraction algorithm such that $\mathcal{M}_{A'}(\theta')$ is the total space of the canonical bundle of a weak toric Fano surface Z, the restriction $\overline{\bigoplus}_{v \in Q_0} L_v|_Z$ of the tautological bundle T of $\mathcal{M}_A(\theta)$ to Z is tilting.*

It is not yet clear whether this is also a necessary condition. We give an example which suggests this might be the case.

Chapter 7 concludes this thesis by conjecturing a link between combinatorial Reid's recipe and the arrow contraction algorithm. The head and tail of the arrow or arrows associated to a line segment τ in strip(α) appear to coincide with the vertices that mark either τ or an endpoint ρ of τ or another line segment in strip(α) attached to ρ by Reid's recipe. We formulate a conjecture based on computational evidence (see Conjecture 7.1) and suggest how this conjecture could be used to show that in the labelling of Σ by Reid's recipe, every nonzero vertex of Q appears 'once' and that combinatorial Reid's recipe for consistent dimer models encodes the relations of the line bundles of $\mathcal{M}_A(\theta)$ in $\mathrm{Pic}(\mathcal{M}_A(\theta))$.

CHAPTER 1

PRELIMINARIES

The aim of this chapter is to provide a basic introduction to dimer models and moduli spaces of quiver representations. We start by defining dimer models as introduced by Hanany et al. [HK05] [FHK$^+$06]. We associate to each dimer model a quiver Q with relations $\mathcal{R}$ and a characteristic polygon $\Delta(\Gamma)$. We then review some classical toric geometry and present King's construction of the moduli space $\mathcal{M}_A(\theta, \underline{d})$ of θ-stable representations of Q with relations $\mathcal{R}$ of dimension vector $\underline{d}$. After introducing the nondegeneracy and consistency conditions for dimer models, we describe the link between Γ and $\mathcal{M}_A(\theta, \underline{d})$ in the case when θ is generic and $\underline{d} = \underline{1}$. Finally, we recall Reid's recipe as introduced by Reid for a special kind of dimer models whose associated quiver is the McKay quiver of G for some finite abelian subgroup G of $\mathrm{SL}(3, \mathbb{C})$.

1.1 Dimer models and their quivers with relations

We define a *graph* to be a triple $(\mathfrak{N}, \mathfrak{E}, \mathfrak{r})$ consisting of a set of nodes $\mathfrak{N}$, a set of edges $\mathfrak{E}$ and a relation $\mathfrak{r}$ that associates to every edge a pair of nodes called its *endnodes*. A graph is said to be *bipartite* if

1. the set of nodes $\mathfrak{N}$ is the union of two disjoint sets $\mathfrak{B}$ and $\mathfrak{W}$, and
2. every edge in $\mathfrak{E}$ has an endnode in $\mathfrak{B}$ and an endnode in $\mathfrak{W}$.

We may choose a colour for each of the disjoint sets of nodes $\mathfrak{B}$ and $\mathfrak{W}$. We will refer to nodes in $\mathfrak{B}$ as black nodes while nodes in $\mathfrak{W}$ will be called white nodes. A bipartite graph with a choice of colouring is a *bicoloured graph*. A black node is said to be *connected* to a white node (and vice versa) if there exists an edge in $\mathfrak{E}$ whose endnodes are the black and white nodes. Associate to any bicoloured graph a one-dimensional CW complex whose 0-cells are the nodes in $\mathfrak{N} = \mathfrak{B} \sqcup \mathfrak{W}$ and 1-cells the edges in $\mathfrak{E}$.

Let $\mathbb{T} := \mathbb{R}^2/\mathbb{Z}^2$ be the real two-torus. The torus $\mathbb{T}$ inherits an orientation from the standard orientation of $\mathbb{R}^2$. An *embedding* of a bicoloured graph $(\mathfrak{B}, \mathfrak{W}, \mathfrak{E})$ into the torus $\mathbb{T}$ is an injective continuous map from its associated one-dimensional CW

complex to the torus. When an embedding exists, we identify the nodes and edges of the bicoloured graph with their images under this map.

Definition 1.1. A *dimer model* is a bicoloured graph $\Gamma = (\mathfrak{B}, \mathfrak{W}, \mathfrak{E})$ embedded in $\mathbb{T}$ with the following two properties:

1. Γ has no univalent nodes, and
2. every connected component of $\mathbb{T} \setminus \mathfrak{E}$ is simply connected.

A *tile* of Γ is the closure of a connected component in $\mathbb{T} \setminus \mathfrak{E}$. In this way, Γ is a CW complex whose 0-cells are the black and white nodes of Γ, 1-cells the edges in $\mathfrak{E}$, and 2-cells its tiles, such that $|\Gamma| = \mathbb{T}$.

Definition 1.2. A *quiver* Q is the quadruple $(Q_0, Q_1, \mathsf{h}, \mathsf{t})$ consisting of a set of vertices Q_0, a set of arrows Q_1 and maps $\mathsf{h}, \mathsf{t} : Q_1 \to Q_0$ which give an orientation to its arrows. For $a \in Q_1$, we call $\mathsf{h}(a)$ the *head* of a and $\mathsf{t}(a)$ the *tail* of a.

A *path* p of length k ($k \geq 1$) in Q is a sequence of arrows $a_k a_{k-1} \cdots a_1$ with $\mathsf{h}(a_j) = \mathsf{t}(a_{j+1})$ for $1 \leq j \leq k-1$. The path has head $\mathsf{h}(p) := \mathsf{h}(a_k)$ and tail $\mathsf{t}(p) := \mathsf{t}(a_0)$. Every vertex $v \in Q_0$ also determines a path e_v called the *trivial path* of v with $\mathsf{h}(e_v) = \mathsf{t}(e_v) = v$. Trivial paths are said to be paths of length 0. A path p in Q is said to be a *cycle* if the head and tail of p coincide. A *relation* in Q is a non-zero $\mathbb{C}$-linear combination of paths of length at least two sharing a common head and a common tail. Let $\mathcal{R}$ be a set of relations in Q. We call $Q := (Q_0, Q_1, \mathsf{h}, \mathsf{t}, \mathcal{R})$ a *quiver with relations*.

Definition 1.3. The *path algebra* $\mathbb{C}Q$ of a quiver $Q = (Q_0, Q_1, \mathsf{h}, \mathsf{t})$ is the associative algebra whose underlying $\mathbb{C}$-vector space has basis the set of paths in Q. The trivial paths are orthogonal idempotent elements of $\mathbb{C}Q$, i.e.

$$e_v \cdot e_{v'} = \begin{cases} e_v & \text{if } v = v' \\ 0 & \text{otherwise} \end{cases}$$

Moreover, for any path p in Q, $e_{\mathsf{h}(p)} \cdot p \cdot e_{\mathsf{t}(p)} = p$. The product of any two paths p and p' is defined as concatenation when possible, and zero otherwise:

$$p \cdot p' = \begin{cases} pp' & \text{if } \mathsf{h}(p') = \mathsf{t}(p) \\ 0 & \text{otherwise} \end{cases} .$$

Every dimer model Γ encodes the information of a quiver with relations Q in the following way. Consider the dual tiling of the bicoloured graph Γ in $\mathbb{T}$. Tiles of Γ are dual to vertices which make the set Q_0. Edges in Γ are dual to arrows connecting vertices in Q_0. The choice of orientation of the arrows comes from the colouring of the graph Γ. Fix the convention that black vertices are to the left of every arrow, while white vertices are to the right.

To define the set of relations $\mathcal{R}$ of Q we introduce the superpotential W of a quiver Q. Let Q be the quiver dual to a dimer model Γ. A *face* F of Q is the closure of any connected component of the complement $\mathbb{T} \setminus Q_1$. We denote the set of faces of Q by Q_2. Faces of Q are dual to nodes of Γ. The fixed orientation means that arrows on

the boundary of faces dual to white nodes are oriented clockwise, while those around a face dual to a black node have an anticlockwise orientation. Consider the quotient $\mathbb{C}Q_{\text{cyc}} := \mathbb{C}Q/[\mathbb{C}Q, \mathbb{C}Q]$, where $[\mathbb{C}Q, \mathbb{C}Q]$ is the complex vector space spanned by all commutators in $\mathbb{C}Q$. The quotient $\mathbb{C}Q_{\text{cyc}}$ has basis corresponding to all cycles in Q up to cyclic shift. For any face $F \in Q_2$, the cycle of arrows around its boundary, denoted ∂F, is a basis element of $\mathbb{C}Q_{\text{cyc}}$. The *superpotential* W of Q is defined to be the element of $\mathbb{C}Q_{\text{cyc}}$ determined by the faces of Q in the following way:

$$W := \sum_{F \in Q_2} (-1)^F \partial F,$$

where $(-1)^F$ takes the value 1 when F is dual to a black node of Γ, and the value -1 when F is dual to a white node of Γ. The set of relations $\mathcal{R}$ of the quiver Q dual to Γ is the set $\left\{ \frac{\partial}{\partial a} W \mid a \in Q_1 \right\}$, where the map $\frac{\partial}{\partial a} : \mathbb{C}Q_{\text{cyc}} \to \mathbb{C}Q$ is defined for every basis element c of $\mathbb{C}Q_{\text{cyc}}$ to be

$$\frac{\partial}{\partial a} c = \begin{cases} p' & \text{if } \exists\ p \in \mathbb{C}Q \text{ such that } [p] = c \text{ and } p = p' \cdot a \\ 0 & \text{otherwise} \end{cases}.$$

Remark 1.4. Since every arrow $a \in Q_1$ appears only in two oppositely oriented faces F_+ and F_- of Q, we can write every relation in $\mathcal{R}$ as $p_+ - p_-$, where $p_\pm$ is the path around $F_\pm$ starting at $\mathsf{h}(a)$ and finishing at $\mathsf{t}(a)$.

Throughout this thesis we will only consider quivers which come from a dimer model, and thus have a superpotential W and a set of relations $\mathcal{R}$ associated to them.

Definition 1.5. The *Jacobian algebra* of a quiver Q with superpotential W and set of relations $\mathcal{R}$ is the quotient algebra

$$A := \mathbb{C}Q/I_{\mathcal{R}}$$

where $I_{\mathcal{R}}$ denotes the two-sided ideal of $\mathbb{C}Q$ generated by set of relations in $\mathcal{R}$.

Example 1.6. One of the simplest examples of a dimer model comes from the tiling of $\mathbb{R}^2$ by hexagons. The dashed lines in Figure 1.1 indicate a fundamental domain, and the induced CW complex on $\mathbb{T}$ is a dimer model that has one black node, one white node, three edges and one tile. The dual quiver Q of Γ is depicted in Figure 1.2. It has a single vertex v, three arrows, one white face F_+ and a black face F_-. The path algebra $\mathbb{C}Q$ is the free algebra $\mathbb{C}\langle a_1, a_2, a_3 \rangle$ generated by the elements a_1, a_2 and a_3 each corresponding to the arrows marked by $1, 2$ and 3, respectively. Note that the element $e_v \in \mathbb{C}Q$ is the identity. The superpotential of Q is

$$W = \partial F_+ - \partial F_- = a_1 a_2 a_3 - a_1 a_3 a_2.$$

The set of relations $\mathcal{R}$ has three elements

$$\frac{\partial}{\partial a_1} W = a_2 a_3 - a_3 a_2, \quad \frac{\partial}{\partial a_2} W = a_3 a_1 - a_1 a_3, \text{ and } \frac{\partial}{\partial a_3} W = a_1 a_2 - a_2 a_1.$$

Thus, the Jacobian algebra A of Q is $\mathbb{C}\langle a_1, a_2, a_3 \rangle / I_{\mathcal{R}} \cong \mathbb{C}[a_1, a_2, a_3]$ the polynomial

ring in three variables.

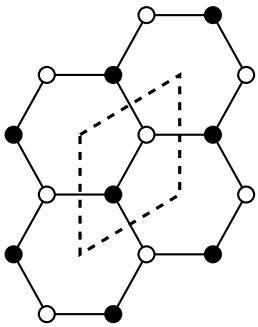

Figure 1.1: *A dimer model coming from the tiling of* $\mathbb{R}^2$ *by hexagons*

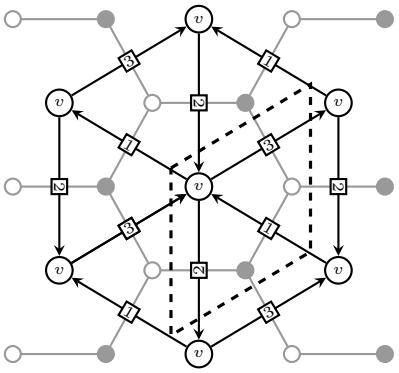

Figure 1.2: *The dual quiver to the dimer model coming from the tiling of* $\mathbb{R}^2$ *by hexagons*

In general, the Jacobian algebra of a quiver dual to a dimer model is noncommutative.

Example 1.7. Let G be a finite abelian subgroup of $\mathrm{SL}(3,\mathbb{C})$ of order r and let $\mathrm{Irr}(G)$ denote the set of irreducible representations of G. Since G is abelian, every irreducible representation is one-dimensional and the number of irreducible representations is the order of the group. The inclusion of G in $\mathrm{SL}(3,\mathbb{C})$ gives a three-dimensional representation which decomposes into irreducible representations $\varrho_1 \oplus \varrho_2 \oplus \varrho_3$. The *McKay quiver* Q of the subgroup G is the quiver with r vertices, one for each element of $\mathrm{Irr}(G)$. For every $\varrho \in \mathrm{Irr}(G)$, there is an arrow $a_i^{\varrho} \in Q_1$ with tail at vertex $\varrho\varrho_i$ $(1 \leq i \leq 3)$ and head at vertex ϱ. Every such quiver is dual to a dimer model with r hexagonal tiles [UY11]. The Jacobian algebra A of Q is isomorphic to the noncommutative skew group algebra $\mathbb{C}[x,y,z] * G$ [CMT07, Proposition 2.8].

Notation 1.8. Let Γ be a dimer model with dual quiver Q and let a be an arrow of Q. We write $\mathfrak{e}_a$ for the edge in Γ dual to a.

1.2 Perfect matchings and the characteristic polygon

A *perfect matching* of a bipartite graph $(\mathfrak{B},\mathfrak{W},\mathfrak{E})$ is a subset of edges $\Pi \subset \mathfrak{E}$ such that each node in $\mathfrak{B} \sqcup \mathfrak{W}$ is the endnode of precisely one edge in Π.

Definition 1.9. A dimer model $\Gamma = (\mathfrak{B},\mathfrak{W},\mathfrak{E})$ is *nondegenerate* if for every edge of $\mathfrak{E}$ there is a perfect matching Π of Γ containing it.

Remark 1.10. It is easy to verify whether a dimer model is nondegerate. Broomhead [Bro12, Remark 2.12] remarks that as a consequence of Hall's theorem a dimer model is nondegenerate if and only if $|\mathfrak{B}| = |\mathfrak{W}|$ and every proper subset of black nodes of size n is connected to at least $n+1$ white nodes, and vice versa. Broomhead refers to this condition as the *strong marriage condition*.

Following Ishii–Ueda [IU09, Section 4.2], we use perfect matchings to define the characteristic polygon $\Delta(\Gamma)$ associated to a dimer model Γ. The universal cover $\pi\colon \mathbb{R}^2 \to \mathbb{T}$ enables one to pull back a dimer model Γ to a bicoloured graph $\widetilde{\Gamma}$ on $\mathbb{R}^2$. We identify a perfect matching Π on Γ with its lift to a $\mathbb{Z}^2$-periodic perfect matching of $\widetilde{\Gamma}$. Fix a reference perfect matching Π_1. For any perfect matching Π, the union of $\Pi \cup \Pi_1$ splits $\mathbb{R}^2$ into connected components.

Definition 1.11. Define the *height function* h_{Π,Π_1} as a locally-constant function on $\mathbb{R}^2 \setminus (\Pi \cup \Pi_1)$ which increases by one when one crosses

(a) an edge $\mathfrak{e} \in \Pi_1$ with a black node on the right; or

(b) an edge $\mathfrak{e} \in \Pi$ with a white node on the right; and

decreases by one when one crosses

(a) an edge $\mathfrak{e} \in \Pi_1$ with a white node on the right; or

(b) an edge $\mathfrak{e} \in \Pi$ with a black node on the right.

The height function is determined up to the addition of a constant. We use the height function to define the *height change* $h(\Pi, \Pi_1) := (h_x(\Pi, \Pi_1), h_y(\Pi, \Pi_1)) \in \mathbb{Z}^2$ of the perfect matching Π with respect to Π_1 as follows

$$h_x(\Pi, \Pi_1) = h_{\Pi,\Pi_1}(p + (1,0)) - h_{\Pi,\Pi_1}(p)$$
$$h_y(\Pi, \Pi_1) = h_{\Pi,\Pi_1}(p + (0,1)) - h_{\Pi,\Pi_1}(p).$$

The height change does not depend on the choice of point $p \in \mathbb{R}^2 \setminus (\Pi \cup \Pi_1)$. Moreover, for any three perfect matchings Π, Π_1 and Π_2

$$h(\Pi, \Pi_2) = h(\Pi, \Pi_1) - h(\Pi_2, \Pi_1). \tag{1.2.1}$$

Height changes are elements of $\mathbb{Z}^2$ and thus can be considered as elements of the cohomology group $H^1(\mathbb{T}, \mathbb{Z}) \cong \mathbb{Z}^2$ of $\mathbb{T}$.

Definition 1.12. Define the *characteristic polygon* $\Delta(\Gamma)$ of a dimer model Γ to be the convex hull

$$\Delta(\Gamma) = \mathrm{Conv}\{h(\Pi, \Pi_1) \in \mathbb{Z}^2 \mid \Pi \text{ a perfect matching of } \Gamma\} \subset \mathbb{R}^2.$$

By equation (1.2.1), computing the characteristic polygon with a different choice of reference perfect matching results in a translation of the original characteristic polygon.

Example 1.13. As an example, consider the dimer model Γ in Figure 1.3 drawn together with its dual quiver Q.

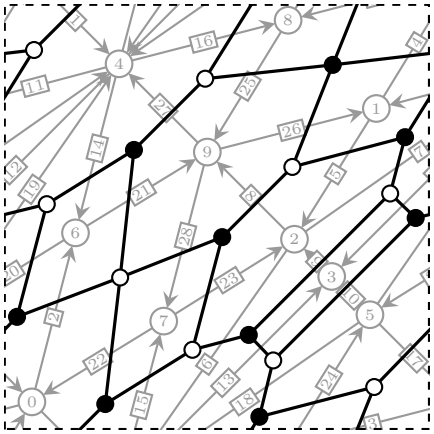

Figure 1.3: *A dimer model with its dual quiver*

The dimer model has sixty perfect matchings, listed in Table A.1 in Appendix A. Choose Π_1 as the reference perfect matching. Figure 1.4 shows the unions $\Pi_i \cup \Pi_1$ for $i = 2, 10, 11$. Edges in $\Pi_1 \setminus \Pi_i$ are coloured in grey. Using Figure 1.4 we can compute the height changes $h(\Pi_2, \Pi_1), h(\Pi_{10}, \Pi_1)$ and $h(\Pi_{11}, \Pi_1)$ as follows:

$$\begin{aligned} h(\Pi_2, \Pi_1) &= (0-0, (0+1)-0) = (0, 1) \\ h(\Pi_{10}, \Pi_1) &= ((0-1)-0, (0+2)-0) = (-1, 2) \\ h(\Pi_{11}, \Pi_1) &= ((0-1)-0, (0+2)-0) = (-1, 2) \end{aligned}$$

for a special choice of point p.

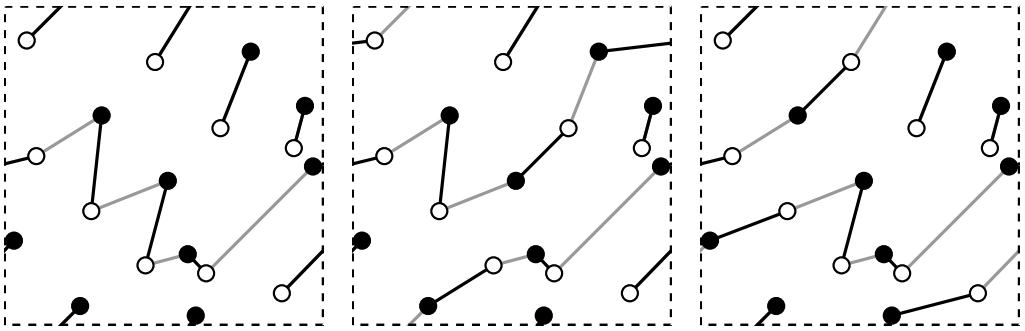

(a) $\Pi_2 \cup \Pi_1$ (b) $\Pi_{10} \cup \Pi_1$ (c) $\Pi_{11} \cup \Pi_1$

Figure 1.4: *The unions* $\Pi_i \cup \Pi_1$ *for* $i = 2, 10, 11$

Note that $h(\Pi_{10}, \Pi_1) = h(\Pi_{11}, \Pi_1)$. In general the height changes of any two perfect matchings may give the same lattice point $\rho \in \mathbb{Z}^2$. In fact, the sixty perfect matchings of Γ only give ten distinct lattice points (see Table A.1).

Figure 1.5 shows ten perfect matchings $\Pi_1, \Pi_2, \ldots, \Pi_{10}$ chosen so that their height changes are all different. Plotting the lattice points $h(\Pi_i, \Pi_1)$ $(1 \leq i \leq 10)$ and taking their convex hull gives the characteristic polygon $\Delta(\Gamma)$ of Γ, which in this case is the elongated hexagon depicted in Figure 1.6. For $1 \leq i \leq 10$, we mark the lattice point $h(\Pi_i, \Pi_1)$ in $\Delta(\Gamma)$ by i.

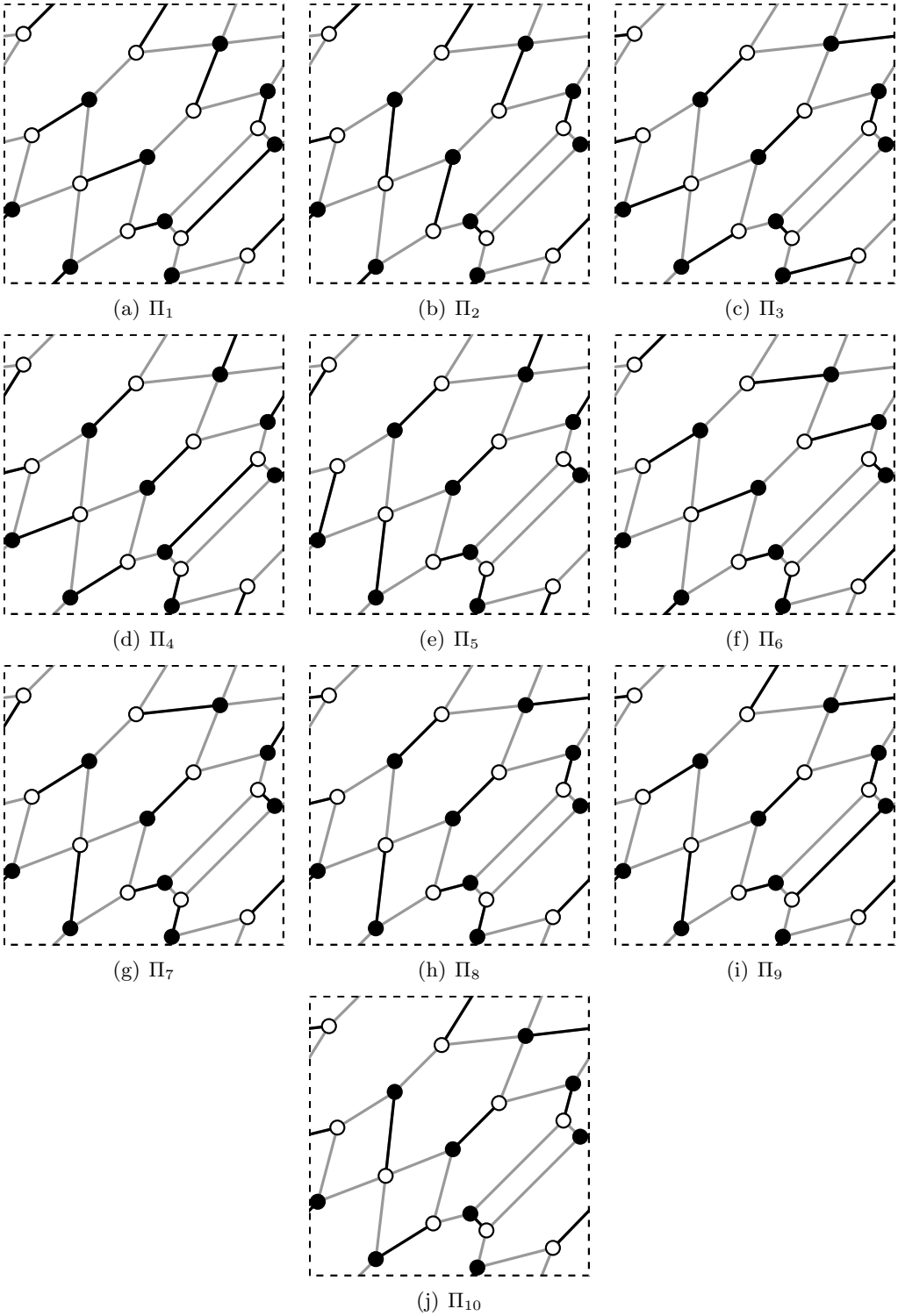

(a) Π_1 (b) Π_2 (c) Π_3

(d) Π_4 (e) Π_5 (f) Π_6

(g) Π_7 (h) Π_8 (i) Π_9

(j) Π_{10}

Figure 1.5: *Ten perfect matchings of the dimer model* Γ *in Figure 1.3*

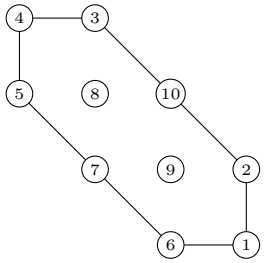

Figure 1.6: *Characteristic polygon* $\Delta(\Gamma)$ *of the dimer model* Γ *in Figure 1.3*

1.3 Toric varieties

We now recall some classical toric geometry as presented in [CLS11]. The theory begins with a (complex) algebraic *torus* T, which is an affine variety isomorphic to $\left(\mathbb{C}^\times\right)^n$ for some $n \in \mathbb{N}$. The torus T inherits a group structure from $\left(\mathbb{C}^\times\right)^n$. Write $M \cong \mathbb{Z}^n$ for the character lattice of T and $N := \mathrm{Hom}_{\mathbb{Z}}(M, \mathbb{Z})$ for its dual lattice.

Definition 1.14. An *affine toric variety* X is an irreducible normal affine variety that contains a torus T as a dense open subset such that the action of T on itself extends to an action on the whole of X.

Affine toric varieties can be encoded by means of cones in $N_{\mathbb{R}} := N \otimes \mathbb{R}$. A *polyhedral cone* in $N_{\mathbb{R}}$ is a subset $\sigma = \mathrm{Cone}(S) = \{\sum_{u \in S} \lambda_u u \mid \lambda_u \geq 0\} \subset N_{\mathbb{R}}$ for some $S \subset N$. For a polyhedral cone σ, the dual cone $\sigma^\vee := \{m \in M_{\mathbb{R}} \mid \langle m, u\rangle \geq 0 \; \forall u \in \sigma\}$ is a polyhedral cone in $M_{\mathbb{R}} := M \otimes \mathbb{R}$. A *face* of σ is $\tau = H_m \cap \sigma \subset N_{\mathbb{R}}$ where H_m is the hyperplane $\{u \in N_{\mathbb{R}} \mid \langle m, u\rangle = 0\}$ for some $m \in \sigma^\vee$. A face of a polyhedral cone is a polyhedral cone and the intersection of any two faces is a face. A polyhedral cone $\sigma = \mathrm{Cone}(S)$ is said to be *rational* if S is finite. It is *strongly convex* if the zero cone $\{0\} := \mathrm{Cone}(\emptyset)$ is a face of σ. The latter is equivalent to σ containing no positive-dimensional subspaces of $N_{\mathbb{R}}$. Given a rational polyhedral cone $\sigma \subset N_{\mathbb{R}}$, the subset $S_\sigma = \sigma^\vee \cap M \subset M$ forms a saturated semigroup.

Theorem 1.15. *Let* $\sigma \subset N_{\mathbb{R}}$ *be a rational polyhedral cone. Then,* $U_\sigma := \mathrm{Spec}(\mathbb{C}[S_\sigma])$ *is an affine toric variety. Moreover,* σ *is strongly convex if and only if* $T = N \otimes_{\mathbb{Z}} \mathbb{C}^\times$ *is the dense open torus of* U_σ*.*

We say a cone σ is smooth if and only if its minimal generators form part of a $\mathbb{Z}$-basis of N. When σ is a strongly convex rational polyhedral cone, U_σ is smooth if and only if σ is smooth. Note that if τ is a face of σ, there is a natural embedding $U_\tau \hookrightarrow U_\sigma$.

We can extend the definition of an affine toric variety by introducing the notion of fans.

Definition 1.16. A fan Σ in $N_{\mathbb{R}}$ is a collection of strongly convex rational polyhedral cones in $N_{\mathbb{R}}$ such that:

1. Every face of a cone in Σ is also a cone in Σ; and
2. The intersection of any two cones is a face of each one of them.

Write $\Sigma(i)$ for the set of all i-dimensional cones of Σ. Cones $\rho \in \Sigma(1)$ are called *rays*.

Define a *toric variety* X_Σ to be the variety covered by charts $U_\sigma = \operatorname{Spec}(\mathbb{C}[S_\sigma])$ for all cones $\sigma \in \Sigma$, where U_σ and $U_{\sigma'}$ are glued along the open subsets U_τ where τ is a common face of σ and σ'. The variety X_Σ is smooth if and only every cone σ of Σ is smooth. We will be particularly interested in toric varieties which are *semiprojective*. These are characterised as varieties of the form $\operatorname{Proj}(\mathbb{C}[S])$ for some $\mathbb{Z}$-graded semigroup algebra $\mathbb{C}[S]$. A semiprojective toric variety is said to be projective if the 0-graded piece $\mathbb{C}[S]_0 = \mathbb{C}$.

Recall that for every $\sigma \in \Sigma$, there is a bijective correspondence between points of $U_\sigma = \operatorname{Spec}(\mathbb{C}[S_\sigma])$ and semigroup homomorphisms $S_\sigma \to \mathbb{C}$ [CLS11, Proposition 1.3.1]. Define the *distinguished point* of U_σ to be the semigroup homomorphism $\gamma_\sigma : S_\sigma \to \mathbb{C}$ which sends an element $m \in S_\sigma$ to 1 if $m \in \sigma^\perp \cap M$ and to 0 otherwise. Now, consider the action of T on X_Σ. The point γ_σ determines a torus orbit $O(\sigma) = T \cdot \gamma_\sigma \subseteq X_\Sigma$.

Theorem 1.17 (The Orbit-Cone Correspondence)**.** *For a toric variety X_Σ with fan Σ in $N_\mathbb{R}$ there is a bijective correspondence between its set of cones and the set of T-orbits of X_σ given by $\sigma \to O(\sigma)$. If n is the dimension of T, $\dim O(\sigma) = n - \dim \sigma$. Moreover, for any cone σ of Σ, the affine open subset U_σ is the union $\bigcup_{\tau \text{ a face of } \sigma} O(\tau)$.*

Suppose X_Σ is a smooth toric variety. By the Orbit-Cone Correspondence, one-dimensional cones of Σ correspond to codimension one T-orbits in X_Σ. For every ray $\rho \in \Sigma(1)$, let D_ρ denote the T-invariant prime divisor $\overline{O(\rho)}$ on X_Σ, where the overline denotes the closure of the orbit. Write $u_\rho \in N$ for the primitive lattice point of ρ, and $d = |\Sigma(1)|$ for the number of T-invariant divisors of X_Σ. Since X_Σ is smooth, every Weil divisor is Cartier. Assume that the vectors $\{u_\rho \in N \mid \rho \in \Sigma(1)\}$ span $N_\mathbb{R}$, then we have the following short exact sequence:

$$0 \longrightarrow M \xrightarrow{\text{div}} \mathbb{Z}^d \xrightarrow{\deg} \operatorname{Pic}(X_\Sigma) \longrightarrow 0 \tag{1.3.1}$$

where $\mathbb{Z}^d$ is the lattice of all T-invariant Cartier divisors of X_Σ. The injective map $\text{div} : M \to \mathbb{Z}^d$ sends an element $m \in M$ to the divisor $\Sigma_{\rho \in \Sigma(1)} \langle m, u_\rho \rangle D_\rho$. The degree map $\deg : \mathbb{Z}^d \to \operatorname{Pic}(X_\Sigma)$ sends a Cartier divisor D to the invertible sheaf $\mathcal{O}_{X_\Sigma}(D)$. The *Cox ring* $S := \mathbb{C}[x_\rho \mid \rho \in \Sigma(1)]$ of the toric variety X_Σ is isomorphic to the semigroup algebra $\mathbb{N}^d$, the subsemigroup of $\mathbb{Z}^d$ consisting of effective torus-invariant Weil divisors on X_Σ. For any torus-invariant divisor $D = \sum_{\rho \in \Sigma(1)} a_\rho D_\rho \in \mathbb{Z}^d$ we write $x^D := \prod_{\rho \in \Sigma(1)} x_\rho^{a_\rho}$ for the corresponding Laurent monomial. For $L \in \operatorname{Pic}(X_\Sigma)$, the set of torus-invariant effective divisors on X_Σ satisfying $\mathcal{O}_{X_\Sigma}(D) \cong L$ is $\deg^{-1}(L) \cap \mathbb{N}^d$, so

$$H^0(X_\Sigma, \mathcal{O}_{X_\Sigma}(D)) = \bigoplus_{D \in \deg^{-1}(L) \cap \mathbb{N}^d} \mathbb{C} x^D.$$

In particular, every torus-invariant section of L is of the form x^D for some divisor $D \in \deg^{-1}(L) \cap \mathbb{N}^d$.

Recall the following definitions:

Definition 1.18. A normal toric variety is *Gorenstein* if its canonical divisor is Cartier.

Definition 1.19. Let X be an irreducible variety. A *resolution of singularities* of X is a proper morphism $f : Y \to X$ such that Y is smooth and irreducible and

$f^{-1}(X \setminus X_{\text{sing}}) \cong X \setminus X_{\text{sing}}$. If the morphism is projective, we say the resolution is *projective*. When X is a normal Gorenstein variety we say a resolution of singularities $f : Y \to X$ is *crepant* if $K_Y = f^*(K_X)$.

For a fan Σ in $N_{\mathbb{R}}$, we say Σ' is a refinement of Σ if every cone of Σ' is contained in a cone Σ and $\bigcup_{\sigma \in \Sigma'} \sigma = \bigcup_{\sigma \in \Sigma} \sigma$.

Theorem 1.20. *Every fan Σ has a refinement Σ' such that the morphism $f : X_{\Sigma'} \to X_\Sigma$ is a resolution of singularities.*

Let U_σ be a three-dimensional Gorenstein toric singularity, where σ has primitive ray generator $u_1, u_2, \ldots, u_k$. The Gorenstein condition means that there exists a monomial $m \in M$ such that $\langle m, u_i \rangle = 1$ for all $1 \leq i \leq k$, i.e. all u_i lie in a common hyperplane at height one. A smooth subdivision of σ into a fan Σ determines a crepant resolution X_Σ if the generators of all the subcones of Σ lie in the same hyperplane, i.e. if Σ is determined completely by a triangulation of the slice Δ of σ. We will abuse notation by identifying Σ with this triangulation of Δ. In particular, we identify:

(1) rays in the fan Σ with lattice points in the triangulation of Δ, typically denoted $\rho \in \Sigma(1)$;

(2) two-dimensional cones in the fan Σ with line segments in the triangulation of Δ, typically denoted $\tau \in \Sigma(2)$; and

(3) three-dimensional cones in the fan Σ with triangles in the triangulation of Δ, typically denoted $\sigma \in \Sigma(3)$.

Suppose X_Σ is a smooth three-dimensional toric variety. For any $\sigma \in \Sigma(3)$, $U_\sigma = \operatorname{Spec}(\mathbb{C}[\sigma^\vee \cap M]) \cong \operatorname{Spec} \mathbb{C}[t_1, t_2, t_3] \cong \mathbb{C}^3$. We can express t_1, t_2, t_3 as Laurent monomials in the variables of the Cox ring $S = \mathbb{C}[x_\rho \mid \rho \in \Sigma(1)]$ of X_Σ, as follows. Find the inner-pointing normal vectors to each of the three two-dimensional cones of σ. Each vector gives a lattice point in M. Using the injective map $\operatorname{div} : M \to \mathbb{Z}^d$ from the short exact sequence (1.3.1), we get a Cartier divisor $D = \Sigma_{\rho \in \Sigma(1)} a_\rho D_\rho$ for each lattice point. Finally, the monomial $x^D = \Pi_{\rho \in \Sigma(1)} x_\rho^{a_\rho} \in S$ defines a coordinate of σ for t_i.

Example 1.21. Let X_Σ be the smooth three-dimensional toric variety defined by the fan Σ in Figure 1.7. We compute the three coordinates for the cone $\sigma \in \Sigma(3)$ with ray generators ρ_8, ρ_9 and ρ_{10}. Choose coordinates for the lattice N so that

$$u_{\rho_8} = (-1, 1, 1), \quad u_{\rho_9} = (0, 0, 1) \text{ and } u_{\rho_{10}} = (1, 0, 1).$$

The inner pointing normal vectors to the three two-dimensional cones of σ are:

$$m_{8,9} = u_{\rho_8} \times u_{\rho_9} = (1, 1, 0),\ m_{9,10} = u_{\rho_9} \times u_{\rho_{10}} = (0, 1, 0),\ m_{10,8} = u_{\rho_{10}} \times u_{\rho_8} = (-1, -2, 1).$$

Using the injective map $\operatorname{div} : M \to \mathbb{Z}^d$ from the short exact sequence (1.3.1), we

associate to each of these vectors a divisor of X_Σ as follows:

$$\begin{aligned} D_{8,9} &= \sum_{\rho\in\Sigma(1)} \langle m_{8,9}, u_\rho\rangle D_\rho = \langle (1,1,0),(1,-1,1)\rangle D_{\rho_1} + \cdots + \langle (1,1,0),(0,1,1)\rangle D_{\rho_{10}} \\ &= D_{\rho_2} + D_{\rho_3} - D_{\rho_5} - D_{\rho_6} - D_{\rho_7} + D_{\rho_{10}} \\ D_{8,10} &= 2D_{\rho_1} + D_{\rho_2} - D_{\rho_3} - D_{\rho_4} + 2D_{\rho_6} + D_{\rho_7} + D_{\rho_9} \\ D_{9,10} &= -D_{\rho_1} - D_{\rho_2} + D_{\rho_3} + 2D_{\rho_4} + 2D_{\rho_5} + D_{\rho_7} + D_{\rho_8} \end{aligned}$$

The Laurent monomials

$$x^{D_{8,9}} = \frac{x_{\rho_2}x_{\rho_3}x_{\rho_{10}}}{x_{\rho_5}x_{\rho_6}x_{\rho_7}},\ x^{D_{8,10}} = \frac{x_{\rho_1}^2 x_{\rho_2} x_{\rho_6}^2 x_{\rho_7} x_{\rho_9}}{x_{\rho_3}x_{\rho_4}},\ \text{and } x^{D_{9,10}} = \frac{x_{\rho_3} x_{\rho_4}^2 x_{\rho_5}^2 x_{\rho_7} x_{\rho_8}}{x_{\rho_1}x_{\rho_2}}$$

give the three coordinates of the chart $U_\sigma \cong \mathbb{C}^3$ in terms of the variables of the Cox ring of X_Σ.

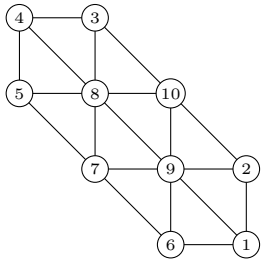

Figure 1.7: *The fan Σ encoding a crepant resolution of X*

1.4 Quiver representations and their moduli spaces

Let $Q = (Q_0, Q_1, \mathsf{h}, \mathsf{t})$ be a quiver. A *representation* W of a quiver Q over $\mathbb{C}$ consists of a collection of complex vector spaces W_v, one for each vertex $v \in Q_0$, and a $\mathbb{C}$-linear map $\phi_a : W_{\mathsf{t}(a)} \to W_{\mathsf{h}(a)}$ for each arrow $a \in Q_1$. More compactly, we write $W = \left(\bigoplus_{v\in Q_0} W_v, \{\phi_a\}_{a\in Q_1}\right)$. A representation is said to be *finite-dimensional* if for all $v \in Q_0$, W_v is a finite-dimensional vector space. The dimension vector of a finite-dimensional representation is the nonnegative tuple $\underline{d} = (\dim W_v)_{v\in Q_0}$. For any two representations W, W' of the quiver Q, a morphism $g : W \to W'$ consists of a $\mathbb{C}$-linear map $g_v : W_v \to W'_v$ for each vertex $v \in Q_0$, such that for all arrows $a \in Q_1$, the following diagram commutes:

$$\begin{array}{ccc} W_{\mathsf{t}(a)} & \xrightarrow{\phi_a} & W_{\mathsf{h}(a)} \\ {\scriptstyle g_{\mathsf{t}(a)}}\downarrow & & \downarrow{\scriptstyle g_{\mathsf{h}(a)}} \\ W'_{\mathsf{t}(a)} & \xrightarrow{\phi'_a} & W'_{\mathsf{h}(a)} \end{array}$$

The morphism $g : W \to W'$ is said to be an *isomorphism* of quiver representations if and only if for all $v \in Q_0$ the map g_v is an isomorphism of vector spaces.

Define $\mathrm{Rep}(Q)$ to be the category whose objects are representations of the quiver Q and morphisms are the morphism between quiver representations. Let $\mathrm{Mod}-\mathbb{C}Q$ denote the category of left $\mathbb{C}Q$-modules. We use lower case to denote the category $\mathrm{rep}(Q)$ of finite-dimensional representations of Q and the category $\mathrm{mod}-\mathbb{C}Q$ of finite-dimensional left $\mathbb{C}Q$-modules. The following is a well-known result:

Proposition 1.22. *[ASS06, Theoreom III 1.6] There is an equivalence of categories* $\mathrm{Rep}(Q) \cong \mathrm{Mod}-\mathbb{C}Q$ *which restricts to an equivalence* $\mathrm{rep}(Q) \cong \mathrm{mod}-\mathbb{C}Q$ *between the categories of finite-dimensional representations of* Q *and finite-dimensional left* $\mathbb{C}Q$*-modules.*

Proof. We first define a functor from $\mathrm{Mod}-\mathbb{C}Q$ to $\mathrm{Rep}(Q)$ on objects. Given a left $\mathbb{C}Q$-module M with module structure $\mu\colon \mathbb{C}Q \times M \to M$, we obtain $\mathbb{C}$-linear maps $\phi_{e_v}\colon M \to M$ satisfying $\phi_{e_v}(m) = \mu(e_v, m)$ for all $v \in Q_0$. Set $W_v := \phi_{e_v}(M)$. Note that $W_v \cap W_v' = \{0\}$ for $v \neq v'$ as $e_v \cdot e_v' = 0$. Similarly, each $a \in Q_1$ defines a $\mathbb{C}$-linear map $\phi_a\colon M \to M$ satisfying $\phi_a(m) = \mu(a, m)$, and the diagram

$$\begin{array}{ccc} M & \xrightarrow{\phi_a} & M \\ {\scriptstyle \phi_{e_{\mathsf{t}(a)}}}\downarrow & & \downarrow{\scriptstyle \phi_{e_{\mathsf{h}(a)}}} \\ M & \xrightarrow{\phi_a} & M \end{array}$$

commutes, so in fact $\phi_a\colon W_{\mathsf{t}(a)} \to W_{\mathsf{h}(a)}$. Thus, M determines a quiver representation $W = \left(\bigoplus_{v\in Q_0} W_v, \{\phi_a\}_{a\in Q_1}\right)$ of Q. One can extend this assignment to morphisms, giving the required functor.

Now we define a functor on objects in the opposite direction. Given a representation $W = (\bigoplus_{v\in Q_0} W_v, \{\phi_a\}_{a\in Q_1})$, set $M := \bigoplus_{v\in Q_0} W_v$. For $v \in Q_0$ define first a $\mathbb{C}Q_0$-module structure $\mu\colon \mathbb{C}Q_0 \times M \to M$ by setting $\mu(e_v, m) = m$ for all $m \in W_v$ and $\mu(e_v, m) = 0$ otherwise. Next, for $a \in Q_1$ and $m \in M$, define $\mu(a, m) = \phi_a(m)$ if $m \in W_{\mathsf{t}(a)}$ and $\mu(a, m) = 0$ otherwise. Every nontrivial path is a composition of arrows, so we obtain the required module structure $\mu\colon \mathbb{C}Q \times M \to M$ that makes M into a left $\mathbb{C}Q$-module. Again, this assignment extends to morphisms, and it is easy to see that these operations are inverse.

For the second statement, note that the functors above take finite-dimensional representations of Q to finite-dimensional left $\mathbb{C}Q$-modules, and vice versa. Therefore, the restrictions of the functors to finite-dimensional object give the second equivalence. □

A representation of a quiver Q with relations $\mathcal{R}$ is defined to be a representation $W = \left(\bigoplus_{v\in Q_0} W_v, \{\phi_a\}_{a\in Q_1}\right)$ with the added condition that the linear maps $\{\phi_a\}_{a\in Q_1}$ satisfy the relations $\mathcal{R}$. Define $\mathrm{Rep}(Q, \mathcal{R})$ to be the category of representations of the quiver Q with relations $\mathcal{R}$. Let $\mathrm{rep}(Q, \mathcal{R})$ denote the category of finite-dimensional representations of the quiver Q with relations $\mathcal{R}$. The equivalences of categories in Proposition 1.22 translate into

$$\mathrm{Rep}(Q, \mathcal{R}) \cong \mathrm{Mod}-A \text{ and } \mathrm{rep}(Q, \mathcal{R}) \cong \mathrm{mod}-A$$

for $A = \mathbb{C}Q/I_{\mathcal{R}}$.

Following King [Kin94], we now present the construction of the fine moduli space of quiver representations of Q with dimension vector $\underline{d}$. We first recall some standard definitions and results from Geometric Invariant Theory (GIT) [MFK94].

Let G be a linearly reductive group acting algebraically on an affine variety $X = \mathrm{Spec}(R)$. The set of *G-orbits* of X is $X/G = \{G \cdot x \mid x \in X\}$. For $g \in G$, the morphism $\varphi_g : X \to X$ defining the action of g on X comes from a homomorphism $\varphi_g^* : R \to R$. Therefore, the action of G on X induces an action on R defined for $f \in R$ by $g \cdot f = \varphi_{g^{-1}}^*(f)$. This action determines the *ring of invariants* $R^G = \{f \in R \mid g \cdot f = f \text{ for all } g \in G\}$. As G is linearly reductive, R^G is finitely generated as a $\mathbb{C}$-algebra and $\mathrm{Spec}\big(R^G\big)$ is an affine variety.

Definition 1.23. The map $\pi : X \to Y$ is a *good categorical quotient* of X by G if:

(i) For any open set $V \subset Y$, the map $\mathcal{O}_Y(V) \to \mathcal{O}_X(\pi^{-1}(V))$ induces an isomorphism $\mathcal{O}_Y(V) \cong \mathcal{O}_X(\pi^{-1}(V))^G$;

(ii) For any G-invariant closed set $U \subset X$, $\pi(U)$ is closed; and

(iii) For any two disjoint G-invariant closed sets $U, U' \subset X$, $\pi(U) \cap \pi(U') = \emptyset$.

We write $\pi : X \to X/\!\!/G$ for a good categorical quotient of X by G. Good categorical quotients satisfy the following properties:

Proposition 1.24. *Let $\pi : X \to X/\!\!/G$ be a good categorical quotient of X by G. Then:*

(i) The map π is surjective;

(ii) For any two points $x, y \in X$

$$\pi(x) = \pi(y) \iff \overline{G \cdot x} \cap \overline{G \cdot y} \neq \emptyset,$$

where the overline denotes the closure of the orbits.

Definition 1.25. A *geometric quotient* of X by G is a good categorical quotient $\pi : X \to X/\!\!/G$ that satisfies the following equivalent conditions:

(i) All G-orbits are closed in X;

(ii) $X/\!\!/G$ is a G-orbit space, i.e. π induces a bijection $\{G-\text{orbits of } X\} \cong X/\!\!/G$; and

(iii) For any two points $x, y \in X$

$$\pi(x) = \pi(y) \iff x \text{ and } y \text{ lie in the same } G\text{-orbit.}$$

Let $\chi : G \to \mathbb{C}^\times$ be a character of G. We say $f \in R$ is a *χ-semi-invariant* function if for all $x \in X$ and $g \in G$

$$f(g \cdot x) = \chi(g) f(x).$$

Let R_χ denote the complex vector space of all χ-semi-invariant functions.

Definition 1.26. The *GIT quotient* of X by G corresponding to χ is the semiprojective variety $X/\!\!/_\chi G := \mathrm{Proj}\big(\bigoplus_{n \geq 0} R_{\chi^n}\big)$.

Note that when $\chi = 0$, $X/\!\!/_0 G = \operatorname{Spec}\big(R^G\big)$. The GIT quotient $X/\!\!/_\chi G$ is projective over $\operatorname{Spec}\big(R^G\big)$, the degree zero part of the graded ring.

We define the semistable and stable loci $X^{ss}(\chi)$ and $X^s(\chi)$ of X with respect to χ as follows:

$$X^{ss}(\chi) := \{x \in X \mid \exists\, n \geq 1 \text{ and } f \in R_{\chi^n} \text{ with } f(x) \neq 0\}$$
$$X^s(\chi) := \{x \in X^{ss}(\chi) \mid G \cdot x \text{ is closed in } X^{ss}(\chi) \text{ and } G_x \text{ is finite}\},$$

where $G_x := \{g \in G \mid g \cdot x = x\}$ is the *stabiliser* of x by G.

Proposition 1.27. *Let $X/\!\!/_\chi G$ be the GIT quotient of X by G corresponding to χ. Then:*

(i) The map $\pi : X^{ss}(\chi) \to X/\!\!/_\chi G$ is a good categorical quotient of $X^{ss}(\chi)$ by G; and

(ii) The open subset $X^s(\chi) \subseteq X^{ss}(\chi)$ gives a geometric quotient $\pi : X^s(\chi) \to X/G \subset X/\!\!/_\chi G$.

Now, let Q be a quiver, fix a dimension vector $\underline{d} := (d_v)_{v \in Q_0}$ and let $W_v = \mathbb{C}^{d_v}$. The set of all representations of Q with vector spaces W_v $(v \in Q_0)$

$$\operatorname{Rep}(Q, \underline{d}) = \bigoplus_{a \in Q_1} \operatorname{Hom}\big(W_{\mathsf{t}(a)}, W_{\mathsf{h}(a)}\big)$$

is an affine space. The group $\mathfrak{G} := \prod_{v \in Q_0} \operatorname{GL}(d_v, \mathbb{C})$ acts on $\operatorname{Rep}(Q, \underline{d})$ by conjugation:

$$(g_v)_{v \in Q_0} \cdot (\phi_a)_{a \in Q_1} = (g_{\mathsf{h}(a)} \phi_a g_{\mathsf{t}(a)}^{-1})_d a \in Q_1.$$

$\operatorname{Rep}(Q, \underline{d})$ contains an affine subscheme $\mathbb{V}_{\mathcal{R}}$ consisting of those representations of Q with dimension vector $\underline{d}$ that satisfy the relations $\mathcal{R}$.

Consider the rational vector space

$$\Theta := \left\{ \theta \in \operatorname{Hom}\big(\mathbb{Z}^{Q_0}, \mathbb{Q}\big) \;\middle|\; \sum_{v \in Q_0} \theta_v d_v = 0 \right\}.$$

For any representation $W \in \operatorname{Rep}(Q, \underline{d})$ define $\theta(W) := \theta(\underline{d})$. Any $\theta \in \Theta$ determines a fractional character χ_θ of $\mathfrak{G}$ by $\chi_\theta(g) := \prod_{v \in Q_0} \det(g_v)^{\theta_v}$.

Definition 1.28. A representation $W \in \operatorname{Rep}(Q, \underline{d})$ is said to be *θ-semistable* (resp. *θ-stable*) if and only if $\theta(W) = 0$ and $\theta(W') \geq 0$ (resp. $\theta(W') > 0$) for every nonzero proper subrepresentation $W' \subset W$. A parameter $\theta \in \Theta$ is said to be *generic* if every θ-semistable representation is also θ-stable.

Definition 1.29. Two θ-semistable representations W, W' of Q are said to be *S-equivalent* if their composition series of θ-stable representations have the same composition factors.

King [Kin94] showed that the notion of θ-semistability (resp. θ-stability) for a representation W coincides with the notion of χ_θ-semistability (resp. χ_θ-stability) for the corresponding point $[W] \in \operatorname{Rep}(Q, \underline{d})$. Moreover:

Proposition 1.30. *Let R denote the coordinate ring of the affine scheme $\mathbb{V}_{\mathcal{R}}$. Then for $\theta \in \Theta$:*

(i) The scheme

$$\mathcal{M}_A(\theta, \underline{d}) := \operatorname{Proj}\left(\bigoplus_{n\geq 0} R_{\chi_\theta^n}\right)$$

is a coarse moduli space of θ-semistable representations of Q with dimension vector $\underline{d}$ up to S-equivalence;

(ii) The scheme $\mathcal{M}_A(\theta, \underline{d})$ is projective over $\mathbb{V}_{\mathcal{R}} /\!\!/_0 \mathfrak{G}$; and

(iii) When θ is generic and $\underline{d}$ is primitive, $\mathcal{M}_A(\theta, \underline{d})$ is the fine moduli space of isomorphism classes of θ-stable representations of Q with dimension vector $\underline{d}$.

Notation 1.31. We will be interested in the representations of a quiver Q with relations $\mathcal{R}$ with dimension vector $\underline{1}$. In light of Proposition 1.22, henceforth we use θ-stable A-modules to refer to θ-stable representations of Q with dimension vector $\underline{1}$ satisfying the relations $\mathcal{R}$ of Q. When θ is generic, we write $\mathcal{M}_A(\theta) := \mathcal{M}_A(\theta, \underline{1})$ for the fine moduli space of θ-stable A-modules.

As $\mathcal{M}_A(\theta)$ is the fine moduli space of θ-stable A-modules, it carries a universal family

$$T = \bigoplus_{v \in Q_0} L_v(\theta)$$

called the tautological bundle of $\mathcal{M}_A(\theta)$, and a tautological $\mathbb{C}$-algebra homomorphism

$$\phi : A \to \operatorname{End}_{\mathcal{O}_{\mathcal{M}_A(\theta)}}(T).$$

Choose a vertex $0 \in Q_0$ and set $L_0 \cong \mathcal{O}_{\mathcal{M}_A(\theta)}$. For a point $y \in \mathcal{M}_A(\theta)$, let $\iota : \{y\} \hookrightarrow \mathcal{M}_A(\theta)$ be its closed immersion. The tautological bundle T on $\mathcal{M}_A(\theta)$ pulls back to $\bigoplus_{v\in Q_0} W_v$, and the maps $\{L_{\mathsf{t}(a)}(\theta) \to L_{\mathsf{h}(a)}(\theta) \mid a \in Q_1\}$ restrict to maps $\{\varphi_a : W_{\mathsf{t}(a)} \to W_{\mathsf{h}(a)} \mid a \in Q_1\}$ that determine a θ-stable A-module $M_y(\theta)$.

Definition 1.32. For any point $y \in \mathcal{M}_A(\theta)$, define $M_y(\theta)$ to be the *θ-stable A-module parametrised by y*, which is the fibre of the tautological bundle T.

Ishii–Ueda studied the moduli space $\mathcal{M}_A(\theta)$ for the case when Q is the dual quiver to a nondegenerate dimer model Γ. Theorem 1.33 summarises some of their results (see [IU08, Proposition 5.1, Proposition 6.3, Theorem 6.4]).

Theorem 1.33. *Let Γ be a nondegenerate dimer model and suppose θ is generic. The moduli space $\mathcal{M}_A(\theta)$ is a crepant resolution of $X := \operatorname{Spec}\big(\mathbb{C}[\sigma^\vee \cap M]\big)$ where σ the cone over the characteristic polygon $\Delta(\Gamma)$.*

Example 1.34. Let $G \subset \mathrm{SL}(3, \mathbb{C})$ be a finite abelian subgroup and write Γ for its corresponding dimer model (see Example 1.7). Recall that $Q_0 = \operatorname{Irr}(G)$ and let $v_0 \in Q_0$ denote the trivial representation. For any stability parameter $\theta = (\theta_v) \in \Theta$ satisfying $\theta_v > 0$ for $v \neq v_0$, the moduli space $\mathcal{M}_A(\theta)$ coincides with the G-Hilbert scheme introduced by Nakamura [Nak01].

Example 1.35. Recall the dimer model Γ introduced in Example 1.13. The parameter $\theta = (-9, 1, 1, \ldots, 1)$ is generic (see Lemma 3.2) and the fine moduli space of θ-stable A-modules is the three-dimensional toric variety encoded by the fan Σ in Figure 1.7.

1.5 Zigzag paths and the consistency condition

We now introduce the notion of a zigzag path which is key in the definition of a consistent dimer model.

Definition 1.36. A *zigzag path* on a bicoloured graph $(\mathfrak{B}, \mathfrak{W}, \mathfrak{E})$ in an oriented surface is a path which turns maximally right at white nodes and maximally left at black nodes.

Zigzag paths are either periodic or infinite. We parametrise a zigzag path $\mathfrak{z}$ in an oriented surface by a map $\gamma_{\mathfrak{z}} : \mathbb{Z} \to \mathfrak{E}$ satisfying the following two conditions:

(i) For all $i \in \mathbb{Z}$, $\mathsf{h}(\gamma_{\mathfrak{z}}(i)) = \mathsf{t}(\gamma_{\mathfrak{z}}(i+1))$; and

(ii) The path $\mathfrak{z}$ turns maximally right at $\mathsf{h}(\gamma_{\mathfrak{z}}(2i))$ and maximally left at $\mathsf{h}(\gamma_{\mathfrak{z}}(2i+1))$.

The following definition is independent of the choice of parametrisation $\gamma_{\mathfrak{z}}$ as defined above.

Definition 1.37. An edge $\mathfrak{e}$ of a zigzag path $\mathfrak{z}$ is called a *zig* (resp. *zag*) of $\mathfrak{z}$ if $\mathfrak{e}$ is the image of and even (resp. odd) integer under the map $\gamma_{\mathfrak{z}}$.

Any edge $\mathfrak{e}$ of a bicoloured graph in an oriented surface determines at most two zigzag paths, depending on whether $\mathfrak{e}$ is a zig or a zag edge. We denote these paths by $\mathrm{zig}(\mathfrak{e})$ and $\mathrm{zag}(\mathfrak{e})$, respectively.

Two infinite zigzag paths in a bicoloured graph $(\mathfrak{B}, \mathfrak{W}, \mathfrak{E})$ are said to *intersect* if and only if they share an odd number of consecutive edges in $\mathfrak{E}$. Suppose two infinite zigzag paths $\mathfrak{z}$ and $\mathfrak{z}'$ intersect each other twice and let $\mathfrak{e}$ and $\mathfrak{e}'$ be edges in the two different intersections. We say the pair $\mathfrak{z}$ and $\mathfrak{z}'$ *intersect each other more than once in the same direction* if and only if either $\gamma_{\mathfrak{z}}(\mathfrak{e}) < \gamma_{\mathfrak{z}}(\mathfrak{e}')$ and $\gamma_{\mathfrak{z}'}(\mathfrak{e}) < \gamma_{\mathfrak{z}'}(\mathfrak{e}')$ or $\gamma_{\mathfrak{z}}(\mathfrak{e}) > \gamma_{\mathfrak{z}}(\mathfrak{e}')$ and $\gamma_{\mathfrak{z}'}(\mathfrak{e}) > \gamma_{\mathfrak{z}'}(\mathfrak{e}')$. Two zigzag paths are said to *share a common node* $\mathfrak{n}$ if and only if they both pass through the node $\mathfrak{n}$.

Remark 1.38. If a node of a dimer model is bivalent and its edges have only it as a common node, it is possible to remove the bivalent node to produce a new dimer model. When Γ is a nondegenerate dimer model, any bivalent node must be connected to two distinct nodes, as otherwise Γ would not satisfy the strong marriage condition introduced in Remark 1.10. Moreover, if Γ' is a dimer model obtained from a nondegenerate dimer model Γ by removing its bivalent nodes, the Jacobian algebra of the quiver dual to Γ is isomorphic to the Jacobian algebra of the quiver dual to Γ'. There also exists a natural bijection between the set of zigzag paths of Γ and Γ' (see [Bro12, Section 2.1.5] and [IU09, Section 5.1]). Note that if the bicoloured graph has no bivalent nodes, two zigzag paths intersect if and only if they share an edge.

Assumption 1.39. *In light of Remark 1.38, we will assume throughout this thesis that every nondegenerate dimer model has no bivalent nodes.*

Let $\mathfrak{z}$ be a zigzag path in Γ. Since Γ is a bicoloured graph embedded in the torus $\mathbb{T}$, zigzag paths are periodic.

Definition 1.40. The *slope* of a zigzag path is its homology class $[\mathfrak{z}] \in H_1(\mathbb{T}, \mathbb{Z}) \cong \mathbb{Z}^2$.

The set of slopes $(u, v) \in \mathbb{Z}^2$ of zigzag paths of Γ which are not homologically trivial has a natural cyclic order when thought of as elements of the unit circle

$$\frac{(u, v)}{\sqrt{u^2 + v^2}} \in S^1.$$

Similarly, every node in Γ has a natural cyclic order given by the directions of the outgoing paths passing through the node. The following consistency condition for a dimer model, first introduced by Gulotta [Gul08], requires both these natural cyclic orders to coincide:

Definition 1.41. A dimer model Γ is said to be *properly-ordered* if

1. no zigzag path of Γ is homologically trivial;
2. no zigzag path of Γ intersects itself on the universal cover;
3. two zigzag paths of Γ with the same homology class do not share a common node; and
4. for every node of Γ, the natural cyclic order of the zigzag paths passing through it coincides with the natural cyclic order determined by their slopes.

Ishii–Ueda [IU11b, Definition 3.5] introduced the following consistency condition for dimer models:

Definition 1.42. A dimer model Γ is said to be *consistent* if

1. no zigzag path of Γ is homologically trivial;
2. no zigzag path of Γ intersects itself on the universal cover; and
3. no pair of zigzag paths on the universal cover intersect each other more than once in the same direction.

Ishii–Ueda's consistency condition is equivalent to Gulotta's properly-ordered condition:

Proposition 1.43. *[IU11b, Lemmata 4.2, 4.3] A dimer model Γ is properly-ordered if and only if Γ is consistent.*

Remark 1.44. There are several notions of consistency for dimer models in the literature. Broomhead [Bro12, Definition 5.12] introduced a notion of algebraic consistency, which by results of Bocklandt [Boc12] and Ishii–Ueda [IU11b] is equivalent to Ishii–Ueda's consistency condition. We shall not define Broomhead's notion of algebraic consistency as we do not use it except in Proposition 1.47 below.

Let Γ be a dimer model and let $\{\mathfrak{z}_1, \mathfrak{z}_2, \ldots, \mathfrak{z}_k\}$ be the set of all zigzag paths in Γ. We can assume that the zigzag paths $\mathfrak{z}_1, \mathfrak{z}_2, \ldots, \mathfrak{z}_k$ are ordered cyclically anticlockwise starting from a randomly chosen zigzag path $\mathfrak{z}_1$. We now define a sequence $(b_i)_{i=1}^k$ of elements of $\mathbb{Z}^2$ by setting $b_0 = (0,0)$ and $b_{i+1} = b_i + [\mathfrak{z}_{i+1}]'$ $(0 \leq i \leq k-1)$ where $[\mathfrak{z}_{i+1}]'$ denotes the vector normal to $[\mathfrak{z}_{i+1}]$ obtained by rotating $[\mathfrak{z}_{i+1}]$ by 90 degrees in the positive direction. If every edge in Γ appears in two distinct zigzag paths, once as a zig and once as a zag, we have $b_k = (0,0)$ and we can define the zigzag polygon of Γ as follows.

Definition 1.45. The *zigzag polygon* is the convex hull of the set of points $\{b_1, b_2, \ldots, b_k\}$.

The following is a result of Gulotta [Gul08, Theorem 3.3] and Ishii–Ueda [IU09, Theorem 11.1]:

Theorem 1.46. *For a consistent dimer model Γ, the characteristic polygon of Γ coincides with the zigzag polygon of Γ up to translation.*

Consistency is a stronger condition for a dimer model than nondegeneracy. Indeed, Broomhead [Bro12, Definition 3.2] defines consistency for a dimer model as a strengthening of the nondegeneracy condition. Ishii–Ueda [IU09, Proposition 7.1] also showed that a consistent dimer model is non-degenerate. Broomhead [Bro12] proved the following result for consistent dimer models:

Proposition 1.47. *Let Γ be a consistent dimer model with dual quiver Q. The centre $Z(A)$ of the Jacobian algebra A of Q is isomorphic to the Gorenstein semigroup algebra $\mathbb{C}[\sigma^\vee \cap M]$, where σ is the cone over $\Delta(\Gamma)$. In particular, $X := \operatorname{Spec}(Z(A))$ is a Gorenstein affine toric threefold.*

For θ generic, Craw–Quintero-Vélez [CQV12] give a GIT construction of a toric subvariety Y_θ of $\mathcal{M}_A(\theta, \underline{1})$ which they call the *coherent component* of $\mathcal{M}_A(\theta, \underline{1})$. The subvariety Y_θ admits a birational morphism $f : Y_\theta \to X := \operatorname{Spec}(Z(A))$ obtained by variation of GIT [CQV12, Proposition 2.14]. This result strengthens Theorem 1.33:

Theorem 1.48. *Let Γ be a consistent dimer model with θ generic. The moduli space $\mathcal{M}_A(\theta)$ is a toric variety that gives a crepant resolution $f : \mathcal{M}_A(\theta) \to X$ of the Gorenstein affine toric threefold $X := \operatorname{Spec}(Z(A))$.*

Consistency is also enough to show an equivalence between the bounded derived category $D^b(\operatorname{coh}(\mathcal{M}_A(\theta)))$ of coherent sheaves on $\mathcal{M}_A(\theta)$ and the bounded derived category $D^b(\operatorname{mod} -A)$ of finite-dimensional A-modules:

Theorem 1.49. *[IU09] Let Γ be a consistent dimer model with θ generic and let $T = \bigoplus_{v \in Q_0} L_v$ be the universal family of A-modules on $\mathcal{M}_A(\theta)$. Then:*

1. *The tautological $\mathbb{C}$-algebra homomorphism $\phi : A \to \operatorname{End}_{\mathcal{O}_{\mathcal{M}_A(\theta)}}(T)$ is an isomorphism; and*

2. *The tautological bundle T is tilting. In particular, the functors*

$$\begin{aligned} \mathbf{R}\operatorname{Hom}_{\mathcal{O}_{\mathcal{M}_A(\theta)}}(T, -) &\colon D^b(\operatorname{coh}(\mathcal{M}_A(\theta))) \to D^b(\operatorname{mod} -A) \\ - \overset{\mathbf{L}}{\otimes}_A T &\colon D^b(\operatorname{mod} -A) \to D^b(\operatorname{coh}(\mathcal{M}_A(\theta))) \end{aligned}$$

give an equivalence of triangulated categories.

Remark 1.50. Ishii–Ueda [IU13, Section 7] remark that the functor $\mathbf{R}\operatorname{Hom}_{\mathcal{O}_{\mathcal{M}_A(\theta)}}(T,-)$ is an equivalence of categories if and only if the functor

$$\Phi(-) = \mathbb{R}\Gamma(T \otimes -)\colon D^b(\operatorname{coh}(\mathcal{M}_A(\theta))) \to D^b(\operatorname{mod} -A)$$

is an equivalence too. The functor Φ sends the structure sheaf $\mathcal{O}_y$ of a point $y \in \mathcal{M}_A(\theta)$ to the A-module M_y introduced in Definition 1.32.

Definition 1.51. An A-module M is *nilpotent* if there exists $n \in \mathbb{N}$ such that any path of length greater than n acts on M by 0. We write $\operatorname{mod}_0 -A$ for the full subcategory of $\operatorname{mod} -A$ consisting of all nilpotent modules. Following Ishii–Ueda [IU13, Section 7], the functor Φ from Remark 1.50 induces a functor Φ_0 from $\operatorname{coh}_0(\mathcal{M}_A(\theta))$, the full subcategory of $\operatorname{coh}(\mathcal{M}_A(\theta))$ consisting of coherent sheaves supported on the fibre over the unique-torus invariant point x_0 of X, to $\operatorname{mod}_0 -A$.

The tautological $\mathbb{C}$-algebra isomorphism $\phi\colon A \to \operatorname{End}_{\mathcal{O}_{\mathcal{M}_A(\theta)}}(T)$ from Theorem 1.49 associates to each path p in Q a torus-invariant section

$$\phi(p) = x^{\operatorname{div}(p)}$$

of the line bundle $L_{\mathsf{h}(p)} \otimes L_{\mathsf{t}(p)}^{-1}$, where the *label* (or *labelling divisor*) on p is the torus-invariant divisor $\operatorname{div}(p) = \sum_{a \in \operatorname{supp}(p)} \operatorname{div}(a) \in \mathbb{N}^{\Sigma(1)}$ on $\mathcal{M}_A(\theta)$. Since $L_0 \cong \mathcal{O}_{\mathcal{M}_A(\theta)}$ we have the following result:

Lemma 1.52. *The tautological bundle $T = \bigoplus_{v \in Q_0} L_v$ satisfies $L_v \cong \mathcal{O}_{\mathcal{M}_A(\theta)}(\operatorname{div}(p))$ for each vertex $v \in Q_0$, where p is any path from the vertex 0 to the vertex v.*

The main result of Bender–Mozgovoy [BM09, Theorem 4.2] presents the following formula for the labelling divisors in terms of the torus-invariant prime divisors in $\mathcal{M}_A(\theta)$:

$$x^{\operatorname{div}(a)} = \prod_{\{\rho \in \Sigma(1) \mid \mathfrak{e}_a \in \Pi_\rho\}} x_\rho. \tag{1.5.1}$$

Example 1.53. Consider the dimer model Γ introduced in Example 1.13. Figure 1.5 shows all θ-stable perfect matchings $\Pi_i := \Pi_{\rho_i}$ $(0 \le i \le 10)$ of Γ for $\theta = (-9, 1, 1, \ldots, 1)$. The quiver Q dual to Γ has 28 arrows. By equation (1.5.1), a divisor $D_i := D_{\rho_i}$ appears in the label $\operatorname{div}(a)$ of an arrow $a \in Q_1$ if its dual edge $\mathfrak{e}_a$ lies in its corresponding perfect matching Π_i. For example, the label of the arrow a_1 with tail at vertex 0 and head at vertex 4 is $\operatorname{div}(a_1) = D_1 + D_2 + D_6$, as its dual edge appears in Π_1, Π_2 and Π_6. It is a simple exercise using Figure 1.5 to verify that the labels of the arrows of Q are those presented in Figure 1.8, where an arrow marked $i_1 i_2 \cdots i_j$ has labelling divisor $D_{i_1} + D_{i_2} + \cdots + D_{i_j}$.

1.6 Reid's recipe for McKay quivers

Reid [Rei97] computed G-Hilb$(\mathbb{C}^3)$ for several examples of $G \subset \mathrm{SL}(3,\mathbb{C})$ and introduced a recipe which marks the interior lattice points and interior line segments of the toric

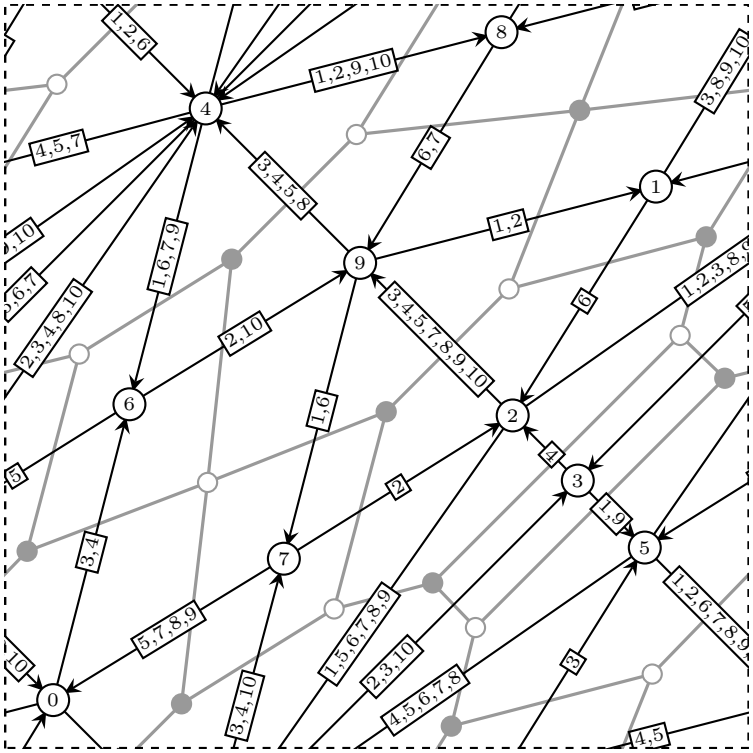

Figure 1.8: *The quiver Q dual to the dimer model Γ from Figure 1.3 with labels*

fan Σ of G-Hilb($\mathbb{C}^3$) with irreducible representations of G. This decoration encodes the relations between the line bundles in the Picard group of G-Hilb($\mathbb{C}^3$). Craw [Cra05] proved that Reid's recipe can be done for any finite abelian subgroup $G \subset SL(3,\mathbb{C})$. The proof uses a deep understanding of the crepant resolution G-Hilb($\mathbb{C}^3$) of $X := \mathbb{C}^3/G$, in particular knowledge of the Craw–Reid algorithm [CR02] which gives an explicit construction of the fan Σ of G-Hilb($\mathbb{C}^3$). We now describe the marking of Σ by Reid's recipe.

To every line segment τ of Σ we can associate a G-invariant ratio of monomials in the Cox ring $S = \mathbb{C}[x,y,z]$ of X, in a similar way as in Example 1.21. Both monomials in each ratio lie in the same character space of the G-action on S. Mark every line segment τ with the character ϱ if and only if the monomials associated to τ lie in the ϱ character space. The marking of the interior lattice points is done case by case depending on the valency of $\rho \in \Sigma(1)$. Note that the valency of ρ can only be $3, 4, 5$ or 6 [CR02, Section 1.3]. The marking of lattice points is defined as follows:

(i) If the valency of $\rho \in \Sigma(1)$ is 3, a single character ϱ marks all three line segments with endpoint ρ and we mark the lattice point ρ with the character $\chi = \varrho\varrho$;

(ii) If the valency of $\rho \in \Sigma(1)$ is 4, two distinct characters ϱ_1 and ϱ_2 mark a pair of line segments with endpoint ρ. Mark ρ with the character $\chi = \varrho_1\varrho_2$;

(iii) If the valency of $\rho \in \Sigma(1)$ is 5, two distinct characters ϱ_1 and ϱ_2 mark a pair of line segments with endpoint ϱ. The fifth line segments is marked with a third distinct character of G. Mark ρ with $\chi = \varrho_1\varrho_2$;

(iv) If the valency of $\rho \in \Sigma(1)$ is 6 either

(a) Two distinct characters ϱ_1 and ϱ_2 mark a pair of line segments with endpoint ϱ and the remaining two line segments are marked by another two different characters of G. In this case, we mark ρ with the character $\chi = \varrho_1\varrho_2$; or

(b) Three distinct characters ϱ_1, ϱ_2 and ϱ_3 mark a pair of line segments each with endpoint ρ and we mark ρ with the characters χ_1 and χ_2 of G such that $\chi_1\chi_2 = \varrho_1\varrho_2\varrho_3$, as defined in [Cra05, Lemma 3.4].

Theorem 1.54. *[Cra05, Corollary 4.6] Every nontrivial character of G appears once on Σ as:*

(i) a character χ marking a lattice point $\rho \in \Sigma(1)$; or

(ii) a character ϱ marking a line segment $\tau \in \Sigma(2)$, or possibly several line segments each sharing an endpoint with another line segment marked with ϱ.

Recall that the McKay quiver Q of G is dual to a hexagonal dimer model Γ in $\mathbb{T}$. The Jacobian algebra A of Q is the skew group algebra $\mathbb{C}[x, y, z] * G$. The quiver Q has a vertex for each irreducible representation of G. Let $v_0 \in Q_0$ denote the trivial representation of G. For any stability parameter $\theta = (\theta_v) \in \Theta$ satisfying $\theta_v > 0$ for all $v \neq v_0$, the moduli space $\mathcal{M}_A(\theta)$ is the G-Hilbert scheme. The tautological bundle T of $\mathcal{M}_A(\theta)$ decomposes into the direct sum of line bundles, one for each irreducible representation of G. Let Σ be the toric fan of $\mathcal{M}_A(\theta)$. The set of relations in $\mathrm{Pic}(\mathcal{M}_A(\theta))$ between the line bundles can be stated using Reid's recipe:

Theorem 1.55. *[Cra05, Theorem 6.1] The following relations hold in* $\mathrm{Pic}(X_\Sigma)$.

(i) $L_\chi = L_\varrho \otimes L_\varrho$ when $\chi = \varrho\varrho$ marks a trivalent lattice point $\rho \in \Sigma(1)$;

(ii) $L_\chi = L_{\varrho_1} \otimes L_{\varrho_2}$ when $\chi = \varrho_1\varrho_2$ is the only character marking a lattice point $\rho \in \Sigma(1)$ of valency 4, 5 or 6;

(iii) $L_{\chi_1} \otimes L_{\chi_2} = L_{\varrho_1} \otimes L_{\varrho_2} \otimes L_{\varrho_3}$ when χ_1 and χ_2 satisfying $\chi_1\chi_2 = \varrho_1\varrho_2\varrho_3$ mark a lattice point $\rho \in \Sigma(1)$ of valency 6.

Moreover, these relations generate all other relations between the tautological line bundles in $\mathrm{Pic}(X_\Sigma)$.

Reid [Rei97] and Craw [Cra05] computed G-Hilb$(\mathbb{C}^3)$ and Reid's recipe for several large examples of finite abelian subgroups $G \subset \mathrm{SL}(3, \mathbb{C})$. We now present a small example to illustrate the recipe and theorems above.

Example 1.56. Let G be the finite abelian subgroup of $\mathrm{SL}(3, \mathbb{C})$ generated by the diagonal matrix $\mathrm{diag}(\varepsilon, \varepsilon^2, \varepsilon^3)$, where ε is a primitive sixth root of unity. Figure 1.9 shows the toric fan of G-Hilb$(\mathbb{C}^3)$ decorated using Reid's recipe. Note that every nontrivial character of G appears once as described in Theorem 1.54. The only nontrivial relation in $\mathrm{Pic}(G\text{-Hilb}(\mathbb{C}^3))$ between its tautological line bundles comes from the interior lattice point of its toric fan $L_5 = L_2 \otimes L_3$.

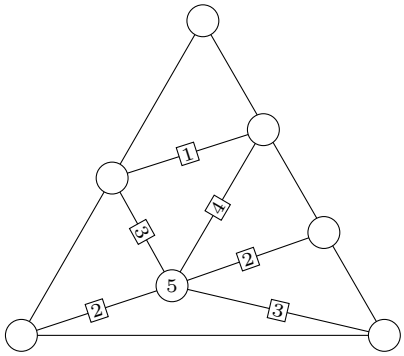

Figure 1.9: *The fan of G-*Hilb$(\mathbb{C}^3)$ *decorated using Reid's recipe*

CHAPTER 2

JIGSAW TRANSFORMATIONS

The aim of this chapter is to study fundamental hexagons for nondegenerate dimer models, and to provide a dimer model analogue of Nakamura's 'G-igsaw transformations' of monomial G-clusters for any finite abelian subgroup $G \subset \mathrm{SL}(3,\mathbb{C})$.

For a nondegenerate dimer model Γ with Jacobian algebra A, and for any generic stability parameter θ, Ishii-Ueda [IU08] associated a fundamental domain - a 'fundamental hexagon' - of the universal cover of Γ to every torus-invariant θ-stable A-module, and hence computed the toric coordinate charts on the fine moduli space $\mathcal{M}_A(\theta)$. For any pair of adjacent 3-dimensional cones $\sigma_\pm \in \Sigma(\theta)$ in the toric fan defining $\mathcal{M}_A(\theta)$, we show how to pass between the fundamental hexagons for the torus-invariant A-modules $M_{\sigma_\pm}$ in a manner that generalises G-igsaw transformations for the G-Hilbert scheme.

2.1 The fundamental hexagon

Let $\Gamma = \{\mathfrak{B}, \mathfrak{W}, \mathfrak{E}\}$ be a nondegenerate dimer model in $\mathbb{T}$ and let $Q = \{Q_0, Q_1, \mathsf{h}, \mathsf{t}, \mathcal{R}\}$ be its dual quiver with relations. Let A be the Jacobian algebra of Γ and write $\Delta(\Gamma)$ for the characteristic polygon of Γ. Recall from Chapter 1 that:

(i) the cone σ over the characteristic polygon $\Delta(\Gamma)$ defines an affine toric variety $X = \mathrm{Spec}(\mathbb{C}[\sigma^\vee \cap M]$; and

(ii) for any generic $\theta \in \Theta$, the fine moduli space $\mathcal{M}_A(\theta)$ of θ-stable A-modules provides a crepant resolution $\mathcal{M}_A(\theta) \to X$.

Throughout this chapter, let $\theta \in \Theta$ be generic and let $\Sigma := \Sigma(\theta) \subseteq N_{\mathbb{R}}$ denote the fan of the toric variety $\mathcal{M}_A(\theta)$.

Definition 2.1. Let $M = \left(\bigoplus_{v \in Q_0} W_v, \{\phi_a\}_{a \in Q_1}\right)$ be a representation of Q. The *cosupport* of M is the subset

$$\mathrm{cosupp}(M) := \{\mathfrak{e}_a \mid \phi_a = 0\} \subset \mathfrak{E}$$

of edges of Γ.

Let $\rho \in \Sigma(1)$ be a ray and let $O_\rho \subset \mathcal{M}_A(\theta)$ denote the corresponding two-dimensional open orbit of the action by the dense torus. For any point $y \in O_\rho$, define

$$\Pi_\rho(\theta) := \operatorname{cosupp}(M_y(\theta)) \subset \mathfrak{E},$$

where $M_y(\theta)$ is the θ-stable A-module associated to the point $y \in \mathcal{M}_A(\theta)$ by Definition 1.32. The subset $\Pi_\rho(\theta) \subseteq \mathfrak{E}$ does not depend on the choice of point $y \in O_\rho$, and it is a perfect matching by Ishii–Ueda [IU08, Lemma 6.1]. We call any such perfect matching a *θ-stable perfect matching*. We now use these perfect matchings to associate a θ-stable A-module to each cone of Σ. For $\sigma \in \Sigma$, write $\sigma(1) := \{\rho \in \Sigma(1) \mid \rho \subseteq \sigma\}$, where the zero cone $\sigma = \{0\}$ satisfies $\sigma(1) = \emptyset$.

Definition 2.2. Let $\theta \in \Theta$ be generic and let Σ denote the fan of $\mathcal{M}_A(\theta)$. For any cone $\sigma \in \Sigma$, the *θ-stable A-module associated to σ* is $M_\sigma(\theta) = (\oplus_{v \in Q_0}\mathbb{C}, \{\psi_a\}_{a \in Q_1})$, where

$$\psi_a := \begin{cases} 0 & \text{if } \mathfrak{e}_a \in \bigcup_{\rho \in \sigma(1)} \Pi_\rho(\theta) \\ 1 & \text{otherwise} \end{cases}.$$

The following result establishes in particular that $M_\sigma(\theta)$ is a θ-stable A-module for every generic $\theta \in \Theta$ and for every cone $\sigma \in \Sigma$.

Lemma 2.3. *Let $\theta \in \Theta$ be generic and let Σ denote the fan of $\mathcal{M}_A(\theta)$. For all $\sigma \in \Sigma$ there exists a unique point $y \in O_\sigma \subseteq \mathcal{M}_A(\theta)$ such that $M_\sigma(\theta) = M_y(\theta)$.*

Proof. This is a restatement of results from Ishii–Ueda [IU08] and Mozgovoy [Moz09], so we only sketch the proof. For $\sigma \in \Sigma$, we claim that the point $(\psi_a) \in \mathbb{C}^{Q_1}$ defined by the scalars from Definition 2.2 is a θ-stable point of the subscheme $\mathbb{V}_\mathcal{R} \subseteq \mathbb{C}^{Q_1}$ cut out by the relations and, moreover, that the corresponding point $y := [(\psi_a)] \in \mathcal{M}_A(\theta)$ lies in O_σ. The proof is case-by-case according to the dimension of $\sigma \in \Sigma$ as follows. For $0 \in \Sigma$, we have $\psi_a = 1$ for all $a \in Q_1$, so $(\psi_a) \in \mathbb{V}_\mathcal{R} \cap (\mathbb{C}^\times)^{Q_1}$. Every point in $(\mathbb{C}^\times)^{Q_1}$ is θ-stable for all $\theta \in \Theta$, so $y := [(\psi_a)]$ satisfies $y \in \big(\mathbb{V}_\mathcal{R} \cap (\mathbb{C}^\times)^{Q_1}\big)/(\mathbb{C}^\times)^{Q_0} = O_0 \subset \mathcal{M}_A(\theta)$ as required. For $\rho \in \Sigma(1)$ and $\tau \in \Sigma(2)$, the result is due to Ishii–Ueda [IU09, Lemma 6.2] and Mozgovoy [Moz09, Corollary 4.19] respectively. For $\sigma \in \Sigma(3)$, the statement is [IU08, Lemma 4.5] (see also [Moz09, Corollary 4.18]). □

Remark 2.4. If ρ is an interior lattice point of Σ, the A-module M_ρ is nilpotent. Indeed, as ρ is interior, the point $y \in \mathcal{M}_A(\theta)$ such that $M_y = M_\rho$ lies in $f^{-1}(x_0)$, where $f : \mathcal{M}_A \to X$ is the crepant resolution of X and x_0 is the unique torus-invariant point of X. Remark 1.50 introduces the functor $\Phi\colon D^b(\operatorname{coh}(\mathcal{M}_A(\theta))) \to D^b(\operatorname{mod} -A)$ that takes the structure sheaf $\mathcal{O}_y$ of y to the A-module M_y. Since y lies over x_0, by Definition 1.51 $\mathcal{O}_y \in \operatorname{coh}_0(\mathcal{M}_A(\theta))$ and the functor Φ_0 induced by Φ takes $\mathcal{O}_y$ to $M_y \in \operatorname{mod}_0 -A$, i.e. M_y is nilpotent.

Lemma 2.3 relies on the description of the coordinates on the affine toric chart $U_\sigma \subseteq \mathcal{M}_A(\theta)$ by Ishii–Ueda [IU08, Lemma 4.5]. We now recall some of the combinatorics from their construction. For $\sigma \in \Sigma(3)$, consider the θ-stable A-module $M_\sigma(\theta)$ and let $Q_\sigma := Q_{M_\sigma}$ denote the subquiver that supports $M_\sigma(\theta)$. The universal cover $\pi\colon \mathbb{R}^2 \longrightarrow \mathbb{T}$ of the two-dimensional torus lifts Q to a $\mathbb{Z}^2$-periodic infinite quiver $\widetilde{Q}$ in $\mathbb{R}^2$. Similarly, Γ is lifted to regular cell decomposition $\widetilde{\Gamma}$ of $\mathbb{R}^2$, in which the 2-cells are polygonal tiles,

each corresponding to a unique vertex v of $\widetilde{Q}$. Fix a vertex $v_0 \in Q_0$ and lift it to a vertex $\widetilde{v_0} \in \widetilde{Q}_0$ with $\pi(\widetilde{v_0}) = v_0 \in Q_\sigma$. Since $M_\sigma(\theta)$ is torus-invariant, for any path p in Q_σ from v_0 to a vertex v in Q_σ, the end point of its lift $\widetilde{p}$ does not depend on the choice of p. Thus, the map π lifts Q_σ to a subquiver $\widetilde{Q_\sigma}$ of $\widetilde{Q}$ such that $\pi\colon \widetilde{Q_\sigma} \to Q_\sigma$ is an isomorphism [IU08, Lemma 4.1].

Definition 2.5. For $\sigma \in \Sigma(3)$, the *fundamental hexagon* $\mathrm{Hex}(\sigma)$ is the subset of $\mathbb{R}^2$ covered by the tiles corresponding to vertices of $\widetilde{Q_\sigma}$. The *honeycomb tiling* of $\mathbb{R}^2$ induced by σ is the tiling of $\mathbb{R}^2$ given by the union of the $\mathbb{Z}^2$-translates of $\mathrm{Hex}(\sigma)$. Consider the $\mathbb{Z}^2$-periodic *graph of* σ

$$\mathrm{Graph}(\sigma) := \bigcup_{n\in\mathbb{Z}^2} (\partial\,\mathrm{Hex}(\sigma) + n)$$

obtained as the union of the $\mathbb{Z}^2$-translates of the boundary of $\mathrm{Hex}(\sigma)$, and let $\mathrm{supp}(\mathrm{Graph}(\sigma))$ denote the set of edges of $\widetilde{\Gamma}$ that lie in $\mathrm{Graph}(\sigma)$.

Remarks 2.6.

1. Both $\widetilde{Q_\sigma}$ and $\mathrm{Hex}(\sigma)$ are defined uniquely up to the choice of the lift $\widetilde{v_0} \in \widetilde{Q}$ of the vertex v_0, i.e., up to translations by $\mathbb{Z}^2$.

2. Since $\widetilde{Q_\sigma}$ is isomorphic to the subquiver Q_σ that supports the θ-stable A-module $M_\sigma(\theta)$, the tiles in $\mathrm{Hex}(\sigma)$ correspond one-to-one with vertices of Q_0. In particular, $\partial\,\mathrm{Hex}(\sigma)$ bounds a fundamental domain of $\widetilde{\Gamma}$.

3. Since $\mathrm{Graph}(\sigma)$ is $\mathbb{Z}^2$-periodic in $\mathbb{R}^2$, we may regard it as a subset of the torus $\mathbb{T}$, in which case $\mathrm{supp}(\mathrm{Graph}(\sigma))$ becomes a subset of the set of edges $\mathfrak{E}$ of Γ. This identification gives

$$\mathrm{supp}(\mathrm{Graph}(\sigma)) \subseteq \mathrm{cosupp}(M_\sigma(\theta)). \tag{2.1.1}$$

   Moreover, since $\partial\,\mathrm{Hex}(\sigma) \subseteq \mathrm{Graph}(\sigma)$, we may regard the edges in the boundary of $\mathrm{Hex}(\sigma)$ as a subset of $\mathrm{cosupp}(M_\sigma)$ which is itself a subset of the torus $\mathbb{T}$. In particular, whenever we work with a set of edges in $\widetilde{\Gamma}$ that lie in $\partial\,\mathrm{Hex}(\sigma)$ for some $\sigma \in \Sigma(3)$, we may regard the edges as a subset of the set of edges $\mathfrak{E}$ of Γ.

When combined with Remarks 2.6(2) above, the next key result of Ishii–Ueda [IU08, Lemma 4.4] and the discussion that follows it justifies the terminology of Definition 2.5.

Lemma 2.7. *For $\sigma \in \Sigma(3)$, there are six trivalent nodes of* $\mathrm{Graph}(\sigma)$ *lying on* $\partial\,\mathrm{Hex}(\sigma)$. *All other nodes of* $\mathrm{Graph}(\sigma)$ *have valency two.*

Each trivalent node in $\mathrm{Graph}(\sigma)$ corresponds to a corner of three hexagons in the honeycomb tiling of $\mathbb{R}^2$, while the bivalent nodes arise along the sides of the hexagon. Ishii–Ueda [IU08, Lemma 4.5] showed that if $\mathfrak{n}_1, \mathfrak{n}_2, \ldots, \mathfrak{n}_6$ are the six trivalent nodes of $\mathrm{Graph}(\sigma)$ lying clockwise around $\partial\,\mathrm{Hex}(\sigma)$, then the nodes $\mathfrak{n}_1, \mathfrak{n}_3$ and $\mathfrak{n}_5$ lie in one $\mathbb{Z}^2$-orbit in $\mathbb{R}^2$ and $\mathfrak{n}_2, \mathfrak{n}_4$ and $\mathfrak{n}_6$ lie in a different one. One of these orbits consists of white nodes of $\widetilde{\Gamma}$, and the other of black nodes. Hence, the boundary of $\mathrm{Hex}(\sigma)$ is made up of three distinct sides, each appearing twice; opposite sides of the hexagon are identified under π. See Figure 2.1 for a schematic picture of a fundamental hexagon in part of the honeycomb tiling.

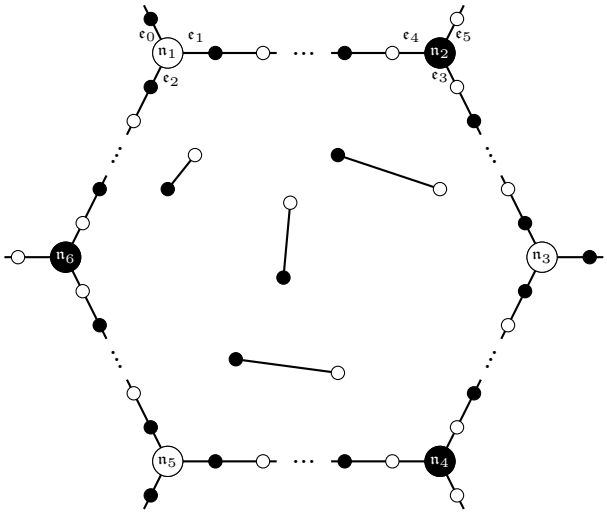

Figure 2.1: *Schematic of a fundamental hexagon*

Definition 2.8. An edge $\mathfrak{e} \in \operatorname{cosupp}(M_\sigma(\theta))$ is a *boundary edge of* $\operatorname{Hex}(\sigma)$ if $\mathfrak{e} \in \operatorname{supp}(\operatorname{Graph}(\sigma))$, and otherwise it is an *interior edge of* $\operatorname{Hex}(\sigma)$.

Example 2.9. Consider the cone $\sigma \in \Sigma(3)$ generated by the rays $\rho_8, \rho_9, \rho_{10}$ in the toric diagram of the crepant resolution from Example 1.35. Figure 2.2 shows the lifts of both the quiver Q_σ that supports $M_\sigma(\theta)$ and the cosupport of $M_\sigma(\theta)$ to the universal cover. The green dashed arrows in Figure 2.2 represent a choice of the quiver $\widetilde{Q_\sigma}$, while the red dashed edges of $\widetilde{\Gamma}$ show all edges in the boundary of a choice of $\operatorname{Hex}(\sigma)$. Note that $\operatorname{Graph}(\sigma)$ provides all boundary edges in the honeycomb tiling for σ, and it is characterised as the unique connected component of the subset of dashed and solid edges in Figure 2.2 consisting of more than a single edge.

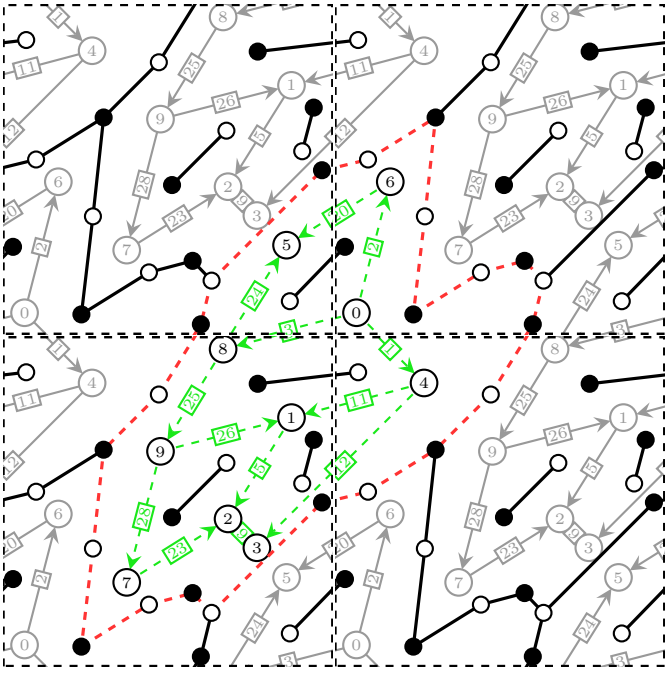

Figure 2.2: *The honeycomb tiling and fundamental hexagon for* σ

2.2 Ishii–Ueda's local coordinates and perfect matchings

We now summarise results from Ishii-Ueda [IU08] to explain how the fundamental hexagon $\mathrm{Hex}(\sigma)$ can be used to describe the coordinates of the affine chart $U_\sigma \cong \mathbb{C}^3$.

For $\sigma \in \Sigma(3)$, write $M_\sigma(\theta) = (\oplus_{v\in Q_0}\mathbb{C}, \{\psi_a\}_{a\in Q_1})$. The affine chart $U_\sigma \subseteq \mathcal{M}_A(\theta)$ parametrises the set of all θ-stable A-modules $(\oplus_{v\in Q_0}\mathbb{C}, \{\phi_a\}_{a\in Q_1})$ satisfying $\phi_a = 1$ for arrows $a \in Q_1$ with $\psi_a = 1$ [IU08, Lemma 4.3]. It follows that for $y \in U_\sigma$, the θ-stable A-module $M_y(\theta) := (\oplus_{v\in Q_0}\mathbb{C}, \{\varphi_a\}_{a\in Q_1})$ is determined by the maps φ_a corresponding to arrows $a \in Q_1$ with $\psi_a = 0$.

To investigate the values of these maps, let $\mathfrak{n}_1, \mathfrak{n}_2, \ldots, \mathfrak{n}_6$ label the trivalent nodes around the boundary of $\mathrm{Hex}(\sigma)$ in clockwise order. Let $\mathfrak{e}_0, \mathfrak{e}_1, \ldots, \mathfrak{e}_5$ be the edges around $\mathfrak{n}_1$ and $\mathfrak{n}_2$, respectively, arranged also in an clockwise direction, so that $\mathfrak{e}_1$ and $\mathfrak{e}_4$ lie along the same side of the hexagon $\mathrm{Hex}(\sigma)$ (see Figure 2.1). For $i = 0, 1, \ldots, 5$, write t_i for the value of the map φ_{a_i} where a_i is the arrow in Q dual to $\mathfrak{e}_i$. The relations $\{p_+(a) - p_-(a) \in \mathbb{C}Q \mid a \in Q_1\}$ determined by the dimer model Γ imply that the edges along the side starting with $\mathfrak{e}_i$ must correspond to maps with alternating values t_i and $t_{\overline{i+1}} \cdot t_{\overline{i-1}}$ for $i = 0, 1, 2$, where the overline denotes addition modulo 3. Therefore, $t_0 = t_3$, $t_1 = t_4$ and $t_2 = t_5$. Since the maps in $M_\sigma(\theta)$ are commutative and, for any arrow $a \in Q_1$, we have $ap_+(a) = ap_-(a)$, the value of the path $ap_+(a)$ does not depend on the arrow $a \in Q_1$. Thus, for any interior edge $\mathfrak{e}$ of $\mathrm{Hex}(\sigma)$, $\varphi_{a_\mathfrak{e}} = t_0t_1t_2$. Hence, any choice of values $t_0, t_1, t_2 \in \mathbb{C}$ for the maps $\varphi_{a_0}, \varphi_{a_1}, \varphi_{a_2}$ determines the values of the rest of the maps of $M_y(\theta)$, giving an isomorphism $U_\sigma \cong \mathbb{C}^3$ that sends the torus-invariant point $y = [M_\sigma(\theta)] \in U_\sigma$ to the origin of $\mathbb{C}^3$. Figure 2.3 records the value of $\varphi_{a_\mathfrak{e}}$ for every edge $\mathfrak{e} \in \mathrm{cosupp}(M_\sigma)$.

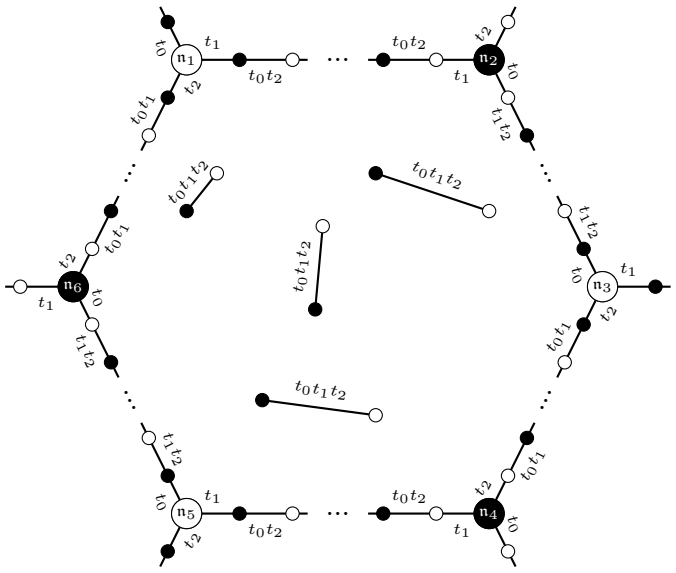

Figure 2.3: *A fundamental hexagon with the values of its maps*

To restate this result in terms of perfect matchings, let $\rho_0, \rho_1, \rho_2 \in \Sigma(1)$ denote the rays in σ, and write $\Pi_0(\theta), \Pi_1(\theta), \Pi_2(\theta)$ for the corresponding θ-stable perfect matchings. Recall from Definition 2.2, that the cosupport of $M_\sigma(\theta)$ is equal to the union of $\Pi_0(\theta), \Pi_1(\theta)$ and $\Pi_2(\theta)$. For $0 \leq i \leq 2$, let $(\mathfrak{e}_{i,1}, \mathfrak{e}_{i,2}, \ldots, \mathfrak{e}_{i,2k_i+1})$ be the chains of edges making the three inequivalent sides of the boundary of $\mathrm{Hex}(\sigma)$; in light of Re-

marks 2.6(3), these edges may be chosen from $\mathfrak{E} \subset \mathbb{T}$. Mozgovoy [Moz09, Corollary 4.18] noted that the set of edges

$$\Pi_i' := \operatorname{cosupp}(M_\sigma(\theta)) \setminus \big(\{\mathfrak{e}_{j,2k+1} \mid 0 \leq k \leq k_j, j \neq i\} \cup \{\mathfrak{e}_{i,2k} \mid 1 \leq k \leq k_i\}\big) \quad (2.2.1)$$

is a perfect matching of Γ and, moreover, these are the only perfect matchings in $\operatorname{cosupp}(M_\sigma(\theta))$. They must therefore coincide with the θ-stable perfect matchings $\Pi_0(\theta), \Pi_1(\theta)$ and $\Pi_2(\theta)$. Relabelling if necessary gives $\Pi_i' = \Pi_i(\theta)$ for $0 \leq i \leq 2$. Equation (2.2.1) implies the following:

Corollary 2.10. *Let $\sigma \in \Sigma(3)$ and consider an edge $\mathfrak{e} \in \operatorname{cosupp}(M_\sigma(\theta))$. For $0 \leq i \leq 2$, we have $\mathfrak{e} \in \Pi_i(\theta)$ if and only if the edge $\mathfrak{e}$ is labelled with Π_i in Figure 2.4. That is, either:*

1. *$\mathfrak{e}$ is an interior edge of $\operatorname{Hex}(\sigma)$, in which case $\mathfrak{e} \in \bigcap_{i=0}^{2} \Pi_i(\theta)$; or*
2. *$\mathfrak{e}$ is a boundary edge of $\operatorname{Hex}(\sigma)$, in which case $\mathfrak{e}$ is one of the edges in a chain $(\mathfrak{e}_{j,1}, \mathfrak{e}_{j,2}, \ldots, \mathfrak{e}_{j,2k_j+1})$ in $\operatorname{Graph}(\sigma)$ linking adjacent trivalent points of $\operatorname{Hex}(\sigma)$, for some $0 \leq j \leq 2$. The edges $\mathfrak{e}_{j,1}, \mathfrak{e}_{j,2}, \ldots, \mathfrak{e}_{j,2k_j+1}$ belong alternately to either a single perfect matching $\Pi_j(\theta)$ or to two perfect matchings $\Pi_{\overline{j-1}}(\theta) \cap \Pi_{\overline{j+1}}(\theta)$, where the overline denotes addition modulo 3.*

In particular, $\operatorname{Graph}(\sigma) \subset \mathbb{T}$ is the unique connected component of the locus $\bigcup_{0 \leq i \leq 2} \Pi_i(\theta) \subset \mathbb{T}$ comprising more than a single edge.

Example 2.11. Consider again the cone $\sigma \in \Sigma(3)$ generated by the rays $\rho_8, \rho_9, \rho_{10}$ in the toric diagram of the crepant resolution introduced in Example 1.35. The perfect matchings Π_8, Π_9, Π_{10} are shown in Figure 1.5, and it is a simple exercise to verify the statement of Corollary 2.10 in this case by comparing Figure 2.2.

2.3 Meandering walks

In this section we generalise the notion of a zig-zag path by associating a walk in a nondegenerate dimer model Γ to any line segment $\tau \in \Sigma(2)$, where $\Sigma := \Sigma(\theta)$ is the toric fan of the moduli space $\mathcal{M}_A(\theta)$ defined by any generic stability parameter $\theta \in \Theta$.

Definition 2.12. Let Π, Π' be θ-stable perfect matchings of Γ. The *symmetric difference* of Π and Π' is the subset $\Pi \ominus \Pi' := (\Pi \cup \Pi') \setminus (\Pi \cap \Pi')$ of edges in Γ. For $\tau \in \Sigma(2)$, let ρ, ρ' be the two ray generators of τ. The *meandering walk of τ* is the set $\mathfrak{m}_\tau := \Pi_\rho \ominus \Pi_{\rho'}$ of edges in Γ. We justify the terminology later.

Remark 2.13. Definition 2.12 generalises the notion of a σ-strand introduced by Logvinenko [Log04, Definition 6.59] to the setting of dimer models.

By Corollary 2.10, if ρ and ρ' are the endpoints of a line segment τ in a triangle $\sigma \in \Sigma(3)$, the edges along two adjacent sides of the boundary of $\operatorname{Hex}(\sigma)$ belong alternately to $\Pi_\rho(\theta)$ and $\Pi_{\rho'}(\theta)$. Therefore, the edges in a meandering walk $\mathfrak{m}_\tau$ make a cycle in Γ, and edges along any two adjacent sides of the fundamental hexagon $\operatorname{Hex}(\sigma)$ belong to one of the meandering walks $\mathfrak{m}_\tau$ for τ a two-dimensional cone in σ. We illustrate this

in Figure 2.4, where ρ_0, ρ_1, ρ_2 are the ray generators in σ and $\Pi_i := \Pi_{\rho_i}(\theta)$ $(0 \leq i \leq 2)$ denotes the corresponding θ-stable perfect matchings. Let $\mathfrak{m}_{i,j}$ denote the meandering walk $\mathfrak{m}_\tau$ where τ is a line segment in σ with endpoints ρ_i and ρ_j. Figure 2.4 shows $\mathrm{Hex}(\sigma)$ in part of the honeycomb tiling with edges labelled by the perfect matchings each belongs to. Edges along each side of $\partial\,\mathrm{Hex}(\sigma)$ are in the intersection of two meandering walks.

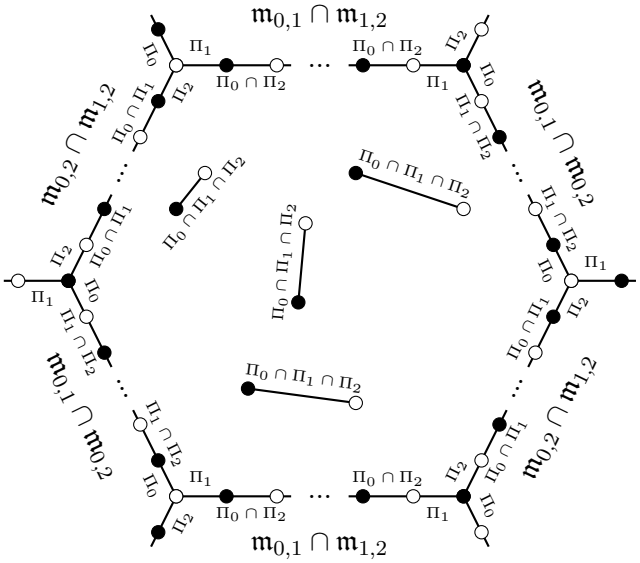

Figure 2.4: *The meandering walks and perfect matchings associated to* $\mathrm{Hex}(\sigma)$

To this point, each meandering walk is just a set of edges whose support is a cycle in Γ. We wish to trace the edges in such cycles, and to do this we have to choose a direction along each of them. For this, let $\mathfrak{T}$ denote the set of all tiles of Γ and consider the chain complex

$$0 \xrightarrow{\partial_3} \mathbb{Z}^{\mathfrak{T}} \xrightarrow{\partial_2} \mathbb{Z}^{\mathfrak{E}} \xrightarrow{\partial_1} \mathbb{Z}^{\mathfrak{B} \sqcup \mathfrak{W}} \xrightarrow{\partial_0} 0$$

which computes the homology of $\mathbb{T}$. The boundary operator ∂_1 sends an edge $\mathfrak{e} \in \mathfrak{E}$ to $\mathfrak{w}(\mathfrak{e}) - \mathfrak{b}(\mathfrak{e})$, where $\mathfrak{w}(\mathfrak{e})$ and $\mathfrak{b}(\mathfrak{e})$ are the white and black endnodes of $\mathfrak{e}$, respectively. A perfect matching Π of Γ gives a 1-chain $\sum_{\mathfrak{e} \in \Pi} \mathfrak{e}$. The difference of 1-chains associated to a pair of perfect matchings Π and Π' is a 1-cycle, whose homology class we denote by $[\Pi - \Pi'] \in H_1(\mathbb{T}, \mathbb{Z})$. This class is equivalent to the class of a 1-cycle supported on the symmetric difference $\Pi \ominus \Pi' = (\Pi \cup \Pi') \setminus (\Pi \cap \Pi')$.

Given any $\tau \in \Sigma(2)$, we may turn the meandering walk $\mathfrak{m}_\tau$ into a directed meandering walk by setting it to be the cycle supported on $\mathfrak{m}_\tau$ together with a choice of direction determined by the choice of either $[\Pi_\rho(\theta) - \Pi_{\rho'}(\theta)]$ or $[\Pi_{\rho'}(\theta) - \Pi_\rho(\theta)]$. For a meandering walk $\mathfrak{m}_\tau$, we denote either choice of direction by $[\mathfrak{m}_\tau]$. In general, the homology class of $\mathfrak{m}_\tau$ is normal to τ:

Lemma 2.14. *Let Σ be the fan of $\mathcal{M}_A(\theta)$ for $\theta \in \Theta$ generic. For either choice of direction on the meandering walk $\mathfrak{m}_\tau$ of $\tau \in \Sigma(2)$, its homology class $[\mathfrak{m}_\tau] \in H_1(\mathbb{T}, \mathbb{Z}) \cong \mathbb{Z}^2$ is normal to the line segment τ.*

Proof. For every $\tau \in \Sigma(2)$, let $\rho, \rho' \in \Sigma(1)$ be its ray generators and let $\sigma \in \Sigma(3)$ be any cone containing it. The meandering walk $\mathfrak{m}_\tau$ passes through two of the three distinct sides of the fundamental hexagon $\mathrm{Hex}(\sigma)$. Choose coordinates so that the homology class of $\mathfrak{m}_\tau$ is $(0,1)$. Figure 2.5 below depicts a part of $\mathrm{Graph}(\sigma)$ in the universal cover of $\mathbb{T}$: the thicker edges of $\mathrm{Graph}(\sigma)$ indicate the edges in the lift of $\mathfrak{m}_\tau$ to the universal cover $\widetilde{\Gamma}$. The dashed lines indicate a fundamental domain of $\mathbb{T}$. Computing the height change $h(\Pi_\rho(\theta), \Pi_{\rho'}(\theta))$, we get that $h(\Pi_\rho(\theta), \Pi_{\rho'}(\theta)) = (1,0) \in H^1(\mathbb{T}, \mathbb{Z})$, as there exists a path from $(0,0)$ to $(1,0)$ that crosses an edge $\mathfrak{e} \in \Pi_{\rho'}$ with a black node on the right when moving from a connected component of $\mathbb{R}^2 \setminus (\Pi_\rho \cup \Pi_{\rho'})$ to another, and both $(0,0)$ and $(0,1)$ lie in the same connected component of $\mathbb{R}^2 \setminus (\Pi_\rho \cup \Pi_{\rho'})$ (see Definition 1.11). Since $h(\Pi_\rho(\theta), \Pi_{\rho'}(\theta))$ indicates the direction of the line segment τ connecting the nodes ρ and ρ' and $h(\Pi_\rho(\theta), \Pi_{\rho'}(\theta)) \cdot [\mathfrak{m}_\tau] = (1,0) \cdot (0,1) = 0$, $\mathfrak{m}_\tau$ is normal to the line segment τ.

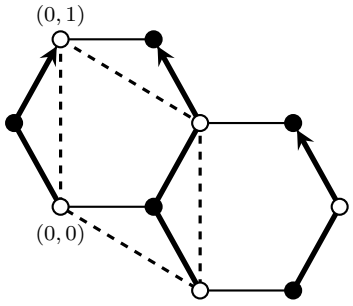

Figure 2.5: *The meandering walk* $\mathfrak{m}_\tau$ *with* $[\mathfrak{m}_\tau] = (0,1)$

□

Remark 2.15. Let Γ be a consistent dimer model. By Theorem 1.46, there is a one-to-one correspondence between the set of zigzag paths of Γ and the set of line segments on the boundary of $\Delta(\Gamma)$. Moreover, Ishii–Ueda [IU09, Theorem 11.1] showed that for θ generic, each zigzag path $\mathfrak{z}$ in Γ is supported on the symmetric difference of the θ-stable perfect matchings of ρ and ρ', where ρ and ρ' are the ray generators of the line segment in $\partial\Delta$ corresponding to $\mathfrak{z}$. Therefore, every zigzag path $\mathfrak{z}$ in Γ is a directed meandering walk with the choice of direction $[\Pi_{\rho'} - \Pi_\rho]$, where ρ' is adjacent to ρ in a clockwise direction. An edge $\mathfrak{e} \in \mathrm{supp}(\mathfrak{z})$ is a zig (resp. zag) of $\mathfrak{z}$ if $\mathfrak{e}$ lies in $\Pi_{\rho'}$ (resp. Π_ρ).

Remark 2.16. The name meandering walk was chosen as the cycle of $\mathbb{T}$ supported on the set of edges making a meandering walk does not always turn maximally right at white nodes and maximally left at black nodes, but rather, it meanders.

2.4 Generalised Nakamura jigsaw transformations

For any finite abelian subgroup $G \subseteq \mathrm{SL}(3,\mathbb{C})$, Nakamura [Nak01] introduced an algorithm to construct a crepant resolution of $\mathbb{C}^3/G$ where the key step in each iteration of the algorithm was a combinatorial procedure called a 'G-igsaw transformation'. The crepant resolution produced by this algorithm is G-Hilb$(\mathbb{C}^3)$ which, by Example 1.34, coincides with the fine moduli space of θ-stable A-modules for $A = \mathbb{C}[x,y,z]*G$ and for a special choice of stability parameter θ. We now generalise Nakamura's algorithm to

construct the fine moduli space $\mathcal{M}_A(\theta)$ for any nondegenerate dimer model Γ and any generic stability parameter θ. Our construction differs from those introduced previously by Mozgovoy [Moz09] and Craw–Quintero-Vélez [CQV12].

Let $\sigma_\pm \in \Sigma(3)$ be adjacent cones in Σ with $\tau = \sigma_+ \cap \sigma_- \in \Sigma(2)$ the common two-dimensional cone. Let ρ_0, ρ_1, ρ_2 and ρ_1, ρ_2, ρ_3 denote the rays in σ_+ and σ_-, respectively. Write $M_+ := M_{\sigma_+}$ and $M_- := M_{\sigma_-}$ for the θ-stable A-modules of σ_+ and σ_-, and write $\mathrm{Hex}(\sigma_+)$ and $\mathrm{Hex}(\sigma_-)$ for their fundamental hexagons (choose any lift, see Remark 2.6(1)).

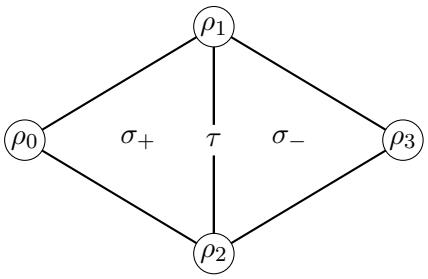

Figure 2.6: *Cones σ_+ and σ_- in the triangulation Σ*

Definition 2.17. Consider the subset $\bigcup_{i=0}^{3} \Pi_i(\theta)$ of edges of Γ. Define a *jigsaw piece of τ* to be the closure of any connected component of $\mathbb{T} \setminus \bigcup_{i=0}^{3} \Pi_i(\theta)$.

Remark 2.18. Each jigsaw piece of τ coincides with a union of tiles of Γ. Since we may lift tiles to $\widetilde{\Gamma}$, we often draw the jigsaw pieces in the universal cover. While the choice of lift is not unique, we often refer to any choice of lift of a given jigsaw piece as being a 'jigsaw piece' itself. The terminology is chosen to suggest that one might move jigsaw pieces around in $\widetilde{\Gamma}$ by deliberately choosing different lifts. In fact, this procedure plays the essential role in the jigsaw transformations introduced in Theorem 2.21 below.

Proposition 2.19. *Let $\sigma_\pm \in \Sigma(3)$ satisfy $\tau = \sigma_+ \cap \sigma_-$ as in Figure 2.6 above, and regard*

$$c_- := \mathfrak{m}_{1,3} \cap \mathfrak{m}_{2,3} \tag{2.4.1}$$

as a subset of the edges in the boundary of $\mathrm{Hex}(\sigma_-)$. The closure of any connected component of $\mathrm{Hex}(\sigma_+) \setminus c_-$ is a jigsaw piece of τ, and every jigsaw piece of τ arises in this way. In particular, if we cut $\mathrm{Hex}(\sigma_+)$ along the edges of c_- then we obtain precisely the jigsaw pieces of τ.

Proof. The rays ρ_1, ρ_2 are contained in both σ_+ and σ_-, so the fundamental hexagons $\mathrm{Hex}(\sigma_\pm)$ share two of their three distinct boundary sides, namely those along the meandering walk $\mathfrak{m}_{1,2}$. We also know the edges of $\mathfrak{m}_{0,1} \cap \mathfrak{m}_{0,2}$ traverse the third boundary side of $\mathrm{Hex}(\sigma_+)$, and cutting $\mathrm{Hex}(\sigma_+)$ along the set c_- requires that we cut along the edges of $\mathfrak{m}_{1,3} \cap \mathfrak{m}_{2,3}$. All together then, the edges that cut out the connected components of $\mathrm{Hex}(\sigma_+) \setminus c_-$ are those in the set

$$\mathfrak{C} := \mathfrak{m}_{1,2} \cup (\mathfrak{m}_{0,1} \cap \mathfrak{m}_{0,2}) \cup (\mathfrak{m}_{1,3} \cap \mathfrak{m}_{2,3}). \tag{2.4.2}$$

This set contains every edge in the boundary of both $\mathrm{Hex}(\sigma)$ and $\mathrm{Hex}(\sigma_-)$. If we regard both $\mathrm{Graph}(\sigma_\pm)$ as subsets of $\mathbb{T}$ as in Remark 2.6(3), we have that

$$\pi(\mathfrak{C}) = \pi\big(\partial\,\mathrm{Hex}(\sigma_+)\big) \cup \pi\big(\partial\,\mathrm{Hex}(\sigma_-)\big) = \mathrm{Graph}(\sigma_+) \cup \mathrm{Graph}(\sigma_-).$$

Now Corollary 2.10 implies that this subset of $\mathbb{T}$ is the unique connected component of the locus $\bigcup_{0\leq i\leq 3}\Pi_i(\theta)$ comprising more than a single edge. Definition 2.17 implies that we may ignore isolated edges of $\bigcup_{0\leq i\leq 3}\Pi_i(\theta)$ when computing the jigsaw pieces, so the jigsaw pieces of τ are precisely the (images under π of the) closures of the connected components of $\mathrm{Hex}(\sigma_+)\setminus c_-$. □

Remarks 2.20. 1. By symmetry, a similar statement holds for the cut of $\mathrm{Hex}(\sigma_-)$ along

$$c_+ := \mathfrak{m}_{0,1} \cap \mathfrak{m}_{0,2} \tag{2.4.3}$$

in $\partial\,\mathrm{Hex}(\sigma_+)$. The proof goes through verbatim if we transpose the numbers 0 and 3 throughout.

2. Since $\mathrm{Hex}(\sigma_+)$ and $\mathrm{Hex}(\sigma_-)$ are different, there are necessarily at least two jigsaw pieces of τ.

Proposition 2.19 and Remark 2.20(1) imply the following result:

Theorem 2.21 (Generalised jigsaw transformation)**.** *Given the θ-stable A-module M_+, we may cut the corresponding fundamental hexagon* $\mathrm{Hex}(\sigma_+)$ *along the edges of c_- and rearrange the resulting jigsaw pieces (i.e., translate each piece by a carefully chosen element of $\mathbb{Z}^2$) in order to obtain* $\mathrm{Hex}(\sigma_-)$ *and hence produce the corresponding θ-stable A-module M_-.*

Example 2.22. Let $G \subset \mathrm{SL}(3,\mathbb{C})$ be a finite abelian subgroup, let $A = \mathbb{C}[x,y,z] * G$ denote the skew group algebra and write Γ for the corresponding consistent dimer model (see Example 1.34). The jigsaw transformations described above recover the G-igsaw transformations introduced by Nakamura [Nak01] in constructing the G-Hilbert scheme of $\mathbb{C}^3$.

Recall that jigsaw pieces are by definition closed subsets of $\mathbb{T}$.

Definition 2.23. We say that an edge $\mathfrak{e} \in \mathfrak{E}$ is an *interior* edge of a jigsaw piece if $\mathfrak{e}$ is not contained in the boundary of the jigsaw piece.

Let Q^+ and Q^- denote the quivers that support the A-modules M_+ and M_-, respectively. Write Q_0^+ and Q_1^+ for the sets of vertices and arrows of the quiver Q^+. Similarly, Q_0^- and Q_1^- denote the sets of vertices and arrows of the quiver Q^-

Corollary 2.24. *Let $a \in Q_1$ have head and tail dual to tiles in different jigsaw pieces of τ. If $a \in Q_1^+$ then $\mathfrak{e}_a \in \Pi_3$. If $a \in Q_1^-$ then $\mathfrak{e}_a \in \Pi_0$*

Proof. Suppose first that $a \in Q_1^+$. Proposition 2.19 shows that $\mathfrak{e}_a \in c_- = \mathrm{supp}(\mathfrak{m}_{1,3} \cap \mathfrak{m}_{2,3})$, so either $\mathfrak{e}_a \in \Pi_3$ or $\mathfrak{e}_a \in \Pi_1 \cap \Pi_2$. However, $\mathfrak{e}_a \notin \mathrm{cosupp}(M_+) = \bigcup_{i=0}^2 \Pi_i$ because $a \in Q_1^+$, giving $\mathfrak{e}_a \in \Pi_3$ as required. A similar proof works for the case when $a \in Q_1^-$. □

Example 2.25. Consider the dimer from Example 1.13. Let $\sigma_{\pm} \in \Sigma(3)$ be the cones such that $\rho_7, \rho_8, \rho_9 \in \sigma_+(1)$ and $\rho_8, \rho_9, \rho_{10} \in \sigma_-(1)$ as in Figure 1.7. Figure 2.7 illustrates that the edges from $\bigcup_{7\leq i\leq 10} \Pi_i(\theta)$ decompose the fundamental domain of $\mathbb{T}$ into two jigsaw pieces. Edges in $\mathfrak{m}_{1,2}$ (and its $\mathbb{Z}^2$-translates) are shown in blue, while edges in c_+ and c_- are coloured green and red respectively. We illustrate several copies of the fundamental hexagons $\mathrm{Hex}(\sigma_{\pm})$ for clarity.

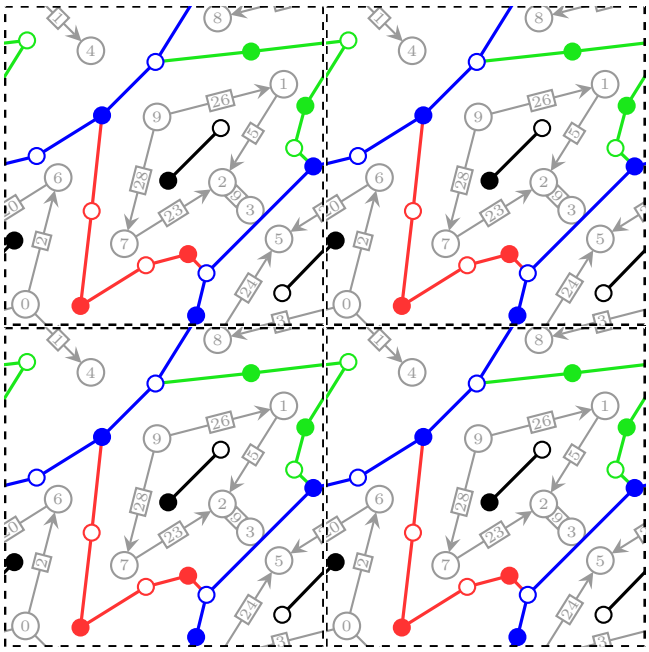

Figure 2.7: *The lift of the edges in* $\bigcup_{7\leq i\leq 10} \Pi_i(\theta)$ *to the universal cover of* $\mathbb{T}$

The fundamental hexagon $\mathrm{Hex}(\sigma_-)$ has boundary comprising edges in red and blue, and the green edges of c_+ split this hexagon into two pieces. Since the union of all edges in blue, red and green is precisely $\bigcup_{7\leq i\leq 10} \Pi_i(\theta)$, we see that these two pieces are precisely the jigsaw pieces of τ. If we keep one of these pieces in place, say that in Figure 2.7 containing the tile dual to the vertex of the quiver labelled 0, and translate the second jigsaw piece along the direction of the blue edges until it sits on the opposite side of the first jigsaw piece, then we cover precisely $\mathrm{Hex}(\sigma_+)$ whose boundary edges are blue and green.

Finally, we discuss some properties of the cuts $c_{\mp}$ of the fundamental hexagons $\mathrm{Hex}(\sigma_{\pm})$.

Lemma 2.26. *The cuts* $c_{\mp}$ *of the fundamental hexagons* $\mathrm{Hex}(\sigma_{\pm})$ *satisfy the following:*

(a) Neither c_- *nor* c_+ *intersects itself;*

(b) If the cuts $c_{\mp}$ *intersect each other, they do so along an odd number of edges;*

(c) If $c_{\mp}$ *meets* $\mathrm{Graph}(\sigma_{\pm})$ *at* $\mathfrak{n}_1$ *and* $\mathfrak{n}_2$ *consecutively, the nodes* $\mathfrak{n}_1$ *and* $\mathfrak{n}_2$ *have different colours.*

Proof. For (a), if c_- intersects itself at a node $\mathfrak{n}$ of $\widetilde{\Gamma}$, then at least three edges of c_- touch $\mathfrak{n}$. Edges on c_- belong alternately to $\Pi_3(\theta)$ and $\Pi_1(\theta) \cap \Pi_2(\theta)$, so two of the three edges touching $\mathfrak{n}$ belong to either set of edges. This is a contradiction because $\Pi_i(\theta)$

are perfect matchings ($i = 1, 2, 3$). The proof for c_+ is similar. For (b), suppose c_- and c_+ intersect. Edges along c_- and c_+ belong alternately to $\Pi_3(\theta)$ and $\Pi_1(\theta) \cap \Pi_2(\theta)$, and to $\Pi_0(\theta)$ and $\Pi_1(\theta) \cap \Pi_2(\theta)$ respectively. Thus the chain of edges along which c_+ and c_- intersect must begin and end with an edge in $\Pi_1(\theta) \cap \Pi_2(\theta)$. Therefore there must be an odd number of them. Finally, for (c), suppose c_- intersects $\mathrm{Graph}(\sigma_+)$ at $\mathfrak{n}_1$ and $\mathfrak{n}_2$, consecutively. Let $\mathfrak{e}_1$ and $\mathfrak{e}_2$ be the first and last edge between $\mathfrak{n}_1$ and $\mathfrak{n}_2$. If $\mathfrak{e}_1 \notin \mathrm{supp}(\mathrm{Graph}(\sigma_+))$, then $\mathfrak{e}_2 \notin \mathrm{supp}(\mathrm{Graph}(\sigma_+))$ and $\mathfrak{e}_1, \mathfrak{e}_2 \in \Pi_0$. Otherwise, $\mathfrak{e}_1, \mathfrak{e}_2 \in \mathrm{supp}(\mathrm{Graph}(\sigma_+))$ and $\mathfrak{e}_1$ coincides with $\mathfrak{e}_2$. In both cases, $\mathfrak{e}_1$ and $\mathfrak{e}_2$ belong to the same set of perfect matchings, and thus $\mathfrak{n}_1$ and $\mathfrak{n}_2$ must have different colours. The same prove holds for c_+ and $\mathrm{Graph}(\sigma_-)$. □

CHAPTER 3

DEFINITION OF REID'S RECIPE

Reid [Rei97] calculated the toric fan Σ of the A-Hilbert scheme A-Hilb$(\mathbb{C}^3)$ for several examples of finite abelian subgroups $A \subset \mathrm{SL}(3,\mathbb{C})$, and in each case introduced a recipe to mark the interior lattice points and line segments of Σ by irreducible representations of A. Craw [Cra05] later proved that this recipe can be carried out for any finite abelian subgroup $A \subset \mathrm{SL}(3,\mathbb{C})$.

In this chapter, we generalise Reid's recipe so that it can be carried out for the toric fan Σ of a particular variety $\mathcal{M}_A$ associated to any consistent dimer model Γ. This recipe marks the interior lattice points and line segments of the fan Σ by vertices of the quiver Q dual to Γ. New phenomena can be observed in this generalisation: line segments in Σ may be marked by more than a single vertex; and vertices may mark more than a single lattice point in Σ. We provide several examples to illustrate the construction, and we establish that this new marking is compatible (as far as can be verified) with 'Geometric Reid's recipe for dimer models' in the sense of Bocklandt–Craw–Quintero-Vélez [BCQV15].

3.1 The 0-generated stability parameter and the module $M(\tau)$

Let Γ be a nondegenerate dimer model with dual quiver Q. Choose once and for all a vertex $0 \in Q_0$. We refer to the tile of Γ dual to 0 as the *zero tile*.

Definition 3.1. A stability parameter $\theta := (\theta_v) \in \Theta$ is said to be 0-*generated* if $\theta_v > 0$ for all $v \neq 0$.

Lemma 3.2. *If $\theta \in \Theta$ is 0-generated, then θ is generic.*

Proof. Let M be a θ-semistable A-module of dimension vector $\underline{1}$. To show θ is generic we must show M is θ-stable. Let $N := (\oplus_{v\in Q_0} W_v, \{\phi_a\}_{a\in Q_1})$ be a nonzero proper submodule of M, so $\theta(N) \geq 0$. Since $\theta(M) = 0$, we have $\theta_0 = -\sum_{v\neq 0} \theta_v$. If $W_0 \neq 0$, then properness of N implies $\theta(N) = \theta_0 + \sum_{v\neq 0} \theta(W_v) < 0$ which is a contradiction. Thus $W_0 = 0$ and hence $\theta(N) > 0$. □

Remark 3.3. It is well known that for any 0-generated stability parameter $\theta \in \Theta$, an A-module M of dimension vector $\underline{1}$ is θ-stable if and only if for all $v \in Q_0$ there exists a path in Q_M from 0 to v (see for example Bocklandt–Craw–Quintero-Vélez [BCQV15, Lemma 3.1(ii)]).

From now on, let $\theta \in \Theta$ be a 0-generated stability parameter.

Notation 3.4. To simplify notation, we write $\mathcal{M}_A$, L_v, M_σ and Π_ρ in place of $\mathcal{M}_A(\theta)$, $L_v(\theta)$, $M_\sigma(\theta)$ and $\Pi_\rho(\theta)$ respectively. We continue to let $\Sigma := \Sigma(\theta)$ denote the toric fan of the moduli space $\mathcal{M}_A$.

Choose once and for all a lift $\widetilde{0} \in \widetilde{Q}$ of the zero vertex. We refer to the tile of $\widetilde{\Gamma}$ dual to $\widetilde{0}$ as the *zero tile in* $\widetilde{\Gamma}$. From now on, for every three-dimensional cone $\sigma \in \Sigma$ in the toric fan of $\mathcal{M}_A$ we choose the lift $\widetilde{Q_\sigma}$ of the subquiver $Q_\sigma \subset Q$ where the vertex $\widetilde{0}$ plays the role of the vertex $\widetilde{v_0}$ as in Section 2.1. It follows that the fundamental hexagon $\mathrm{Hex}(\sigma)$ of every three-dimensional cone $\sigma \in \Sigma(3)$ contains the zero tile in $\widetilde{\Gamma}$.

We now study jigsaw transformations of torus-invariant θ-stable A-modules for a 0-generated stability parameter $\theta \in \Theta$. Choose adjacent three-dimensional cones $\sigma_\pm \in \Sigma(3)$ and let $\tau := \sigma_+ \cap \sigma_-$ be the common face of dimension two as in Figure 2.6. As before, let $M_\pm := M_{\sigma_\pm}$ denote the θ-stable A-modules associated to the three-dimensional cones $\sigma_\pm$, and write $Q^\pm := Q_{M_\pm}$ for the quivers that support these modules. Write $Q_0^\pm$ and $Q_1^\pm$ for the sets of vertices and arrows of $Q^\pm$. It is often convenient to think of $Q^\pm$ as subquivers of $\widetilde{Q}$ in the universal cover as in Example 2.9, where each vertex of $Q_0^\pm$ is drawn inside the dual tile in the corresponding fundamental hexagon $\mathrm{Hex}(\sigma_\pm)$.

Definition 3.5. The *zero jigsaw piece* of any interior line segment $\tau \in \Sigma(2)$ in the triangulation Σ is the jigsaw piece in Γ containing the zero tile. Let $\mathrm{Jig}_\tau(0)$ denote this jigsaw piece.

Recall that both $\mathrm{Hex}(\sigma_+)$ and $\mathrm{Hex}(\sigma_-)$ can be obtained by glueing together the jigsaw pieces of τ. One may ask how many jigsaw pieces of τ lie adjacent to $\mathrm{Jig}_\tau(0)$ in $\mathrm{Hex}(\sigma_+)$ or $\mathrm{Hex}(\sigma_-)$.

Lemma 3.6. *The zero jigsaw piece in* $\mathrm{Hex}(\sigma_\pm)$ *is adjacent to only one jigsaw piece in* $\mathrm{Hex}(\sigma_\pm)$ *that we denote* $\mathrm{Jig}_\tau^\pm(1)$*, and the common boundary of* $\mathrm{Jig}_\tau(0)$ *and* $\mathrm{Jig}_\tau^\pm(1)$ *in* $\mathrm{Hex}(\sigma_\pm)$ *is a single chain of edges from* $c_\mp$*.*

Proof. We give the argument for $\mathrm{Hex}(\sigma_+)$; the argument for $\mathrm{Hex}(\sigma_-)$ is identical except that we swap $+$ and $-$ throughout. Proposition 2.19 implies that every edge in the boundary of each jigsaw piece in $\mathrm{Hex}(\sigma_+)$ lies in either $\partial\,\mathrm{Hex}(\sigma_+) \setminus c_-$ or in c_-. The boundary edges of $\mathrm{Jig}_\tau(0)$ do not all lie in $\partial\,\mathrm{Hex}(\sigma_+) \setminus c_-$ because $\mathrm{Hex}(\sigma_+)$ and $\mathrm{Hex}(\sigma_-)$ are different. Equally, the boundary edges of $\mathrm{Jig}_\tau(0)$ do not all lie in c_-, because Lemma 2.26(a) asserts that c_- does not intersect itself. We claim that the boundary of $\mathrm{Jig}_\tau(0)$ is made up precisely of a chain of edges in c_- and a chain of edges in $\partial\,\mathrm{Hex}(\sigma_+) \setminus c_-$. To see this, note that each chain of edges from c_- in $\partial\,\mathrm{Jig}_\tau(0)$ starts and ends at a node on $\partial\,\mathrm{Hex}(\sigma_+)$. Suppose $\mathrm{Jig}_\tau(0)$ has boundary made of more than one chain of edges from c_-. Figure 3.1 shows the fundamental hexagon $\mathrm{Hex}(\sigma_+)$. The dashed lines indicate all edges in c_-. The shaded area in the fundamental hexagon is

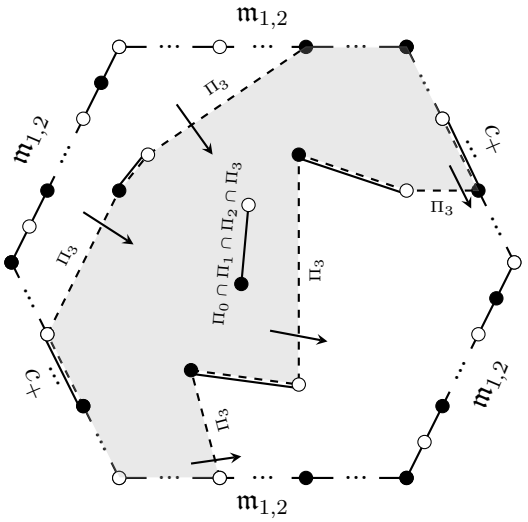

Figure 3.1: *A zero jigsaw piece in* $\mathrm{Hex}(\sigma_+)$ *with two chains of edges from* c_-

the zero jigsaw piece $\mathrm{Jig}_\tau(0)$ with boundary made of two disjoint chains of edges from c_-. The interior edges of $\mathrm{Hex}(\sigma_+)$ which are not labelled belong to all four perfect matchings Π_0, Π_1, Π_2 and Π_3, thus arrows dual to those edges are not in Q^+ or Q^-. Without loss of generality, suppose that the first chain of edges from c_- in $\partial\,\mathrm{Jig}_\tau(0)$ starts at a black node on $\partial\,\mathrm{Hex}(\sigma_+)$. Lemma 2.26 part (c) implies that the chain of edges will end at a white node on $\partial\,\mathrm{Hex}(\sigma_+)$. By Lemma 2.26 part (b), c_- and c_+ will intersect along an odd number of edges, so the second chain of edges from c_- in $\partial\,\mathrm{Jig}_\tau(0)$ starts at a white node on $\partial\,\mathrm{Hex}(\sigma_+)$. It ends at a black node on $\partial\,\mathrm{Hex}(\sigma_+)$ by Lemma 2.26 part (c). Therefore, the edges in $\Pi_3 \setminus (\Pi_0 \cup \Pi_1 \cup \Pi_2)$ which make up one of the disjoint chains of edges of c_- along $\partial\,\mathrm{Jig}_\tau(0)$ are dual to arrows in Q^+ with tail at vertices dual to tiles in a non-zero jigsaw piece and head at vertices dual to tiles in $\mathrm{Jig}_\tau(0)$. Let $v \in Q_0$ be one of the vertices dual to a tile in a nonzero jigsaw piece such that there exists an arrow in Q^+ with tail at v and head at a vertex dual to a tile in $\mathrm{Jig}_\tau(0)$. Then, there is no path in Q^+ from any vertex dual to a tile in $\mathrm{Jig}_\tau(0)$ to v. In particular, there is no path in Q^+ from 0 to v, contradicting our choice of stability parameter θ (see Remark 3.3). Hence, there cannot be more than one chain of edges from c_- in $\partial\,\mathrm{Jig}_\tau(0)$, and the result follows. □

Our next goal is to show that the modules $M_\pm$ share a common quotient module $M(\tau)$, and to do this we first define the subquiver $Q(\tau)$ of Q that supports $M(\tau)$.

Lemma 3.7. *Let* $\mathfrak{e}_a \in \mathfrak{E}$ *be an interior edge of a jigsaw piece of* τ*. If the dual arrow satisfies* $a \in Q_1^+ \cup Q_1^-$*, then in fact* $a \in Q_1^+ \cap Q_1^-$*. In particular,*

$$\{a \in Q_1^+ \mid \mathfrak{e}_a \text{ is an interior edge of } \mathrm{Jig}_\tau(0)\} = \{a \in Q_1^- \mid \mathfrak{e}_a \text{ is an interior edge of } \mathrm{Jig}_\tau(0)\}.$$

Proof. Since $\mathfrak{e}_a \in \mathfrak{E}$ is an interior edge of a jigsaw piece of τ, Definition 2.17 and Corollary 2.10 imply that either $\mathfrak{e}_a \notin \bigcup_{0\le i\le 3} \Pi_i$, or $\mathfrak{e}_a \in \bigcap_{0\le i\le 3} \Pi_i$. The assumption $a \in Q_1^+ \cup Q_1^-$ is equivalent to $\mathfrak{e}_a \notin \bigcap_{0\le i\le 3} \Pi_i$. It follows that $\mathfrak{e}_a \notin \bigcup_{0\le i\le 3} \Pi_i$ which is equivalent to $a \in Q_1^+ \cap Q_1^-$ as required. The second statement is immediate. □

Definition 3.8. Let $Q(\tau)$ be the subquiver of Q with vertex set

$$Q_0(\tau) := \{v \in Q_0 \mid v \text{ is dual to a tile in } \mathrm{Jig}_\tau(0)\}$$

and arrow set

$$\begin{aligned} Q_1(\tau) &:= \{a \in Q_1^+ \mid \mathfrak{e}_a \text{ is an interior edge of } \mathrm{Jig}_\tau(0)\} \\ &= \{a \in Q_1^- \mid \mathfrak{e}_a \text{ is an interior edge of } \mathrm{Jig}_\tau(0)\}, \end{aligned}$$

where the equality follows from Lemma 3.7. Define $M(\tau) := (\oplus_{v \in Q_0(\tau)}\mathbb{C}, \{\phi_a\}_{a \in Q_1})$ by setting

$$\phi_a = \begin{cases} 1 & \text{if } a \in Q_1(\tau) \\ 0 & \text{else} \end{cases}.$$

Remark 3.9. We regard $M(\tau)$ as a representation of Q (that is, a $\mathbb{C}Q$-module) with dimension vector $\underline{d} := (d_v) \in \mathbb{N}^{Q_0}$ given by $d_v = 1$ for $v \in Q_0(\tau)$ and $d_v = 0$ otherwise. Notice that

1. at least one entry of $\underline{d}$ equals 1, because $\mathrm{Jig}_\tau(0)$ is non-empty; and
2. at least one entry of $\underline{d}$ equals 0, because there are at least two jigsaw pieces of τ.

The next result establishes in particular that $M(\tau)$ is an A-module (note that $M(\tau)$ is not equal to the θ-stable A-module M_τ associated to the cone $\tau \in \Sigma(2)$ in Definition 2.2).

Proposition 3.10. *There exist nonzero proper A-submodules $N_\pm(\tau) \subset M_\pm$ such that*

$$M_+/N_+(\tau) \cong M(\tau) \cong M_-/N_-(\tau).$$

Proof. Recall that $M_+ = (\oplus_{v \in Q_0}\mathbb{C}, \{\psi_a\}_{a \in Q_1})$, where $\psi_a = 1$ for $a \in Q_1^+$ and $\psi_a = 0$ otherwise. Define a $\mathbb{C}Q$-module $N_+(\tau) := (\oplus_{v \in Q_0 \setminus Q_0(\tau)}\mathbb{C}, \{\phi_a\}_{a \in Q_1})$ by setting

$$\phi_a = \begin{cases} 1 & \text{if } a \in Q_1^+ \text{ and } \mathsf{t}(a), \mathsf{h}(a) \in Q_0 \setminus Q_0(\tau) \\ 0 & \text{else} \end{cases}.$$

To show that $N_+(\tau)$ is an A-submodule of M_+, we must show that there does not exist $a \in Q_1^+$ with $\mathsf{t}(a) \in Q_0 \setminus Q_0(\tau)$ and $\mathsf{h}(a) \in Q_0(\tau)$. Suppose for a contradiction that $a \in Q_1^+$ is one such arrow. The head of a is dual to a tile in $\mathrm{Jig}_\tau(0)$ and the tail is not, so Lemma 3.6 implies that $\mathsf{t}(a)$ is dual to a tile in $\mathrm{Jig}_\tau^+(1)$ and, moreover, that the dual edge $\mathfrak{e}_a \in c_-$ lies in the unique chain of edges from c_- that forms part of the boundary of $\mathrm{Jig}_\tau(0)$. The edges of c_- alternate between those in Π_3 and those in $\Pi_1 \cap \Pi_2$, and we know $\mathfrak{e}_a \in \Pi_3$ by Corollary 2.24. Since $\mathsf{t}(a)$ is dual to a tile in $\mathrm{Jig}_\tau^+(1)$ and $\mathsf{h}(a)$ is dual to a tile in $\mathrm{Jig}_\tau(0)$, it follows that every arrow $b \in Q_1^+$ in the opposite direction (that is, $\mathsf{t}(b) \in Q_0(\tau)$ and $\mathsf{h}(b) \in Q_0 \setminus Q_0(\tau)$) satisfies $\mathfrak{e}_b \in \Pi_1 \cap \Pi_2$. However, $\mathrm{cosupp}(M_+) = \bigcup_{0 \le i \le 2} \Pi_i$, so no such arrow $b \in Q_1^+$ can exist. This is a contradiction, because a vertex $v_0 \in Q_0 \setminus Q_0(\tau)$ exists by Remark 3.9 and there must exist at least one path in Q^+ from 0 to v_0 by Remark 3.9. This contradiction proves the claim, so $N_+(\tau)$ is a $\mathbb{C}Q$-submodule of M_+. Regarding M_+ as a representation of the quiver Q,

we have that $N_+(\tau)$ is a subrepresentation of M_+. Since M_+ satisfies the relations $\mathcal{R}$ in Q, it follows that $N_+(\tau)$ does as well, so $N_+(\tau)$ is an A-submodule of M_+.

The quotient A-module $M_+/N_+(\tau)$ is isomorphic to $(\oplus_{v\in Q_0(\tau)}\mathbb{C}, \{\varphi_a\}_{a\in Q_1})$ where

$$\varphi_a = \begin{cases} 1 & \text{if } a \in Q_1^+ \text{ and } \mathtt{t}(a), \mathtt{h}(a) \in Q_0(\tau) \\ 0 & \text{else} \end{cases} .$$

If an arrow $a \in Q_1^+$ has both head and tail in $Q_0(\tau)$, then the dual edge $\mathfrak{e}_a$ is an interior edge of $\mathrm{Jig}_\tau(0)$, so this quotient module is $M(\tau)$ as required. The proof of the analogous result for $N_-(\tau)$ is identical, except in that we swap $+$ with $-$ and 0 with 3 throughout. □

Remark 3.11. As in the proof of Lemma 3.6, one can show that the only arrows in $Q^\pm$ with head dual to a tile in $\mathrm{Jig}_\tau^\pm(1)$ have tail dual to a tile in $\mathrm{Jig}_\tau(0) \cup \mathrm{Jig}_\tau^\pm(1)$. Using a similar argument to the one in the proof of Lemma 3.10, suppose there exists an arrow in $Q^\pm$ from a tile in a jigsaw piece $\mathrm{Jig}_\tau(i)$ $(i \neq 0, 1)$ to a tile in $\mathrm{Jig}_\tau(1)$. Then, there are no arrows in $Q^\pm$ from tiles in $\mathrm{Jig}_\tau(1)$ to tiles in $\mathrm{Jig}_\tau(i)$. Hence, for any tile v in $\mathrm{Jig}_\tau(i)$, there does not exist a path in $Q^\pm$ from 0 to it, a contradiction as $M_\pm$ is θ-stable.

Example 3.12. Consider the dimer model Γ with dual quiver Q presented in Figure 3.2. The fan Σ of $\mathcal{M}_A$ for $\theta = (-7, 1, 1, \ldots, 1)$ is depicted in Figure 3.3.

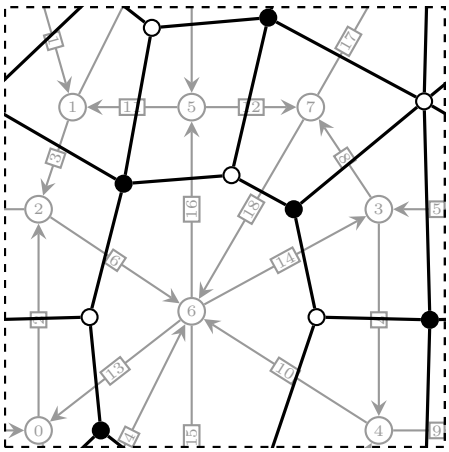

Figure 3.2: *The dimer model* Γ *with dual quiver* Q

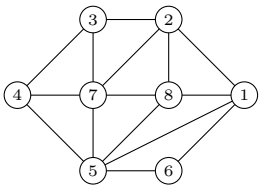

Figure 3.3: *The fan* Σ *of* $\mathcal{M}_A$

Let σ_+ and σ_- denote the cones of Σ with ray generators ρ_5, ρ_7, ρ_8 and ρ_2, ρ_7, ρ_8, respectively. The arrows and vertices in Figure 3.4 show the lift of the quiver Q_{σ_+} that supports M_{σ_+} to the universal cover of Γ.

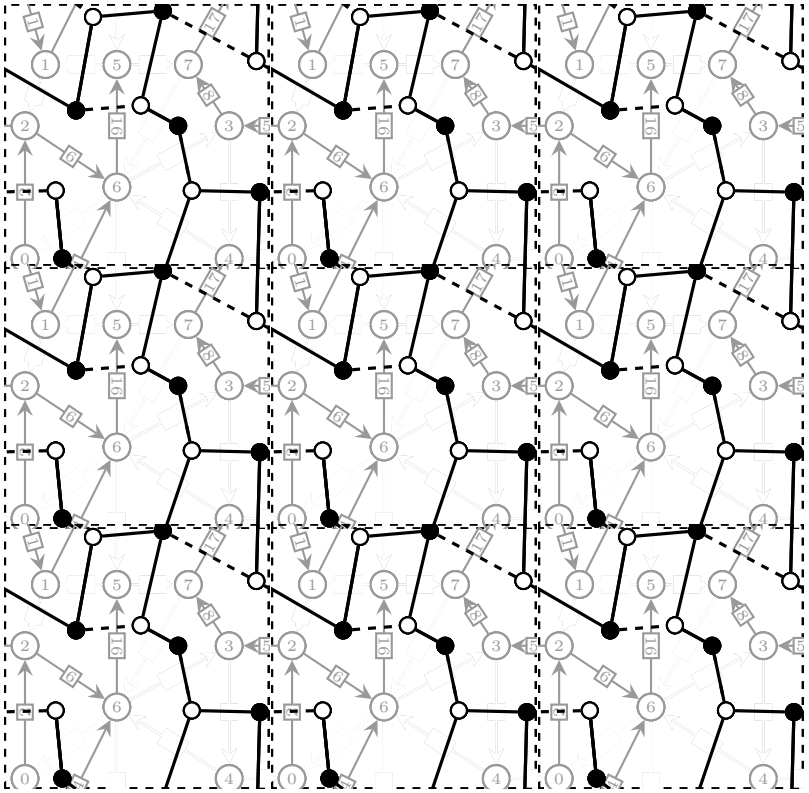

Figure 3.4: *The honeycomb tiling of* $\mathbb{R}^2$ *by* $\mathrm{Hex}(\sigma_+)$ *and the lift of edges in* c_-

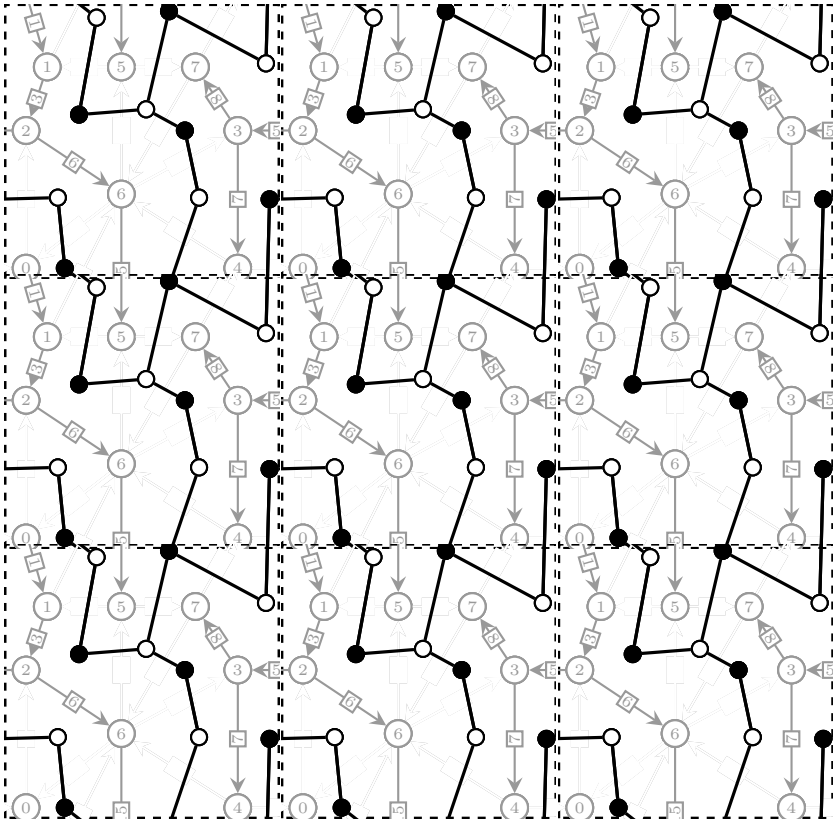

Figure 3.5: *The honeycomb tiling of* $\mathbb{R}^2$ *by* $\mathrm{Hex}(\sigma_-)$

The zero jigsaw piece has two tiles, while the one jigsaw piece is made out of the tiles dual to the vertices $2, 3, 6$ and 7. The jigsaw pieces can be rearranged to give the fundamental hexagon $\mathrm{Hex}(\sigma_-)$ depicted in Figure 3.5.

3.2 On consistency and sections of tautological bundles

The modules $N_\pm(\tau)$ from Proposition 3.10 are not isomorphic in general. Nevertheless, our goal in this section is to prove that the set of minimal A-module generators of $N_\pm$ coincide. For this we must recall some geometric properties of the tautological bundle $T = \bigoplus_{v \in Q_0} L_v$ on the fine moduli space $\mathcal{M}_A$, where A is the Jacobian algebra of a consistent dimer model Γ.

Assumption 3.13. *From now on, assume that Γ is a consistent dimer model.*

Recall from Chapter 1 that every torus-invariant section of a line bundle L on the toric variety $\mathcal{M}_A$ is a multiple of a monomial x^D in the Cox ring $S := \mathbb{C}[x_\rho \mid \rho \in \Sigma(1)]$ of $\mathcal{M}_A$. Since Γ is a consistent dimer model, the tautological $\mathbb{C}$-algebra isomorphism $\phi\colon A \to \mathrm{End}_{\mathcal{O}_{\mathcal{M}_A}}(T)$ from Theorem 1.49 associates to each path p in Q the torus-invariant section

$$\begin{aligned} x^{\mathrm{div}(p)} &= \prod_{a \in \mathrm{supp}(p)} x^{\mathrm{div}(a)} \\ &= \prod_{\{\rho \in \Sigma(1) \mid \mathfrak{e}_a \in \Pi_\rho\}} x_\rho \qquad \text{by (1.5.1)} \end{aligned}$$

of the line bundle $L_{\mathsf{h}(p)} \otimes L_{\mathsf{t}(p)}^{-1}$. For any $v \in Q_0$, Lemma 1.52 shows that $L_v = \mathcal{O}_{\mathcal{M}_A}(\mathrm{div}(p))$, where p is any path from vertex 0 to vertex v. Hence by restricting to either of the affine open subsets $U_{\sigma_\pm} := U_\pm \subseteq \mathcal{M}_A$, we have that

$$L_v|_{U_\pm} \cong \mathcal{O}_{U_\pm}(\mathrm{div}(p_\pm)),$$

where $p_\pm$ is any path in $Q^\pm$ from 0 to v, so $x^{\mathrm{div}(p_\pm)}$ generates $L_v|_{U_\pm}$ as an $\mathcal{O}_{U_\pm}$-module.

Remark 3.14. Since $L_v = \mathcal{O}_{\mathcal{M}_A}(\mathrm{div}(p_\pm))$, we have $\mathsf{h}(p_+) = \mathsf{h}(p_-)$ as vertices of Q. However, the lifts to the universal cover of the paths $p_\pm$ differ in general (unless $v = 0$, in which case $L_0 \cong \mathcal{O}_{\mathcal{M}_A}$ when $p_\pm$ both equal the trivial path at vertex 0).

Let $\sigma_\pm \in \Sigma(3)$ satisfy $\tau = \sigma_+ \cap \sigma_-$ as in Figure 2.6. The cones σ_+ and σ_- have ray generators ρ_0, ρ_1, ρ_2 and ρ_1, ρ_2, ρ_3, respectively.

Lemma 3.15. *For $v \in Q_0^+$, let p be a path in Q^+ from vertex 0 to vertex v. Then v is dual to a tile in $\mathrm{Jig}_\tau^+(1)$ if and only if x_{ρ_3} appears with multiplicity one in the labelling section $x^{\mathrm{div}(p)}$.*

Proof. The path p must traverse one arrow a with tail in $\mathrm{Jig}_\tau(0)$ and head in $\mathrm{Jig}_\tau^+(1)$, so $\mathfrak{e}_a \in \Pi_3$ by Corollary 2.24 and hence $x_{\rho_3} | x^{\mathrm{div}(a)}$. By the proof of Lemma 3.6, since p is a path in Q^+, the path p cannot travel from $\mathrm{Jig}_\tau^+(1)$ to $\mathrm{Jig}_\tau(0)$. Therefore, every other arrow a' in the path p has head and tail in the same jigsaw piece, either $\mathrm{Jig}_\tau(0)$ or $\mathrm{Jig}_\tau^+(1)$, so the dual edge $\mathfrak{e}_{a'}$ is an interior edge in a jigsaw piece of τ. Since $a' \in Q_1^+$,

Lemma 3.7 implies that $a' \in Q_1^-$. In particular, x_{ρ_3} does not divide $x^{\mathrm{div}(a')}$ because $\mathrm{cosupp}(M_-) = \bigcup_{1\leq i\leq 3} \Pi_i$. Thus, a is the only arrow in the path p whose label is divisible by x_{ρ_3}, so the multiplicity of x_{ρ_3} in $x^{\mathrm{div}(a)}$ equals one as required. □

Remark 3.16. A vertex $v \in Q_0^-$ is dual to a tile in $\mathrm{Jig}_\tau^-(1)$ if and only if x_{ρ_0} appears with multiplicity one in the section $x^{\mathrm{div}(p)}$ on any path p in Q_1^- from vertex 0 to vertex v. The proof is identical to that of Lemma 3.15 except in that we replace + by − and 0 by 3 throughout.

Proposition 3.17. *There exists a jigsaw piece* $\mathrm{Jig}_\tau(1) \subset \mathbb{T}$ *that lifts to the jigsaw piece* $\mathrm{Jig}_\tau^+(1)$ *in* $\mathrm{Hex}(\sigma_+)$ *and to* $\mathrm{Jig}_\tau^-(1)$ *in* $\mathrm{Hex}(\sigma_-)$.

Proof. We first compute the toric coordinate function on the chart U_+ corresponding to the face τ of σ_+ satisfying $\tau = \sigma_+ \cap \sigma_-$. Let $m \in M$ be the primitive vector that lies perpendicular to the cone τ such that $\langle m, n\rangle \geq 0$ for all $n \in \sigma_+$. Since $\rho_1, \rho_2 \subset \tau$, we have $\langle m, v_{\rho_1}\rangle = \langle m, v_{\rho_2}\rangle = 0$. Also, since ρ_0 and ρ_3 lie on opposite sides of τ, our choice of m gives $\langle m, v_{\rho_0}\rangle > 0$ and $\langle m, v_{\rho_3}\rangle < 0$, and since m is a primitive generator and both cones $\sigma_\pm$ are basic, we have $\langle m, v_{\rho_0}\rangle = 1$ and $\langle m, v_{\rho_3}\rangle = -1$. Thus, the toric coordinate function on U_+ corresponding to the face τ of σ_+ satisfies $x^m = (x_{\rho_0}/x_{\rho_3}) \cdot x^{m'}$, where $x^{m'} \in \mathbb{C}[M]$ is independent of $x_{\rho_0}, x_{\rho_1}, x_{\rho_2}, x_{\rho_3}$.

Let $v \in Q_0$ be dual to a tile of $\mathrm{Jig}_\tau^+(1)$ in $\mathrm{Hex}(\sigma_+)$ and let $p_\pm$ be any path in $Q^\pm$ from 0 to v. We now compute the generating section $x^{\mathrm{div}(p_-)}$ of $L_v|_{U_-}$ directly from $x^{\mathrm{div}(p_+)}$ using the transition function for L_v from U_+ to U_-. Indeed, given the section $x^{\mathrm{div}(p_+)}$ that generates $L_v|_{U_+}$, the section $x^{\mathrm{div}(p_-)}$ that generates $L_v|_{U_-}$ is then obtained by multiplying $x^{\mathrm{div}(p_+)}$ by the minimal power of the above Laurent monomial x^m such that the resulting Laurent monomial lies in $\mathbb{C}[\sigma_-^\vee \cap M]$, as $m \in M$ is the primitive vector perpendicular to the common face τ of σ_+ and σ_-. Putting this together gives

$$x^{\mathrm{div}(p_-)} = x^{\mathrm{div}(p_+)} \cdot \left(\frac{x_{\rho_0}}{x_{\rho_3}} \cdot x^{m'}\right)^d \in \mathbb{C}[\sigma_-^\vee \cap M] \tag{3.2.1}$$

for some Laurent monomial $x^{m'} \in \mathbb{C}[M]$ that is independent of $x_{\rho_0}, x_{\rho_1}, x_{\rho_2}, x_{\rho_3}$, where $d \in \mathbb{N}$ is the minimal non-negative integer such that (3.2.1) holds. Now, p_- is a path in the quiver Q^- and $\Pi_3 \subseteq \mathrm{cosupp}(Q^-)$, so the left hand side of (3.2.1) is independent of x_{ρ_3}. The same is true of $x^{m'}$, and yet x_{ρ_3} appears in $x^{\mathrm{div}(p_+)}$ with multiplicity one by Lemma 3.15, so we have $d = 1$.

We now claim that the vertex $v = \mathsf{h}(p_-) \in Q_0^-$ is dual to a tile in $\mathrm{Jig}_\tau^-(1)$. To see this, note that p_+ is a path in Q^+ and $\Pi_0 \subseteq \mathrm{cosupp}(Q^+)$, so $x^{\mathrm{div}(p_+)}$ is independent of x_{ρ_0}. The monomial $x^{m'}$ is also independent of x_{ρ_0}, and since $d = 1$ we conclude from equation (3.2.1) that x_{ρ_0} appears in $x^{\mathrm{div}(p_-)}$ with multiplicity one. The claim follows directly from Remark 3.16.

Thus far, we know that for a vertex $v \in Q_0$ such that $v = \mathsf{h}(p_+) \in Q_0^+$ is dual to a tile in $\mathrm{Jig}_\tau^+(1)$, we have that the vertex $v = \mathsf{h}(p_-) \in Q_0^-$ is dual to a tile in $\mathrm{Jig}_\tau^-(1)$. This is true for the vertex v dual to some tile in $\mathrm{Jig}_\tau^+(1)$, and hence for the vertices dual to every tile in $\mathrm{Jig}_\tau^+(1)$. The statement is symmetric, so $\mathrm{Jig}_\tau^\pm(1)$ are two lifts of the same jigsaw piece of τ as required. □

Remark 3.18. The non-negative integer d from equation (3.2.1) equals the degree of the line bundle L_v on the toric curve $C_\tau \cong \mathbb{P}^1$ in $\mathcal{M}_A$ defined by $\tau \in \Sigma(2)$.

Definition 3.19. Let $Q_\pm(\tau)$ denote the subquiver of $Q^\pm$ that supports the A-module $N_\pm(\tau)$. Explicitly, $Q_\pm(\tau)$ has vertex set $Q_0 \setminus Q_0(\tau)$ and arrow set $\{a \in Q_1^\pm \mid \mathsf{t}(a), \mathsf{h}(a) \in Q_0 \setminus Q_0(\tau)\}$.

Corollary 3.20. *The set of minimal A-module generators of $N_\pm(\tau)$ coincide. Equivalently, the source vertices of the quivers $Q_\pm(\tau)$ coincide.*

Proof. We claim that the source vertices of the quivers $Q_\pm(\tau)$ are dual to tiles in $\mathrm{Jig}_\tau^\pm(1)$. To see this, let $v \in Q_0 \setminus Q_0(\tau)$ be any vertex. By our choice of stability parameter $\theta \in \Theta$, there exist paths $p^\pm$ in the quivers $Q^\pm$, each with tail at 0 and head at v. Lemma 3.6 implies that each path $p^\pm$ travels along precisely one arrow $a^\pm$ with tail in $Q_0(\tau)$ and head in $Q_0 \setminus Q_0(\tau)$. Thus, there is a path in $Q_\pm(\tau)$ from the vertex $\mathsf{h}(a^\pm)$ to the vertex v, and the claim follows because $\mathsf{h}(a^\pm)$ is dual to a tile in $\mathrm{Jig}_\tau^\pm(1)$.

To complete the proof, Remark 3.11 implies that the only arrows of $Q_\pm(\tau)$ with head dual to a tile of $\mathrm{Jig}_\tau^\pm(1)$ have tail dual to a tile of $\mathrm{Jig}_\tau^\pm(1)$. It follows from the above claim that the source vertices of $Q_\pm(\tau)$ are precisely the source vertices of the quivers with vertex set $\{v \in Q_0^\pm \mid v \text{ is dual to a tile in } \mathrm{Jig}_\tau^\pm(1)\}$ and arrow set $\{a \in Q_1^\pm \mid \mathfrak{e}_a \text{ is an interior edge of } \mathrm{Jig}_\tau^\pm(1)\}$. These latter two quivers coincide by Proposition 3.17, and hence so do the source vertices of the quivers $Q_\pm(\tau)$. □

3.3 Combinatorial Reid's recipe

We are now in a position to introduce Reid's recipe for a consistent dimer model Γ. We first introduce the recipe for interior line segments of Σ.

Definition 3.21 (**Reid's recipe for interior line segments**)**.** Let $\tau \in \Sigma(2)$ define an interior line segment of Σ. We say a vertex $v \in Q_0$ *marks the line segment* τ if v is one of the common source vertices of the quivers $Q_\pm(\tau)$ as in Corollary 3.20

Remarks 3.22.

1. Reid's recipe never marks an interior line segment with the vertex $0 \in Q_0$, because the zero vertex cannot be a vertex of $Q_\pm(\tau)$.
2. Reid's recipe does not mark boundary line segments of Σ with any vertices, because any such line segment $\tau \in \Sigma(2)$ is not of the form $\tau = \sigma_+ \cap \sigma_-$ for cones $\sigma_\pm \in \Sigma(3)$.

We now introduce Reid's recipe for marking interior lattice points of Σ. For $v \in Q_0$, write $S_v := \mathbb{C}e_v$ for the corresponding vertex simple A-module. For any θ-stable A-module M, the module S_v is contained in the socle of M if and only if S_v is a submodule of M, in which case we write $S_v \subseteq \mathrm{soc}(M)$.

Definition 3.23 (**Reid's recipe for interior lattice points**)**.** Let $\rho \in \Sigma(1)$ define an interior lattice point of Σ. We say that a vertex $v \in Q_0$ *marks the lattice point* ρ if for every torus-invariant point $y \in D_\rho$, $S_v \subseteq \mathrm{soc}(M_y)$ where M_y is the θ-stable A-module associated to the point $y \in \mathcal{M}_A$.

Remarks 3.24. 1. Reid's recipe never marks a lattice point with the vertex $0 \in Q_0$ because our choice of stability parameter θ ensures that for any dimer model Γ, S_0 is never in $\mathrm{soc}(M_y)$ for every torus-invariant point $y \in \mathcal{M}_A$.

2. Note that for $\rho \in \Sigma(1)$ and $v \in Q_0$, $S_v \subseteq \mathrm{soc}(M_\rho)$ implies that $S_v \subseteq \mathrm{soc}(M_y)$ for every torus-invariant point $y \in D_\rho$. Indeed, if $S_v \subseteq \mathrm{soc}(M_\rho)$ every arrow in M_y with tail at vertex v is zero. As the zero arrows of M_ρ are zero in M_y, $S_v \subseteq \mathrm{soc}(M_y)$.

3. Reid's recipe marks every interior lattice point of Σ with at least one vertex of Q. Indeed, if $\rho \in \Sigma(1)$ defines an interior lattice point, Remark 2.4 shows that the A-module M_ρ is nilpotent. It follows that there exists a nonzero vertex $v \in Q_0$ such that M_ρ contains S_v as a submodule, in which case vertex v marks ρ by the previous remark.

Example 3.25. Consider the dimer model from Example 1.13. The fan of $\mathcal{M}_A$ for the 0-generated stability parameter $\theta = (-9, 1, 1, \ldots, 1)$ is presented in Example 1.35. By looking at the jigsaw transformation in Example 2.25, it is clear from Figure 2.7 that the primitive generators of the degree 1 jigsaw piece are 3 and 9. Hence, the vertices 3 and 9 mark the unique line segment $\tau \in \Sigma$ with $\rho_8, \rho_9 \subset \tau$. Figure 3.6 presents the perfect matchings associated to the rays ρ_8 and ρ_9 and their underlying quiver. Both S_2 and S_5 lie in the socle of M_{ρ_8}, while only S_2 lies in the socle of M_{ρ_3}. Hence, vertices 2 and 5 mark the lattice point ρ_8, while the vertex 2 marks the lattice point ρ_9. By drawing the underlying quivers of the θ-stable A-modules M_y for all torus-invariant points y in D_{ρ_8} and D_{ρ_9}, one can verify that these are the only vertices marking the lattice points ρ_8 and ρ_9.

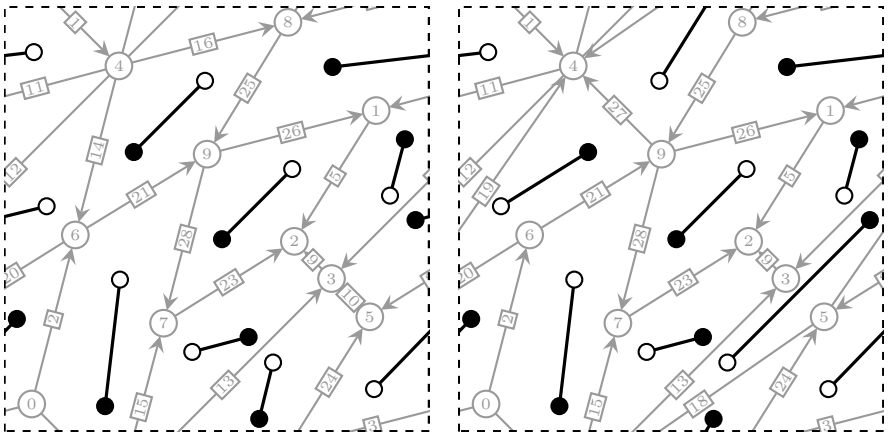

(a) Π_8 (b) Π_9

Figure 3.6: *The θ-stable perfect matchings Π_8 and Π_9 for Example 1.35*

Remark 3.26. The combinatorial input required for computing Reid's recipe is the set of θ-stable perfect matchings of Γ. Raf Bocklandt has written a code in GAP which produces for any choice of convex polygon Δ a quiver Q dual to a dimer model Γ with characteristic polygon Δ. The output of the code also includes the set of θ-stable perfect matchings of Γ, for whatever choice of generic stability parameter θ.

3.4 Compatibility with classical Reid's recipe

Now that we have defined Reid's recipe for a consistent dimer model, we must verify that our description is compatible with that in the literature. We begin with the classical Reid's recipe from Reid [Rei97] and Craw [Cra05].

Theorem 3.27 (**Reid's recipe for the G-Hilbert scheme**). *Let G be a finite abelian subgroup of $\mathrm{SL}(3,\mathbb{C})$ and let Σ be the fan of the G-Hilbert scheme. Reid's recipe for Σ as in Definitions 3.21 and 3.23 agrees with the classical recipe from Reid [Rei97] and Craw [Cra05].*

Proof. In the classical version of Reid's recipe for the G-Hilbert scheme, the vertex set of the McKay quiver Q is the set $\mathrm{Irr}(G)$ of isomorphism classes of irreducible representation of G.

Consider first the marking of an interior lattice point $\rho \in \Sigma(1)$. Craw–Ishii [CI04, Proposition 9.1] proved that a vertex $v \in Q_0$ of the McKay quiver marks ρ in the classical recipe if and only if S_v is a submodule of every G-cluster defined by a torus-invariant point of D_ρ. This agrees with the marking from Definition 3.23.

Now let $\tau \in \Sigma(2)$ be an interior line segment in Σ. To each τ we associated a G-invariant ratio $m_\tau^+ : m_\tau^-$ of monomials in the Cox ring $S = \mathbb{C}[x,y,z]$ of $X := \mathbb{C}^3/G$. A vertex v marks the line segment τ if v is the common character space of the monomials $m_\tau^\pm$. We now show that this marking is compatible with Definition 3.21. In G-Hilb$(\mathbb{C}^3)$, a G-igsaw transformation along τ from σ_+ to σ_- moves every tile v such that the label of the path from 0 to v is divisible by m_τ. Let v be the unique vertex such that $\mathrm{div}(p) = m_\tau^-$. The vertex v is the unique irredundant generator of the degree one jigsaw piece $\mathrm{Jig}_\tau^+(1)$, and by Proposition 3.17 and Corollary 3.20 the marking of interior line segments in Δ by the classical recipe of Reid and Craw agrees with that by Definition 3.21. □

Remark 3.28. It follows from [Cra05, Corollary 4.6] that at least in the case of the G-Hilbert scheme, every vertex of the quiver Q appears 'once' in the marking of interior lattice points and line segments of Σ.

3.5 Compatibility with geometric Reid's recipe

We now consider geometric Reid's recipe in the sense of Cautis-Logvinenko [CL09], Logvinenko [Log10], Cautis–Craw–Logvinenko [CCL12] and Bocklandt–Craw–Quintero-Vélez [BCQV15]. We will show that the marking of interior lattice points by vertices of Q according to Definition 3.23 is compatible with the generalisation by Bocklandt–Craw–Quintero-Vélez [BCQV15, Theorem 1.4] of the work of Logvinenko [Log10, Theorem 1.1]. We can only give a partial link here, namely, for the marking of interior lattice points and certain line segments that are marked with a single vertex. For the general statements we need first to prove that every vertex of Q appears 'once' on the fan Σ.

Rather than using the functor $- \overset{\mathbf{L}}{\otimes}_A T \colon D^b(\mathrm{mod}\, -A) \to D^b(\mathrm{coh}(\mathcal{M}_A))$ from Theo-

rem 1.49 we consider

$$\Psi(-) := T^\vee \overset{\mathbf{L}}{\otimes}_A -\colon D^b(\operatorname{mod} -A) \to D^b(\operatorname{coh}(\mathcal{M}_A))$$

where $T^\vee = \bigoplus_v L_v^{-1}$. This equivalence is chosen to be compatible with the equivalence considered by [CL09]. Recall that for $v \in Q_0$, we write S_v for the vertex simple A-module $\mathbb{C}e_v$. Bocklandt–Craw–Quintero-Vélez [BCQV15, Theorem 1.4] studied the image $\Psi(S_v)$ for v a vertex of a quiver Q dual to a consistent dimer model generalising [Log10, Theorem 1.1]:

Theorem 3.29. *[BCQV15, Theorem 1.4] Let Γ be a consistent dimer model with dual quiver Q. Then for any $v \in Q_0$, $\Psi(S_v)$ is quasi-isomorphic to one of the following:*

(i) L_v^{-1} restricted to a connected union of compact irreducible torus-invariant divisors;

(ii) L_v^{-1} restricted to a compact torus-invariant curve;

(iii) $\mathcal{F}[1]$ for a sheaf $\mathcal{F}$ supported on a connected union of compact torus-invariant divisors;

(iv) The dualising complex of the compact exceptional locus $f^{-1}(x_0)$, where $f : \mathcal{M}_A \to X$ is a crepant resolution and x_0 is the unique torus-invariant point of X.

The insight of geometric Reid's recipe, due to Cautis–Logvinenko [CL09], and expanded upon by Logvinenko [Log10] and Cautis–Craw–Logvinenko [CCL12], is that the support of the object $\Psi(S_v)$ is closely related to classical Reid's recipe. Theorem 3.29 parts (i) and (ii) suggest a marking of the interior lattice points and some of the interior line segments of Σ by vertices of Q. For the purposes of this thesis, geometric Reid's recipe marks a lattice point ρ with the vertex $v \in Q_0$ if $\Psi(S_v)$ is quasi-isomorphic to L_v^{-1} restricted to the compact irreducible torus-invariant divisor D_ρ. It marks a line segment τ of Σ with the vertex $v \in Q_0$ if $\Psi(S_v)$ is quasi-isomorphic to L_v^{-1} restricted to the compact torus-invariant curve C_τ. The next result provides the appropriate generalisation to consistent dimer models of a result of Cautis–Craw–Logvinenko [CCL12, Proposition 4.8].

Lemma 3.30. *Let $\sigma \in \Sigma(3)$ and suppose S_v lies in the socle of the corresponding torus-invariant θ-stable A-module M_σ. Then the vertex v marks either:*

1. *an edge of the triangle σ, i.e., there exists $\tau \in \Sigma(2)$ with $\tau \subset \sigma$ such that v marks τ. In this case, S_v lies in the socle of every θ-stable A-module in the curve C_τ; or*

2. *a node of the triangle σ, i.e., there exists $\rho \in \Sigma(1)$ with $\rho \subset \sigma$ such that v marks ρ. In this case, S_v lies in the socle of every θ-stable A-module in the divisor D_ρ.*

Proof. Let $y \in \mathcal{M}_A$ denote the torus-invariant point defined by the cone $\sigma \in \Sigma(3)$, so $M_y = M_\sigma$ by Lemma 2.3. Since S_v lies in the socle of M_σ, Remark 3.24(1) implies that v is not the zero vertex. Bocklandt–Craw–Quintero-Vélez [BCQV15, Propositions 3.4, 4.7, Lemma 4.8] shows

$$Z_v = \left\{ y \in \mathcal{M}_A \mid S_v \subseteq \operatorname{soc}(M_y) \right\}$$

is either a single $(-1,-1)$-curve or a connected union of compact torus-invariant divisors in $\mathcal{M}_A$. We have $S_v \subseteq \operatorname{soc}(M_y)$ by assumption, hence $y \in Z_v$. We consider two cases.

If Z_v is a $(-1,-1)$-curve in $\mathcal{M}_A$ then there exists $\tau \in \Sigma(2)$ such that $Z_v = C_\tau$, so S_v lies in the socle of every θ-stable A-module in C_τ. Also, $y \in Z_v = C_\tau$ so the inclusion-reversing correspondence between orbit-closures in $\mathcal{M}_A$ and cones in Σ gives $\tau \subset \sigma$. By the proof of [BCQV15, Lemma 4.10], the tile dual to v is the only tile in Γ not contained in the zero jigsaw piece. Hence, v marks the line segment τ by Reid's recipe.

Otherwise, Z_v is a torus-invariant divisor. Since $y \in Z_v$, there exists $\rho \in \Sigma(1)$ such that $y \in D_\rho \subseteq Z_v$, so S_v lies in the socle of every θ-stable A-module in D_ρ and hence v marks ρ by Definition 3.23. Apply the inclusion-reversing correspondence between orbit closures in $\mathcal{M}_A$ and cones in Σ to the inclusion $y \in D_\rho$, giving $\rho \subset \sigma$ as required. □

We now strengthen Lemma 3.30 slightly in order to present a geometric result:

Proposition 3.31. *Let $v \in Q_0$ be a nonzero vertex. If $H^0(\Psi(S_v)) \neq 0$, then either:*

1. *there exists a line segment $\tau \in \Sigma(2)$ such that vertex v marks τ, and the corresponding torus-invariant curve satisfies $C_\tau = \operatorname{supp}(\Psi(S_v))$; or*
2. *there exists a lattice point $\rho \in \Sigma(1)$ such that vertex v marks ρ, and the corresponding torus-invariant divisor satisfies $D_\rho \subseteq \operatorname{supp}(\Psi(S_v))$.*

Proof. Since v is a nonzero vertex and $H^0(\Psi(S_v)) \neq 0$, Bocklandt–Craw–Quintero-Vélez [BCQV15, Proposition 4.7] gives $\sigma \in \Sigma(3)$ such that the corresponding torus-invariant θ-stable A-module M_σ contains S_v in its socle. Now Lemma 3.30 produces either:

1. an interior line segment $\tau \in \Sigma(2)$ such that v marks τ, and S_v lies in the socle of every θ-stable A-module in the curve C_τ; or
2. an interior lattice point $\rho \in \Sigma(1)$ such that v marks ρ, and S_v lies in the socle of every θ-stable A-module in the divisor D_ρ.

It remains to note [BCQV15, Proposition 3.4] that since $H^0(\Psi(S_v)) \neq 0$, the support of the object $\Psi(S_v)$ is precisely the locus $\{y \in \mathcal{M}_A \mid S_v \subseteq \operatorname{soc}(M_y)\}$. □

The next result provides a partial link between combinatorial Reid's recipe and geometric Reid's recipe.

Theorem 3.32 (**Geometric Reid's recipe for lattice points**). *Let $v \in Q_0$ be a nonzero vertex and let $\rho \in \Sigma(1)$ be an interior lattice point of the triangulation Σ. Then v marks ρ according to Reid's recipe if and only if the divisor D_ρ is contained in the support of the sheaf $\Psi(S_v)$.*

Proof. Lemma 3.30 implies that v marks ρ if and only if S_v lies in the socle of some (equivalently, every) θ-stable A-module in the divisor D_ρ. This is equivalent to having D_ρ in the support of $\Psi(S_v)$ by Bocklandt–Craw–Quintero-Vélez [BCQV15, Proposition 1.3]. □

3.6 Conjectures regarding combinatorial Reid's recipe

We expect that in the marking of the fan Σ by combinatorial Reid's recipe, every nonzero vertex of Q appears 'once' in the following sense:

Conjecture 3.33. *In the marking of Σ by combinatorial Reid's recipe, every nonzero vertex v of Q appears either:*

1. *marking a collection of lattice points, connected by line segments of Σ ;*
2. *marking a single line segment τ;*
3. *marking a collection of line segments in Σ, such that any τ marked with v shares an endpoint with another line segment τ' marked with v.*

Moreover, a vertex $v \in Q_1$ marks a single line segment of Σ by combinatorial Reid's recipe if and only if S_v lies in the socle of every θ-stable A-module in the curve C_τ, as in Proposition 3.31.

We also expect combinatorial Reid's recipe to encode the relations between the line bundles in $\mathrm{Pic}(\mathcal{M}_A)$:

Conjecture 3.34. *Let ρ be an interior line segment. Then the following relation holds in* $\mathrm{Pic}(\mathcal{M}_A)$*:*

$$\bigotimes_{v \text{ marks } \rho} L_v = \bigotimes_{\substack{v \text{ marks at least} \\ 2 \text{ line segments} \\ \text{attached to } \rho}} L_v \bigotimes_{\substack{v \text{ marks more than} \\ 2 \text{ line segments} \\ \text{attached to } \rho}} L_v.$$

The search for a proof of these two conjectures has led us to the arrow contraction algorithm, which is motivated in the following chapter. The connection with the arrow contraction algorithm is explained in Chapter 7 (see Corollary 7.1).

3.7 Examples

Example 3.35. Let G be a finite abelian subgroup of $\mathrm{SL}(3,\mathbb{C})$. By Corollary 3.27, the examples calculated in Reid [Rei97], Craw [Cra05] and Cautis–Logvinenko [CL09] illustrate combinatorial Reid's recipe for consistent dimer models. Example 1.56 illustrates combinatorial Reid's recipe for a dimer model Γ dual to the McKay quiver Q of G, where $G \subset \mathrm{SL}(3,\mathbb{C})$ is generated by the diagonal matrix $\mathrm{diag}(\varepsilon, \varepsilon^2, \varepsilon^3)$, ε a primitive sixth root of unity.

Example 3.36. Consider the dimer model from Example 1.35. The stability parameter $\theta = (-9, 1, 1, \ldots, 1)$ is 0-generated and the fan Σ of $\mathcal{M}_A$ is presented in Figure 1.7. Geometric Reid's recipe suggests the marking of Σ presented in Figure 3.7(a). Combinatorial Reid's recipe gives a complete marking of the interior lattice points and interior line segments of the toric fan. Notice that unlike classical Reid's recipe, two vertices, 3 and 9, mark an interior line segment of Σ. Also, the vertex 2 marks two interior lattice points of Σ. Moreover, the recipe for lattice points is not determined by the shape of the incoming line segments and their marking, as one of the interior lattice points of Σ is marked by two vertices of Q while the other by a single one.

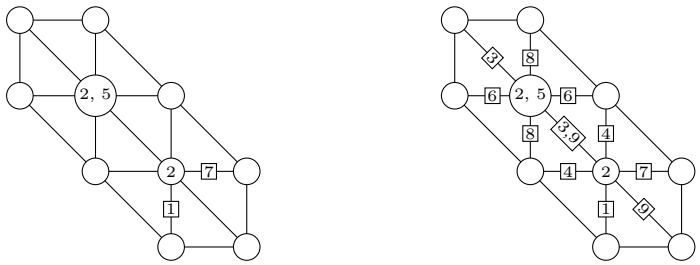

(a) Geometric (b) Combinatorial

Figure 3.7: *Marking of* Σ *by geometric and combinatorial Reid's recipe*

Example 3.37. Figure 3.8 shows a consistent dimer model with its dual quiver. The stability parameter $\theta = (-21, 1, 1, \ldots, 1)$ is 0-generated. The fan Σ of $\mathcal{M}_A$ is depicted in Figure 3.9. The interior line segments and nodes of Σ are decorated using geometric and combinatorial Reid's recipe. While geometric Reid's recipe only marks a single line segment in Σ, combinatorial Reid's recipe marks every interior line segment with a vertex of Q.

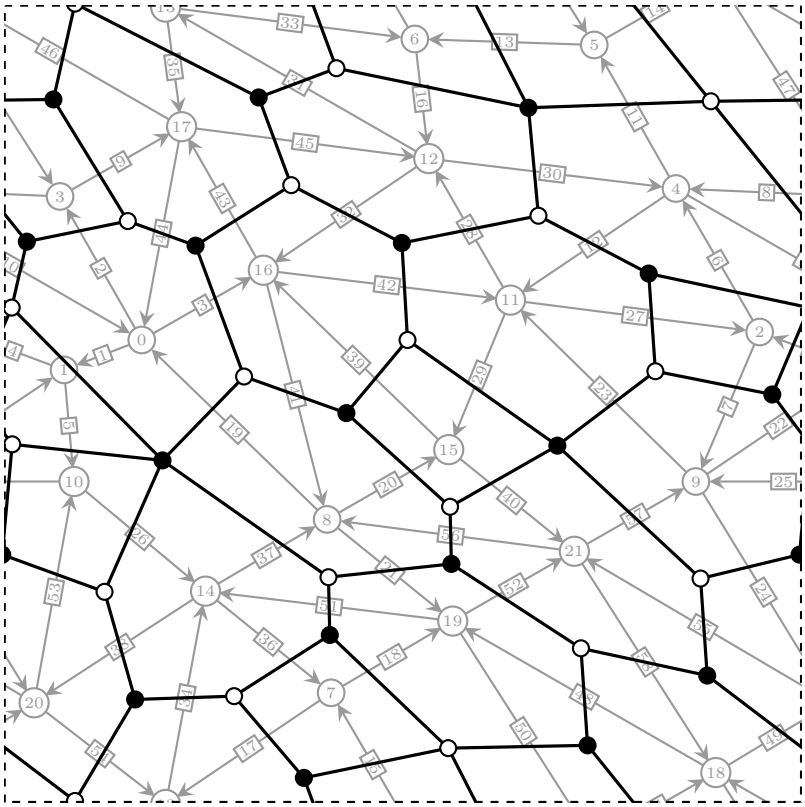

Figure 3.8: *A dimer model with its dual quiver*

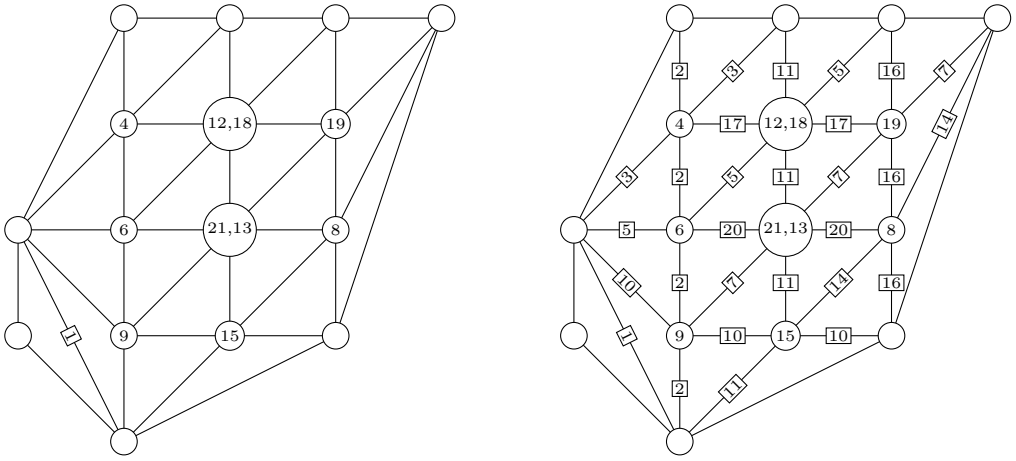

(a) Geometric (b) Combinatorial

Figure 3.9: *Marking of* Σ *by geometric and combinatorial Reid's recipe*

Example 3.38. Consider the dimer model in Figure 3.10. The fan Σ of $\mathcal{M}_A$ for $\theta = (-25, 1, 1, \ldots, 1)$ is depicted in Figure 3.11. The interior line segments and interior lattice points of Σ are decorated using geometric and combinatorial Reid's recipe.

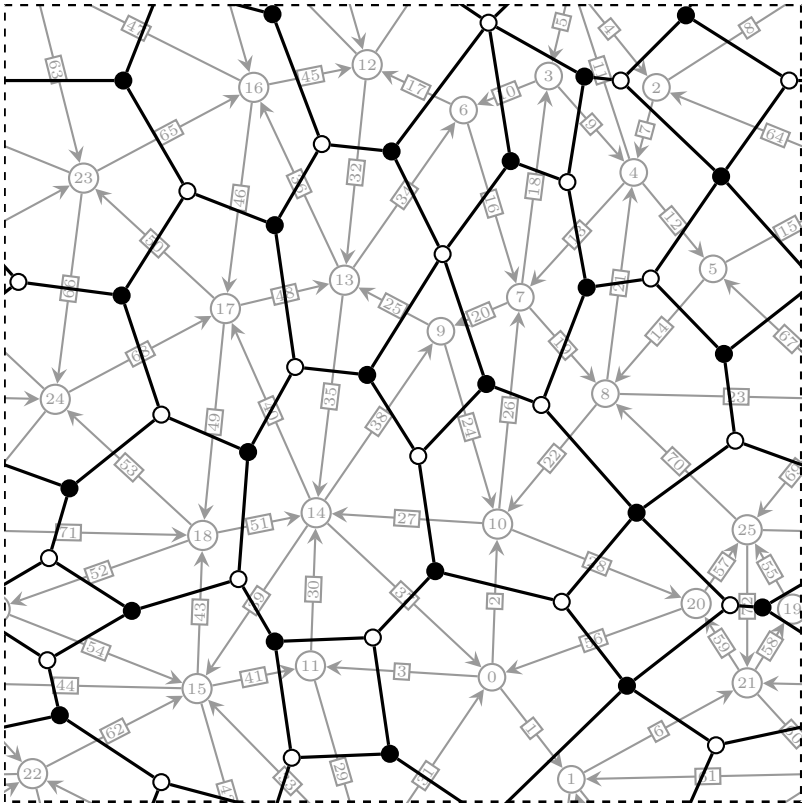

Figure 3.10: *A dimer model with its dual quiver*

The first thing to note in this example is that there exists an interior lattice point of valency 7. This is unlike the fan of the G-Hilbert scheme, for G a finite abelian subgroup of $\mathrm{SL}(3, \mathbb{C})$, which Craw [CR02, Section 1.3] showed only has interior lattice points of valency $3, 4, 5$ and 6. Combinatorial Reid's recipe for Σ also shows two vertices

7 and 21 marking a single interior line segment and one vertex 8 marking two interior lattice points of Σ.

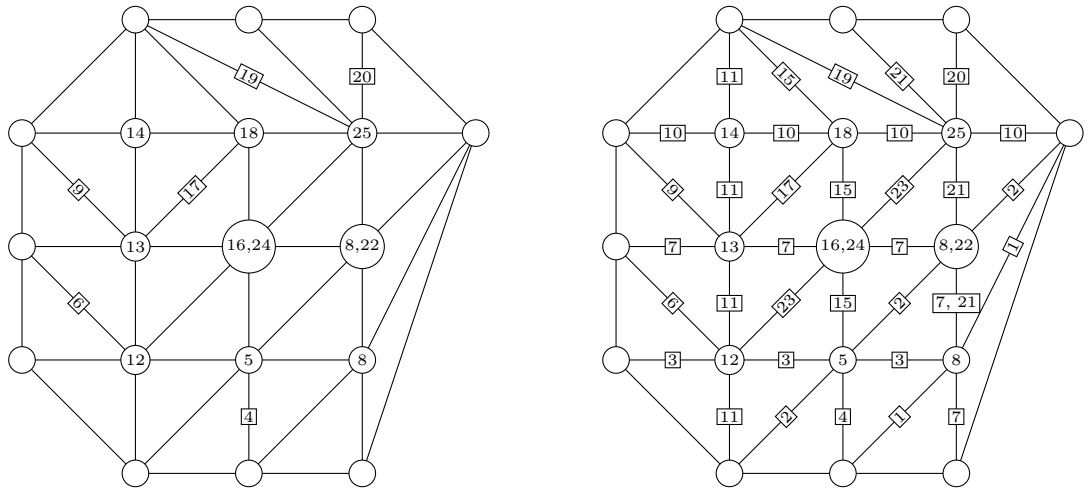

(a) Geometric (b) Combinatorial

Figure 3.11: *Marking of Σ by geometric and combinatorial Reid's recipe*

CHAPTER 4

THE CONVEX POLYGON Δ' AND THE OPEN SUBVARIETY Y'

This chapter motivates the arrow contraction algorithm. We begin by introducing an example which illustrates many of the results presented in the remaining of this thesis. We then associate to any arrow α in Q with tail at vertex 0 a convex polygon Δ' and an open subvariety Y' of $\mathcal{M}_A(\theta)$, for θ 0-generated and Γ a consistent dimer model dual to Q. The aim of the arrow contraction algorithm will be to produce a new consistent dimer model Γ' from our original consistent dimer model Γ, such that the characteristic polygon of Γ' is Δ' and the moduli space $\mathcal{M}_{A'}(\theta')$, for θ' a 0-generated stability parameter, is Y'. Lemma 4.9 gives the first link between combinatorial Reid's recipe and the toric fan of Y'.

4.1 Motivating example

Consider the consistent dimer model Γ from Example 3.38. Figure 4.1 shows the dual quiver Q of Γ. The characteristic polygon $\Delta(\Gamma)$ of Γ is an irregular heptagon. The toric fan Σ of the moduli space $\mathcal{M}_A$ of θ-stable A-modules for the 0-generated stability parameter $\theta = (-25, 1, 1, \ldots, 1)$ is presented in Figure 4.2. The fan has 19 rays $\rho_1, \rho_2, \ldots, \rho_{19}$, marked $1, 2, \ldots, 19$ in the toric picture, each corresponding to a torus-invariant prime divisor $D_i := D_{\rho_i}$ in $\mathcal{M}_A$ with θ-stable perfect matching Π_i $(1 \leq i \leq 19)$. The isomorphism $\phi : A \to \mathrm{End}(T)$ between the Jacobian algebra of Q and the endomorphism algebra of the tautological bundle of $\mathcal{M}_A$ gives a label $\mathrm{div}(a)$ to each arrow $a \in Q_1$. Figure 4.3 shows the quiver Q with a selection of the arrows labelled. An arrow a in Figure 4.3 labelled by $i_1, i_2, \ldots, i_j$ has labelling divisor $\mathrm{div}(a) = D_{i_1} + D_{i_2} + \ldots + D_{i_j}$. For a list containing all of the labels for the arrows of Q see Appendix B.

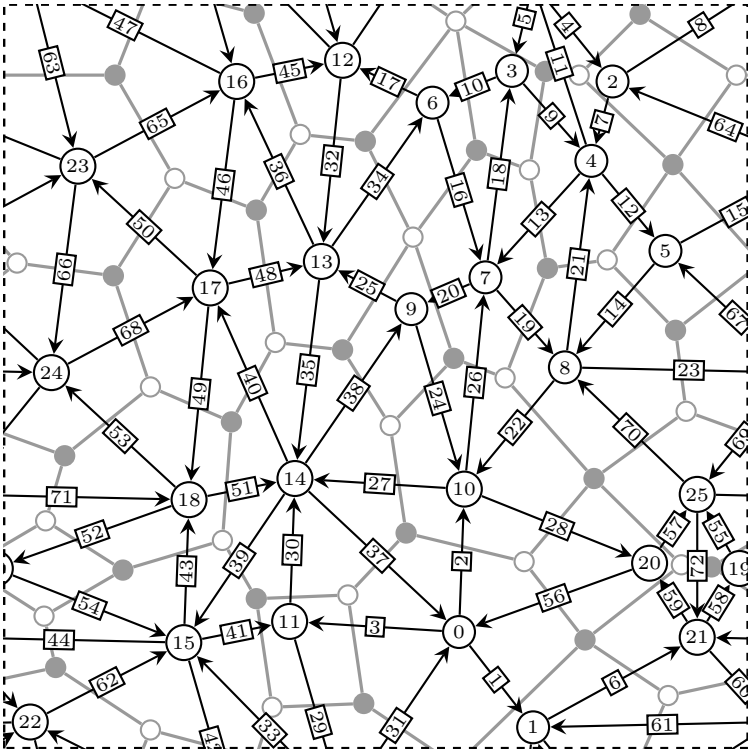

Figure 4.1: *The quiver Q dual to the dimer model from Example 3.38*

Pick the arrow a_3 in Q with tail at vertex 0 and head at vertex 11. The arrow has labelling divisor $\mathrm{div}(a_3) = D_4 + D_5 + D_8$. Note that the torus-invariant prime divisors D_4, D_5 and D_8 correspond to adjacent lattice points ρ_4, ρ_5, ρ_8 on the boundary of the characteristic polygon $\Delta(\Gamma)$. Moreover, the complement of all the triangles in Σ containing one of the boundary lattice points ρ_4, ρ_5 or ρ_8 defines a convex polygon Δ'. It is easy to verify that this is also the case for the arrows a_1 and a_2 in Q. In fact, both statements hold for any arrow α with tail at vertex 0 (see Lemma 4.3 and Proposition 4.6). Therefore, any choice of arrow $\alpha \in Q_1$ with tail at vertex 0 determines a convex polygon Δ' and strip of triangles $\mathrm{strip}(\alpha)$. For $\alpha = a_3 \in Q_1$, Figure 4.2 shows its convex polygon Δ'. Its strip of triangles $\mathrm{strip}(a_3)$ is depicted in Figure 4.4 together with the names we use to denote the triangles and line segments contained in it.

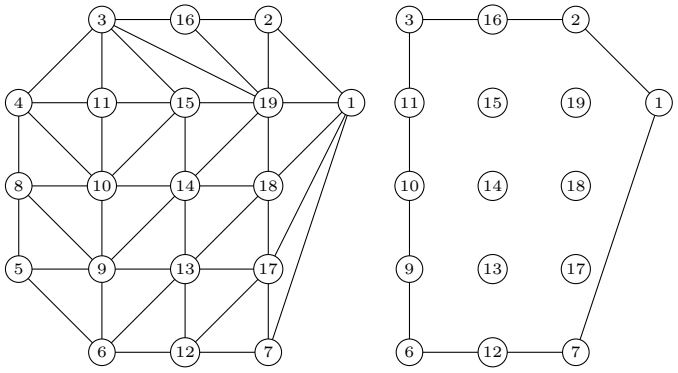

(a) The toric fan Σ (b) Δ' for $a_3 \in Q_1$

Figure 4.2: *The toric fan of $\mathcal{M}_A$ and convex polygon Δ' for $a_3 \in Q_1$*

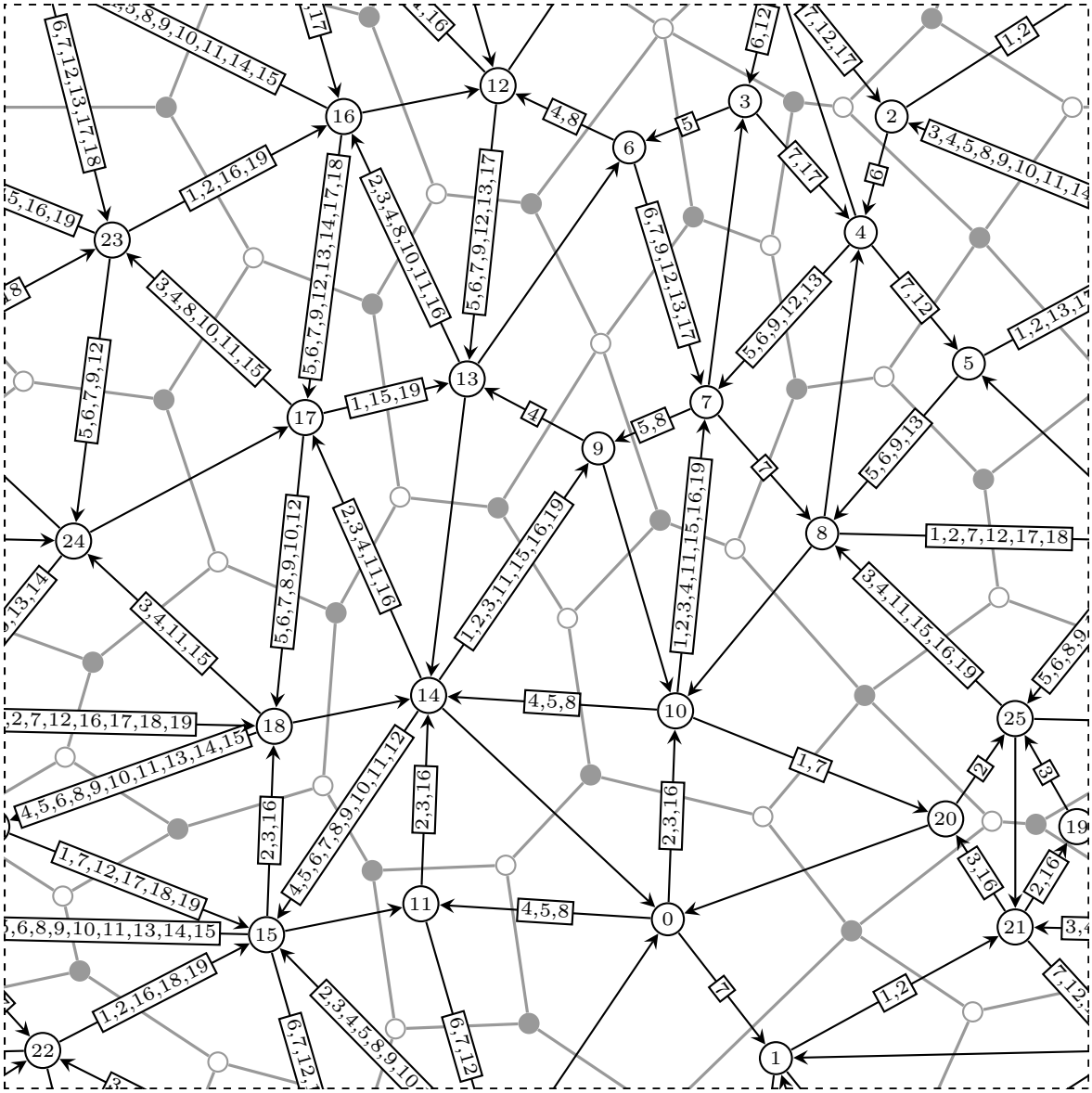

Figure 4.3: *The quiver Q with a selection of arrows labelled*

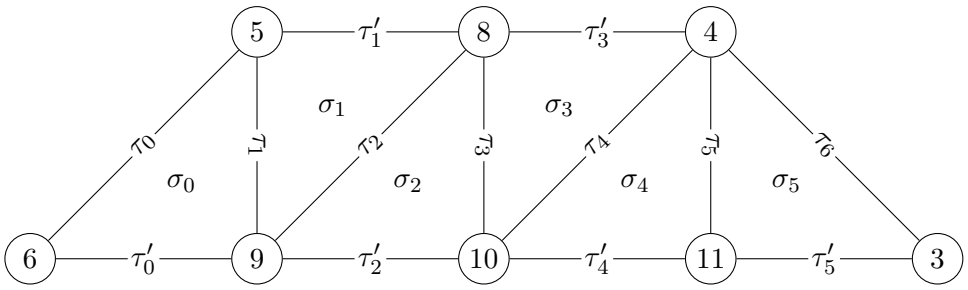

Figure 4.4: *Strip of triangles* $\mathrm{strip}(a_3)$

We would like to construct a consistent dimer model Γ' whose characteristic polygon is Δ'. For this, we define a subset of edges $\mathcal{S}_{a_3} \subset \mathfrak{E}$ that will be removed from Γ in order to produce Γ'. Recall from Definition 2.12 that for any line segment τ in Σ with endnodes ρ and ρ', we define the meandering walk $\mathfrak{m}_\tau$ of τ to be the set of of edges in the symmetric difference $\Pi_\rho \ominus \Pi_{\rho'}$. By Corollary 2.10, every meandering walk is the support of a cycle in Γ. Note that the line segments τ_0, τ_1', τ_3' and τ_6 are all boundary line segments on $\Delta(\Gamma)$, and Remark 2.15 shows that their meandering walks support zigzag paths. We will use the meandering walks of the line segments in $\mathrm{strip}(a_3)$ to define the set of edges $\mathcal{S}_{a_3}$.

For $0 \leq i \leq 6$ and $0 \leq j \leq 5$, write $\mathfrak{m}_i$ and $\mathfrak{m}_j'$ for the meandering walks of τ_i and τ_j', respectively. In order to create a dimer model Γ' that is consistent, we consider what its zig-zag paths must look like. By Theorem 1.46, there should be one zigzag path $\mathfrak{z}$ for each line segment τ in the boundary of Δ', such that $\mathrm{supp}(\mathfrak{z}) = \mathfrak{m}_\tau$ and the homology class of $\mathfrak{z}$ is the inward-pointing normal vector to τ. As Γ is consistent, Γ already has a zigzag path for every boundary line segment of Δ except for $\tau_0', \tau_2', \tau_4'$ and τ_5'. By Lemma 2.14, the homology classes of the meandering walks $\mathfrak{m}_0', \mathfrak{m}_2', \mathfrak{m}_4', \mathfrak{m}_5'$ are normal to the line segment $\tau_0', \tau_2', \tau_4'$ and τ_5', respectively, making them candidates for the missing zigzag paths. Thus, every edge we remove from Γ should not be an edge in any of these meandering walks. Edges in $\mathcal{S}_{a_3}$ would ideally prevent the zigzag paths $\mathfrak{m}_0, \mathfrak{m}_1', \mathfrak{m}_3', \mathfrak{m}_6$ from appearing in Γ' and would make the meandering walks $\mathfrak{m}_0', \mathfrak{m}_2', \mathfrak{m}_4', \mathfrak{m}_5'$ into zigzag paths. Table 4.1 lists all meandering walks $\mathfrak{m}_\tau$ for τ a line segment in $\mathrm{strip}(a_3)$. To simplify notation $\mathfrak{e}_i$ denotes the edges in Γ dual to the arrow a_i in Q.

Walk	Edges
$\mathfrak{m}_0$	$\mathfrak{e}_3, \mathfrak{e}_{29}, \mathfrak{e}_{33}, \mathfrak{e}_{42}, \mathfrak{e}_{47}, \mathfrak{e}_{63}, \mathfrak{e}_{64}, \mathfrak{e}_7, \mathfrak{e}_{11}, \mathfrak{e}_5, \mathfrak{e}_{10}, \mathfrak{e}_{16}, \mathfrak{e}_{20}, \mathfrak{e}_{24}, \mathfrak{e}_{27}, \mathfrak{e}_{37}$
$\mathfrak{m}_1$	$\mathfrak{e}_3, \mathfrak{e}_{31}, \mathfrak{e}_{10}, \mathfrak{e}_{16}, \mathfrak{e}_{20}, \mathfrak{e}_{24}, \mathfrak{e}_{27}, \mathfrak{e}_{37}$
$\mathfrak{m}_2$	$\mathfrak{e}_3, \mathfrak{e}_{31}, \mathfrak{e}_{17}, \mathfrak{e}_{32}, \mathfrak{e}_{36}, \mathfrak{e}_{46}, \mathfrak{e}_{50}, \mathfrak{e}_{66}, \mathfrak{e}_{67}, \mathfrak{e}_{14}, \mathfrak{e}_{21}, \mathfrak{e}_{13}, \mathfrak{e}_{18}, \mathfrak{e}_{16}, \mathfrak{e}_{20}, \mathfrak{e}_{24}, \mathfrak{e}_{27}, \mathfrak{e}_{37}$
$\mathfrak{m}_3$	$\mathfrak{e}_3, \mathfrak{e}_{31}, \mathfrak{e}_{17}, \mathfrak{e}_{34}, \mathfrak{e}_{20}, \mathfrak{e}_{24}, \mathfrak{e}_{27}, \mathfrak{e}_{37}$
$\mathfrak{m}_4$	$\mathfrak{e}_3, \mathfrak{e}_{31}, \mathfrak{e}_{17}, \mathfrak{e}_{34}, \mathfrak{e}_{25}, \mathfrak{e}_{35}, \mathfrak{e}_{40}, \mathfrak{e}_{49}, \mathfrak{e}_{53}, \mathfrak{e}_{69}, \mathfrak{e}_{70}, \mathfrak{e}_{22}, \mathfrak{e}_{26}, \mathfrak{e}_{24}, \mathfrak{e}_{27}, \mathfrak{e}_{37}$
$\mathfrak{m}_5$	$\mathfrak{e}_3, \mathfrak{e}_{31}, \mathfrak{e}_{17}, \mathfrak{e}_{34}, \mathfrak{e}_{25}, \mathfrak{e}_{38}, \mathfrak{e}_{27}, \mathfrak{e}_{37}$
$\mathfrak{m}_6$	$\mathfrak{e}_3, \mathfrak{e}_{31}, \mathfrak{e}_{17}, \mathfrak{e}_{34}, \mathfrak{e}_{25}, \mathfrak{e}_{38}, \mathfrak{e}_{27}, \mathfrak{e}_2, \mathfrak{e}_{56}, \mathfrak{e}_{59}, \mathfrak{e}_{72}, \mathfrak{e}_{55}, \mathfrak{e}_{52}, \mathfrak{e}_{43}, \mathfrak{e}_{39}, \mathfrak{e}_{30}$
$\mathfrak{m}_0'$	$\mathfrak{e}_{29}, \mathfrak{e}_{33}, \mathfrak{e}_{42}, \mathfrak{e}_{47}, \mathfrak{e}_{63}, \mathfrak{e}_{64}, \mathfrak{e}_7, \mathfrak{e}_{11}, \mathfrak{e}_5, \mathfrak{e}_{31}$
$\mathfrak{m}_1'$	$\mathfrak{e}_{10}, \mathfrak{e}_{18}, \mathfrak{e}_{13}, \mathfrak{e}_{21}, \mathfrak{e}_{14}, \mathfrak{e}_{67}, \mathfrak{e}_{66}, \mathfrak{e}_{50}, \mathfrak{e}_{46}, \mathfrak{e}_{36}, \mathfrak{e}_{32}, \mathfrak{e}_{17}$
$\mathfrak{m}_2'$	$\mathfrak{e}_{16}, \mathfrak{e}_{18}, \mathfrak{e}_{13}, \mathfrak{e}_{21}, \mathfrak{e}_{14}, \mathfrak{e}_{67}, \mathfrak{e}_{66}, \mathfrak{e}_{50}, \mathfrak{e}_{46}, \mathfrak{e}_{36}, \mathfrak{e}_{32}, \mathfrak{e}_{34}$
$\mathfrak{m}_3'$	$\mathfrak{e}_{20}, \mathfrak{e}_{26}, \mathfrak{e}_{22}, \mathfrak{e}_{70}, \mathfrak{e}_{69}, \mathfrak{e}_{53}, \mathfrak{e}_{49}, \mathfrak{e}_{40}, \mathfrak{e}_{35}, \mathfrak{e}_{25}$
$\mathfrak{m}_4'$	$\mathfrak{e}_{24}, \mathfrak{e}_{26}, \mathfrak{e}_{22}, \mathfrak{e}_{70}, \mathfrak{e}_{69}, \mathfrak{e}_{53}, \mathfrak{e}_{49}, \mathfrak{e}_{40}, \mathfrak{e}_{35}, \mathfrak{e}_{38}$
$\mathfrak{m}_5'$	$\mathfrak{e}_{37}, \mathfrak{e}_2, \mathfrak{e}_{56}, \mathfrak{e}_{59}, \mathfrak{e}_{72}, \mathfrak{e}_{55}, \mathfrak{e}_{52}, \mathfrak{e}_{43}, \mathfrak{e}_{39}, \mathfrak{e}_{30}$

Table 4.1: *Edges of the meandering walks coming from line segments in* $\mathrm{strip}(a_3)$

The first thing to note from Table 4.1 is that $\mathfrak{e}_3$, the arrow dual to our chosen arrow $a_3 \in Q_1$, appears in all the meandering walks $\mathfrak{m}_0, \mathfrak{m}_1, \ldots, \mathfrak{m}_6$. This is always the case for any $\alpha \in Q_1$ with tail at vertex 0 (see proof of Lemma 5.5). Also note that the meandering walks $\mathfrak{m}_0', \mathfrak{m}_2', \mathfrak{m}_4', \mathfrak{m}_5'$ share no edges and each of their edges belongs to one of the zigzag paths $\mathfrak{m}_0, \mathfrak{m}_1', \mathfrak{m}_3', \mathfrak{m}_6$ of Γ. For example, $\mathfrak{m}_0'$ consists of nine edges from $\mathfrak{m}_0$ and one edge from $\mathfrak{m}_6$. The meandering walk $\mathfrak{m}_2'$ shares an edge with $\mathfrak{m}_0$,

ten edges with $\mathfrak{m}'_1$ and an edge with $\mathfrak{m}_6$. Therefore, $\mathfrak{m}'_0, \mathfrak{m}'_2, \mathfrak{m}'_4, \mathfrak{m}'_5$ have each a natural direction inherited from the zigzag paths they share edges with. The edges at which these meandering walks with their natural direction fail to be zigzag are zigs and zags of $\mathfrak{m}_0, \mathfrak{m}'_1, \mathfrak{m}'_3, \mathfrak{m}_6$:

$$\mathfrak{s}_0 = \mathfrak{e}_3 \in \mathfrak{m}_0 \cap \mathfrak{m}_6,\ \mathfrak{s}_1 = \mathfrak{e}_{10} \in \mathfrak{m}_0 \cap \mathfrak{m}'_1,\ \mathfrak{s}_2 = \mathfrak{e}_{17} \in \mathfrak{m}_6 \cap \mathfrak{m}'_1,$$
$$\mathfrak{s}_3 = \mathfrak{e}_{20} \in \mathfrak{m}_0 \cap \mathfrak{m}'_3,\ \mathfrak{s}_4 = \mathfrak{e}_{25} \in \mathfrak{m}_6 \cap \mathfrak{m}'_3,\ \mathfrak{s}_5 = \mathfrak{e}_{27} \in \mathfrak{m}_0 \cap \mathfrak{m}_6.$$

These edges make the set $\mathcal{S}_{a_3} = (\mathfrak{m}_0 \cup \mathfrak{m}_6) \setminus (\mathfrak{m}'_0 \cup \mathfrak{m}'_2 \cup \mathfrak{m}'_4 \cup \mathfrak{m}'_5)$ as introduced in Definition 5.4.

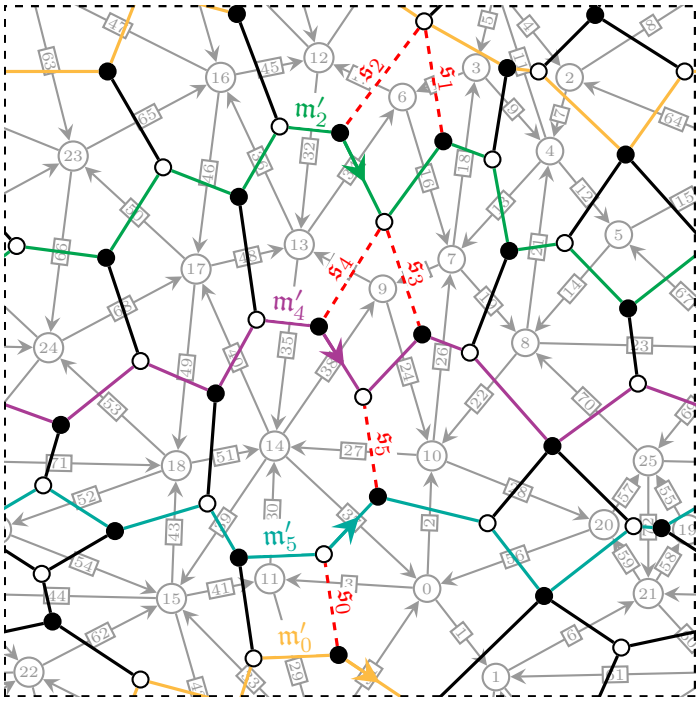

Figure 4.5: *The meandering walks $\mathfrak{m}'_0, \mathfrak{m}'_2, \mathfrak{m}'_4, \mathfrak{m}'_5$ and the edges at which they fail to be zigzag*

Figure 4.5 shows the meandering walks $\mathfrak{m}'_0, \mathfrak{m}'_2, \mathfrak{m}'_4, \mathfrak{m}'_5$ with their natural direction and the edges in $\mathcal{S}_{a_3}$. Notice that the edges in the set $\mathcal{S}_{a_3}$ are those that prevent the lower meandering walks $\mathfrak{m}'_0, \mathfrak{m}'_2, \mathfrak{m}'_4, \mathfrak{m}'_5$ from turning maximally right at a white node and maximally left at a black node, i.e., they prevent these walks from being zigzags (see Lemma 6.10 and Remark 6.11). Observe that the endnodes of each of the edges in $\mathcal{S}_{a_3}$ is a trivalent node of a fundamental hexagon $\mathrm{Hex}(\sigma)$ for σ a triangle in $\mathrm{strip}(a_3)$. Indeed, the black endnode of $\mathfrak{e}_3$ is attached to the edges $\mathfrak{e}_3 \in \mathfrak{m}_0 \cap \mathfrak{m}_1$, $\mathfrak{e}_{29} \in \mathfrak{m}_0 \cap \mathfrak{m}'_0$ and $\mathfrak{e}_{31} \in \mathfrak{m}_1 \cap \mathfrak{m}'_0$, making it a trivalent node of $\mathrm{Hex}(\sigma_0)$. Write $\mathfrak{b}_i$ and $\mathfrak{w}_i$ for the black and white trivalent nodes of $\mathrm{Hex}(\sigma_i)$ $(0 \leq i \leq 5)$, respectively. It is an easy exercise to verify that for $0 \leq i \leq 5$, the edge $\mathfrak{s}_i$ has endnodes $\mathfrak{w}_{\overline{i-1}}$ and $\mathfrak{b}_i$, where the overline denotes addition modulo 6.

Figure 4.6 shows a schematic depicting all edges in $\mathcal{S}_{a_3}$ and all meandering walks $\mathfrak{m}_\tau$ for τ a line segment in $\mathrm{strip}(a_3)$, called the circuit diagram for a_3. The circuit diagram encodes much of the structure described earlier. Although in this example $\mathfrak{w}_0 = \mathfrak{w}_1$ and $\mathfrak{w}_2 = \mathfrak{w}_3$, we intentionally draw the circuit diagram in its most general form assuming

there is an even number of edges (possibly zero) connecting two trivalent nodes of the same colour in Γ. Notice that the walk $\mathfrak{m}_1$ splits from $\mathfrak{m}_0$ at $\mathfrak{b}_0$ and travels up to $\mathfrak{w}_1$ with each of $\mathfrak{m}_i$ (for $2 \leq i \leq 6$). At $\mathfrak{w}_1$ it splits from these, travelling along $\mathfrak{m}'_0$ until it rejoins $\mathfrak{m}_0$ at $\mathfrak{w}_0$, and then travels with $\mathfrak{m}_0$ until $\mathfrak{b}_0$, when it completes a cycle around $\mathbb{T}$. The meandering walks $\mathfrak{m}_2, \mathfrak{m}_3, \mathfrak{m}_4$ and $\mathfrak{m}_5$ exhibit a similar behaviour. All of them split from $\mathfrak{m}_0$ at $\mathfrak{b}_0$ and travel with $\mathfrak{m}_6$ until a trivalent node of a triangle in strip(a_3), when they split from $\mathfrak{m}_6$ to eventually rejoin $\mathfrak{m}_0$ at another trivalent node. For $1 \leq i \leq 5$, the walk $\mathfrak{m}_i$ splits from $\mathfrak{m}_6$ before the walks $\mathfrak{m}_{i+1}, \mathfrak{m}_{i+2}, \ldots, \mathfrak{m}_5$ do, and rejoins $\mathfrak{m}_0$ after $\mathfrak{m}_1, \mathfrak{m}_2, \ldots, \mathfrak{m}_{i-1}$ do. Because of this orderly behaviour, the walks $\mathfrak{m}_1, \mathfrak{m}_2, \mathfrak{m}_3, \mathfrak{m}_4$ and $\mathfrak{m}_5$ appear to make a Mexican wave in the circuit diagram.

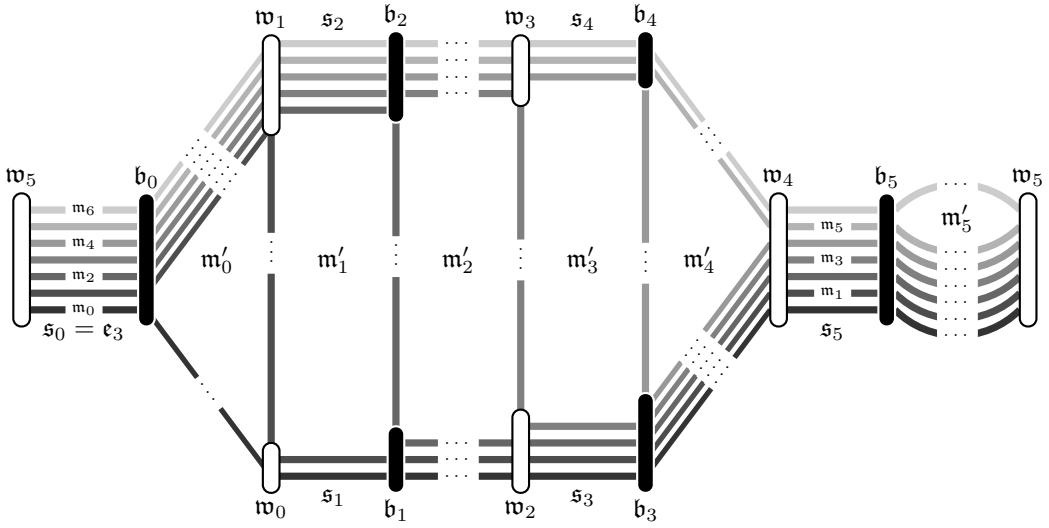

Figure 4.6: *Circuit diagram for a_3*

4.2 The convex polygon Δ' and the open subvariety Y'

Let $\Gamma = \{\mathfrak{B}, \mathfrak{W}, \mathfrak{E}\}$ be a consistent dimer model and let $Q = \{Q_0, Q_1, \mathsf{h}, \mathsf{t}, \mathcal{R}\}$ be its dual quiver with relations. Write A for the Jacobian algebra of Q. Recall that for a 0-generated stability parameter θ (see Definition 3.1):

(i) The moduli space $\mathcal{M}_A$ of θ-stable A-modules provides a projective crepant resolution $f : \mathcal{M}_A \to X$ of the affine Gorenstein toric threefold $X := \mathrm{Spec}(Z(A))$; and

(ii) The tautological $\mathbb{C}$-algebra morphism $\phi : A \to \mathrm{End}_{\mathcal{O}_{\mathcal{M}_A}}(T)$ between the algebra A and the endomorphism algebra of the tautological bundle $\bigoplus_{v \in Q_0} L_v$ on $\mathcal{M}_A$ is an isomorphism.

The tautological $\mathbb{C}$-algebra isomorphism $\phi : A \to \mathrm{End}_{\mathcal{O}_{\mathcal{M}_A}}(T)$ associates to each path p a label $\mathrm{div}(p)$. A divisor D is said to be a *summand* of $\mathrm{div}(p)$ if and only if $\mathrm{div}(p) - D \geq 0$. Every lattice point ρ in Σ corresponds to a torus-invariant prime divisor D_ρ. It follows from equation (1.5.1) that for $a \in Q_1$, D_ρ is a summand of $\mathrm{div}(a)$ if and only if its dual edge $\mathfrak{e}_\alpha$ lies in the θ-stable perfect matching Π_ρ.

We distinguish between two different types of prime divisors:

Definition 4.1. Every lattice point $\rho \in \Sigma$ lies either:

(i) on the boundary of Δ, in which case we call D_ρ a *boundary divisor* of $\mathcal{M}_A$; or

(ii) in the interior of Δ, in which case we call D_ρ an *interior divisor* of $\mathcal{M}_A$.

Lemma 4.2. *Let a be an arrow in Q_1 with head at vertex 0. Then every interior divisor of $\mathcal{M}_A$ is a summand of* $\operatorname{div}(a)$.

Proof. Let x_0 denote the unique-torus invariant point of X. Pick any point $y \in \mathcal{M}_A$ in an interior divisor D_ρ, so that $y \in f^{-1}(x_0)$, where $f : \mathcal{M}_A \to X$ is a crepant resolution of X. By [BCQV15, Lemma 3.1 (ii)], all maps in M_y with head at vertex 0 are zero. Therefore, $\mathfrak{e}_a$ is an edge of the perfect matching Π_ρ and D_ρ is a summand of $\operatorname{div}(a)$. As this holds for every interior divisor D_ρ of $\mathcal{M}_A$, the result follows. □

Suppose the characteristic polygon $\Delta(\Gamma)$ of Γ has n lattice points $\rho_0, \rho_1, \ldots, \rho_{n-1}$ arranged clockwise around its boundary. For $0 \leq i \leq n-1$, let $D_i := D_{\rho_i}$ and $\Pi_i := \Pi_{\rho_i}$ denote the boundary divisor and the θ-stable perfect matching associated to ρ_i. Recall from Remark 2.15 that any zigzag path in Γ is supported on the symmetric difference of two θ-stable perfect matchings coming from adjacent boundary divisors. For $0 \leq i \leq n-1$, write $\mathfrak{z}_i$ for the zigzag path supported on the symmetric difference $\Pi_i \ominus \Pi_{\overline{i+1}}$, where the overline denotes addition modulo n.

Pick once and for all an arrow $\alpha \in Q_1$ with tail at vertex 0.

Lemma 4.3. *After relabelling the boundary divisors, there exist consecutive boundary divisors $D_1, D_2, \cdots, D_r$ in $\Delta(\Gamma)$ such that* $\operatorname{div}(\alpha) = D_1 + D_2 + \cdots + D_r$ *for some $1 \leq r \leq n-1$.*

Proof. Since Γ is consistent, the edge $\mathfrak{e}_\alpha$ appears in exactly two distinct zigzag paths, once as a zig and once as a zag. Without loss of generality, assume $\mathfrak{e}_\alpha$ lies in the support of $\mathfrak{z}_0$ and $\mathfrak{z}_r$ for some $1 \leq r \leq n-1$. Recall that for $0 \leq i \leq n-1$, an edge $\mathfrak{e} \in \operatorname{supp}(\mathfrak{z}_i) = \Pi_i \ominus \Pi_{\overline{i+1}}$ is a zig (resp. zag) of $\mathfrak{z}_i$ if and only if $\mathfrak{e}$ lies in $\Pi_{\overline{i+1}}$ (resp. Π_i). Hence either $\operatorname{zig}(\mathfrak{e}_\alpha) = \mathfrak{z}_0$ and $\operatorname{zag}(\mathfrak{e}_\alpha) = \mathfrak{z}_r$, in which case $\mathfrak{e}_\alpha \in \Pi_1 \cap \Pi_r$, or $\operatorname{zag}(\mathfrak{e}_\alpha) = \mathfrak{z}_0$ and $\operatorname{zig}(\mathfrak{e}_\alpha) = \mathfrak{z}_r$ which implies that $\mathfrak{e}_\alpha \in \Pi_0 \cap \Pi_{\overline{r+1}}$.

Suppose the first holds and $\mathfrak{e}_\alpha \in \Pi_1 \cap \Pi_r$. The fact that $\mathfrak{e}_\alpha$ is not in the support of $\mathfrak{z}_i$ for $i \neq 1, r$ means both that $\mathfrak{e}_\alpha \in \Pi_2, \Pi_3, \cdots, \Pi_{r-1}$ and $\mathfrak{e}_\alpha \notin \Pi_{\overline{r+1}}, \Pi_{\overline{r+2}}, \ldots, \Pi_n, \Pi_0$. Therefore, the only boundary divisors that appear as summands of the label of α are $D_1, D_2, \ldots, D_r$, whose lattice points $\rho_1, \rho_1, \ldots, \rho_r$ lie in a segment of the boundary of $\Delta(\Gamma)$. When $\operatorname{zag}(\mathfrak{e}_\alpha) = \mathfrak{z}_0$ and $\operatorname{zig}(\mathfrak{e}_\alpha) = \mathfrak{z}_r$ the same argument shows that the boundary divisors in the label of α are $D_{\overline{r+1}}, D_{\overline{r+2}}, \ldots, D_0$. Their corresponding lattice points also lie in a segment of the boundary of $\Delta(\Gamma)$. After relabelling, $\operatorname{div}(\alpha) = D_1 + D_2 + \cdots + D_r$ for some $1 \leq r \leq n-1$.

It remains to show that every summand of $\operatorname{div}(\alpha)$ is a boundary divisor. The edge $\mathfrak{e}_\alpha$ dual to the arrow α shares a node with an edge $\mathfrak{e}_a$ dual to an arrow $a \in Q_1$ with head at vertex 0. By Lemma 4.2, all interior divisors of $\mathcal{M}_A$ are summands of $\operatorname{div}(a)$. Therefore, $\mathfrak{e}_a \in \Pi_\rho$ for all interior divisors D_ρ. It follows that $\mathfrak{e}_\alpha \notin \Pi_\rho$ for all interior divisors D_ρ of $\mathcal{M}_A$, as Π_ρ is a perfect matching. Hence, no interior divisor of $\mathcal{M}_A$ is a summand of $\operatorname{div}(\alpha)$. □

Remark 4.4. The proof of Lemma 4.3 also shows that the segment of the boundary of $\Delta(\Gamma)$ determined by lattice points of the summands of $\mathrm{div}(\alpha)$ is bounded by the line segments corresponding to the zigzag paths $\mathrm{zig}(\mathfrak{e}_\alpha)$ and $\mathrm{zag}(\mathfrak{e}_\alpha)$. Raf Bocklandt proved this result and Lemma 4.3 independently in unpublished work.

Definition 4.5. By Lemma 4.3, after relabelling the boundary divisors, there exist consecutive boundary divisors $D_1, D_2, \cdots, D_r$ in $\Delta(\Gamma)$ such that $\mathrm{div}(\alpha) = D_1 + D_2 + \ldots + D_r$ for some $1 \leq r \leq n-1$. Define

$$\Sigma' := \{\sigma \in \Sigma \mid \rho_i \nsubseteq \sigma \text{ for all } 1 \leq i \leq r\} \tag{4.2.1}$$

to be the fan made of all cones $\sigma \in \Sigma$ such that ρ_i is not a ray of σ $(1 \leq i \leq r)$. Write $\Delta' := \Sigma' \cap \Delta(\Gamma)$ for the cross-section of Σ' at height one.

Proposition 4.6. *The subset Δ' of Δ is a convex polygon.*

Proof. Our choice of 0-generated stability parameter θ implies that the line bundle $L_{\mathsf{h}(\alpha)}$ is globally generated and that the subset of $\Delta(\Gamma)$

$$P(\alpha) := \left\{ p \in \Delta(\Gamma) \;\middle|\; \begin{array}{c} \exists\ \sigma \in \Sigma(3) \text{ such that } p \in \sigma \cap \Delta(\Gamma) \text{ and} \\ x^{\mathrm{div}(\alpha)} \text{ generates } L_{\mathsf{h}(\alpha)}|_{U_\sigma} \text{ as an } \mathcal{O}_{U_\sigma}\text{-module} \end{array} \right\}$$

is convex (see proof of [Cra05, Lemma 5.3(i)]). Hence, it suffices to show that $\Delta' = P(\alpha)$. Let $\sigma \in \Sigma(3)$ be a three-dimensional cone and let $y \in U_\sigma \subseteq \mathcal{M}_A$ denote the origin in $U_\sigma \cong \mathbb{C}^3$. Suppose $p \in \sigma \cap \Delta(\Gamma)$. Then, $p \in P(\alpha)$ if and only if the corresponding torus-invariant θ-stable representation M_σ has a path from 0 to $v \in Q_0$ that begins along the arrow α. Recall that the cosupport of M_σ is the union of the three perfect matchings corresponding to the rays of σ. Therefore, $\alpha \in Q_1$ is in M_σ if and only if $\rho \nsubseteq \sigma$ for all $\rho \in \Sigma_\alpha(1) := \{\rho \in \Sigma(1) | \, \mathrm{div}(\alpha) - D_\rho \geq 0\}$. This is true if and only if σ is a cone in Σ'. Hence, the equality holds, and the result follows. □

Definition 4.7. A polygon is said to be *nondegenerate* if not all of its vertices lie on a straight line.

Theorem 4.8. *Suppose Δ' is a nondegenerate polygon. Let Y' denote the toric variety defined by the fan Σ' from (4.2.1) and let $\sigma' := \left\{ \sum_{\lambda_\rho \geq 0} \lambda_\rho u_\rho \in N_\mathbb{R} \mid u_\rho \in \Delta' \right\}$ denote the cone over Δ'. Then:*

1. *Y' is the open subvariety of $\mathcal{M}_A$ satisfying $Y' = \mathcal{M}_A \setminus \mathrm{supp}(\mathrm{div}(\alpha))$;*
2. *Y' is a crepant resolution of the affine Gorenstein toric variety $U_{\sigma'}$.*

Proof. This follows from Proposition 4.6. As Δ' is a nondegenerate convex polygon, the cone σ' defines a three-dimensional affine toric variety $U_{\sigma'}$. The variety $U_{\sigma'}$ is Gorenstein as all the primitive ray generators of σ' lie in a hyperplane. The nondegeneracy and convexity of Δ' also imply that the fan Σ' defines a three-dimensional toric variety Y'. The variety Y' is smooth as each of its cones is a cone of $\mathcal{M}_A$, which is itself a smooth variety. As Σ' is a subfan of Σ, Y' is a subvariety of $\mathcal{M}_A$, and by construction $Y' = \mathcal{M}_A \setminus \mathrm{supp}(\mathrm{div}(\alpha))$. Finally, since Σ' is determined completely by a triangulation of the slice Δ' of σ', Y' is a crepant resolution of $U_{\sigma'}$. □

The following lemma gives the first connection between combinatorial Reid's recipe, the arrow α and certain line segments of Σ':

Lemma 4.9. *The line segments along $\partial\Sigma' \setminus \partial\Sigma$ have label $\mathsf{h}(\alpha)$ by Reid's recipe, as line segments of Σ.*

Proof. Consider a jigsaw transformation along any of the line segments τ in $\partial\Sigma' \setminus \partial\Sigma$. We need to show that $\mathsf{h}(\alpha)$ is the generator of the quiver $Q_{\pm}(\tau)$. First, note that the tile dual to $\mathsf{h}(\alpha)$ is not in $\mathrm{Jig}_{\tau}(0)$, as the arrow α is contained in the the perfect matchings of $D_1, \ldots, D_r$. Therefore, $\mathsf{h}(\alpha)$ is a vertex of $Q_{\pm}(\tau)$. Suppose $\mathsf{h}(\alpha)$ is not a generator of $Q_{\pm}(\tau)$, then there exists a path p in Q from 0 to a vertex $v \in Q_0$ such that $\mathrm{div}(p)$ is a summand of $\mathrm{div}(\alpha)$. In particular, there exists an arrow α' with tail at zero, such that $\mathrm{div}(\alpha')$ is a summand of $\mathrm{div}(\alpha)$. The divisor $D = \mathrm{div}(\alpha) - \mathrm{div}(\alpha')$ defines a section of $L_{\mathsf{h}(\alpha)} \otimes L^{-1}_{\mathsf{t}(\alpha')}$ and hence a path in Q. So, there is a relation in which α appears as a linear term, a contradiction, as Γ has no bivalent nodes. □

CHAPTER 5

THE SUBSET OF EDGES $\mathcal{S}_\alpha$

In Chapter 4, we associated to each arrow $\alpha \in Q_1$ with tail at vertex 0 a convex polygon Δ' and an open subvariety $Y' \hookrightarrow \mathcal{M}_A$. The aim of the arrow contraction algorithm is to generate a new dimer model Γ' from Γ, whose associated affine Gorenstein toric variety is $U_{\sigma'}$, for σ' the cone over Δ', and its moduli space of θ'-stable A'-modules, for θ' a 0-generated stability parameter, is Y'. In order to define Γ' we need to determine a subset of edges $\mathcal{S}_\alpha \subseteq \mathfrak{E}$ that will be removed from Γ.

In this chapter, we define the set $\mathcal{S}_\alpha$ in terms of the meandering walks of line segments in a strip of triangles strip(α). Assuming Conjecture 5.7, we give two alternative characterisations of $\mathcal{S}_\alpha$ using the triangles in strip(α) and the trivalent nodes of their fundamental hexagons (see Proposition 5.15 and Theorem 5.16). These characterisations will be useful in proving that the dimer model obtained from Γ by removing the edges in $\mathcal{S}_\alpha$ is consistent (see Theorem 6.15). We conclude the chapter by introducing the circuit diagram for α, which gives a schematic depiction of the edges in $\mathcal{S}_\alpha$ and all meandering walks $\mathfrak{m}_\tau$, where τ is a line segment in strip(α).

5.1 The strip of triangles strip(α)

Let Γ be a consistent dimer model with dual quiver Q. For a 0-generated stability parameter θ, let Σ denote the fan of $\mathcal{M}_A$. Fix $\alpha \in Q_1$ with tail at vertex 0.

Definition 5.1. Define

$$\text{strip}(\alpha) := \Sigma \setminus \Sigma'$$

to be the set of triangles in the complement of Σ'.

The geometry of strip(α) forces it to be a strip of triangles, which justifies the notation.

Let $\sigma_0, \ldots, \sigma_k$ be the $k+1$ triangles along the strip strip(α) arranged in a clockwise direction. For $1 \leq i \leq k$, let τ_i denote the line segment $\sigma_{i-1} \cap \sigma_i$. Write τ_0 and τ_{k+1} to be the line segments of σ_0 and σ_k which form part of the boundary of Σ. For $0 \leq i \leq k$, write τ_i' for the line segment of σ_i that does not coincide with either τ_{i-1} or τ_i.

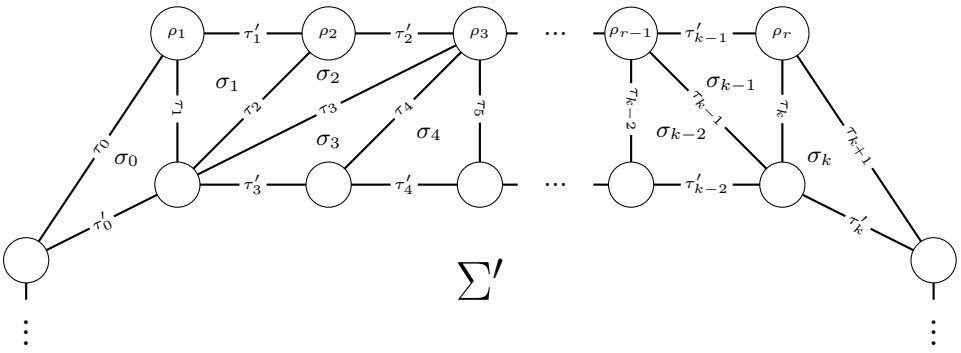

Figure 5.1: *A typical strip* strip(α)

We distinguish between two different types of triangles in strip(α):

Definition 5.2. For $0 \leq i \leq k$, each τ'_i is either:

(i) on the boundary of Σ', in which case we call σ_i a *lower triangle*; or

(ii) on the boundary Σ, in which case we call σ_i an *upper triangle*.

Recall that to any two-dimensional cone τ in Σ we associate a subset of edges of Γ called the meandering walk $\mathfrak{m}_\tau$ of τ (see Definition 2.12).

Definition 5.3. For τ a line segment in strip(α), the meandering walk $\mathfrak{m}_\tau$ is called:

(i) a *lower meandering walk* of strip(α) if $\tau = \tau'_i$ for a lower triangle σ_i $(0 \leq i \leq k)$;

(ii) a *middle meandering walk* of strip(α) if $\tau = \tau_i$ for $1 \leq i \leq k$;

(iii) an *upper meandering walk* of strip(α) if $\tau = \tau'_i$ for an upper triangle σ_i $(0 \leq i \leq k)$ or $\tau = \tau_0$ or τ_k.

To simplify notation, we write $\mathfrak{m}_i$ and $\mathfrak{m}'_i$ for the meandering walks $\mathfrak{m}_{\tau_i}$ and $\mathfrak{m}_{\tau'_i}$ $(0 \leq i \leq k)$ and $\mathfrak{m}_{k+1}$ for $\mathfrak{m}_{\tau_{k+1}}$. Both upper and lower meandering walks carry a natural direction as follows:

(i) Every upper meandering walk supports a zigzag path in Γ (see Remark 2.15) which has a direction determined by the fact that it turns maximally right at white nodes and maximally left at black nodes;

(ii) To each lower meandering walk $\mathfrak{m}_\tau$ we assign the direction $[\Pi_{\rho'} - \Pi_\rho]$, where ρ and ρ' are the ray generators of τ and ρ' is adjacent to ρ in a clockwise direction along the boundary of Σ'. With this convention, the homology class of a lower meandering walk is the inward-pointing normal vector to the boundary edge of Δ'.

We use the meandering walks of strip(α) to define a subset of edges $\mathcal{S}_\alpha \subset \mathfrak{E}$ as follows:

Definition 5.4. Define the subset of $\mathfrak{E}$ given by

$$\mathcal{S}_\alpha := (\mathfrak{m}_0 \cup \mathfrak{m}_{k+1}) \setminus \bigcup_{\substack{\mathfrak{m} \text{ a lower} \\ \text{meandering} \\ \text{walk}}} \mathfrak{m}.$$

Lemma 5.5. *The edge $\mathfrak{e}_\alpha$ is an element of $\mathcal{S}_\alpha$.*

Proof. The edge $\mathfrak{e}_\alpha$ lies in $\mathrm{supp}(\mathfrak{z}_0) = \mathfrak{m}_0$ and $\mathrm{supp}(\mathfrak{z}_r) = \mathfrak{m}_{k+1}$. For all $1 \leq i \leq k$, write ρ_i' and ρ_i'' for the ray generators of τ_i. Since by Lemma 4.3 the label $\mathrm{div}(\alpha) = D_1 + D_2 + \cdots + D_r$ contains no interior divisors, $\mathfrak{e}_\alpha \in \Pi_{\rho_i'} \ominus \Pi_{\rho_i''} = \mathfrak{m}_i$ for all $1 \leq i \leq k$. Moreover, as $\mathfrak{e}_\alpha$ is an edge in $\mathfrak{m}_0, \mathfrak{m}_1, \ldots, \mathfrak{m}_{k+1}$, $\mathfrak{e}_\alpha \notin \mathfrak{m}_i'$ for all $0 \leq i \leq k$. In particular, $\mathfrak{e}_\alpha \notin \mathfrak{m}$ for every lower meandering walk $\mathfrak{m}$ and hence $\mathfrak{e}_\alpha$ is an element of $\mathcal{S}_\alpha$. □

Lemma 5.6. *The black and white endnodes of $\mathfrak{e}_\alpha$ are the black and white trivalent nodes of* $\mathrm{Hex}(\sigma_0)$ *and* $\mathrm{Hex}(\sigma_k)$*, respectively.*

Proof. By the proof of Lemma 5.5, $\mathfrak{e}_\alpha$ is an edge in $\mathfrak{m}_0, \mathfrak{m}_1, \ldots, \mathfrak{m}_{k+1}$. Moreover, since $\mathfrak{m}_0$ and $\mathfrak{m}_{k+1}$ support the zigzag paths $\mathfrak{z}_0$ and $\mathfrak{z}_r$ and the edge $\mathfrak{e}_\alpha$ is a zig of $\mathfrak{z}_0$ and a zag of $\mathfrak{z}_r$, the edges $\mathfrak{e} \in \mathfrak{m}_0$ and $\mathfrak{e}' \in \mathfrak{m}_{k+1}$ following $\mathfrak{e}_\alpha$ are dual to arrows with head at vertex 0. Therefore, by Lemma 4.2 the labels $\mathrm{div}(a_\mathfrak{e})$ and $\mathrm{div}(a_{\mathfrak{e}'})$ have all the interior divisors of $\mathcal{M}_A$ as their summands. It follows that $\mathfrak{e} \in \mathfrak{m}_0 \cap \mathfrak{m}_1 \cap \cdots \cap \mathfrak{m}_k \cap \mathfrak{m}_k'$ and $\mathfrak{e}' \in \mathfrak{m}_0' \cap \mathfrak{m}_1 \cap \mathfrak{m}_2 \cap \cdots \cap \mathfrak{m}_{k+1}$. Therefore the white node common to both $\mathfrak{e}$ and $\mathfrak{e}_\alpha$ and the black node common to both $\mathfrak{e}'$ and $\mathfrak{e}_\alpha$ are the white and black trivalent nodes of $\mathrm{Hex}(\sigma_k)$ and $\mathrm{Hex}(\sigma_0)$, respectively. □

5.2 Walking along $\mathfrak{m}_0$ and $\mathfrak{m}_{k+1}$

In this section, we describe the behaviour of the middle meandering walks $\mathfrak{m}_1, \mathfrak{m}_2, \ldots, \mathfrak{m}_k$ as we travel along $\mathfrak{m}_0$ and $\mathfrak{m}_{k+1}$. This understanding will enable us to characterise the edges in $\mathcal{S}_\alpha$ in terms of the triangles in $\mathrm{strip}(\alpha)$ and the trivalent nodes of their fundamental hexagons (see Theorem 5.16).

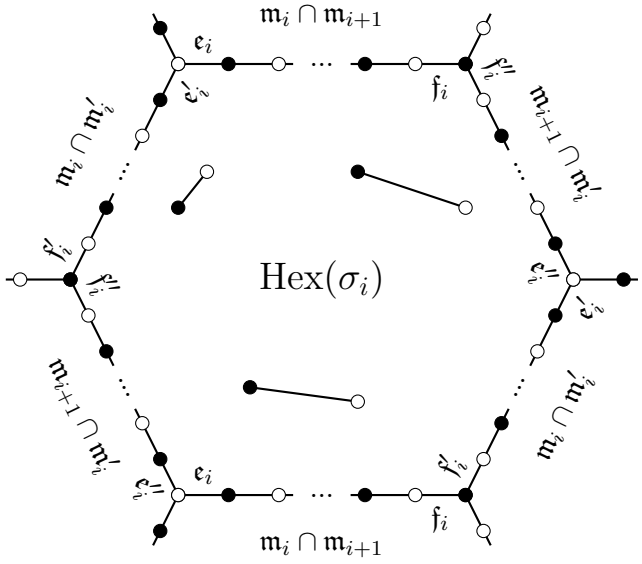

Figure 5.2: *Edges $\mathfrak{e}_i, \mathfrak{e}_i', \mathfrak{e}_i''$ and $\mathfrak{f}_i, \mathfrak{f}_i', \mathfrak{f}_i''$ in* $\mathrm{Hex}(\sigma_i)$

For the purposes of this section, we assign to $\mathfrak{m}_0$ and $\mathfrak{m}_{k+1}$ the direction opposite to that of the zigzag paths supported on them. We say two meandering walks *travel together* between two nodes $\mathfrak{n}$ and $\mathfrak{n}'$ if they share a sequence of edges $\{\mathfrak{e}_1, \mathfrak{e}_2, \ldots, \mathfrak{e}_j\}$ in

$\mathfrak{E}$ and $\mathfrak{n}$ and $\mathfrak{n}'$ are endpoints of $\mathfrak{e}_1$ and $\mathfrak{e}_j$, respectively. We say two meandering walks travelling together along a set of edges $\{\mathfrak{e}_1, \mathfrak{e}_2, \ldots, \mathfrak{e}_j\}$ *split* at the endnode $\mathfrak{n}$ of $\mathfrak{e}_j$ if the edges following $\mathfrak{e}_j$ are different for both meandering walks. For $0 \leq i \leq k$, write $\mathfrak{w}_i$ and $\mathfrak{b}_i$ for the white and black trivalent nodes of $\mathrm{Hex}(\sigma_i)$ in Γ and let $\mathfrak{e}_i$, $\mathfrak{e}_i'$ and $\mathfrak{e}_i''$ and $\mathfrak{f}_i$, $\mathfrak{f}_i'$ and $\mathfrak{f}_i''$ denote the edges in $\partial\,\mathrm{Hex}(\sigma_i)$ around $\mathfrak{w}_i$ and $\mathfrak{b}_i$, respectively so that $\mathfrak{e}_i, \mathfrak{f}_i \in \mathfrak{m}_i \cap \mathfrak{m}_{i+1}$, $\mathfrak{e}_i', \mathfrak{f}_i' \in \mathfrak{m}_i \cap \mathfrak{m}_i'$ and $\mathfrak{e}_i'', \mathfrak{f}_i'' \in \mathfrak{m}_{i+1} \cap \mathfrak{m}_i'$, as depicted in Figure 5.2.

5.2.1 Walking along $\mathfrak{m}_0$

We assume the following conjecture:

Conjecture 5.7. *Let σ_i and σ_{i+1} be triangles in the strip* $\mathrm{strip}(\alpha)$*, then:*

(i) If σ_i is an lower triangle and σ_{i+1} is a upper triangle, $\mathfrak{e}_i \in \mathfrak{m}_{i+1}'$;

(ii) If σ_i is an upper triangle and σ_{i+1} is a lower triangle, $\mathfrak{f}_i \in \mathfrak{m}_{i+1}'$;

(iii) If σ_i and σ_{i+1} are lower triangles, $\mathfrak{e}_i \in \mathfrak{m}_{i+2}$ and $\mathfrak{f}_{i+1} \in \mathfrak{m}_0$;

(iv) If σ_i and σ_{i+1} are upper triangles, $\mathfrak{f}_i \in \mathfrak{m}_{i+2}$ and $\mathfrak{e}_{i+1} \in \mathfrak{m}_0$;

(v) If $\mathfrak{e} \in \mathfrak{m}_0 \cap \mathfrak{m}_1 \cap \cdots \mathfrak{m}_i \cap \mathfrak{m}_i'$ for an upper meandering walk $\mathfrak{m}_i'$, $\mathfrak{e}$ is not an edge in any lower meandering walk of $\mathrm{strip}(\alpha)$*.*

Lemmata 5.8 – 5.11 enable us to describe the walk along $\mathfrak{m}_0$ inductively as we jump between adjacent triangles in the strip $\mathrm{strip}(\alpha)$ in a clockwise direction.

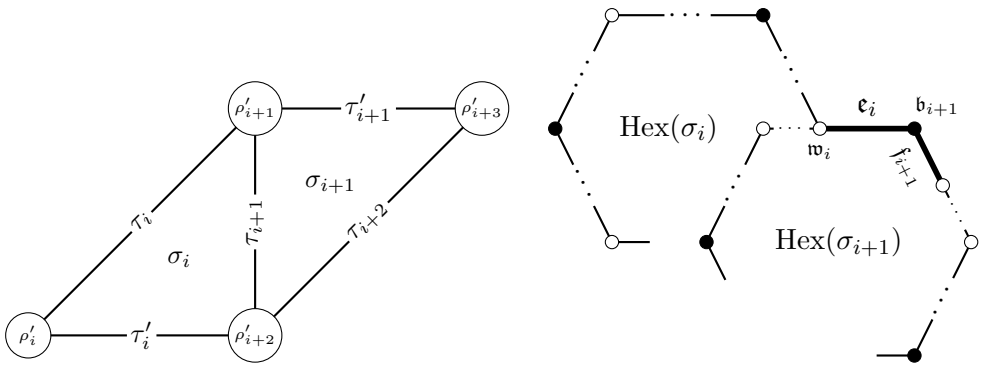

(a) A lower and an upper triangle in $\mathrm{strip}(\alpha)$ (b) The nodes of $\mathfrak{e}_i$ are $\mathfrak{w}_i$ and $\mathfrak{b}_{i+1}$

Figure 5.3: *Depiction of results in Lemma 5.8*

Lemma 5.8. *Suppose σ_i is a lower triangle and σ_{i+1} is an upper triangle and suppose:*

(i) The edge $\mathfrak{e}_i$ lies in $\mathfrak{m}_0, \mathfrak{m}_1, \ldots, \mathfrak{m}_{i+1}$; and

(ii) $\mathfrak{m}_0, \mathfrak{m}_1, \ldots, \mathfrak{m}_{i+1}$ travel together from $\mathfrak{w}_i$ until $\mathfrak{b}_0$.

Then the white and black nodes of $\mathfrak{e}_i$ are the white trivalent node $\mathfrak{w}_i$ of $\mathrm{Hex}(\sigma_i)$ *and the black trivalent node $\mathfrak{b}_{i+1}$ of* $\mathrm{Hex}(\sigma_{i+1})$*. Moreover:*

(i') The edge $\mathfrak{f}_{i+1}$ lies in $\mathfrak{m}_0, \mathfrak{m}_1, \ldots, \mathfrak{m}_{i+2}$; and

(ii') $\mathfrak{m}_0, \mathfrak{m}_1, \ldots, \mathfrak{m}_{i+2}$ *travel together from* $\mathfrak{b}_{i+1}$ *until* $\mathfrak{b}_0$.

Proof. By Conjecture 5.7 (i), $\mathfrak{e}_i \in \mathfrak{m}'_{i+1}$. Since σ_{i+1} is an upper triangle, $\mathfrak{m}'_{i+1}$ is a zigzag path. Thus $\mathfrak{e}_i \in \mathfrak{m}_0 \cap \mathfrak{m}'_{i+1}$, both zigzag paths. By assumption, Γ has no bivalent nodes. Therefore $\mathfrak{m}_0$ and $\mathfrak{m}'_{i+1}$ split at the black node of $\mathfrak{e}_i$. Note that the black node of $\mathfrak{e}_i$ is not $\mathfrak{b}_0$, as $\mathfrak{e}_i \notin \mathfrak{m}_{i+2}$. Since $\mathfrak{m}_0, \ldots, \mathfrak{m}_{i+1}$ travel together from $\mathfrak{w}_i$ until $\mathfrak{b}_0$, the black node of $\mathfrak{e}_i$ is the black trivalent node $\mathfrak{b}_{i+1}$ of $\mathrm{Hex}(\sigma_{i+1})$. As we have not met $\mathfrak{b}_0$, the edge $\mathfrak{f}_{i+1}$ lies in $\mathfrak{m}_0, \mathfrak{m}_1, \ldots, \mathfrak{m}_{i+2}$. Moreover, by the time we reach $\mathfrak{b}_0$ again, we must be travelling along $\mathfrak{m}_0, \mathfrak{m}_1, \ldots, \mathfrak{m}_k$. So, we cannot meet $\mathfrak{w}_{i+1}$ along $\mathfrak{m}_0$, as this would imply $\mathfrak{m}_{i+1}$ and $\mathfrak{m}_{i+2}$ stop travelling together and we cannot meet $\mathfrak{b}_{i+1}$ again before $\mathfrak{b}_0$ as $\mathfrak{m}_0$ does intersect itself. Hence, $\mathfrak{m}_0, \ldots, \mathfrak{m}_{i+2}$ travel together from $\mathfrak{b}_{i+1}$ until $\mathfrak{b}_0$. □

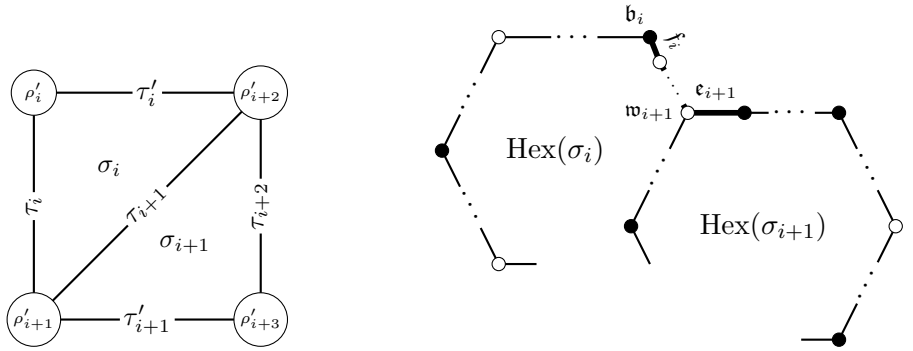

(a) An upper and a lower triangle in strip(α)

(b) The walks $\mathfrak{m}_0, \mathfrak{m}_1, \ldots, \mathfrak{m}_{i+1}$ meet $\mathfrak{w}_{i+1}$ travelling along the thickened edges

Figure 5.4: *Depiction of results in Lemma 5.9*

Lemma 5.9. *Suppose σ_i is an upper triangle and σ_{i+1} is a lower triangle and suppose:*

(i) The edge $\mathfrak{f}_i$ lies in $\mathfrak{m}_0, \mathfrak{m}_1, \ldots, \mathfrak{m}_{i+1}$; and

(ii) $\mathfrak{m}_0, \mathfrak{m}_1, \ldots, \mathfrak{m}_{i+1}$ travel together from $\mathfrak{b}_i$ until $\mathfrak{b}_0$.

Then, the walks $\mathfrak{m}_0, \ldots, \mathfrak{m}_{i+1}$ meet $\mathfrak{w}_{i+1}$ and moreover:

(i') The edge $\mathfrak{e}_{i+1}$ lies in $\mathfrak{m}_0, \mathfrak{m}_1, \ldots, \mathfrak{m}_{i+2}$; and

(ii') $\mathfrak{m}_0, \mathfrak{m}_1, \ldots, \mathfrak{m}_{i+2}$ travel together from $\mathfrak{w}_{i+1}$ until $\mathfrak{b}_0$.

Proof. By Conjecture 5.7 (ii), $\mathfrak{f}_i \in \mathfrak{m}'_{i+1}$. Travel along $\mathfrak{m}_{i+1}, \mathfrak{m}'_{i+1}$ until the next trivalent node of $\mathrm{Hex}(\sigma_{i+1})$. Since $\mathfrak{f}_i \in \Pi_{\rho'_{i+1}}$ and edges from $\mathfrak{b}_i$ onwards belong alternatively to $\Pi_{\rho'_{i+1}}$ and $\Pi_{\rho'_i} \cap \Pi_{\rho'_{i+2}} \cap \Pi_{\rho'_{i+3}}$, the trivalent node is white (see Figure 5.4(a)). As none of the edges between $\mathfrak{b}_i$ and $\mathfrak{w}_{i+1}$ belongs to $\mathfrak{m}_{i+1}$, we do not meet $\mathfrak{b}_0$ before $\mathfrak{w}_{i+1}$. Therefore, $\mathfrak{e}_{i+1}$ lies in $\mathfrak{m}_0, \mathfrak{m}_1, \ldots, \mathfrak{m}_{i+2}$. Moreover, by the time we reach $\mathfrak{b}_0$ again, we must be travelling along $\mathfrak{m}_0, \mathfrak{m}_1, \ldots, \mathfrak{m}_k$. So, we cannot meet $\mathfrak{b}_{i+1}$ along $\mathfrak{m}_0$, as this would imply that $\mathfrak{m}_i$ and $\mathfrak{m}_{i+1}$ stop travelling together. Hence, $\mathfrak{m}_0, \ldots, \mathfrak{m}_{i+2}$ travel together from $\mathfrak{w}_{i+1}$ until $\mathfrak{b}_0$ □

Lemma 5.10. *Suppose σ_i and σ_{i+1} are lower triangles and suppose:*

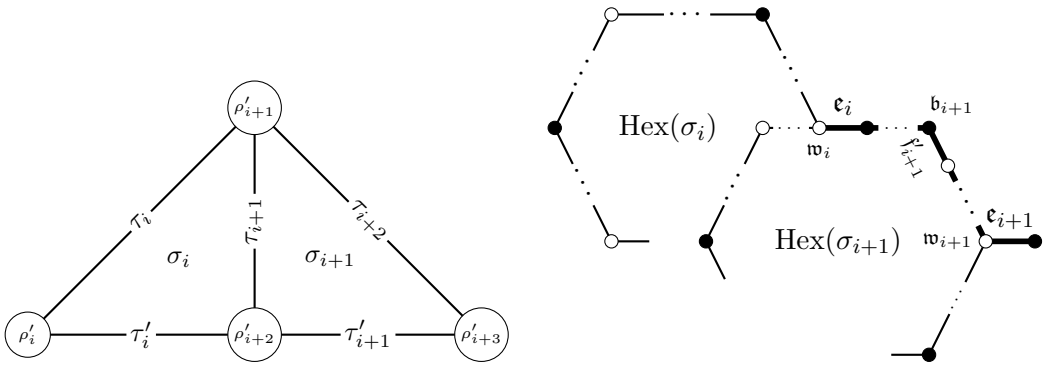

(a) Two lower triangles in strip(α)

(b) The walks $\mathfrak{m}_0, \mathfrak{m}_1, \ldots, \mathfrak{m}_{i+1}$ meet $\mathfrak{b}_{i+1}$ and $\mathfrak{w}_{i+1}$ travelling along the thickened edges

Figure 5.5: *Depiction of results in Lemma 5.10*

(i) The edge $\mathfrak{e}_i$ lies in $\mathfrak{m}_0, \mathfrak{m}_1, \ldots, \mathfrak{m}_{i+1}$; and

(ii) $\mathfrak{m}_0, \mathfrak{m}_1, \ldots, \mathfrak{m}_{i+1}$ travel together from $\mathfrak{w}_i$ until $\mathfrak{b}_0$.

Then the walks $\mathfrak{m}_0, \ldots, \mathfrak{m}_{i+1}$ meet $\mathfrak{b}_{i+1}$ and $\mathfrak{w}_{i+1}$ and moreover:

(i') The edge $\mathfrak{e}_{i+1}$ lies in $\mathfrak{m}_0, \mathfrak{m}_1, \ldots, \mathfrak{m}_{i+2}$; and

(ii') $\mathfrak{m}_0, \mathfrak{m}_1, \ldots, \mathfrak{m}_{i+2}$ travel together from $\mathfrak{w}_{i+1}$ until $\mathfrak{b}_0$.

Proof. By Conjecture 5.7 (iii), $\mathfrak{e}_i \in \mathfrak{m}_{i+2}$ and $\mathfrak{f}_{i+1} \in \mathfrak{m}_0$. Travel along $\mathfrak{m}_i, \mathfrak{m}_{i+1}$ until the next trivalent node of $\mathrm{Hex}(\sigma_{i+1})$. Since $\mathfrak{e}_i \in \Pi_{\rho'_{i+1}}$ and edges from $\mathfrak{w}_i$ onwards belong alternatively to $\Pi_{\rho'_{i+1}}$ and $\Pi_{\rho'_i} \cap \Pi_{\rho'_{i+2}} \cap \Pi_{\rho'_{i+3}}$, the trivalent node is black (see Figure 5.5(a)). By conjecture, $\mathfrak{f}_{i+1} \in \mathfrak{m}_0$ and we know $\mathfrak{f}_{i+1} \in \mathfrak{m}_i \cap \mathfrak{m}_{i+1}$. Therefore, we could had not passed through $\mathfrak{b}_0$ before $\mathfrak{b}_{i+1}$ and $\mathfrak{f}'_{i+1}$ lies in $\mathfrak{m}_0, \mathfrak{m}_1, \ldots, \mathfrak{m}_{i+1}, \mathfrak{m}'_{i+1}$. Now, travel along $\mathfrak{m}_{i+1}, \mathfrak{m}'_{i+1}$ until the white trivalent node $\mathfrak{w}_{i+1}$. As an edge along $\partial\,\mathrm{Hex}(\sigma_{i+1})$ cannot lie in $\mathfrak{m}_{i+1}, \mathfrak{m}'_{i+1}$ and $\mathfrak{m}_{i+2}$, we do not meet $\mathfrak{b}_0$ before $\mathfrak{w}_{i+1}$. Thus, $\mathfrak{e}_{i+1}$ lies in $\mathfrak{m}_0, \mathfrak{m}_1, \ldots, \mathfrak{m}_{i+2}$, Moreover, we cannot meet another trivalent node of $\mathrm{Hex}(\sigma_{i+1})$ before meeting $\mathfrak{b}_0$, as $\mathfrak{m}_0$ does not intersect itself. Hence, $\mathfrak{m}_0, \ldots, \mathfrak{m}_{i+2}$ travel together from $\mathfrak{w}_{i+1}$ until $\mathfrak{b}_0$ □

Lemma 5.11. *Suppose σ_i and σ_{i+1} are upper triangles and suppose:*

(i) The edge $\mathfrak{f}_i$ lies in $\mathfrak{m}_0, \mathfrak{m}_1, \ldots, \mathfrak{m}_{i+1}$; and

(ii) $\mathfrak{m}_0, \mathfrak{m}_1, \ldots, \mathfrak{m}_{i+1}$ travel together from $\mathfrak{b}_i$ until $\mathfrak{b}_0$.

Then $\mathfrak{m}_0, \ldots, \mathfrak{m}_{i+1}$ meet $\mathfrak{w}_{i+1}$ and $\mathfrak{b}_{i+1}$. The white and black nodes of $\mathfrak{e}'_i$ are the white and black trivalent nodes of $\mathrm{Hex}(\sigma_{i+1})$*. Moreover:*

(i') The edge $\mathfrak{f}_{i+1}$ lies in $\mathfrak{m}_0, \mathfrak{m}_1, \ldots, \mathfrak{m}_{i+2}$; and

(ii') $\mathfrak{m}_0, \mathfrak{m}_1 \ldots, \mathfrak{m}_{i+2}$ travel together from $\mathfrak{b}_{i+1}$ until $\mathfrak{b}_0$.

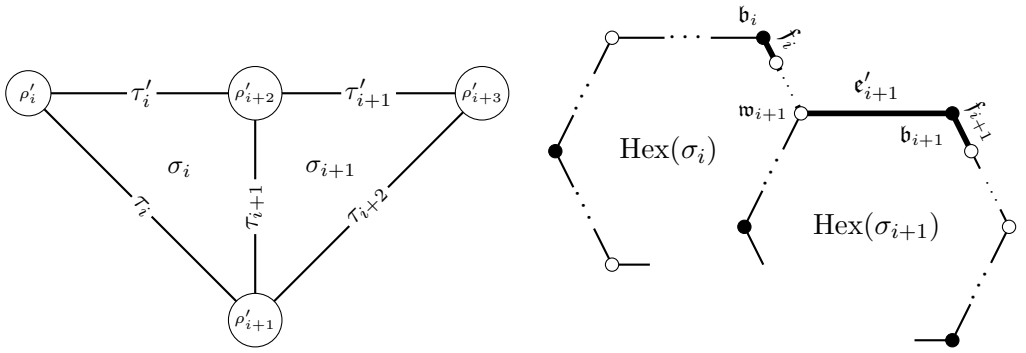

(a) Two upper triangles in strip(α)

(b) The walks $\mathfrak{m}_0, \mathfrak{m}_1, \ldots, \mathfrak{m}_{i+1}$ meet $\mathfrak{w}_{i+1}$ and $\mathfrak{b}_{i+1}$ travelling along the thickened edges. The nodes of $\mathfrak{e}'_{i+1}$ are $\mathfrak{w}_{i+1}$ and $\mathfrak{b}_{i+1}$.

Figure 5.6: *Depiction of results in Lemma 5.8*

Proof. By Conjecture 5.7 (ii), $\mathfrak{f}_i \in \mathfrak{m}_{i+2}$ and $\mathfrak{e}_{i+1} \in \mathfrak{m}_0$. Travel along $\mathfrak{m}_{i+1}, \mathfrak{m}_{i+2}$ until the next trivalent node of $\mathrm{Hex}(\sigma_{i+1})$. Since $\mathfrak{f}_i \in \Pi_{\rho'_{i+1}}$ and edges from $\mathfrak{b}_i$ onwards belong alternatively to $\Pi_{\rho'_{i+1}}$ and $\Pi_{\rho'_i} \cap \Pi_{\rho'_{i+2}} \cap \Pi_{\rho'_{i+3}}$, the trivalent node is white (see Figure 5.6(a)). By conjecture, $\mathfrak{e}_{i+1} \in \mathfrak{m}_0$ and we know $\mathfrak{e}_{i+1} \in \mathfrak{m}_i \cap \mathfrak{m}_{i+1}$. Thus, we could not had passed through $\mathfrak{b}_0$ before $\mathfrak{w}_{i+1}$ and $\mathfrak{e}'_{i+1}$ lies in $\mathfrak{m}_0, \mathfrak{m}_1, \ldots, \mathfrak{m}_i, \mathfrak{m}'_{i+1}$. Since σ_{i+1} is an upper triangle, $\mathfrak{m}'_{i+1}$ is a zigzag path. As Γ has no bivalent nodes, $\mathfrak{m}_0$ and $\mathfrak{m}'_{i+1}$ split at the black node of $\mathfrak{f}'_{i+1}$. The edge $\mathfrak{f}'_{i+1}$ does not lie in $\mathfrak{m}_{i+1}$ and hence its black node is not $\mathfrak{b}_0$. Therefore, after the black node of $\mathfrak{f}'_{i+1}$, $\mathfrak{m}_0, \mathfrak{m}_1, \ldots, \mathfrak{m}_{i+1}$ travel together, which implies that the black node is in fact $\mathfrak{b}_{i+1}$. It follows that $\mathfrak{e}_{i+1}$ lies in $\mathfrak{m}_0, \mathfrak{m}_1, \ldots, \mathfrak{m}_{i+2}$. Since $\mathfrak{m}_0$ does not intersect itself, $\mathfrak{m}_{i+1}$ and $\mathfrak{m}_{i+2}$ travel together at least up to $\mathfrak{b}_0$ and thus $\mathfrak{m}_0, \mathfrak{m}_1, \ldots, \mathfrak{m}_{i+2}$ travel together from $\mathfrak{b}_{i+1}$ until $\mathfrak{b}_0$. □

We now describe an inductive mechanism that traces a cycle of the walk $\mathfrak{m}_0$ around $\mathbb{T}$ starting and finishing at $\mathfrak{e}_\alpha$, as we jump between adjacent triangles in strip(α) in a clockwise direction.

Algorithm 5.12. *Algorithm to trace a cycle of the walk $\mathfrak{m}_0$ around $\mathbb{T}$ starting and finishing at $\mathfrak{e}_\alpha$:*

1. *Start at $\mathfrak{e}_\alpha$. By Lemma 5.6, the black node of $\mathfrak{e}_\alpha$ is the black trivalent node of* $\mathrm{Hex}(\sigma_0)$. *Travel from $\mathfrak{b}_0$ to $\mathfrak{w}_0$ along edges in $\mathfrak{m}_0 \cap \mathfrak{m}'_0$. The edge $\mathfrak{e}_0$ attached to $\mathfrak{w}_0$ satisfies the initial conditions of Lemma 5.8 and Lemma 5.10.*

2. *Use either Lemma 5.8 or Lemma 5.10, depending on whether σ_1 is an upper or lower triangle, to trace $\mathfrak{m}_0$ from $\mathfrak{w}_0$ to a trivalent node of* $\mathrm{Hex}(\sigma_1)$.

3. *For $1 \leq i \leq k-1$, use the appropriate Lemma to trace $\mathfrak{m}_0$ from a trivalent node of* $\mathrm{Hex}(\sigma_i)$ *to a trivalent node of* $\mathrm{Hex}(\sigma_{i+1})$, *depending on whether σ_i and σ_{i+1} are upper or lower triangles.*

4. *The last triangle σ_k in* strip(α) *is a lower triangle, so we finish at the white trivalent node $\mathfrak{w}_k$ of* $\mathrm{Hex}(\sigma_k)$ *with $\mathfrak{e}_k$ in $\mathfrak{m}_0, \ldots, \mathfrak{m}_k$. By Lemma 5.6, $\mathfrak{e}_k = \mathfrak{e}_\alpha$ and the black node of $\mathfrak{e}_k$ is $\mathfrak{b}_0$. Therefore, we have completed tracing a cycle of $\mathfrak{m}_0$ around $\mathbb{T}$.*

5.2.2 Walking along $\mathfrak{m}_{k+1}$

A similar inductive mechanism can be used to trace a cycle of the walk $\mathfrak{m}_{k+1}$ around $\mathbb{T}$, starting and finishing at $\mathfrak{e}_\alpha$, as we jump between adjacent triangles in strip(α) in an anticlockwise direction. To obtain the equivalent statements of the Lemmata 5.8 – 5.11 for the case $\mathfrak{m}_{k+1}$:

(i) Replace $\mathfrak{b}_0$ by $\mathfrak{w}_k$;

(ii) Replace $\mathfrak{m}_0, \mathfrak{m}_1, \ldots, \mathfrak{m}_{i+1}$ by $\mathfrak{m}_i, \mathfrak{m}_{i+1}, \ldots, \mathfrak{m}_{k+1}$ and replace $\mathfrak{m}_0, \mathfrak{m}_1, \ldots, \mathfrak{m}_{i+2}$ by $\mathfrak{m}_{i-1}, \mathfrak{m}_i, \ldots, \mathfrak{m}_{k+1}$;

(iii) For the fixed index $0 \leq i \leq k-1$, replace the black nodes $\mathfrak{b}_i$ and $\mathfrak{b}_{i+1}$ by white nodes $\mathfrak{w}_i$ and $\mathfrak{w}_{i+1}$, and vice versa;

(iv) For the fixed index $0 \leq i \leq k-1$, replace the edges $\mathfrak{e}_i$ and $\mathfrak{e}_{i+1}$ by $\mathfrak{f}_i$ an $\mathfrak{f}_{i+1}$, and vice versa;

(v) Replace the indices $i+1$ from nodes, edges and cones by $i-1$; and

(vi) In the case of Lemma 5.11, replace $\mathfrak{e}'_{i+1}$ by $\mathfrak{f}''_{i-1}$.

For example, Lemma 5.8 becomes:

Lemma 5.13. *Suppose σ_i is a lower triangle and σ_{i-1} is an upper triangle and suppose:*

(i) The edge $\mathfrak{f}_i$ lies in $\mathfrak{m}_i, \mathfrak{m}_{i+1}, \ldots, \mathfrak{m}_{k+1}$; and

(ii) $\mathfrak{m}_i, \mathfrak{m}_{i+1}, \ldots, \mathfrak{m}_{k+1}$ travel together from $\mathfrak{b}_i$ until $\mathfrak{w}_k$.

Then the black and white nodes of $\mathfrak{e}_i$ are the black trivalent node $\mathfrak{b}_i$ of Hex(σ_i) *and the white trivalent node $\mathfrak{w}_{i-1}$ of* Hex(σ_{i-1})*. Moreover:*

(i') The edge $\mathfrak{e}_{i-1}$ lies in $\mathfrak{m}_{i-1}, \mathfrak{m}_i, \ldots, \mathfrak{m}_{k+1}$; and

(ii') $\mathfrak{m}_{i-1}, \mathfrak{m}_i, \ldots, \mathfrak{m}_{k+1}$ travel together from $\mathfrak{w}_{i-1}$ until $\mathfrak{w}_k$.

A similar conjecture to Conjecture 5.7 is needed in order to prove the equivalent statements of the Lemmata 5.8 – 5.11 for the case $\mathfrak{m}_{k+1}$. It can be obtained from Conjecture 5.7 in a manner similar to how the equivalent statements were obtained.

We can deduce more information about the edges in the intersection of the meandering walks $\mathfrak{m}_0, \mathfrak{m}_1, \ldots, \mathfrak{m}_{i+2}$ from Lemma 5.8 and Lemma 5.11 by using their equivalent statements for the meandering walk $\mathfrak{m}_{k+1}$.

Lemma 5.14. *If σ_i and σ_{i+1} are both lower (resp. upper) triangles, there exists an edge in $\mathfrak{m}_0, \mathfrak{m}_1, \ldots, \mathfrak{m}_{k+1}$ whose nodes are $\mathfrak{w}_i$ and $\mathfrak{b}_{i+1}$ ($\mathfrak{b}_i$ and $\mathfrak{w}_{i+1}$, respectively).*

Proof. Suppose σ_i and σ_{i+1} are both lower triangles. Consider the edges $\mathfrak{e}_i$ and $\mathfrak{f}_{i+1}$ attached to $\mathfrak{w}_i$ and $\mathfrak{b}_{i+1}$, respectively. By Lemma 5.10, $\mathfrak{e}_i$ lies in $\mathfrak{m}_0, \mathfrak{m}_1, \ldots, \mathfrak{m}_{i+2}$. The equivalent Lemma for $\mathfrak{m}_{k+1}$ shows that $\mathfrak{f}_{i+1}$ lies in $\mathfrak{m}_i, \mathfrak{m}_{i+1}, \ldots, \mathfrak{m}_{k+1}$. Since, $\mathfrak{m}_0, \mathfrak{m}_1, \ldots, \mathfrak{m}_{i+2}$ travel together from $\mathfrak{w}_i$ to $\mathfrak{b}_{i+1}$, and $\mathfrak{m}_i, \mathfrak{m}_{i+1}, \ldots, \mathfrak{m}_{k+1}$ travel together from $\mathfrak{b}_{i+1}$ to $\mathfrak{w}_i$, both $\mathfrak{e}_i$ and $\mathfrak{f}_{i+1}$ lie in $\mathfrak{m}_0, \mathfrak{m}_1, \ldots, \mathfrak{m}_{k+1}$. As $\mathfrak{m}_0$ and $\mathfrak{m}_{k+1}$ are zigzag paths and Γ has no bivalent nodes, $\mathfrak{e}_i = \mathfrak{f}_{i+1}$ is an edge in $\mathfrak{m}_0, \mathfrak{m}_1, \ldots, \mathfrak{m}_{k+1}$ whose nodes are $\mathfrak{w}_i$ and $\mathfrak{b}_{i+1}$.

A similar proof works for the case when σ_i and σ_{i+1} are both upper triangles. □

5.2.3 Summary of results

Lemmata 5.8 – 5.11 and their equivalent statement for $\mathfrak{m}_{k+1}$ imply that the meandering walks $\mathfrak{m}_0$ and $\mathfrak{m}_{k+1}$ can be partitioned into segments each corresponding to either:

(i) The starting point of the inductive mechanism; or

(ii) A jump between adjacent triangles in strip(α).

Table 5.1 gives a summary of the results in this section. To simplify notation, we write $\mathfrak{m}_{[i,j]}$ for the intersection $\bigcap_{\ell=i}^{j} \mathfrak{m}_\ell$.

	Segment of $\mathfrak{m}_0$	Segment of $\mathfrak{m}_{k+1}$
Starting Point	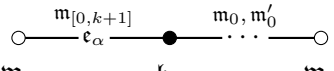 $\mathfrak{m}'_0$ is a lower meandering walk	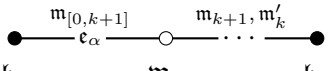 $\mathfrak{m}'_k$ is a lower meandering walk
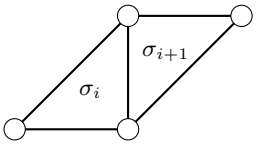	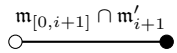 $\mathfrak{m}'_{i+1}$ is an upper meandering walk	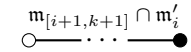 $\mathfrak{m}'_i$ is a lower meandering walk
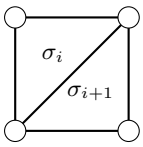	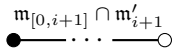 $\mathfrak{m}'_{i+1}$ is a lower meandering walk	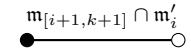 $\mathfrak{m}'_i$ is an upper meandering walk
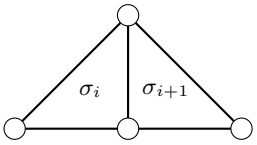	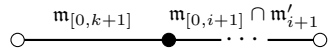 $\mathfrak{m}'_{i+1}$ is a lower meandering walk	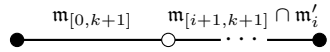 $\mathfrak{m}'_{i+1}$ is a lower meandering walk
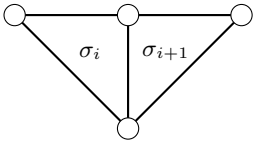	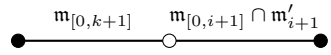 $\mathfrak{m}'_{i+1}$ is an upper meandering walk	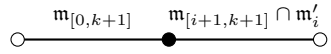 $\mathfrak{m}'_{i+1}$ is an upper meandering walk

Table 5.1: *The walks $\mathfrak{m}_0$ and $\mathfrak{m}_{k+1}$ partitioned into segments*

5.3 New characterisations of the edges in $\mathcal{S}_\alpha$

Recall that for $0 \leq i \leq k+1$, $\mathfrak{b}_i$ and $\mathfrak{w}_i$ denote the black and white trivalent nodes of Hex(σ_i) in Γ and we write $\mathfrak{e}_i$, $\mathfrak{e}'_i$ and $\mathfrak{e}''_i$ and $\mathfrak{f}_i$, $\mathfrak{f}'_i$ and $\mathfrak{f}''_i$ for the edges in $\partial\,\mathrm{Hex}(\sigma_i)$ around $\mathfrak{b}_i$ and $\mathfrak{w}_i$, respectively so that

$$\mathfrak{e}_i, \mathfrak{f}_i \in \mathfrak{m}_i \cap \mathfrak{m}_{i+1}, \quad \mathfrak{e}'_i, \mathfrak{f}'_i \in \mathfrak{m}_i \cap \mathfrak{m}'_i \quad \text{and} \quad \mathfrak{e}''_i, \mathfrak{f}''_i \in \mathfrak{m}_{i+1} \cap \mathfrak{m}'_i,$$

as in Figure 5.2. Throughout this section and for the remainder of this thesis, overline denotes addition modulo $k+1$.

We now use the results from the previous section, summarised in Table 5.1, to give two new characterisations of the edges in S_α in terms of the triangles in strip(α) and the trivalent nodes of their fundamental hexagons:

Proposition 5.15. *Assume Conjecture 5.7 and let $\mathfrak{e}$ be an edge of Γ. Then $\mathfrak{e} \in \mathcal{S}_\alpha$ if and only if*

1. *$\mathfrak{e} \in \mathfrak{m}_0 \setminus \mathfrak{m}_{k+1}$ and there exists an upper triangle σ_i $(1 \leq i \leq k-1)$ in* strip(α) *such that either*
   - *(i) σ_{i-1} is a lower triangle, and the endnodes of $\mathfrak{e}$ are $\mathfrak{w}_{i-1}$ and $\mathfrak{b}_i$; or*
   - *(ii) σ_{i-1} is an upper triangle, and the endnodes of $\mathfrak{e}$ are $\mathfrak{w}_i$ and $\mathfrak{b}_i$.*
2. *$\mathfrak{e} \in \mathfrak{m}_{k+1} \setminus \mathfrak{m}_0$ and there exists an upper triangle σ_i $(1 \leq i \leq k-1)$ in* strip(α) *such that either*
   - *(i) σ_{i+1} is a lower triangle, and the endnodes of $\mathfrak{e}$ are $\mathfrak{w}_i$ and $\mathfrak{b}_{i+1}$; or*
   - *(ii) σ_{i+1} is an upper triangle, and the endnodes of $\mathfrak{e}$ are $\mathfrak{w}_i$ and $\mathfrak{b}_i$.*
3. *$\mathfrak{e} \in \mathfrak{m}_0 \cap \mathfrak{m}_{k+1}$ and there exists $0 \leq i \leq k$ such that either*
   - *(i) σ_i and $\sigma_{\overline{i+1}}$ are both lower triangles, and the endnodes of $\mathfrak{e}$ are $\mathfrak{w}_i$ and $\mathfrak{b}_{\overline{i+1}}$; or*
   - *(ii) σ_i and σ_{i+1} are both upper triangles, and the endnodes of $\mathfrak{e}$ are $\mathfrak{w}_i$ and $\mathfrak{b}_{i+1}$.*

Proof. Note that if $\mathfrak{e}$ is an element of $\mathcal{S}_\alpha \subseteq \mathfrak{m}_0 \cap \mathfrak{m}_{k+1}$, then $\mathfrak{e}$ is an edge of one of the segments listed in Table 5.1. Suppose $\mathfrak{e}$ is an edge in the segment of $\mathfrak{m}_0$ (resp. $\mathfrak{m}_{k+1}$) corresponding to the starting point of the induction mechanism. The only edge of $\mathcal{S}_\alpha$ in that segment is $\mathfrak{e}_\alpha$, as the edges in $\mathfrak{m}_0$ (resp. $\mathfrak{m}_{k+1}$) between $\mathfrak{b}_0$ and $\mathfrak{w}_0$ (resp. $\mathfrak{w}_k$ and $\mathfrak{b}_k$) are elements of the lower meandering walk $\mathfrak{m}'_0$ ($\mathfrak{m}'_k$, respectively). Moreover, $\mathfrak{e}_\alpha \in \mathfrak{m}_0 \cap \mathfrak{m}_k$ satisfies 3(i) when $i = k$. Similarly, the only edge in the segment of $\mathfrak{m}_0$ (resp. $\mathfrak{m}_{k+1}$) corresponding to a jump between two lower triangles σ_i and σ_{i+1} is the edge $\mathfrak{e} \in \mathfrak{m}_0 \cap \mathfrak{m}_1 \cap \cdots \cap \mathfrak{m}_{k+1}$ with endnodes $\mathfrak{w}_i$ and $\mathfrak{b}_{i+1}$ satisfying 3(i).
Now, suppose $\mathfrak{e}$ is the edge in $\mathfrak{m}_0$ ($\mathfrak{m}_{k+1}$) corresponding to the jump between a lower (resp. an upper) triangle σ_i and an upper (resp. a lower) triangle σ_{i+1}. Then, by Conjecture 5.7(v) $\mathfrak{e} \in \mathcal{S}_\alpha$ and $\mathfrak{e}$ satisfies 1(i) (2(i), respectively). Note that no edges in the segment of $\mathfrak{m}_0$ (resp. $\mathfrak{m}_{k+1}$) corresponding to a jump between an upper (resp. a lower) triangle σ_i and a lower (resp. an upper) triangle σ_{i+1} belong to $\mathcal{S}_\alpha$, as they are edges of the lower meandering walk $\mathfrak{m}'_{i+1}$ ($\mathfrak{m}'_i$, respectively). Finally, in the case when σ_i and σ_{i+1} are upper triangles, the corresponding segments of $\mathfrak{m}_0$ and $\mathfrak{m}_{k+1}$ share an edge $\mathfrak{e} \in \mathfrak{m}_{[0,k+1]}$ with nodes $\mathfrak{b}_i$ and $\mathfrak{w}_{i+1}$, satisfying 3(ii). Also, the segment of $\mathfrak{m}_0$ (resp. $\mathfrak{m}_{k+1}$) has another edge in $\mathcal{S}_\alpha$ as described by 1(ii) (2(ii), respectively). Since every edge of $\mathcal{S}_\alpha$ corresponds to one of the listed edges and every listed edge is an element of $\mathcal{S}_\alpha$, this completes the proof. □

For $0 \leq i \leq k+1$, we associate one or three edges of $\mathcal{S}_\alpha$ to every line segment τ_i in strip(α) in the following way:

Theorem 5.16. *Assume Conjecture 5.7 and let $\mathfrak{e}$ be an edge of Γ. Then $\mathfrak{e} \in \mathcal{S}_\alpha$ if and only if for $0 \leq i \leq k$:*

1. *The edge $\mathfrak{e} = \mathfrak{f}_i = \mathfrak{e}_{\overline{i-1}}$ with endnodes $\mathfrak{b}_i$ and $\mathfrak{w}_{\overline{i-1}}$ lies in $\mathfrak{m}_0 \cap \mathfrak{m}_{k+1}$, in which case σ_i and $\sigma_{\overline{i-1}}$ are both lower triangles. We associate to τ_i the edge $\mathfrak{s}_i := \mathfrak{e} \in \mathcal{S}_\alpha$;*
2. *The edge $\mathfrak{e} = \mathfrak{f}'_i = \mathfrak{e}_{i-1}$ with endnodes $\mathfrak{b}_i$ and $\mathfrak{w}_{i-1}$ lies in $\mathfrak{m}_0 \setminus \mathfrak{m}_{k+1}$, in which σ_i and σ_{i-1} are an upper and a lower triangle, respectively. We associate to τ_i the edge $\mathfrak{s}_i := \mathfrak{e} \in \mathcal{S}_\alpha$;*
3. *The edge $\mathfrak{e} = \mathfrak{f}_i = \mathfrak{e}''_{i-1}$ with endnodes $\mathfrak{b}_i$ and $\mathfrak{w}_{i-1}$ lies in $\mathfrak{m}_{k+1} \setminus \mathfrak{m}_0$, in which case σ_i and σ_{i-1} are a lower and an upper triangle, respectively. We associate to τ_i the edge $\mathfrak{s}_i := \mathfrak{e} \in \mathcal{S}_\alpha$;*
4. *The edge $\mathfrak{e}$ is one of $\mathfrak{s}_i := \mathfrak{e}_i = \mathfrak{f}_{i-1} \in \mathfrak{m}_0 \cap \mathfrak{m}_{k+1}$, $\mathfrak{s}'_i := \mathfrak{e}'_i = \mathfrak{f}'_i \in \mathfrak{m}_0 \setminus \mathfrak{m}_{k+1}$ or $\mathfrak{s}''_i := \mathfrak{e}''_i = \mathfrak{f}''_i \in \mathfrak{m}_{k+1} \setminus \mathfrak{m}_0$ with endnodes $\mathfrak{b}_{i-1}$ and $\mathfrak{w}_i$, $\mathfrak{b}_i$ and $\mathfrak{w}_i$ and $\mathfrak{b}_{i-1}$ and $\mathfrak{w}_{i-1}$, respectively. In this case σ_{i-1} and σ_i are both upper triangles and we associate to τ_i the edges $\mathfrak{s}_i, \mathfrak{s}'_i, \mathfrak{s}''_i \in \mathcal{S}_\alpha$.*

Proof. This is essentially a reworking of the Proposition 5.15. Cases 1, 2 and 3 correspond to 3(i), 1(i) and 2(i) in Theorem 5.16, respectively. Case 4 merges 3(ii), 1(ii) and 2(ii). Note that as Proposition 5.15 makes use of Lemmata 5.8-5.11, all of which assume Conjecture 5.7, this result depends on the same conjecture. □

Corollary 5.17. *A node $\mathfrak{n}$ is a trivalent node of* $\mathrm{Hex}(\sigma)$*, for a cone σ in* $\mathrm{strip}(\alpha)$ *if and only if $\mathfrak{n}$ is an endnode of an edge in $\mathcal{S}_\alpha$.*

Proof. By Proposition 5.15, if $\mathfrak{e}$ is an edge in $\mathcal{S}_\alpha$ either there exists a pair of triangles $\sigma_i, \sigma_{\overline{i+1}}$ $(0 \leq i \leq k)$ in $\mathrm{strip}(\alpha)$ such that the endnodes of $\mathfrak{e}$ are trivalent nodes of $\mathrm{Hex}(\sigma_i)$ and $\mathrm{Hex}(\sigma_{\overline{i+1}})$; or there exists a triangle σ in $\mathrm{strip}(\alpha)$ such the endnodes of $\mathfrak{e}$ are the white and black trivalent nodes of $\mathrm{Hex}(\sigma)$. Thus, if $\mathfrak{n}$ is an endnode of an edge in $\mathcal{S}_\alpha$, $\mathfrak{n}$ is a trivalent node of $\mathrm{Hex}(\sigma)$, for σ a cone in $\mathrm{strip}(\alpha)$. For the converse, let σ_i be a cone in $\mathrm{strip}(\alpha)$ $(0 \leq i \leq k)$. By Theorem 5.16, if σ_i is a lower triangle, the edges $\mathfrak{s}_i$ and $\mathfrak{s}_{\overline{i+1}}$ have the black and white trivalent nodes of $\mathrm{Hex}(\sigma_i)$ as their endnodes, respectively. Else σ_i is an upper triangle and either σ_{i-1} and σ_{i+1} are both lower triangles, in which case the black endnode of $\mathfrak{s}_i$ is $\mathfrak{b}_i$ and the white endnode of $\mathfrak{s}_{i+1}$ is $\mathfrak{w}_i$; or σ_{i-1} or σ_{i+1} is an upper triangle and the endnodes of $\mathfrak{s}'_i$ or $\mathfrak{s}''_{i+1}$ are $\mathfrak{b}_i$ and $\mathfrak{w}_i$. □

5.4 Circuit diagrams

Using our understanding of the meandering walks $\mathfrak{m}_0$ and $\mathfrak{m}_{k+1}$, we can deduce information about $\mathfrak{m}'_0, \mathfrak{m}'_1, \ldots, \mathfrak{m}'_k$.

Lemma 5.18. *Assume Conjecture 5.7. For $0 \leq i \leq k$, we can trace the meandering walk $\mathfrak{m}'_i$ by travelling along the zigzag paths of Γ supported on $\mathfrak{m}_0$, $\mathfrak{m}_{k+1}$ and the upper meandering walks of* $\mathrm{strip}(\alpha)$*. Moreover, if the meandering walk $\mathfrak{m}'_i$ splits from one such zigzag path $\mathfrak{z}$ at a node $\mathfrak{n}$ and starts travelling along a new zigzag path $\mathfrak{z}'$, then there exists an edge $\mathfrak{s} \in \mathcal{S}_\alpha$ with endnode $\mathfrak{n}$ such that $\mathfrak{s} \in \mathrm{supp}(\mathfrak{z}) \cap \mathrm{supp}(\mathfrak{z}')$.*

Proof. Both statements are trivially true for all upper meandering walks of strip(α), as they are zigzag paths of Γ (see Definition 5.3). To show both statements hold for all lower meandering walks, we use Lemmata 5.8-5.11 to trace a cycle of $\mathfrak{m}_i'$ ($0 \leq i \leq k$) around $\mathbb{T}$ by travelling between $\mathfrak{b}_i$ and $\mathfrak{w}_i$ twice, first along $\mathfrak{m}_i \setminus \mathfrak{m}_{i+1}$ and then along $\mathfrak{m}_{i+1} \setminus \mathfrak{m}_i$. For $0 \leq i \leq k$, the way the cycle of $\mathfrak{m}_i'$ is completed depends on whether $\sigma_{\overline{i-1}}$, σ_i and $\sigma_{\overline{i+1}}$ are upper or lower triangles. We complete the cycle of a lower meandering walk $\mathfrak{m}_i'$ in the cases when σ_i is between two lower and two upper triangles. All eight cases are summarised in Table 5.2 and their proofs are similar to the ones here presented.

Let $0 \leq i \leq k$. Suppose $\sigma_{\overline{i-1}}, \sigma_i$ and $\sigma_{\overline{i+1}}$ are all lower triangles. If $i \neq 0$, we know by Lemma 5.10 that the walks $\mathfrak{m}_0, \mathfrak{m}_1, \ldots, \mathfrak{m}_i, \mathfrak{m}_i'$ travel together from $\mathfrak{b}_i$ to $\mathfrak{w}_i$. The equivalent statement of Lemma 5.10 for $\mathfrak{m}_{k+1}$ shows that for $i \neq k$ the meandering walks $\mathfrak{m}_i', \mathfrak{m}_{i+1}, \mathfrak{m}_{i+2}, \ldots, \mathfrak{m}_{k+1}$ travel together from $\mathfrak{w}_i$ to $\mathfrak{b}_i$. When $i = 0$ ($i = k$, resp.) $\mathfrak{m}_0$ ($\mathfrak{m}_{k+1}$, resp.) travels from $\mathfrak{w}_0$ ($\mathfrak{w}_k$, resp.) to $\mathfrak{b}_0$ ($\mathfrak{b}_k$ resp.) as τ_0 (τ_{k+1}, resp.) is a line segment in σ_0 (σ_k, resp.). Therefore, every edge of $\mathfrak{m}_i'$ is an edge in the support of a zigzag path supported in either $\mathfrak{m}_0$ or $\mathfrak{m}_{k+1}$. The only nodes where $\mathfrak{m}_i'$ and $\mathfrak{m}_0$, and $\mathfrak{m}_i'$ and $\mathfrak{m}_{k+1}$ split are $\mathfrak{b}_i$ and $\mathfrak{w}_i$. For $i \neq k$, since $\sigma_{\overline{i-1}}, \sigma_i$ and σ_{i+1} are all lower triangles, the edges $\mathfrak{s}_i \in \mathfrak{m}_0 \cap \mathfrak{m}_{k+1}$ and $\mathfrak{s}_{i+1} \in \mathfrak{m}_0 \cap \mathfrak{m}_{k+1}$ of $\mathcal{S}_\alpha$ have endnodes $\mathfrak{b}_i$ and $\mathfrak{w}_i$, respectively (see Theorem 5.16). When $i = k$, the edges $\mathfrak{s}_k, \mathfrak{s}_0 \in \mathfrak{m}_0 \cap \mathfrak{m}_{k+1}$ have $\mathfrak{b}_k$ and $\mathfrak{w}_k$ as endnodes, respectively.

Now suppose σ_{i-1}, σ_i and σ_{i+1} are an upper, a lower and an upper triangle, respectively. By Lemma 5.8 and its equivalent for $\mathfrak{m}_{k+1}$, the nodes $\mathfrak{b}_{i-1}$ and $\mathfrak{w}_i$, and $\mathfrak{b}_i$ and $\mathfrak{w}_{i+1}$ are connected by edges in $\mathfrak{m}_0, \mathfrak{m}_1, \ldots, \mathfrak{m}_i, \mathfrak{m}_i'$ and $\mathfrak{m}_i', \mathfrak{m}_{i+1}, \mathfrak{m}_{i+2}, \ldots, \mathfrak{m}_{k+1}$, respectively. Moreover, the meandering walks $\mathfrak{m}_i'$ and $\mathfrak{m}_{i+1}$ travel together from $\mathfrak{w}_i$ to $\mathfrak{b}_i$ and therefore must travel together from $\mathfrak{w}_i$ to $\mathfrak{w}_{i+1}$. Conjecture 5.7(i) ensures that $\mathfrak{m}_{i+1}'$ also travels with $\mathfrak{m}_i'$ and $\mathfrak{m}_{i+1}$ between $\mathfrak{w}_i$ and $\mathfrak{w}_{i+1}$. By the same argument, the nodes $\mathfrak{b}_{i-1}$ and $\mathfrak{b}_i$ are connected by edges in $\mathfrak{m}_i', \mathfrak{m}_i$ and $\mathfrak{m}_{i-1}'$. So the lower meandering walk $\mathfrak{m}_i'$ can be traced by travelling along the zigzag paths supported on $\mathfrak{m}_0$, $\mathfrak{m}_{i+1}'$, $\mathfrak{m}_{k+1}$ and $\mathfrak{m}_{i-1}'$. The meandering walks supported on $\mathfrak{m}_i'$ and $\mathfrak{m}_0$, $\mathfrak{m}_i'$ and $\mathfrak{m}_{i+1}'$, $\mathfrak{m}_i'$ and $\mathfrak{m}_{k+1}$, and $\mathfrak{m}_i'$ and $\mathfrak{m}_{i-1}'$ split at the nodes $\mathfrak{w}_i$, $\mathfrak{w}_{i+1}$, $\mathfrak{b}_i$ and $\mathfrak{b}_{i-1}$, respectively. The edges $\mathfrak{s}_{i+1}$, $\mathfrak{s}_{i+2}$, $\mathfrak{s}_i$ and $\mathfrak{s}_{i-1}$ have $\mathfrak{w}_i$, $\mathfrak{w}_{i+1}$, $\mathfrak{b}_i$ and $\mathfrak{b}_{i-1}$ as an endnode. By Lemma 5.9 and Lemma 5.8, $\mathfrak{s}_{i+1} \in \mathfrak{m}_0 \cap \mathfrak{m}_{i+1}'$, $\mathfrak{s}_{i+2} \in \mathfrak{m}_{k+1} \cap \mathfrak{m}_{i+1}'$, $\mathfrak{s}_i \in \mathfrak{m}_{k+1} \cap \mathfrak{m}_{i-1}'$ and $\mathfrak{s}_{i-1} \in \mathfrak{m}_0 \cap \mathfrak{m}_{i-1}'$. □

Corollary 5.19. *Every edge in a zigzag path of* Γ *supported on the meandering walk of a line segment in* strip(α) *is an edge in a lower meandering walk of* strip(α) *or an edge in* $\mathcal{S}_\alpha$

Using Lemmata 5.8-5.11 and Lemma 5.18, we draw a schematic, called a *circuit diagram*, depicting all meandering walks $\mathfrak{m}_\tau$ for τ a line segment of strip(α) and edges in $\mathcal{S}_\alpha$. For $\alpha \in Q_1$, use Table 5.2 to draw the cycle of $\mathfrak{m}_i'$ for each $0 \leq i \leq k$. The walks $\mathfrak{m}_0$ and $\mathfrak{m}_{k+1}$ complete the circuit diagram of α, linking every cycle of $\mathfrak{m}_i'$. The following example presents the circuit diagram for a different choice of arrow α in the quiver Q from Section 4.1.

Example 5.20. Consider the dimer model Γ from Section 4.1. Its dual quiver Q is depicted in Figure 4.1. Figure 5.7(a) shows the fan Σ of its moduli space of θ-stable A-modules for the 0-generated stability parameter $\theta = (-25, 1, 1, \ldots, 1)$. Choose α to

σ_{i-1}	σ_i	σ_{i+1}	Cycle $\mathfrak{m}'_i$
Lower triangle	Lower triangle	Lower triangle	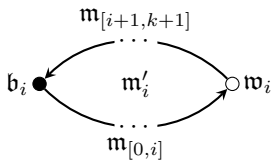
Upper triangle	Lower triangle	Lower triangle	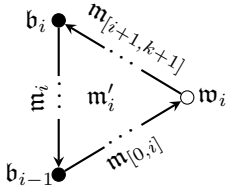
Lower triangle	Lower triangle	Upper triangle	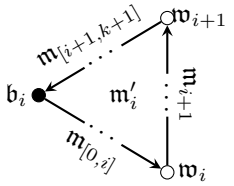
Upper triangle	Lower triangle	Upper triangle	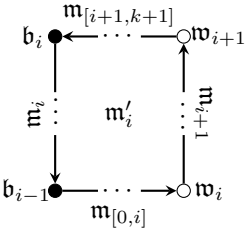
Upper triangle	Upper triangle	Upper triangle	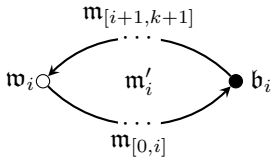
Lower triangle	Upper triangle	Upper triangle	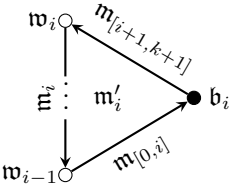
Upper triangle	Upper triangle	Lower triangle	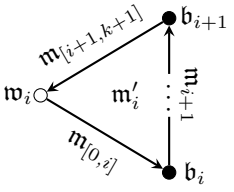
Lower triangle	Upper triangle	Lower triangle	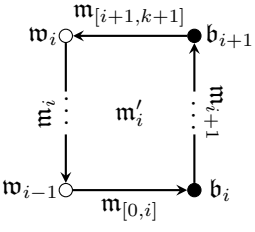

Table 5.2: *Cycles* $\mathfrak{m}'_i$

be the arrow a_2 with tail at vertex 0 and head at vertex 10. The arrow a_2 has labelling divisor $D_2 + D_3 + D_{16}$ (see Figure 4.3). Its respective convex polygon Δ' and strip of triangles strip(a_2) are shown in Figures 5.7(b) and 5.8.

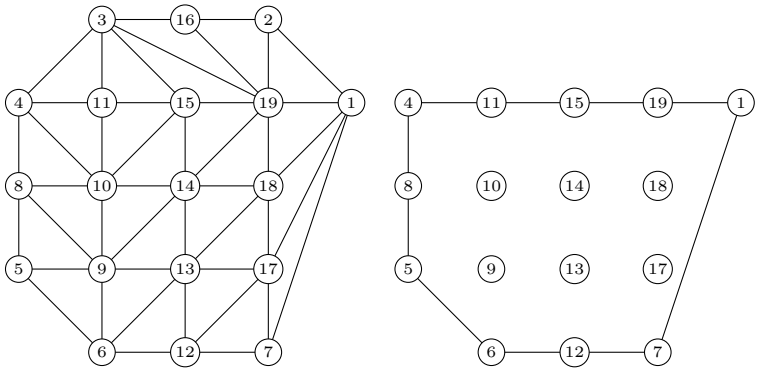

(a) The toric fan Σ (b) Δ' for $a_2 \in Q_1$

Figure 5.7: *The toric fan Σ of $\mathcal{M}_A$ and convex polygon Δ' for $a_2 \in Q_1$*

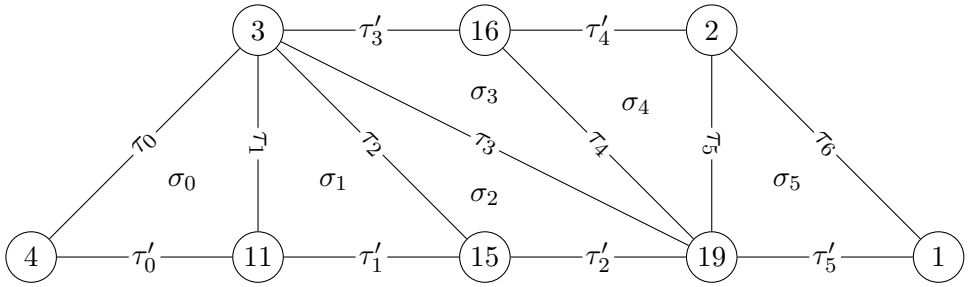

Figure 5.8: *Strip of triangles* strip(a_2)

The subset $\mathcal{S}_{a_2}$ has eight edges all depicted in its circuit diagram in Figure 5.9. As in Figure 4.6, the meandering walks $\mathfrak{m}_i$ $(0 \leq i \leq 6)$ make a 'Mexican wave' as they orderly move from $\mathfrak{m}_6$ to $\mathfrak{m}_0$. Figure 5.10 shows all lower meandering walks of strip(a_2) with their natural direction. Note that no lower meandering walk fails to be zigzag at $\mathfrak{s}_4$.

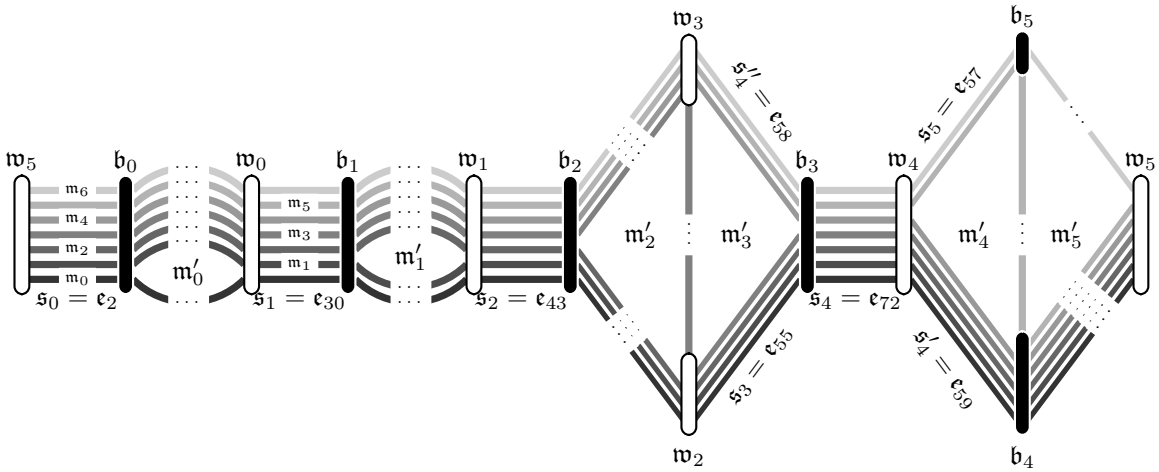

Figure 5.9: *The circuit diagram of a_2*

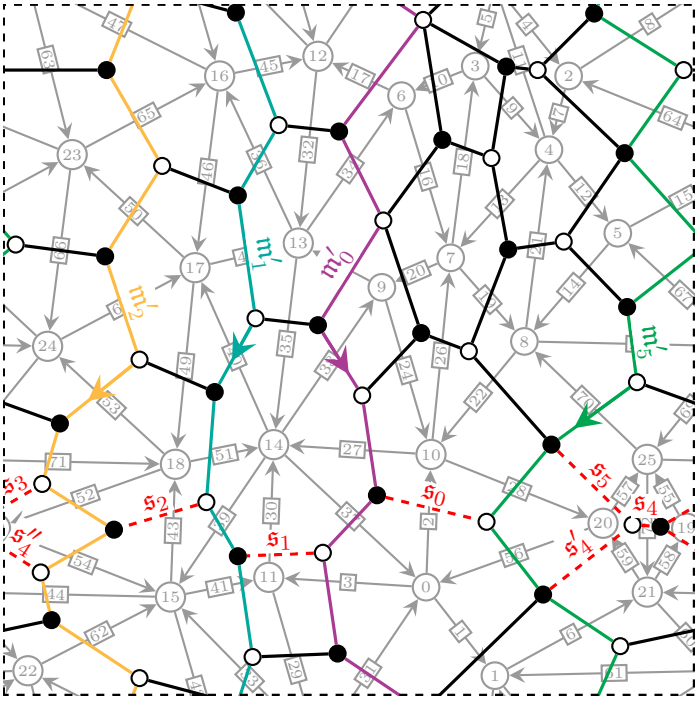

Figure 5.10: *The meandering walks* $\mathfrak{m}'_0, \mathfrak{m}'_1, \mathfrak{m}'_2, \mathfrak{m}'_5$ *and the edges in* $\mathcal{S}_{a_2}$

CHAPTER 6

THE ARROW CONTRACTION ALGORITHM

In this chapter, we describe an algorithm - the arrow contraction algorithm - that allows us to produce new consistent dimer models from old. Any choice of arrow α in the dual quiver of a consistent dimer model Γ with tail at vertex 0, produces a new consistent dimer model Γ' whose corresponding characteristic polygon coincides with Δ'. Ishii–Ueda [IU09] introduced an algorithm which takes a consistent dimer model Γ with characteristic polygon $\Delta(\Gamma)$ to a new consistent dimer model Γ' whose characteristic polygon is the convex hull of $\Delta(\Gamma) \setminus \{\rho\}$, for any choice of corner ρ in $\Delta(\Gamma)$. The arrow contraction algorithm coincides with Ishii–Ueda's in the special case when $\mathrm{div}(\alpha) = D_\rho$ (see Section 6.6). However, the two algorithms are different in general.

6.1 The dimer model Γ'

We start by defining the bicoloured graph Γ' associated to a consistent dimer model $\Gamma := (\mathfrak{E}, \mathfrak{B}, \mathfrak{W})$ and arrow $\alpha \in Q_1$ with tail at vertex 0.

Definition 6.1. Define Γ' to be the bicoloured graph whose set of nodes is the set of nodes $\mathfrak{n}$ of Γ such that $\mathfrak{n}$ is an endnode of an edge in $\mathfrak{E} \setminus \mathcal{S}_\alpha$. Its set of edges is

$$\mathfrak{E}' := \mathfrak{E} \setminus \mathcal{S}_\alpha.$$

By definition, every node of Γ' has an edge of $\mathfrak{E}'$ attached to it. In fact, every node of Γ' is at least bivalent:

Lemma 6.2. *Assume Conjecture 5.7. Then for every node $\mathfrak{n}$ of Γ', there exists at least two edges $\mathfrak{e}, \mathfrak{e}' \in \mathfrak{E}'$, such that $\mathfrak{n}$ is an endnode of both $\mathfrak{e}$ and $\mathfrak{e}'$.*

Proof. Since every node of Γ is at least trivalent, we only need to check those nodes of Γ attached to edges in $\mathcal{S}_\alpha$. To do this, we use the characterisation of the set $\mathcal{S}_\alpha$ introduced in Theorem 5.16, which assumes Conjecture 5.7. Let σ_i be a triangle in

strip(α) ($0 \leq i \leq k$). Throughout this proof, overline denotes addition modulo $k+1$. There are four different cases, two of which we treat together:

1. If $\sigma_{\overline{i-1}}$ and σ_i are both lower triangles, τ_i contributes a single edge $\mathfrak{s}_i$ to $\mathcal{S}_\alpha$ with endnodes $\mathfrak{w}_{\overline{i-1}}$ and $\mathfrak{b}_i$. The lower meandering walks $\mathfrak{m}'_{\overline{i-1}}$ and $\mathfrak{m}'_i$ pass through $\mathfrak{w}_{\overline{i-1}}$ and $\mathfrak{b}_i$, respectively. Thus, at least two edges in $\mathfrak{E}' = \mathfrak{E} \setminus \mathcal{S}_\alpha$ have $\mathfrak{w}_{\overline{i-1}}$ and $\mathfrak{b}_i$ as an endnode.

2. If σ_{i-1} and σ_i are a lower (resp. an upper) and an upper (resp. a lower) triangle, respectively, the line segment τ_i contributes a single edge $\mathfrak{s}_i$ to $\mathcal{S}_\alpha$ with endnodes $\mathfrak{w}_{i-1}$ and $\mathfrak{b}_i$ as well. The lower meandering walk $\mathfrak{m}'_{i-1}$ (resp. $\mathfrak{m}'_i$) passes through the node $\mathfrak{w}_{i-1}$ (resp. $\mathfrak{b}_i$) which is at least bivalent in Γ'. If σ_{i+1} (resp. σ_{i-2}) is a lower triangle, the lower meandering walk $\mathfrak{m}'_{i+1}$ (resp. $\mathfrak{m}'_{i-1}$) passes through $\mathfrak{b}_i$ (resp. $\mathfrak{w}_{i-1}$) and at least two edges of Γ' have $\mathfrak{b}_i$ (resp. $\mathfrak{w}_{i-1}$) as an endnode. Else, σ_{i+1} (resp. σ_{i-2}) is an upper triangle and $\mathfrak{b}_i$ (resp. $\mathfrak{w}_{i-1}$) is attached to $\mathfrak{s}_i$, $\mathfrak{s}'_{i+1}$ (resp. $\mathfrak{s}_{i-1}$) and $\mathfrak{s}''_{i+1}$ (resp. $\mathfrak{s}'_{i-1}$) only. Therefore, $\mathfrak{b}_i$ (resp. $\mathfrak{w}_{i-1}$) is not a node of Γ'.

3. Finally, if σ_{i-1} and σ_i are both upper triangles, τ_i has three edges associated to it: $\mathfrak{s}_i$, $\mathfrak{s}'_i$ and $\mathfrak{s}''_i$ with endnodes $\mathfrak{b}_{i-1}$ and $\mathfrak{w}_i$, $\mathfrak{w}_i$ and $\mathfrak{b}_{i+1}$ and $\mathfrak{w}_{i-1}$ and $\mathfrak{b}_{i-1}$, respectively. The nodes $\mathfrak{b}_{i-1}$ and $\mathfrak{w}_i$ are only attached to edges in $\mathcal{S}_\alpha$ and therefore are not nodes of Γ'. If σ_{i-2} (resp. σ_{i+1}) is a lower triangle, the lower meandering walk $\mathfrak{m}'_{i-2}$ (resp. $\mathfrak{m}'_{i+1}$) passes through the node $\mathfrak{w}_{i-1}$ (resp. $\mathfrak{b}_i$), which means it is at least bivalent in Γ'. Else σ_{i-2} (resp. σ_{i+1}) is an upper triangle and $\mathfrak{w}_{i-1}$ (resp. $\mathfrak{b}_i$) is not an endnode of any edge in $\mathfrak{E}'$.

Therefore, every endnode of an edge in $\mathcal{S}_\alpha$ is either a node in Γ', in which case a lower meandering walk passes through it making it a bivalent node, or is attached only to edges in $\mathcal{S}_\alpha$ and it is not a node of Γ'. □

Notation 6.3. Let S_α denote the subset of arrows of Q dual to the edges in $\mathcal{S}_\alpha$. For $0 \leq i \leq k$, Theorem 5.16 associates to each line segment τ_i in strip(α) three edges $\mathfrak{s}_i, \mathfrak{s}'_i$ and $\mathfrak{s}''_i$ in $\mathcal{S}_\alpha$ if τ_i is between two upper triangles, and a single edge $\mathfrak{s}_i$ otherwise. Write $\check{S}_\alpha$ for the subset of S_α consisting of arrows s_i dual to edges $\mathfrak{s}_i \in \mathcal{S}_\alpha$ associated to line segments τ_i in strip(α) between two upper triangles.

Throughout this chapter we assume the following conjecture:

Conjecture 6.4. *The only cycles of arrows from S_α are those generated by the sets of three arrows dual to edges $\mathfrak{s}_i$, $\mathfrak{s}'_i$ and $\mathfrak{s}''_i$ associated to line segments τ_i ($0 \leq i \leq k$) between two upper triangles.*

Proposition 6.5. *Assume Conjectures 5.7 and 6.4. Then the bicoloured graph Γ' is a dimer model.*

Proof. We know that Γ' is a bicoloured graph embedded in the torus $\mathbb{T}$. By Lemma 6.2, assuming Conjecture 5.7, Γ' has no univalent nodes. It remains to show that every tile of Γ is simply-connected. This follows from Conjecture 6.4. □

One can think of every tile in Γ' as a union of tiles of Γ. As Γ' is a dimer model, it is dual to a quiver Q' with relations $\mathcal{R}'$. Note that the quiver Q' inherits a choice of vertex $0 \in Q'_0$, namely the vertex $v' \in Q'_0$ dual to the tile containing the zero tile of Γ.

Definition 6.6. Let $\overline{Q} := (\overline{Q}_0, \overline{Q}_1, \overline{\mathsf{h}}, \overline{\mathsf{t}}, \overline{\mathcal{R}})$ be a quiver with

(i) set of vertices $\overline{Q}_0 = Q_0$;

(ii) set of arrows $\overline{Q}_1$ containing the set $Q_1 \setminus \check{S}_\alpha$ and an arrow a^{-1} for every arrow $a \in S_\alpha \setminus \check{S}_\alpha$ with $\overline{\mathsf{t}}(a^{-1}) = \overline{\mathsf{h}}(a)$ and $\overline{\mathsf{h}}(a^{-1}) = \overline{\mathsf{t}}(a)$; and

(iii) set of relations $\overline{\mathcal{R}}$ containing the set $\mathcal{R}$ and two additional relations $aa^{-1} - e_{\mathsf{h}(a)}$ and $a^{-1}a - e_{\mathsf{t}(a)}$ for each arrow $a \in S_\alpha \setminus \check{S}_\alpha$.

Proposition 6.7. *Assume Conjectures 5.7 and 6.4. The Jacobian algebra $\overline{A} = \mathbb{C}\overline{Q}/I_{\overline{\mathcal{R}}}$ of $\overline{Q}$ is Morita equivalent to the Jacobian algebra $A' = \mathbb{C}Q'/I_{\mathcal{R}'}$ of Q' dual to the dimer model Γ'.*

Proof. Recall that the equivalence of categories from Proposition 1.22 translates into an equivalence between the category $\operatorname{rep}(Q, \mathcal{R})$ of finite-dimensional representation of a quiver Q with relations $\mathcal{R}$ and the category $\operatorname{mod}-A$ of finite-dimensional left A-modules for $A = \mathbb{C}Q/I_{\mathcal{R}}$. To show Morita equivalence, we define functors between the categories $\operatorname{rep}(Q', \mathcal{R}')$ and $\operatorname{rep}(\overline{Q}, \overline{\mathcal{R}})$.

We start by defining a functor from $\operatorname{rep}(\overline{Q}, \overline{\mathcal{R}})$ to $\operatorname{rep}(Q', \mathcal{R}')$ on objects. Let $\overline{W} = \left(\bigoplus_{\overline{v} \in \overline{Q}_0} \overline{W}_{\overline{v}}, \{\overline{\phi}_{\overline{a}}\}_{\overline{a} \in \overline{Q}_1}\right)$ be a representation of $\overline{Q}$. The set of vertices of $\overline{Q}$ coincides with the set of vertices of Q. The relations $\overline{\mathcal{R}}$ of $\overline{Q}$ ensure that if the tiles dual to two vertices $\overline{v}$ and $\overline{v}'$ in $\overline{Q}_0 = Q_0$ lie in the same tile of Γ', then $\overline{W}_{\overline{v}} \cong \overline{W}_{\overline{v}'}$. For $v \in Q'_0$, let $W_v := \overline{W}_{\overline{v}}$ for any $\overline{v}$ dual to a tile of Γ in the tile of Γ' dual to v. By definition, the set of arrows of $\overline{Q}$ contains the set $Q_1 \setminus S_\alpha$. For $a \in Q'_1 = Q_1 \setminus S_\alpha$, let $\phi_a = \overline{\phi}_{\overline{a}}$ where a and $\overline{a}$ are the same arrow, thought of as elements of Q_1. Thus, a representation $\overline{W}$ of $\overline{Q}$ determines a representation $W = \left(\bigoplus_{v \in Q_0} W_v, \{\phi_a\}_{a \in Q_1}\right)$ of Q, and one can extend this assignment to morphisms between representations.

Now we define a functor on objects between the categories in the opposite direction. Let $W = \left(\bigoplus_{v \in Q'_0} W_v, \{\phi_a\}_{a \in Q'_1}\right)$ be a representation of Q'. The functor sends W to $\overline{W} = \left(\bigoplus_{\overline{v} \in \overline{Q}_0} \overline{W}_{\overline{v}}, \{\overline{\phi}_{\overline{a}}\}_{\overline{a} \in \overline{Q}_1}\right)$, where $\overline{W}_{\overline{v}} := W_v$ for every vertex $\overline{v} \in \overline{Q}_0 = Q_0$ dual to a tile of Γ contained in the tile of Γ' dual to v. Every arrow in $\overline{Q}$ is either in $Q_1 \setminus \check{S}_\alpha$, in $S_\alpha \setminus \check{S}_\alpha$ or is an arrow a^{-1} for $a \in S_\alpha \setminus \check{S}_\alpha$. If $a \in Q_1 \setminus \check{S}_\alpha$, set $\overline{\phi}_{\overline{a}} = \phi_a$, where both $\overline{a}$ and a are the same arrow, thought of as elements of Q_1. For $a \in S_\alpha \setminus \check{S}_\alpha$, choose any nonzero value for the maps $\overline{\phi}_a$. This choice determines the value of the maps $\overline{\phi}_{a^{-1}}$. The relations in $\overline{\mathcal{R}}$ ensure that any other choice of nonzero values for the maps $\overline{\phi}_{\overline{a}}$ ($a \in S_\alpha \setminus \check{S}_\alpha$) gives a new representation of $\overline{Q}$ isomorphic to $\overline{W}$. So a representation of Q' defines a unique representation of $\overline{Q}$ up to isomorphism. This assignment also extends to morphisms. Moreover, the composition of these functors give isomorphic representations and the categories are equivalent. □

Remarks 6.8. 1. Introducing inverted arrows in a quiver Q is a special case of 'universal localisation' in the sense of A. H. Schofield [Sch85, Chapter 4].

2. Note that in the proof of Proposition 6.7 not all the arrows in S_α are inverted. The arrows in $\check{S}_\alpha$ are deleted, since the relations in $\overline{A}$ determine the arrows in $\check{S}_\alpha$, as follows. Suppose $a \in \check{S}_\alpha$. Then there exists arrows $a_1, a_1', a_2, a_2' \in S_\alpha \setminus \check{S}_\alpha$ as in Figure 6.1 below. For $i = 1, 2$, the following relations hold in $\overline{A}$:

$$a_i^{-1}a_i = e_{\mathsf{t}(a_i)} = e_{\mathsf{h}(a)} \qquad (a_i')^{-1}a_i' = e_{\mathsf{t}(a_i')} = e_{\mathsf{h}(a_i)} \qquad a_i'a_ia = q,$$

where q is any small cycle starting at vertex $e_{\mathsf{t}(a)}$. Hence, $a = a_i^{-1}(a_i')^{-1}q \in \overline{A}$.

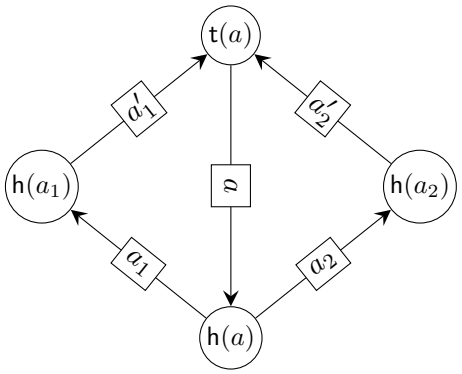

Figure 6.1: *An arrow a in $\check{S}_\alpha$*

6.2 The zigzag polygon of Γ'

In order to show that Γ' is a consistent dimer model, we study its set of zigzag paths.

Definition 6.9. We say a directed meandering walk $\mathfrak{m} = \{\mathfrak{e}_i\}_{i\in\mathbb{Z}}$ in Γ *fails to be zigzag* at an edge $\mathfrak{e} \in \Gamma$ if the presence of $\mathfrak{e}$ prevents the directed meandering walk $\mathfrak{m}$ from turning maximally right at a white node or maximally left at a black node, i.e. if there exists an edge $\mathfrak{e}$ such that for for some $i \in \mathbb{Z}$ the edges $\mathfrak{e}_i, \mathfrak{e}_{i+1}$ and $\mathfrak{e}$ share either

(i) a black node and $\mathfrak{e}$ is between $\mathfrak{e}_i$ and $\mathfrak{e}_{i+1}$ in a clockwise direction; or

(ii) a white node and $\mathfrak{e}$ is between $\mathfrak{e}_{i+1}$ and $\mathfrak{e}_i$ in a clockwise direction.

Recall that every lower meandering walk of strip(α) comes with a natural direction introduced in Definition 5.3. The homology class of a lower meandering walk with its natural direction is the inward-pointing normal vector to the boundary edge of Δ'.

Lemma 6.10. *Assume Conjecture 5.7. The set $\mathcal{S}_\alpha$ contains all edges $\mathfrak{e} \in \mathfrak{E}$ such that $\mathfrak{m}$ fails to be zigzag at $\mathfrak{e}$, for $\mathfrak{m}$ a lower meandering walk with its natural direction.*

Proof. Note that a lower meandering walk $\mathfrak{m}$ only fails to be zigzag when it stops following a zigzag path $\mathfrak{z}$ and starts following a new zigzag path $\mathfrak{z}'$. By Lemma 5.18, which assumes Conjecture 5.7, this only happens at nodes attached to edges in $\mathcal{S}_\alpha$. Moreover, since the edge at which $\mathfrak{m}$ fails to be zigzag is an element of both $\mathfrak{z}$ and $\mathfrak{z}'$, $\mathfrak{m}$ is a zigzag path after removing all edges of $\mathcal{S}_\alpha$. Thus, $\mathcal{S}_\alpha$ contains all edges at which $\mathfrak{m}$ fails to be a zigzag. □

Remark 6.11. In general, the set $\mathcal{S}_\alpha$ is not equal to the set of edges where the lower meandering walks fail to be zigzag. For an example where the latter set is a proper subset of $\mathcal{S}_\alpha$ see Example 5.20.

Suppose $\mathfrak{m}$ is a meandering walk in Γ that does not traverse any edges of $\mathcal{S}_\alpha$, i.e. $\mathfrak{m} \subseteq \mathfrak{E} \setminus \mathcal{S}_\alpha = \mathfrak{E}'$. Then, $\mathfrak{m}$ *induces* uniquely a path $\mathfrak{m}'$ in Γ'.

Lemma 6.12. *Assume Conjectures 5.7 and 6.4. Every zigzag path in Γ' is either:*

1. *a path in Γ' induced by a zigzag path of Γ that traverses no edges of $\mathcal{S}_\alpha$, in which case it is the zigzag to an edge of Δ that is also an edge of Δ'; or*
2. *a path in Γ' induced by a lower meandering walk of $\mathrm{strip}(\alpha)$ with its natural direction.*

Proof. Suppose $\mathfrak{m}$ is a zigzag path of Γ with homology class normal to a line segment in Δ'. By Lemma 5.18, every edge of $\mathcal{S}_\alpha$ is contained in two zigzag paths with homology classes normal to line segments in $\mathrm{strip}(\alpha)$. Therefore, $\mathfrak{m}$ contains no edges in $\mathcal{S}_\alpha$. Thus, $\mathfrak{m}$ induces a path in Γ' which is a zigzag path. Suppose $\mathfrak{m}$ is a lower meandering walk of $\mathrm{strip}(\alpha)$. By Lemma 6.10, the path of Γ' induced by the lower meandering walk $\mathfrak{m}$ with its natural direction is a zigzag path. As every edge of Γ' belongs to two zigzag paths of either type, Γ' has no other zigzag paths. □

Corollary 6.13. *Assume Conjectures 5.7 and 6.4. The zigzag polygon of Γ' coincides with Δ', up to translation.*

Proof. Recall from Definition 1.45 that the zigzag polygon of Γ' is constructed by taking the homology classes of all its zigzag paths $\mathfrak{z}_1, \mathfrak{z}_2, \ldots, \mathfrak{z}_\ell$, cyclically ordered, and defining a sequence of lattice points $b_0 = (0,0)$ and $b_{i+1} = b_i + [\mathfrak{z}_{i+1}]'$ $(0 \leq i \leq \ell - 1)$, where $[\mathfrak{z}_{i+1}]'$ denotes the vector normal to $[\mathfrak{z}_{i+1}]$ obtained by rotating $[\mathfrak{z}_{i+1}]$ by 90 degrees in the positive direction. As every edge of Γ' appears in two distinct zigzag paths, $b_\ell = 0$. The zigzag polygon is the convex hull of the set of points $b_1, b_2, \ldots, b_\ell$. By construction, it is the convex polygon that has a boundary line segment for each zigzag path of Γ. The boundary line segment is normal to the homology class of its zigzag path. Therefore, it suffices to show that for every boundary line segment of Δ', there exists a zigzag path in Γ' whose homology class is the primitive inward-pointing normal vector to the line segment.

By Theorem 1.46, we know that the homology classes of the zigzag paths of Γ' induced by zigzag paths of Γ are in one-to-one correspondence with the primitive inward-pointing normal vectors to line segments in $\partial\Delta'$ which form part of the boundary of $\Delta(\Gamma)$. Moreover, there is a lower meandering walk for each of the remaining boundary line segments of Δ'. By Lemma 6.12, each of these induces a zigzag path in Γ and by Lemma 2.14, the homology classes of these zigzag paths are normal to the line segments in the boundary of Δ' they are associated to. The choice of natural direction ensures that their homology classes are in fact the inward-pointing normal vectors to their associated line segment. □

6.3 Γ' is a consistent dimer model

We now use the fact that the zigzag polygon of Γ' is Δ' to prove that Γ' is a consistent dimer model. Recall the following theorem from Gulotta:

Theorem 6.14. *[Gul08, Theorem 3.1] A dimer model Γ is properly-ordered if and only if its number of tiles is equal to twice the area of its zigzag polygon.*

Theorem 6.15. *Assume Conjectures 5.7 and 6.4. The dimer model Γ' is consistent.*

Proof. Since Γ is a consistent dimer model its zigzag polygon coincides with its characteristic polygon $\Delta(\Gamma)$ [IU09, Theorem 11.1]. Recall that every consistent dimer model is properly-ordered [IU11b, Lemmata 4.2, 4.3]. Now, by definition

$$\text{Area of } \Delta' = \text{Area of } \Delta(\Gamma) - \frac{1}{2}\#\text{ Triangles in strip}(\alpha). \tag{6.3.1}$$

Therefore,

$$\begin{aligned} 2 \times \text{Area of } \Delta' &= 2 \times \text{Area of } \Delta(\Gamma) - \#\text{ Triangles in strip}(\alpha) \\ &= \#\text{ Tiles of } \Gamma - \#\text{ Triangles in strip}(\alpha) \qquad \text{as } \Gamma \text{ properly-ordered.} \end{aligned} \tag{6.3.2}$$

By Theorem 6.14, the dimer model Γ' is properly-ordered if and only if

$$2 \times \text{Area of } \Delta' = \#\text{ Tiles of } \Gamma'. \tag{6.3.3}$$

Putting equations (6.3.2) and (6.3.3) together, Γ' is properly-ordered if and only if

$$\#\text{ Tiles of } \Gamma' = \#\text{ Tiles of } \Gamma - \#\text{ Triangles in strip}(\alpha). \tag{6.3.4}$$

Theorem 5.16, which assumes Conjecture 5.7, associates to every line segment τ_i in strip(α) one or three edges of $\mathcal{S}_\alpha$. By Conjecture 6.4, if $\mathfrak{s}_i \in \mathcal{S}_\alpha$ is associated to a line segment τ_i $(0 \leq i \leq k)$ between two triangles $\sigma_{\overline{i-1}}$ and σ_i and at least one of $\sigma_{\overline{i-1}}$ and σ_i is a lower triangle, the effect of removing $\mathfrak{s}_i$ from Γ is merging two different tiles of Γ into one tile of Γ'. If $\mathfrak{s}_i$, $\mathfrak{s}_i'$ and $\mathfrak{s}_i''$ are the three edges associated to a line segment τ_i in strip(α) $(0 \leq i \leq k)$ between two upper triangles σ_{i-1} and σ_i, $\mathfrak{s}_i$ merges two different tiles $\mathfrak{t}_0$ and $\mathfrak{t}_2$ of Γ into a single tile of Γ'. The edges $\mathfrak{s}_i'$ and $\mathfrak{s}_i''$ merge two other tiles $\mathfrak{t}_1$ with $\mathfrak{t}_2$ and $\mathfrak{t}_3$ with $\mathfrak{t}_0$, respectively, into a tile of Γ'. However, the edges associated to the line segments τ_{i-1} and τ_{i+1} make a bow tie shape with the edges of τ_i merging $\mathfrak{t}_2$ with $\mathfrak{t}_3$ and $\mathfrak{t}_2$ with $\mathfrak{t}_0$, respectively. Therefore, the effect of removing all edges associated to the line segments τ_{i-1}, τ_i and τ_{i+1} is merging four different tiles of Γ into a single tile of Γ'. In summary, for $0 \leq i \leq k$ the effect of removing the edge or edges associated to a line segment τ_i is decreasing the number of tiles of Γ by 1. Since there are $k+1$ triangles in strip(α) and $k+1$ line segments in strip(α) to which we associate one or three edges of $\mathcal{S}_\alpha$, equation (6.3.4) holds and the dimer model Γ' is properly-ordered and hence consistent [IU11b, Lemmata 4.2, 4.3]. □

Remark 6.16. It follows from the proof of Theorem 6.15, that number $|Q_0'|$ of vertices of the quiver Q', which is equal to the number of tiles of Γ', is the number of vertices of Q minus $k+1$, the number of triangles in strip(α).

6.4 Geometric consequences of consistency

Fix $\theta' := (|Q'_0|, 1, 1, \ldots, 1)$. The stability parameter θ' is 0-generated and thus generic (see Definition 3.1 and Remark 3.3). Since Γ' is a consistent, the following corollary follows:

Corollary 6.17. *Assume Conjectures 5.7 and 6.4 and suppose Δ' is a nondegenerate polygon. Let $\sigma' := \left\{\sum_{\lambda_\rho \geq 0} \lambda_\rho u_\rho \in N_{\mathbb{R}} \mid u_\rho \in \Delta'\right\}$ denote the cone over Δ' and let θ' be generic. Then:*

(i) The zigzag polygon Δ' of Γ' coincides with its characteristic polygon $\Delta(\Gamma')$, up to translation;

(ii) The moduli space of θ'-stable A'-modules $\mathcal{M}_{A'}$ is a projective crepant resolution of the Gorenstein toric threefold $X = \operatorname{Spec}(\mathbb{C}[(\sigma')^\vee \cap M])$;

(iii) The tautological algebra morphism $\phi' : T' \to \operatorname{End}_{\mathcal{O}_{\mathcal{M}_{A'}}} A'$ from the tautological bundle $T' = \bigoplus_{v \in Q'_0} L'_v$ of $\mathcal{M}_{A'}$ to the endomorphism algebra of A' is an isomorphism; and

(iv) There is a derived equivalence between the bounded derived category $D^b(\operatorname{coh}(\mathcal{M}_{A'}))$ of coherent sheaves of $\mathcal{M}_{A'}$ and the bounded derived category $D^b(\operatorname{mod} -A')$ of left A'-modules.

Following Ishii-Ueda [IU09, Section 4.9], we define for every quiver Q with relations $\mathcal{R}$ a $\mathbb{C}$-linear category $\mathcal{Q}$ whose set of objects is the set Q_0 of vertices of Q. For any two objects v, v' of $\mathcal{Q}$, the space of morphisms between v and v' is the vector space $e_{v'} \cdot \mathbb{C}Q \cdot e_v$ of paths with tail at vertex v and head at vertex v'. Composition of morphisms is defined to be the product of elements in the path algebra $\mathbb{C}Q$. Note that a representation of Q is a linear functor from the category $\mathcal{Q}$ of Q to the category of complex vector spaces.

Proposition 6.18. *Assume Conjectures 5.7 and 6.4 and suppose Δ' is a nondegenerate polygon. Then, there is an open immersion $j : \mathcal{M}_{A'} \hookrightarrow \mathcal{M}_A$ whose image is the complement of the support of* $\operatorname{div}(\alpha)$*. Moreover, for $v' \in Q'_0$ the tautological line bundle L'_v of $\mathcal{M}_{A'}$ is the restriction of a tautological line bundle L_v of $\mathcal{M}_A$ to $\mathcal{M}_{A'}$, for some $v \in Q_0$. In particular, the tautological bundle T' of $\mathcal{M}_{A'}$ is obtained by restricting a subbundle of the tautological bundle T of $\mathcal{M}_A$ to $\mathcal{M}_{A'}$.*

Proof. There is a functor from the category $\mathcal{Q}$ of the quiver Q dual to Γ to the category $\mathcal{Q}'$ of the quiver Q' dual to Γ'. The functor $F : \mathcal{Q} \to \mathcal{Q}'$ takes a vertex $v \in Q$ to the the vertex $v' \in Q'$ dual to the tile of Γ' containing the tile of Γ dual to v. An arrow $a \in Q_1$ is sent to itself if $a \notin S_\alpha$, the identity if $a \notin S_\alpha \setminus \check{S}_\alpha$ and zero otherwise. Since representations of Q are linear functors from the category $\mathcal{Q}$ to the category of complex vector spaces, the pullback of the functor $F : \mathcal{Q} \to \mathcal{Q}'$ gives a functor $G : \operatorname{mod} A' \to \operatorname{mod} A$, whose image consists of representations $\left(\bigoplus_{v \in Q_0} W_v, \{\phi_a\}_{a \in Q_1}\right)$ satisfying $W_{v_1} = W_{v_2}$ if the functor F sends v_1 and v_2 to the same vertex $v' \in Q'_0$ and $\phi_a = \operatorname{id}_{W_{\mathrm{t}(a)}}$ for every arrow $a \in S_\alpha \setminus \check{S}_\alpha$. This functor induces the open immersion $j : \mathcal{M}_{A'} \hookrightarrow \mathcal{M}_A$.

For the second statement, the tautological bundle T' of $\mathcal{M}_{A'}$ is a family of θ'-stable A'-modules and by the Morita equivalence of Proposition 6.7, we get a family $\overline{T}$ of θ-stable $\overline{A}$-modules which defines a family of θ-stable A-modules. By the universal property of moduli spaces over the image $j(\mathcal{M}_{A'})$, this family is obtained by restriction. □

The following result gives a geometric characterisations of the arrows in S_α:

Corollary 6.19. *Assume Conjectures 5.7 and 6.4 and suppose Δ' is a nondegenerate polygon. Let a be an arrow in S_α. Then, either:*

1. *The arrow a lies in $S_\alpha \setminus \check{S}_\alpha$ and $\operatorname{div}(a)$ is a summand of $\operatorname{div}(\alpha)$; or*
2. *The arrow a lies in $\check{S}_\alpha$ and $\operatorname{div}(a)$ is the complement $\sum_{\rho\in\Sigma(1)} D_\rho - \operatorname{div}(\alpha) = \sum_{\rho\in\Sigma'(1)} D_\rho$.*

Proof. Let a be an arrow in $S_\alpha \setminus \check{S}_\alpha$. The relations $aa^{-1} - e_{\mathsf{h}(a)}$ and $a^{-1}a - e_{\mathsf{t}(a)}$ defined for the quiver $\overline{Q}$ and Proposition 6.18 imply that the maps between the line bundles $L_{t(a)}$ and $L_{h(a)}$ are isomorphisms on the complement of $\operatorname{div}(\alpha)$, hence the labelling divisor of a is a summand of $\operatorname{div}(\alpha)$. Let $a = s_i$ be an arrow in $\check{S}_\alpha$. By Lemma 5.18, the dual edge $\mathfrak{s}_i$ of s_i is a zag of $\mathfrak{z}_0$ and a zig of $\mathfrak{z}_{k+1}$, where $\mathfrak{z}_0$ and $\mathfrak{z}_{k+1}$ are the zigzag paths of Γ supported on $\mathfrak{m}_0$ and $\mathfrak{m}_{k+1}$, respectively. Thus, every boundary divisor which is not a summand of $\operatorname{div}(\alpha)$ is a summand of $\operatorname{div}(s_i)$. Moreover, there exists arrows s_{i+1} and s_i' in $S_\alpha \setminus \check{S}_\alpha$ such that $s_{i+1}s_i's_i$ is a small cycle of Q. Since $s_{i+1}, s_i' \in S_\alpha \setminus \check{S}_\alpha$ their labels are summands of $\operatorname{div}(\alpha)$. Hence, every interior divisor is a summand of $\operatorname{div}(s_i)$ and $\operatorname{div}(s_i) = \sum_{\rho\in\Sigma(1)} D_\rho - \operatorname{div}(\alpha)$. □

6.5 The arrow contraction algorithm

We are now ready to state the arrow contraction algorithm.

Algorithm 6.20 (The Arrow Contraction Algorithm)**.** *Let Γ be a consistent dimer model with dual quiver Q and Jacobian algebra A. We assume Γ has no bivalent nodes and Conjectures 5.7 and 6.4 hold for Γ.*

1. *Pick an arrow $\alpha \in Q_0$ with tail at vertex 0. By Proposition 4.6, we can associate to α a convex polygon Δ'. Assume α is such that Δ' is nondegenerate.*
2. *Find the set of edges $\mathcal{S}_\alpha$ using Definition 5.4 or either characterisations of the sets $\mathcal{S}_\alpha$ (see Proposition 5.15 and Theorem 5.16) or S_α (see Corollary 6.19).*
3. *Remove the edges in $\mathcal{S}_\alpha$ and all nodes of Γ connected only to edges in $\mathcal{S}_\alpha$ from Γ to obtain a new dimer model Γ' with characteristic polygon $\Delta(\Gamma') = \Delta'$.*
4. *The dimer model Γ' is consistent and for 0-generated stability parameters θ and θ', there exists an open immersion $\mathcal{M}_{A'} \hookrightarrow \mathcal{M}_A$, so that the toric fan of $\mathcal{M}_{A'}$ is $\Sigma' := \{\sigma \in \Sigma \mid \rho_i \nsubseteq \sigma \text{ for all } 1 \le i \le r\}$, where Σ is the fan of $\mathcal{M}_A$.*
5. *Since Γ' is consistent, and therefore nondegenerate, we may remove all bivalent nodes of Γ' without altering the number and direction of its zigzag paths or the Jacobian algebra of its dual quiver (see Remark 1.38).*

One can now repeat using Γ' *and* θ'*.*

6.6 Recovering the Ishii–Ueda algorithm

For a consistent dimer model Γ with dual quiver Q and 0-generated stability parameter θ, suppose there exists $\alpha \in Q_1$ with tail at vertex 0 and label $\mathrm{div}(\alpha)$ equal to a torus-invariant primer divisor D_ρ of $\mathcal{M}_A$. Assume without loss of generality that $\mathrm{div}(\alpha) = D_{\rho_1}$. Then, $\mathfrak{e}_\alpha$ is a zig of $\mathfrak{z}_1$ and a zag of $\mathfrak{z}_2$. Since $\mathfrak{z}_1$ and $\mathfrak{z}_2$ intersect and Γ is consistent, the ray ρ_1 is a corner of the characteristic polygon $\Delta(\Gamma)$ of Γ. The polygon Δ' is the convex hull of $\Delta(\Gamma) \setminus \{\rho_1\}$ and the arrow contraction algorithm coincides with Ishii–Ueda's operation [IU09]. Every triangle in $\mathrm{strip}(\alpha)$ is a lower triangle and by Theorem 5.16, the number of edges in $\mathcal{S}_\alpha$ equals the number of triangles in $\mathrm{strip}(\alpha)$. Lemma 5.18 gives an alternative description of the 'new' zigzag paths of Γ, those induced by the lower meandering walks of $\mathrm{strip}(\alpha)$, to that introduced in the proof of [IU09, Proposition 10.1].

Remark 6.21. The fact that Δ' is the characteristic polygon of Γ' [IU09, Proposition 11.2], left largely as an exercise to the reader, requires an understanding of the combinatorics of the Wunram's i-series (see Lemma 10.2 and proof of Proposition 10.1 in [IU09]). Corollary 6.13 provides a simple geometric argument to establish this fact in the special case when the divisor D_ρ equal the label of an arrow α with tail at vertex 0.

Unlike Ishii-Ueda's algorithm, the arrow contraction algorithm is constrained by the labels of the arrows of Q with tail at vertex 0. However, the arrow contraction algorithm preserves the triangulation of Σ, i.e. the toric fan of $\mathcal{M}_{A'}$, for θ' a 0-generated stability parameter, is Σ'.

6.7 Restrictions of the tautological bundle

Given any compact surface $Z \subset \mathcal{M}_A$, we may restrict the tautological bundle to it. The restriction $\bigoplus_{v\in Q_0} L_v|_Z$ contains redundant summands, as some of the line bundles are identified. Write $\overline{\bigoplus}_{v\in Q_0} L_v|_Z$ for the restriction of the tautological bundle T to Z after removing every redundant summand. Craw, King and (independently) Logvinenko observed that for some compact surfaces $Z \subset G\text{-Hilb}(\mathbb{C}^3)$, the restriction of the tautological bundle $\overline{\bigoplus}_{v\in Q_0} L_v|_Z$ is tilting on Z. The arrow contraction algorithm gives a partial explanation for this phenomenon.

Theorem 6.22. *Let* Γ *be a consistent dimer model with Jacobian algebra* A*. If we can obtain a dimer model* Γ' *with Jacobian algebra* A' *from* Γ *by performing the arrow contraction algorithm such that* $\mathcal{M}_{A'}$ *is the total space of the canonical bundle of a weak toric Fano surface* Z*, the restriction* $\overline{\bigoplus}_{v\in Q_0} L_v|_Z$ *of the tautological bundle* T *of* $\mathcal{M}_A$ *to* Z *is tilting.*

Proof. By assumption, there is a sequence of contractions which take the dimer model Γ associated to $\mathcal{M}_A$ to a dimer model Γ' such that $\mathcal{M}_{A'}$ is the total space of the canonical bundle of a weak toric Fano surface Z. Since Γ' was obtained by performing

the arrow contraction algorithm, the dimer model Γ' is consistent. Therefore, the tautological bundle T' of $\mathcal{M}_{A'}$ is tilting. Moreover, by Proposition 6.18, we know T' is obtained by restricting a subbundle of the tautological bundle T of $\mathcal{M}_A$ to $\mathcal{M}_{A'}$. The fact that the bundle T' restricted to Z is tilting is a result of Carqueville–Quintero-Vélez [CQV10, Proposition C.1] and Ishii–Ueda [IU11a, Theorem 7.1]. □

Therefore, the arrow contraction algorithm gives a sufficient condition for which the restriction of the tautological bundle to a weak toric Fano surface Z is tilting. It is not yet clear whether this condition is also a necessary one. The following example suggests that this could be the case.

Example 6.23. Consider the dimer model Γ depicted in Figure 6.2 with its dual quiver. An arrow of the quiver Q marked by $i_1, i_2, \ldots, i_j$ has labelling divisor $D_{i_1} + D_{i_2} + \ldots + D_{i_j}$. The dimer model Γ can be obtained from the dimer model in Example 3.37 by applying the arrow contraction algorithm five times. The toric fan Σ of the moduli space $\mathcal{M}_A$ of θ-stable A-modules, for the 0-generated stability parameter $\theta = (-7, 1, 1, \ldots, 1)$, is depicted in Figure 6.3(a). Figure 6.3(b) shows the labelling of the fan by combinatorial Reid's recipe.

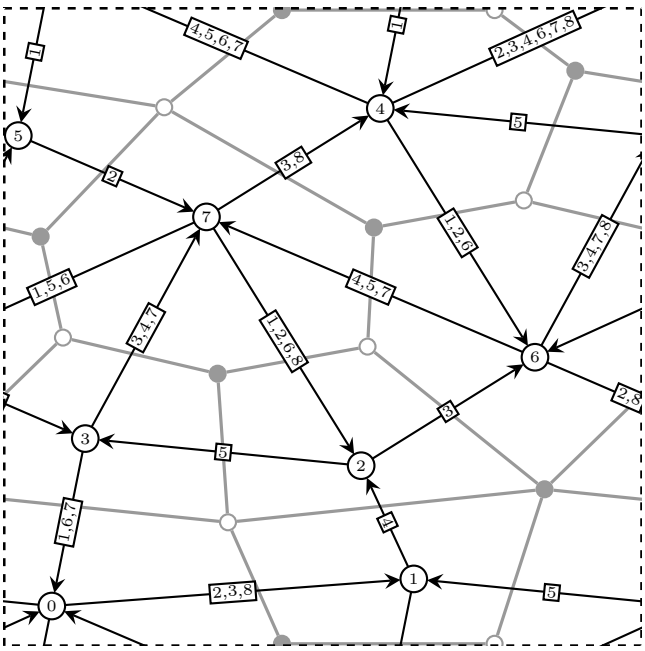

Figure 6.2: *The quiver Q dual to a dimer model Γ with arrows labelled*

The fan contains two compact surfaces Z_1, Z_2 associated to the rays ρ_6 and ρ_7, respectively. Note that since the labels of the arrows with tail at 0 are D_1, $D_2+D_3+D_8$ and D_5, it is not possible to use the arrow contraction algorithm to find a new consistent dimer model Γ' whose characteristic polygon has corners $\rho_1, \rho_2, \rho_5, \rho_8$. Moreover, after removing redundant summands, the restriction of the tautological bundle T of $\mathcal{M}_A$ to Z_1 decomposes into six line bundles, and thus it is not one of the tilting bundles of Z_1.

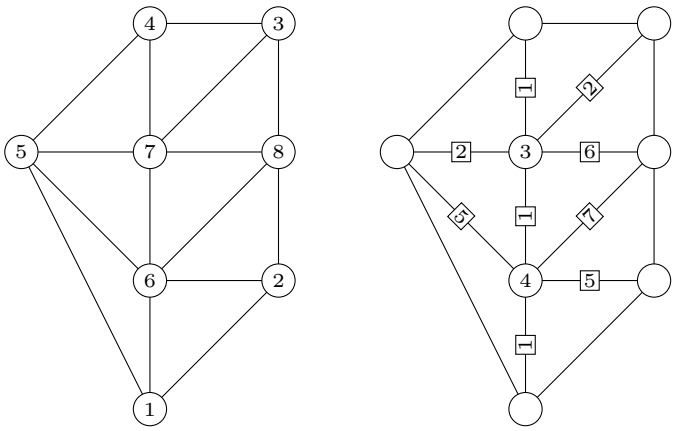

(a) The fan Σ of $\mathcal{M}_A$ (b) Reid's recipe

Figure 6.3: *The fan Σ of $\mathcal{M}_A$ for $\theta = (-7, 1, 1, \ldots, 1)$*

CHAPTER 7

FUTURE DIRECTIONS

We conclude this thesis by suggesting a link between the arrow contraction algorithm and combinatorial Reid's recipe. Numerous computational evidence suggests that the marking of the line segments and lattice points in strip(α) is closely related to the head and tails of the arrows in S_α. We give an explicit conjecture as to the relation of these two and suggest how this conjecture could be used to prove that in a fan Σ marked by Reid's recipe, every vertex of Q appears 'once' and that combinatorial Reid's recipe encodes the relations of the line bundles of $\mathcal{M}_A$ in $\mathrm{Pic}(\mathcal{M}_A)$.

7.1 Example 3.38 revisited

Recall the dimer model Γ introduced in Example 3.38.

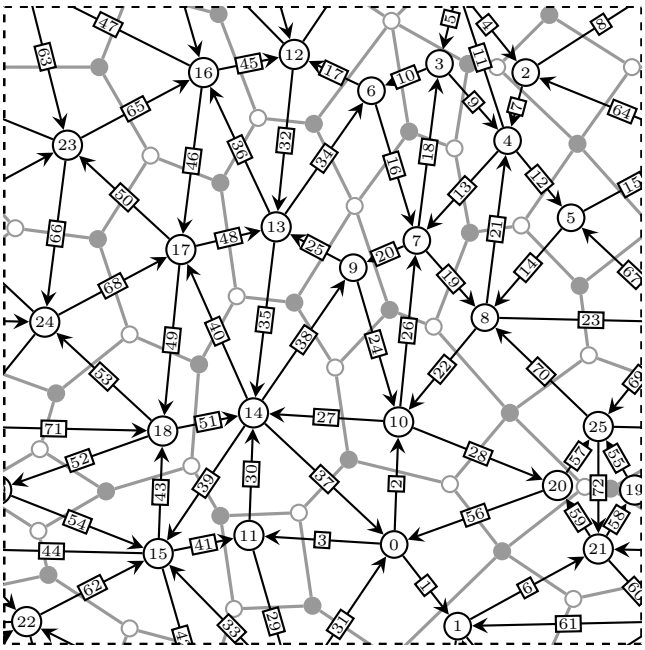

Figure 7.1: *Dimer model from Example 3.38*

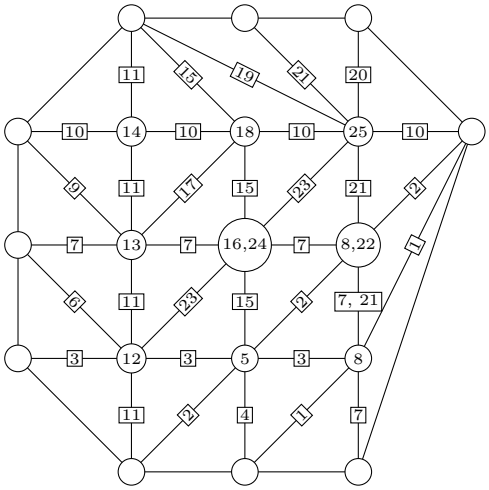

Figure 7.2: *Fan of $\mathcal{M}_A$ for $\theta = (-25, 1, 1, \ldots, 1)$ marked by Reid's recipe*

When $\alpha = a_3$, $\mathcal{S}_{a_3}$ has six edges $\mathfrak{s}_0, \mathfrak{s}_1, \ldots, \mathfrak{s}_5$ one for each line segments τ_i ($0 \leq i \leq 5$) depicted in Figure 7.3 (see Theorem 5.16).

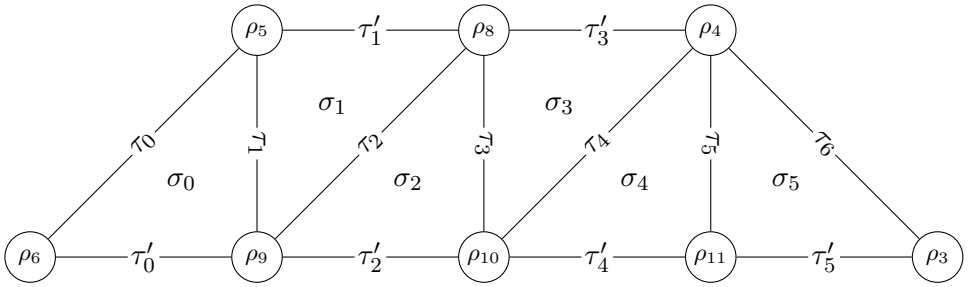

Figure 7.3: *Strip of triangles* $\mathrm{strip}(a_3)$

Table 7.1 lists the arrows in S_{a_3} dual to the edges in $\mathcal{S}_{a_3}$ along with their corresponding labelling divisor, tail and head. Notice the relation between Reid's recipe and the tails and heads of the arrows in S_{a_3}. The arrow s_0 has head at vertex 11, which marks all line segments in the boundary of $\mathrm{strip}(a_3)$ which are not in the boundary of Σ. As the line segments in $\partial\,\mathrm{strip}(\alpha) \setminus \partial\Sigma$ coincide with the line segments in $\partial\Sigma' \setminus \partial\Sigma$, this is Lemma 4.9. For $1 \leq i \leq 5$, the arrow s_i has tail at the vertex marking τ_i by Reid's recipe. The arrows s_2, s_4 and s_5 have head at the vertex marking the unique interior lattice point of Σ in τ_2, τ_4 and τ_5, respectively. The arrows s_1 and s_3 have head at the vertices marking τ_2 and τ_4, respectively.

	Arrow	Label	Tail	Head
s_0	a_3	$D_4 + D_5 + D_8$	0	11
s_1	a_{10}	D_5	3	6
s_2	a_{17}	$D_4 + D_8$	6	12
s_3	a_{20}	$D_5 + D_8$	7	9
s_4	a_{25}	D_4	9	13
s_5	a_{27}	$D_4 + D_5 + D_8$	10	14

Table 7.1: *Labelling divisors, heads and tails for the arrows in S_{a_3}*

A similar behaviour appears in the case when $\alpha = a_2$. Figure 7.4 shows the strip of triangles strip(a_2). From Example 5.20, we know that there are a total of 8 arrows in S_{a_2}. Table 7.2 lists all arrows in S_{a_2} with their labelling divisor, head and tail. As expected, the head of s_0 marks the lines segments in the boundary of strip(a_2) that are not in the boundary of Σ. For $i = 1, 2, 3, 5$, the arrow $s_i \in S_{a_2}$ has tail at the vertex marking the line segment τ_i by Reid's recipe and head at the vertex marking the unique interior lattice point of Σ in τ_i. The arrow s_4 exhibits an opposite behaviour. It has tail at vertex 25, which marks the interior lattice point connected to τ_4 and head at vertex 21, which marks the line segment τ_4. The arrows s_4' and s_4'' both have tail at the vertex marking τ_4 and head at the vertex making τ_5 and τ_3, respectively.

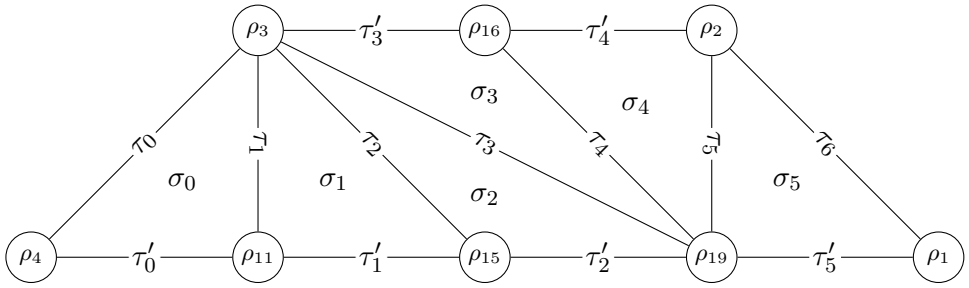

Figure 7.4: *Strip of triangles* strip(a_2)

	Arrow	Label	Tail	Head
s_0	a_2	$D_2 + D_3 + D_{16}$	0	10
s_1	a_{30}	$D_2 + D_3 + D_{16}$	11	14
s_2	a_{43}	$D_2 + D_3 + D_{16}$	15	18
s_3	a_{55}	D_3	19	25
s_4	a_{72}	$\sum_{j=1}^{19} D_j - (D_2 + D_3 + D_{16})$	25	21
s_4'	a_{59}	$D_3 + D_{16}$	21	20
s_4''	a_{58}	$D_2 + D_{16}$	21	19
s_5	a_{57}	D_2	20	25

Table 7.2: *Labelling divisors, heads and tails for the arrows in* S_{a_2}

Finally, when $\alpha = a_1$, Theorem 5.16 tells us that the only arrows in S_{a_1} are $s_0 = a_1$ and $s_1 = a_{19}$. The head of the arrow s_0 is the vertex 1, which marks the boundary line segments of strip(a_1) not in the boundary of Σ, as expected. The arrow s_1 has tail at vertex 7, which marks the unique interior line segment in strip(a_1) and head at vertex 8, which marks the unique interior lattice point of Σ in strip(a_1).

7.2 The conjecture

It is clear from the examples in the previous section that Lemma 4.9 provides the first link between the arrow contraction algorithm and combinatorial Reid's recipe for consistent dimer models. The following conjecture suggests a stronger link between these two:

Conjecture 7.1. *Let Γ be a consistent dimer model and let α be an arrow in its dual quiver Q with tail at vertex 0. The arrows s_i, s_i' and s_i'' denote the arrow or arrows in S_α dual to the edge or edges $\mathfrak{s}_i$, $\mathfrak{s}_i'$ and $\mathfrak{s}_i''$ associated to τ_i (see Theorem 5.16). Let ρ be a lattice point on $\partial\,\mathrm{strip}(\alpha) \setminus \partial\Sigma$ corresponding to an interior divisor D_ρ of $\mathcal{M}_A$. Then, one of the following holds:*

1. *Two lower triangles σ_{i-1} and σ_i on $\mathrm{strip}(\alpha)$ contain the lattice point ρ. Reid's recipe marks the lattice point ρ and the line segment τ_i with distinct vertices v_ρ and v_{τ_i}, respectively, and there exists a line segment τ' in Σ' containing ρ marked by v_{τ_i}. Then*
$$\mathsf{t}(s_i) = v_{\tau_i} \quad \text{and} \quad \mathsf{h}(s_i) = v_\rho.$$

2. *Two lower triangles σ_{i-1} and σ_{i+1} and an upper triangle σ_i contain the lattice point ρ. Reid's recipe marks the line segments τ_i and τ_{i+1} with distinct vertices $v_{\tau_i}, v_{\tau_{i+1}}$ and either:*

   (a) *Reid's recipe marks the lattice point ρ with a unique vertex $v_\rho \in Q_0$ and there exists a line segment τ' in Σ' containing ρ marked with either v_{τ_i} or $v_{\tau_{i+1}}$. Then the arrows s_i and s_{i+1} have tail at v_{τ_i} and $v_{\tau_{i+1}}$, respectively. If v_{τ_i} marks τ'*
   $$\mathsf{t}(s_i) = v_{\tau_i} \qquad \mathsf{h}(s_i) = v_{\tau_{i+1}} \qquad \mathsf{t}(s_{i+1}) = v_{\tau_{i+1}} \qquad \mathsf{h}(s_{i+1}) = v_\rho.$$
   Else, $v_{\tau_{i+1}}$ marks τ' and
   $$\mathsf{t}(s_i) = v_{\tau_i} \qquad \mathsf{h}(s_i) = v_\rho \qquad \mathsf{t}(s_{i+1}) = v_{\tau_{i+1}} \qquad \mathsf{h}(s_{i+1}) = v_{\tau_i}.$$

   (b) *Reid's recipe marks the lattice point ρ with two vertices v_ρ and v_ρ' and there exists line segments τ_1' and τ_2' in Σ' containing ρ marked with v_{τ_i} and $v_{\tau_{i+1}}$, respectively. Then*
   $$\mathsf{t}(s_i) = v_{\tau_i} \qquad \mathsf{h}(s_i) = v_\rho \qquad \mathsf{t}(s_{i+1}) = v_{\tau_{i+1}} \qquad \mathsf{h}(s_{i+1}) = v_\rho'.$$

3. *Two lower triangles σ_{i-2} and σ_{i+1} and two upper triangles σ_{i-1} and σ_i all contain the lattice point ρ. Reid's recipe marks the lattice point ρ and line segments τ_{i-1}, τ_i and τ_{i+1} with distinct vertices $v_\rho, v_{\tau_{i-1}}, v_{\tau_i}$ and $v_{\tau_{i+1}}$ and there exists a line segment τ' in Σ' containing ρ marked with v_{τ_i}. Then*
$$\begin{aligned} &\mathsf{t}(s_{i-1}) = v_{\tau_{i-1}} \qquad \mathsf{h}(s_{i-1}) = v_\rho \qquad \mathsf{t}(s_i') = v_{\tau_i} \qquad \mathsf{h}(s_i') = v_{\tau_{i+1}} \\ &\mathsf{t}(s_{i+1}) = v_{\tau_{i+1}} \qquad \mathsf{h}(s_{i+1}) = v_\rho \qquad \mathsf{t}(s_i'') = v_{\tau_i} \qquad \mathsf{h}(s_i'') = v_{\tau_{i-1}} \\ &\qquad\qquad\qquad\quad \mathsf{t}(s_i) = v_\rho \qquad \mathsf{h}(s_i) = v_{\tau_i}. \end{aligned}$$

Assuming Conjecture 7.1, we would like to use an inductive argument to show that in the marking of Σ with vertices of Q by Reid's recipe, every nonzero vertex appears 'once', in the sense of Conjecture 3.33. To do this, we need to verify that Reid's recipe is recursive with respect to the arrow contraction algorithm. First note that Conjecture 7.1 suggests a labelling of the vertices of Q' by the labels of some of the vertices of Q. Either:

1. The vertex v' of Q' is dual to a tile made up of a single tile $\mathfrak{t}$ of Γ, in which case the label of v' is the label of the vertex $v \in Q_1$ dual to the tile $\mathfrak{t}$; or

2. The vertex v' of Q' is dual to tile made up by merging two or more tiles of Γ, in which case either:

   (a) Its dual tile contains the zero tile of Γ, and we set v' to be the zero vertex of Q'; or

   (b) Its dual tile contains a tile of Γ dual to a vertex $v \in Q_1$ that labels an interior lattice point ρ in $\Sigma \setminus \mathrm{strip}(\alpha)$, and we set $v' = v$; or

   (c) Its dual tile contains no tile of Γ dual to a vertex marking an interior lattice point ρ in $\Sigma \setminus \mathrm{strip}(\alpha)$, but contains a tile dual to a vertex $v \in Q_1$ marking an interior line segments τ in $\Sigma \setminus \mathrm{strip}(\alpha)$, and we set $v' = v$.

Conjecture 7.2. *After performing Reid's recipe for Γ', a vertex v marks an interior lattice point or and interior line segment of Σ' by Reid's recipe if and only if v labels a vertex of Q' and v marks the corresponding interior lattice point or interior line segment of $\Sigma \setminus \mathrm{strip}(\alpha)$.*

The proof of Conjecture 3.33 would be an inductive argument which performs the arrow contraction algorithm as many times as needed to produce the dimer model from Example 1.6. At each stage, the number of vertices will be reduced as tiles of Γ merge to give new tiles of Γ' until we are left with a single vertex, the zero vertex. It is not yet clear that for any consistent dimer model Γ one can always repeatedly perform the arrow contraction algorithm to produce the dimer model from Example 1.6, as the algorithm is only well-defined for when Δ' is a nondegenerate polygon.

Example 7.3. Consider the dimer model Γ with dual quiver Q in Figure 7.5(a). For $\theta = (-9, 1, 1, \ldots, 1)$, the fan Σ of $\mathcal{M}_A$ is depicted in Figure 7.6(a).

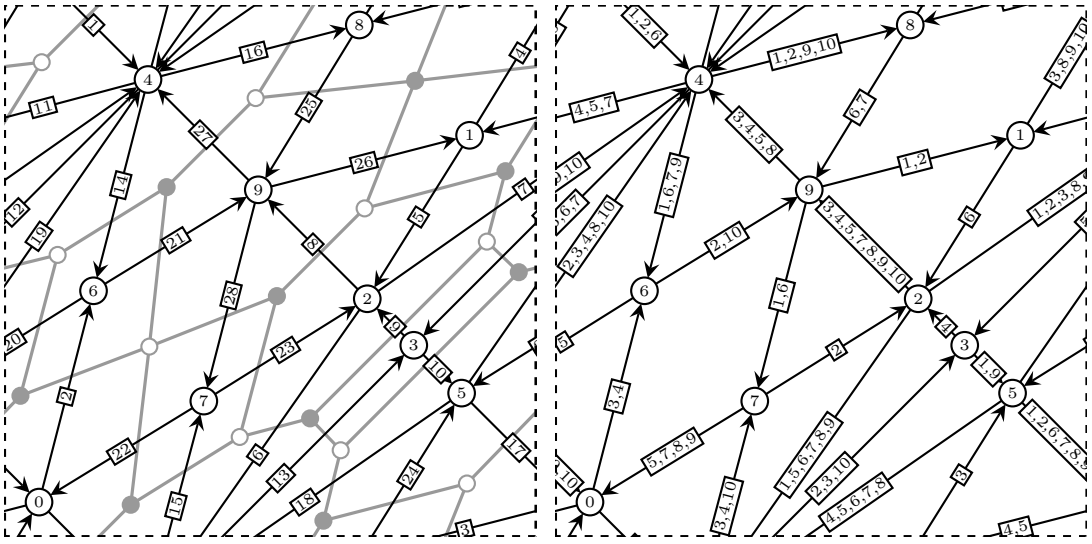

(a) The dimer model Γ and its dual quiver Q (b) The quiver Q with labelled arrows

Figure 7.5: *The dimer model Γ and its dual quiver Q*

Let $\alpha = a_1$, with label $\mathrm{div}(a_1) = D_1 + D_2 + D_6$ (see Figure 7.5(b)). The set $\mathcal{S}_{a_1}$ consists of six edges corresponding to the arrows:

Arrow	Label	Tail	Head
a_1	$D_1 + D_2 + D_6$	0	4
a_{28}	$D_1 + D_6$	9	7
a_{23}	D_2	7	2
a_8	$\sum_{j=1}^{10} D_j - (D_1 + D_2 + D_6)$	2	9
a_{26}	$D_1 + D_2$	9	1
a_5	D_6	1	2

Table 7.3: *Labelling divisors, heads and tails for the arrows in* S_{a_1}

To obtain Γ' from Γ, the zero tile of Γ merges with the tile dual to vertex 4 in Q to make a tile of Γ' dual to the vertex labelled 0 in Q'. The tiles dual to the vertices $1, 2, 7$ and 9 of Q merge into a single tile of Γ'. As the vertex 2 appears labelling an interior lattice point of $\Sigma \setminus \mathrm{strip}(a_1)$, we assign the label 2 to the vertex dual to this tile of Γ'. Note that a lattice point or line segment of Σ' is marked by a vertex v if and only if v marks the corresponding lattice point or line segment of Σ, except for the vertex 9, which does not appear in the marking of Σ' by Reid's recipe. This is expected since 9 labels no vertex of Q'.

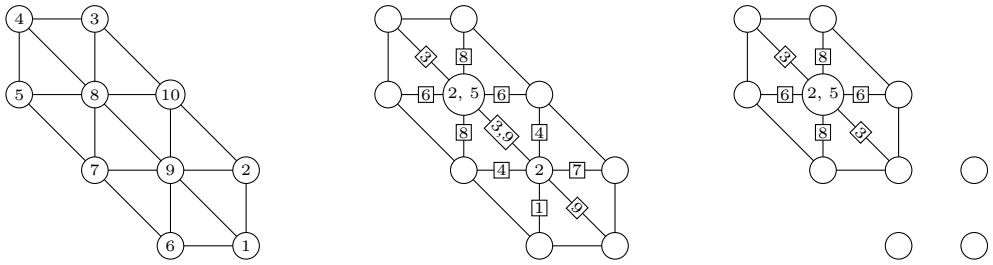

(a) The fan Σ of $\mathcal{M}_A$ (b) Reid's recipe on Σ (c) Reid's recipe on Σ'

Figure 7.6: *The fan* Σ *of* $\mathcal{M}_A$ *and Reid's recipe on* Σ *and* Σ'

Conjecture 7.1 could also be used to show that the relations of the tautological line bundles of $\mathcal{M}_A$ in $\mathrm{Pic}(\mathcal{M}_A)$ are encoded by combinatorial Reid's recipe. Proposition 7.4 shows that the relations from Conjecture 3.34 hold when restricted to some local charts. The proof assumes Conjecture 7.1 and considers each its four cases individually.

Proposition 7.4. *Let* Γ *be a consistent dimer model and let* α *be an arrow in its dual quiver* Q *with tail at vertex* 0*. Assume Conjecture 7.1. For all* $\sigma \nsubseteq \mathrm{strip}(\alpha)$*, the following relations hold in* $\mathrm{Pic}(\mathcal{M}_A)$*:*

1. $L_{v_\rho}\big|_{U_\sigma} = L_{v_{\tau_i}}\big|_{U_\sigma} \otimes L_{\mathsf{h}(\alpha)}\big|_{U_\sigma}$ *in Case 1 of Conjecture 7.1;*
2. $L_{v_\rho}\big|_{U_\sigma} = L_{v_{\tau_i}}\big|_{U_\sigma} \otimes L_{\mathsf{h}(\alpha)}\big|_{U_\sigma}$ *or* $L_{v_\rho}\big|_{U_\sigma} = L_{v_{\tau_{i+1}}}\Big|_{U_\sigma} \otimes L_{\mathsf{h}(\alpha)}\big|_{U_\sigma}$ *in Case 2(a) of Conjecture 7.1, depending on whether* v_{τ_i} *or* $v_{\tau_{i+1}}$ *mark* τ'*;*

3. $L_{v_\rho}\big|_{U_\sigma} \otimes L_{v'_\rho}\Big|_{U_\sigma} = L_{v_{\tau_i}}\big|_{U_\sigma} \otimes L_{v_{\tau_{i+1}}}\Big|_{U_\sigma} \otimes L_{\mathsf{h}(\alpha)}\big|_{U_\sigma}$ *in Case 2(b) of Conjecture 7.1; or*

4. $L_{v_\rho}\big|_{U_\sigma} = L_{v_{\tau_i}}\big|_{U_\sigma} \otimes L_{\mathsf{h}(\alpha)}\big|_{U_\sigma}$ *in Case 3 of Conjecture 7.1.*

Proof. Let s_i, s'_i and s''_i denote the arrow or arrows in S_α dual to the edge or edges $\mathfrak{s}_i$, $\mathfrak{s}'_i$ and $\mathfrak{s}''_i$ associated to τ_i (see Theorem 5.16).

For Case 1, first observe that by Lemma 5.18, the label of the arrow s_i coincides with $\operatorname{div}(\alpha)$. Moreover, the arrow s_i has tail at v_{τ_i} and head at v_ρ. Therefore for all $\sigma \nsubseteq \operatorname{strip}(\alpha)$, there exists a path from 0 to v_ρ in Q_σ, the quiver supporting M_σ, made up of a path from 0 to v_{τ_i} followed by the arrow s_i. This shows that the relation $L_{v_\rho}\big|_{U_\sigma} = L_{v_{\tau_i}}\big|_{U_\sigma} \otimes L_{\mathsf{h}(\alpha)}\big|_{U_\sigma}$ holds, as $L_v|_{U_\sigma} = \mathcal{O}_{U_\sigma}(\operatorname{div}(p))$ where p is a path is a path in Q_σ from 0 to v.

For Case 2(a), Lemma 5.18 says that $\operatorname{div}(s_i) + \operatorname{div}(s_{i+1}) = \operatorname{div}(\alpha)$. Therefore for all $\sigma \nsubseteq \operatorname{strip}(\alpha)$, there exists a path from 0 to v_ρ in Q_σ made up of a path from 0 to either v_{τ_i} or $v_{\tau_{i+1}}$, depending on whether v_{τ_i} or $v_{\tau_{i+1}}$ marks τ', followed by one of s_{i+1} or s_i and then the other. Thus, either $L_{v_\rho}\big|_{U_\sigma} = L_{v_{\tau_i}}\big|_{U_\sigma} \otimes L_{\mathsf{h}(\alpha)}\big|_{U_\sigma}$ or $L_{v_\rho}\big|_{U_\sigma} = L_{v_{\tau_{i+1}}}\Big|_{U_\sigma} \otimes L_{\mathsf{h}(\alpha)}\big|_{U_\sigma}$.

For Case 2(b), again Lemma 5.18 tells us that $\operatorname{div}(s_i)+\operatorname{div}(s_{i+1}) = \operatorname{div}(\alpha)$. Thus for $\sigma \nsubseteq \operatorname{strip}(\alpha)$, there exist paths in Q_σ from 0 to v_ρ and from 0 to v'_ρ made up of a path from 0 to v_{τ_i} followed by the arrow s_i in one case, and a path from 0 to $v_{\tau_{i+1}}$ followed by the arrow s_{i+1} in the other. Hence, $L_{v_\rho}\big|_{U_\sigma} \otimes L_{v'_\rho}\Big|_{U_\sigma} = L_{v_{\tau_i}}\big|_{U_\sigma} \otimes L_{v_{\tau_{i+1}}}\Big|_{U_\sigma} \otimes L_{\mathsf{h}(\alpha)}\big|_{U_\sigma}$.

Finally, for Case 3 we know that $\operatorname{div}(s_{i-1}) + \operatorname{div}(s''_i) = \operatorname{div}(s_{i+1}) + \operatorname{div}(s'_i) = \operatorname{div}(\alpha)$. Moreover for $\sigma \nsubseteq \operatorname{strip}(\alpha)$, there exist a minimum of two paths from 0 to v_ρ. Both start by travelling from 0 to v_{τ_i}, then one goes through s''_i followed by s_{i-1} while the other travels through s'_i and then s_{i+1}. It follows that $L_{v_\rho}\big|_{U_\sigma} = L_{v_{\tau_i}}\big|_{U_\sigma} \otimes L_{\mathsf{h}(\alpha)}\big|_{U_\sigma}$, as required. □

Therefore, to prove Conjecture 3.34, it suffices to show that Conjecture 7.1 holds and that the relations of Proposition 7.4 hold for all $\sigma \subseteq \operatorname{strip}(\alpha)$.

APPENDIX A

PERFECT MATCHINGS OF THE DIMER MODEL IN FIGURE 1.3

Table A.1 lists all perfect matchings of the dimer model in Figure 1.3. We write $\mathfrak{e}_i$ for the edge in Γ dual to the arrow marked by i in Figure 1.3. The last column of the table shows the value of the height change for each perfect matching with respect to Π_1.

Perfect Matching	**Edges**									$h(-,\Pi_1)$
Π_1	$\mathfrak{e}_1$	$\mathfrak{e}_6$	$\mathfrak{e}_7$	$\mathfrak{e}_{10}$	$\mathfrak{e}_{14}$	$\mathfrak{e}_{16}$	$\mathfrak{e}_{17}$	$\mathfrak{e}_{26}$	$\mathfrak{e}_{28}$	(0,0)
Π_2	$\mathfrak{e}_1$	$\mathfrak{e}_7$	$\mathfrak{e}_{13}$	$\mathfrak{e}_{16}$	$\mathfrak{e}_{17}$	$\mathfrak{e}_{19}$	$\mathfrak{e}_{21}$	$\mathfrak{e}_{23}$	$\mathfrak{e}_{26}$	(0,1)
Π_3	$\mathfrak{e}_2$	$\mathfrak{e}_4$	$\mathfrak{e}_7$	$\mathfrak{e}_8$	$\mathfrak{e}_{13}$	$\mathfrak{e}_{15}$	$\mathfrak{e}_{19}$	$\mathfrak{e}_{24}$	$\mathfrak{e}_{27}$	(-2,3)
Π_4	$\mathfrak{e}_2$	$\mathfrak{e}_3$	$\mathfrak{e}_8$	$\mathfrak{e}_9$	$\mathfrak{e}_{11}$	$\mathfrak{e}_{15}$	$\mathfrak{e}_{18}$	$\mathfrak{e}_{19}$	$\mathfrak{e}_{27}$	(-3,3)
Π_5	$\mathfrak{e}_3$	$\mathfrak{e}_6$	$\mathfrak{e}_8$	$\mathfrak{e}_{11}$	$\mathfrak{e}_{12}$	$\mathfrak{e}_{18}$	$\mathfrak{e}_{20}$	$\mathfrak{e}_{22}$	$\mathfrak{e}_{27}$	(-3,2)
Π_6	$\mathfrak{e}_1$	$\mathfrak{e}_5$	$\mathfrak{e}_6$	$\mathfrak{e}_{12}$	$\mathfrak{e}_{14}$	$\mathfrak{e}_{17}$	$\mathfrak{e}_{18}$	$\mathfrak{e}_{25}$	$\mathfrak{e}_{28}$	(-1,0)
Π_7	$\mathfrak{e}_6$	$\mathfrak{e}_8$	$\mathfrak{e}_{11}$	$\mathfrak{e}_{12}$	$\mathfrak{e}_{14}$	$\mathfrak{e}_{17}$	$\mathfrak{e}_{18}$	$\mathfrak{e}_{22}$	$\mathfrak{e}_{25}$	(-2,1)
Π_8	$\mathfrak{e}_4$	$\mathfrak{e}_6$	$\mathfrak{e}_7$	$\mathfrak{e}_8$	$\mathfrak{e}_{17}$	$\mathfrak{e}_{18}$	$\mathfrak{e}_{19}$	$\mathfrak{e}_{22}$	$\mathfrak{e}_{27}$	(-2,2)
Π_9	$\mathfrak{e}_4$	$\mathfrak{e}_6$	$\mathfrak{e}_7$	$\mathfrak{e}_8$	$\mathfrak{e}_{10}$	$\mathfrak{e}_{14}$	$\mathfrak{e}_{16}$	$\mathfrak{e}_{17}$	$\mathfrak{e}_{22}$	(-1,1)
Π_{10}	$\mathfrak{e}_4$	$\mathfrak{e}_7$	$\mathfrak{e}_8$	$\mathfrak{e}_{13}$	$\mathfrak{e}_{15}$	$\mathfrak{e}_{16}$	$\mathfrak{e}_{17}$	$\mathfrak{e}_{19}$	$\mathfrak{e}_{21}$	(-1,2)
Π_{11}	$\mathfrak{e}_1$	$\mathfrak{e}_2$	$\mathfrak{e}_7$	$\mathfrak{e}_{13}$	$\mathfrak{e}_{19}$	$\mathfrak{e}_{23}$	$\mathfrak{e}_{24}$	$\mathfrak{e}_{26}$	$\mathfrak{e}_{27}$	(-1,2)
Π_{12}	$\mathfrak{e}_1$	$\mathfrak{e}_3$	$\mathfrak{e}_5$	$\mathfrak{e}_6$	$\mathfrak{e}_{12}$	$\mathfrak{e}_{18}$	$\mathfrak{e}_{20}$	$\mathfrak{e}_{27}$	$\mathfrak{e}_{28}$	(-2,1)
Π_{13}	$\mathfrak{e}_8$	$\mathfrak{e}_9$	$\mathfrak{e}_{11}$	$\mathfrak{e}_{15}$	$\mathfrak{e}_{17}$	$\mathfrak{e}_{18}$	$\mathfrak{e}_{19}$	$\mathfrak{e}_{21}$	$\mathfrak{e}_{25}$	(-2,2)
Π_{14}	$\mathfrak{e}_4$	$\mathfrak{e}_5$	$\mathfrak{e}_9$	$\mathfrak{e}_{17}$	$\mathfrak{e}_{18}$	$\mathfrak{e}_{19}$	$\mathfrak{e}_{22}$	$\mathfrak{e}_{23}$	$\mathfrak{e}_{27}$	(-2,2)
Π_{15}	$\mathfrak{e}_9$	$\mathfrak{e}_{11}$	$\mathfrak{e}_{17}$	$\mathfrak{e}_{18}$	$\mathfrak{e}_{19}$	$\mathfrak{e}_{22}$	$\mathfrak{e}_{23}$	$\mathfrak{e}_{26}$	$\mathfrak{e}_{27}$	(-2,2)
Π_{16}	$\mathfrak{e}_4$	$\mathfrak{e}_5$	$\mathfrak{e}_9$	$\mathfrak{e}_{15}$	$\mathfrak{e}_{17}$	$\mathfrak{e}_{18}$	$\mathfrak{e}_{19}$	$\mathfrak{e}_{27}$	$\mathfrak{e}_{28}$	(-2,2)
Π_{17}	$\mathfrak{e}_9$	$\mathfrak{e}_{11}$	$\mathfrak{e}_{15}$	$\mathfrak{e}_{17}$	$\mathfrak{e}_{18}$	$\mathfrak{e}_{19}$	$\mathfrak{e}_{26}$	$\mathfrak{e}_{27}$	$\mathfrak{e}_{28}$	(-2,2)
Π_{18}	$\mathfrak{e}_2$	$\mathfrak{e}_3$	$\mathfrak{e}_8$	$\mathfrak{e}_9$	$\mathfrak{e}_{10}$	$\mathfrak{e}_{11}$	$\mathfrak{e}_{14}$	$\mathfrak{e}_{15}$	$\mathfrak{e}_{16}$	(-2,2)
Π_{19}	$\mathfrak{e}_2$	$\mathfrak{e}_3$	$\mathfrak{e}_8$	$\mathfrak{e}_{11}$	$\mathfrak{e}_{12}$	$\mathfrak{e}_{13}$	$\mathfrak{e}_{14}$	$\mathfrak{e}_{15}$	$\mathfrak{e}_{16}$	(-2,2)
Π_{20}	$\mathfrak{e}_3$	$\mathfrak{e}_8$	$\mathfrak{e}_9$	$\mathfrak{e}_{10}$	$\mathfrak{e}_{11}$	$\mathfrak{e}_{15}$	$\mathfrak{e}_{16}$	$\mathfrak{e}_{20}$	$\mathfrak{e}_{21}$	(-2,2)
Π_{21}	$\mathfrak{e}_3$	$\mathfrak{e}_8$	$\mathfrak{e}_{11}$	$\mathfrak{e}_{12}$	$\mathfrak{e}_{13}$	$\mathfrak{e}_{15}$	$\mathfrak{e}_{16}$	$\mathfrak{e}_{20}$	$\mathfrak{e}_{21}$	(-2,2)

Continued on next page

Table A.1 – *Continued from previous page*

Perfect Matching	**Edges**									$h(-,\Pi_1)$
Π_{22}	e_1	e_2	e_3	e_6	e_7	e_8	e_{18}	e_{19}	e_{27}	(-2,2)
Π_{23}	e_1	e_2	e_3	e_5	e_9	e_{18}	e_{19}	e_{23}	e_{27}	(-2,2)
Π_{24}	e_2	e_8	e_9	e_{10}	e_{11}	e_{14}	e_{15}	e_{24}	e_{25}	(-2,2)
Π_{25}	e_2	e_8	e_{11}	e_{12}	e_{13}	e_{14}	e_{15}	e_{24}	e_{25}	(-2,2)
Π_{26}	e_8	e_9	e_{10}	e_{11}	e_{15}	e_{20}	e_{21}	e_{24}	e_{25}	(-2,2)
Π_{27}	e_8	e_{11}	e_{12}	e_{13}	e_{15}	e_{20}	e_{21}	e_{24}	e_{25}	(-2,2)
Π_{28}	e_4	e_6	e_7	e_8	e_{10}	e_{20}	e_{22}	e_{24}	e_{27}	(-2,2)
Π_{29}	e_4	e_5	e_9	e_{10}	e_{20}	e_{22}	e_{23}	e_{24}	e_{27}	(-2,2)
Π_{30}	e_4	e_5	e_{12}	e_{13}	e_{20}	e_{22}	e_{23}	e_{24}	e_{27}	(-2,2)
Π_{31}	e_9	e_{10}	e_{11}	e_{20}	e_{22}	e_{23}	e_{24}	e_{26}	e_{27}	(-2,2)
Π_{32}	e_{11}	e_{12}	e_{13}	e_{20}	e_{22}	e_{23}	e_{24}	e_{26}	e_{27}	(-2,2)
Π_{33}	e_4	e_5	e_9	e_{10}	e_{15}	e_{20}	e_{24}	e_{27}	e_{28}	(-2,2)
Π_{34}	e_4	e_5	e_{12}	e_{13}	e_{15}	e_{20}	e_{24}	e_{27}	e_{28}	(-2,2)
Π_{35}	e_9	e_{10}	e_{11}	e_{15}	e_{20}	e_{24}	e_{26}	e_{27}	e_{28}	(-2,2)
Π_{36}	e_{11}	e_{12}	e_{13}	e_{15}	e_{20}	e_{24}	e_{26}	e_{27}	e_{28}	(-2,2)
Π_{37}	e_4	e_5	e_9	e_{10}	e_{14}	e_{16}	e_{17}	e_{22}	e_{23}	(-1,1)
Π_{38}	e_4	e_5	e_{12}	e_{13}	e_{14}	e_{16}	e_{17}	e_{22}	e_{23}	(-1,1)
Π_{39}	e_1	e_6	e_7	e_8	e_{17}	e_{18}	e_{19}	e_{21}	e_{25}	(-1,1)
Π_{40}	e_1	e_5	e_9	e_{17}	e_{18}	e_{19}	e_{21}	e_{23}	e_{25}	(-1,1)
Π_{41}	e_9	e_{10}	e_{11}	e_{14}	e_{16}	e_{17}	e_{22}	e_{23}	e_{26}	(-1,1)
Π_{42}	e_{11}	e_{12}	e_{13}	e_{14}	e_{16}	e_{17}	e_{22}	e_{23}	e_{26}	(-1,1)
Π_{43}	e_4	e_5	e_9	e_{10}	e_{14}	e_{15}	e_{16}	e_{17}	e_{28}	(-1,1)
Π_{44}	e_4	e_5	e_{12}	e_{13}	e_{14}	e_{15}	e_{16}	e_{17}	e_{28}	(-1,1)
Π_{45}	e_9	e_{10}	e_{11}	e_{14}	e_{15}	e_{16}	e_{17}	e_{26}	e_{28}	(-1,1)
Π_{46}	e_{11}	e_{12}	e_{13}	e_{14}	e_{15}	e_{16}	e_{17}	e_{26}	e_{28}	(-1,1)
Π_{47}	e_1	e_6	e_7	e_{17}	e_{18}	e_{19}	e_{26}	e_{27}	e_{28}	(-1,1)
Π_{48}	e_1	e_2	e_3	e_6	e_7	e_8	e_{10}	e_{14}	e_{16}	(-1,1)
Π_{49}	e_1	e_3	e_6	e_7	e_8	e_{10}	e_{16}	e_{20}	e_{21}	(-1,1)
Π_{50}	e_1	e_2	e_3	e_5	e_9	e_{10}	e_{14}	e_{16}	e_{23}	(-1,1)
Π_{51}	e_1	e_2	e_3	e_5	e_{12}	e_{13}	e_{14}	e_{16}	e_{23}	(-1,1)
Π_{52}	e_1	e_3	e_5	e_9	e_{10}	e_{16}	e_{20}	e_{21}	e_{23}	(-1,1)
Π_{53}	e_1	e_3	e_5	e_{12}	e_{13}	e_{16}	e_{20}	e_{21}	e_{23}	(-1,1)
Π_{54}	e_1	e_2	e_6	e_7	e_8	e_{10}	e_{14}	e_{24}	e_{25}	(-1,1)
Π_{55}	e_1	e_6	e_7	e_8	e_{10}	e_{20}	e_{21}	e_{24}	e_{25}	(-1,1)
Π_{56}	e_1	e_2	e_5	e_9	e_{10}	e_{14}	e_{23}	e_{24}	e_{25}	(-1,1)
Π_{57}	e_1	e_2	e_5	e_{12}	e_{13}	e_{14}	e_{23}	e_{24}	e_{25}	(-1,1)
Π_{58}	e_1	e_5	e_9	e_{10}	e_{20}	e_{21}	e_{23}	e_{24}	e_{25}	(-1,1)
Π_{59}	e_1	e_5	e_{12}	e_{13}	e_{20}	e_{21}	e_{23}	e_{24}	e_{25}	(-1,1)
Π_{60}	e_1	e_6	e_7	e_{10}	e_{20}	e_{24}	e_{26}	e_{27}	e_{28}	(-1,1)

Table A.1: *Perfect matchings for the dimer model in Figure 1.3*

APPENDIX B

LABELS FOR THE ARROWS OF THE QUIVER IN FIGURE 4.1

Table B.1 lists all the labels for the arrows of the quiver in Figure B.1 below. We write a_i for the arrow marked by i in Figure B.1. An arrow a in Table B.1 with label $i_1, i_2, \ldots, i_j$ has labelling divisor $\mathrm{div}(a) = D_{i_1} + D_{i_2} + \ldots + D_{i_j}$.

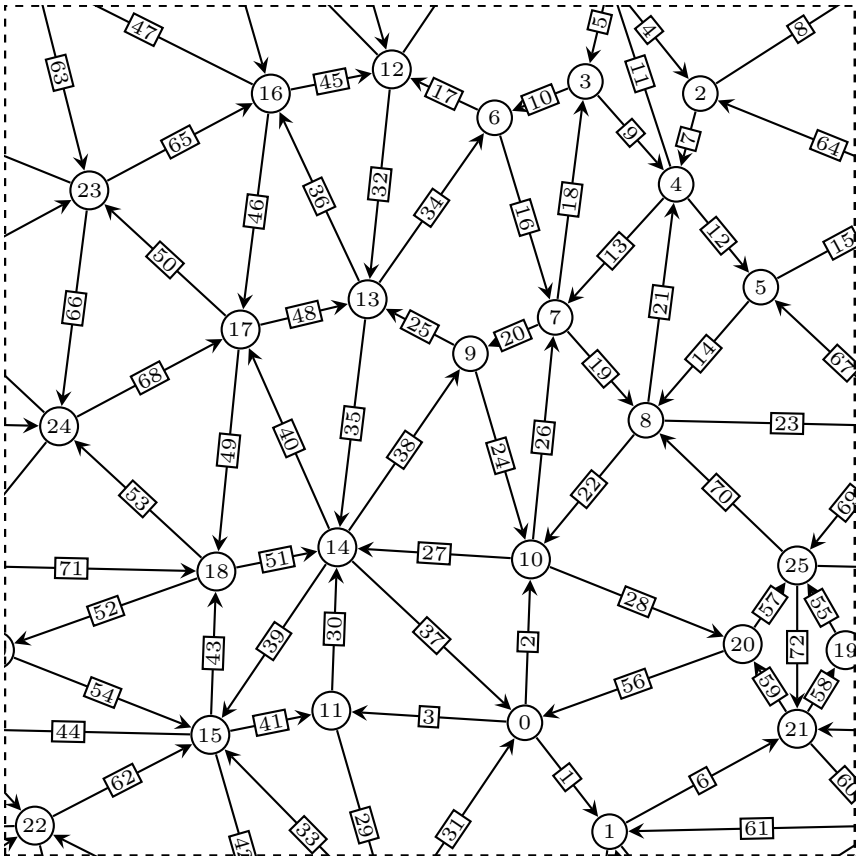

Figure B.1: *The quiver Q from Figure 4.1*

Arrow	**Tail**	**Head**	**Label**
a_1	0	1	7
a_2	0	10	2, 3, 16
a_3	0	11	4, 5, 8
a_4	1	2	7, 12, 17
a_5	1	3	6, 12
a_6	1	21	1, 2
a_7	2	4	6
a_8	2	22	1, 2
a_9	3	4	7, 17
a_{10}	3	6	5
a_{11}	4	1	1, 2, 3, 4, 5, 8, 9, 10, 11, 13, 14, 15, 16, 18, 19
a_{12}	4	5	7, 12
a_{13}	4	7	5, 6, 9, 12, 13
a_{14}	5	8	5, 6, 9, 13
a_{15}	5	23	1, 2, 13, 17, 18
a_{16}	6	7	6, 7, 9, 12, 13, 17
a_{17}	6	12	4, 8
a_{18}	7	3	1, 2, 3, 4, 8, 10, 11, 14, 15, 16, 18, 19
a_{19}	7	8	7
a_{20}	7	9	5, 8
a_{21}	8	4	1, 2, 3, 4, 8, 10, 11, 14, 15, 16, 18, 19
a_{22}	8	10	5, 6, 8, 9, 10, 12, 13, 14, 17, 18
a_{23}	8	24	1, 2, 7, 12, 17, 18
a_{24}	9	10	6, 7, 9, 10, 12, 13, 14, 17, 18
a_{25}	9	13	4
a_{26}	10	7	1, 2, 3, 4, 11, 15, 16, 19
a_{27}	10	14	4, 5, 8
a_{28}	10	20	1, 7
a_{29}	11	12	6, 7, 12
a_{30}	11	14	2, 3, 16
a_{31}	12	0	1, 2, 3, 9, 10, 11, 13, 14, 15, 16, 17, 18, 19
a_{32}	12	13	5, 6, 7, 9, 12, 13, 17
a_{33}	12	15	2, 3, 4, 5, 8, 9, 10, 11, 16
a_{34}	13	6	1, 2, 3, 10, 11, 14, 15, 16, 18, 19
a_{35}	13	14	5, 6, 7, 8, 9, 10, 12, 13, 14, 17, 18
a_{36}	13	16	2, 3, 4, 8, 10, 11, 16
a_{37}	14	0	1, 6, 9, 10, 11, 12, 13, 14, 15, 17, 18, 19
a_{38}	14	9	1, 2, 3, 11, 15, 16, 19
a_{39}	14	15	4, 5, 6, 7, 8, 9, 10, 11, 12
a_{40}	14	17	2, 3, 4, 11, 16
a_{41}	15	11	1, 13, 14, 15, 17, 18, 19
a_{42}	15	16	6, 7, 12, 13, 17

Continued on next page

Table B.1 – *Continued from previous page*

Arrow	**Tail**	**Head**	**Label**
a_{43}	15	18	$2, 3, 16$
a_{44}	15	21	$3, 4, 5, 6, 8, 9, 10, 11, 13, 14, 15$
a_{45}	16	12	$1, 14, 15, 18, 19$
a_{46}	16	17	$5, 6, 7, 9, 12, 13, 14, 17, 18$
a_{47}	16	22	$3, 4, 5, 8, 9, 10, 11, 14, 15$
a_{48}	17	13	$1, 15, 19$
a_{49}	17	18	$5, 6, 7, 8, 9, 10, 12$
a_{50}	17	23	$3, 4, 8, 10, 11, 15$
a_{51}	18	14	$1, 13, 14, 15, 17, 18, 19$
a_{52}	18	19	$4, 5, 6, 8, 9, 10, 11, 13, 14, 15$
a_{53}	18	24	$3, 4, 11, 15$
a_{54}	19	15	$1, 7, 12, 17, 18, 19$
a_{55}	19	25	3
a_{56}	20	0	$4, 5, 6, 8, 9, 10, 11, 12, 13, 14, 15, 17, 18, 19$
a_{57}	20	25	2
a_{58}	21	19	$2, 16$
a_{59}	21	20	$3, 16$
a_{60}	21	22	$7, 12, 17$
a_{61}	22	1	$3, 4, 5, 6, 8, 9, 10, 11, 13, 14, 15, 16, 18, 19$
a_{62}	22	15	$1, 2, 16, 18, 19$
a_{63}	22	23	$6, 7, 12, 13, 17, 18$
a_{64}	23	2	$3, 4, 5, 8, 9, 10, 11, 14, 15, 16, 19$
a_{65}	23	16	$1, 2, 16, 19$
a_{66}	23	24	$5, 6, 7, 9, 12$
a_{67}	24	5	$3, 4, 8, 10, 11, 14, 15, 16, 19$
a_{68}	24	17	$1, 2, 13, 14, 16, 17, 18, 19$
a_{69}	24	25	$5, 6, 8, 9, 10, 13, 14$
a_{70}	25	8	$3, 4, 11, 15, 16, 19$
a_{71}	25	18	$1, 2, 7, 12, 16, 17, 18, 19$
a_{72}	25	21	$1, 4, 5, 6, 7, 8, 9, 10, 11, 12, 13, 14, 15, 17, 18, 19$

Table B.1: *Labels for the arrows of the quiver in Figure B.1*

BIBLIOGRAPHY

[ASS06] Ibrahim Assem, Daniel Simson, and Andrzej Skowroński. *Elements of the representation theory of associative algebras*, volume 65 of *London Mathematical Society Student Texts*. Cambridge University Press, 2006.

[BCQV15] Raf Bocklandt, Alastair Craw, and Alexander Quintero Vélez. Geometric Reid's recipe for dimer models. *Math. Ann.*, 361(3-4):689–723, 2015.

[BM09] Martin Bender and Sergey Mozgovoy. Crepant resolutions and brane tilings II: Tilting bundles. `arXiv:0909.2013`, September 2009.

[Boc12] Raf Bocklandt. Consistency conditions for dimer models. *Glasg. Math. J.*, 54(2):429–447, 2012.

[Bro12] Nathan Broomhead. Dimer models and Calabi-Yau algebras. *Mem. Amer. Math. Soc.*, 215(1011):viii+86, 2012.

[CCL12] Sabin Cautis, Alastair Craw, and Timothy Logvinenko. Derived Reid's recipe for abelian subgroups of $\mathrm{SL}_3(\mathbb{C})$. `arXiv:1205.3110`, to appear in *J. Reine Angew. Math.*, 2012.

[CI04] Alastair Craw and Akira Ishii. Flops of G-Hilb and equivalences of derived categories by variation of GIT quotient. *Duke Math. J.*, 124(2):259–307, 2004.

[CL09] Sabin Cautis and Timothy Logvinenko. A derived approach to geometric McKay correspondence in dimension three. *J. Reine Angew. Math.*, 636:193–236, 2009.

[CLS11] David A. Cox, John B. Little, and Henry K. Schenck. *Toric varieties*, volume 124 of *Graduate Studies in Mathematics*. American Mathematical Society, Providence, RI, 2011.

[CMT07] Alastair Craw, Diane Maclagan, and Rekha R. Thomas. Moduli of McKay quiver representations. II. Gröbner basis techniques. *J. Algebra*, 316(2):514–535, 2007.

[CQV10] Nils Carqueville and Alexander Quintero Vélez. Remarks on quiver gauge theories from open topological string theory. *J. High Energy Phys.*, (3):129, 24, 2010.

[CQV12] Alastair Craw and Alexander Quintero Vélez. Cellular resolutions of non-commutative toric algebras from superpotentials. *Adv. Math.*, 229(3):1516–1554, 2012.

[CR02] Alastair Craw and Miles Reid. How to calculate A-Hilb $\mathbb{C}^3$. In *Geometry of toric varieties*, volume 6 of *Sémin. Congr.*, pages 129–154. Soc. Math. France, Paris, 2002.

[Cra05] Alastair Craw. An explicit construction of the McKay correspondence for A-Hilb $\mathbb{C}^3$. *J. Algebra*, 285(2):682–705, 2005.

[FHK+06] Sebastián Franco, Amihay Hanany, Kristian D. Kennaway, David Vegh, and Brian Wecht. Brane dimers and quiver gauge theories. *J. High Energy Phys.*, 2006, 2006.

[Gul08] Daniel R. Gulotta. Properly ordered dimers, R-charges, and an efficient inverse algorithm. *J. High Energy Phys.*, (10):014, 31, 2008.

[HK05] Amihay Hanany and Kristian D. Kennaway. Dimer models and toric diagrams. `arXiv:hep-th/0511287v2`, 2005.

[IU08] Akira Ishii and Kazushi Ueda. On moduli spaces of quiver representations associated with dimer models. In *Higher dimensional algebraic varieties and vector bundles*, RIMS Kôkyûroku Bessatsu, B9, pages 127–141. Res. Inst. Math. Sci. (RIMS), Kyoto, 2008.

[IU09] Akira Ishii and Kazushi Ueda. Dimer models and the special McKay correspondence. `arXiv:0905.0059`, May 2009.

[IU11a] Akira Ishii and Kazushi Ueda. Dimer models and exceptional collections. `arXiv:0911.4529`, May 2011.

[IU11b] Akira Ishii and Kazushi Ueda. A note on consistency conditions on dimer models. In *Higher dimensional algebraic geometry*, RIMS Kôkyûroku Bessatsu, B24, pages 143–164. Res. Inst. Math. Sci. (RIMS), Kyoto, 2011.

[IU13] Akira Ishii and Kazushi Ueda. Dimer models and crepant resolutions. `arXiv:1303.4028`, March 2013.

[Kin94] Alastair D. King. Moduli of representations of finite-dimensional algebras. *Quart. J. Math. Oxford Ser. (2)*, 45(180):515–530, 1994.

[Log04] Timothy Logvinenko. *Families of G-constellations parametrised by resolutions of quotient singularities.* Ph.D. Thesis. University of Bath, UK, 2004.

[Log10] Timothy Logvinenko. Reid's recipe and derived categories. *J. Algebra*, 324(8):2064–2087, 2010.

[MFK94] David Mumford, John Fogarty, and Frances C. Kirwan. *Geometric Invariant Theory*. Ergebnisse der Mathematik und ihrer Grenzgebiete. Springer-Verlag, Berlin, 1994.

[Moz09] Sergey Mozgovoy. Crepant resolutions and brane tilings I: Toric realization. `arXiv:0908.3475`, August 2009.

[Nak01] Iku Nakamura. Hilbert schemes of abelian group orbits. *J. Algebraic Geom.*, 10(4):757–779, 2001.

[Rei97] Miles Reid. Mckay correspondence. *Proc. of Algebraic Geom. Symposium (Kinosaki, November 1996)*, pages 14–41, 1997.

[Sch85] A.H. Schofield. *Representations of rings over skew fields*, volume 92 of *London Mathematical Society Lecture Notes Series*. Cambridge University Press, 1985.

[UY11] Kazushi Ueda and Masahito Yamazaki. A note on dimer models and McKay quivers. *Comm. Math. Phys.*, 301(3):723–747, 2011.